NAVAL POSTGRADUATE SCHOOL
MONTEREY, CALIFORNIA

THESIS

A STUDY OF POTENTIAL USES FOR WALSH TRANSFORMED IMAGES IN TARGET RECOGNITION

by

Jeffrey H. Davis

December, 1994

Thesis Advisor: D. Scott Davis

Approved for public release; distribution is unlimited.

REPORT DOCUMENTATION PAGE

Form Approved OMB No. 0704-0188

1.AGENCY USE ONLY *(Leave blank)*	2.REPORT DATE	3.REPORT TYPE AND DATES COVERED
	DECEMBER 1994	Master's Thesis

4. TITLE AND SUBTITLE : A STUDY OF POTENTIAL USES FOR WALSH TRANSFORMED IMAGES IN TARGET RECOGNITION

5.FUNDING NUMBERS

6. AUTHOR(S) Jeffrey H. Davis

7. PERFORMING ORGANIZATION NAME(S) AND ADDRESS(ES)
Naval Postgraduate School
Monterey CA 93943-5000

8.PERFORMING ORGANIZATION REPORT NUMBER

9.SPONSORING/MONITORING AGENCY NAME(S) AND ADDRESS(ES)

10.SPONSORING/MONITORING AGENCY REPORT NUMBER

11.SUPPLEMENTARY NOTES
The views expressed in this thesis are those of the author and do not reflect the official policy or position of the Department of Defense or the U.S. Government.

12a. DISTRIBUTION/AVAILABILITY STATEMENT

Approved for public release; distribution is unlimited.

12b.DISTRIBUTION CODE

13.ABSTRACT *(maximum 200 words)*

We conducted an experiment to determine if the unprocessed output of a developmental sensor system could be used to identify military targets. We used a computer to manipulate images of tanks and helicopters to produce data files similar to the expected output of the developmental sensor system. Graphing the data files and comparing the graphs for similarities gave us the basis for judging that the output of the system could be used by an automatic pattern recognition device to correctly recognize military targets. This development could yield advances in automatic target recognition, target acquisition, and battle damage assessment.

14.SUBJECT TERMS: WALSH TRANSFORM, TARGET RECOGNITION, IR DETECTORS

15.NUMBER OF PAGES 252

16.PRICE CODE

17. SECURITY CLASSIFICATION OF REPORT	18. SECURITY CLASSIFICATION OF THIS PAGE	19. SECURITY CLASSIFICATION OF ABSTRACT	20. LIMITATION OF ABSTRACT
Unclassified	Unclassified	Unclassified	UL

NSN 7540-01-280-5500 Standard Form 298 (Rev. 2-89)

Prescribed by ANSI Std. 239-18 298-102

Approved for public release; distribution is unlimited.

A STUDY OF POTENTIAL USES FOR WALSH TRANSFORMED IMAGES IN TARGET RECOGNITION

by

Jeffrey H. Davis
Captain, United States Army
B.S., United States Military Academy, 1983

Submitted in partial fulfillment
of the requirements for the degree of

MASTER OF SCIENCE IN APPLIED PHYSICS

from the

NAVAL POSTGRADUATE SCHOOL
December 1994

Author: Jeffrey H. Davis
Jeffrey H. Davis

Approved by: David Scott Davis
D. Scott Davis, Thesis Advisor

Michael E. Melich, Second Reader

W. B. Colson
William B. Colson, Chairman
Department of Physics

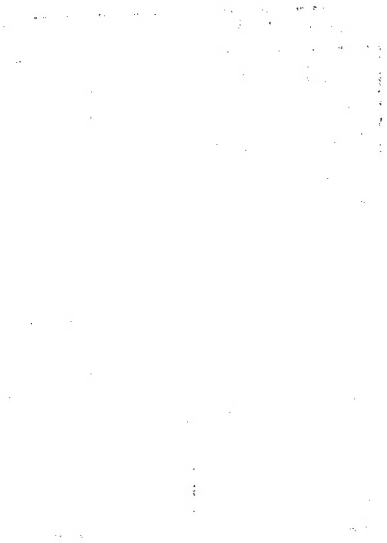

ABSTRACT

We conducted an experiment to determine if the unprocessed output of a developmental sensor system could be used to identify military targets. We used a computer to manipulate images of tanks and helicopters to produce data files similar to the expected output of the developmental sensor system. Graphing the data files and comparing the graphs for similarities gave us the basis for judging that the output of the system could be used by an automatic pattern recognition device to correctly recognize military targets. This development could yield advances in automatic target recognition, target acquisition, and battle damage assessment.

TABLE OF CONTENTS

ACKNOWLEDGMENT

The author would like to acknowledge the financial support of NAVSEA, TAD-PEO for allowing the purchase of the equipment used in this thesis.

I. INTRODUCTION

A. MOTIVATION AND PROBLEM STATEMENT

The research presented in this thesis is a portion of a sensor system development project being done at the Naval Postgraduate School (NPS) in Monterey, California. This project includes the design and prototyping of a new imaging and multispectral imaging sensor system based on a revolutionary approach to conventional image recording methods. Image data is recorded as a sequence of expansion coefficients that express the characteristics of the image as a linear superposition of two dimensional (2-D) basis functions that tile the image plane (Davis, 1994). Applying this approach to infrared (IR) measurements should realize several advantages. Among these advantages are enhanced signal-to-noise ratio (SNR), improved background rejection, and efficient exploitation of discrete IR detector technologies (Kadin et al, 1990). Several of the characteristics and technological aspects of this sensor system have been discussed in previous theses (McKenzie, 1990; Musselman, 1991; Sargent, 1991; Metzger, 1992; Huguenin, 1992; and Middleton, 1994). These theses explored various technological problems associated with the development of the prototype system.

The work described in this thesis does not concern itself with a specific technological question per se. Instead, it addresses a more general and fundamental question about potential applications of the new sensor system once it becomes operational. This project has been motivated by a juxtaposition of two ideas. First, the concept that the device will record the amplitudes or expansion coefficients of an image with respect to a predetermined set of orthogonal basis functions defined across a 2-D image plane, instead of a conventional image. Secondly, that many of the current approaches to automatic pattern recognition (APR) algorithms and their associated digital signal processing techniques operate on 2-D transforms of images rather than on the images themselves (Pratt, 1991). Combining these concerns leads to an exciting question: since the new system will directly record a 2-D transform of an image, can this raw data

contain useful information that can provide an APR capability without further processing? The resolution of that question constitutes the purpose of this thesis research.

B. BACKGROUND

1. Importance Of The Infrared Portion Of The EM Spectrum

Most thermal radiation from terrestrial objects exists in the IR portion of the electromagnetic spectrum. The majority of natural objects of interest are in approximate thermal equilibrium with their environment and radiate approximately as blackbodies (Hecht, 1987), with the bulk of their irradiance in the 5 - 25 μm wavelength range , while machines that burn fuel radiate more power at shorter wavelengths due to their higher temperatures. Infrared spectra can convey information about an object's chemical composition and thermodynamic characteristics. That information can be used to determine or to estimate an objects identity with a greater ease than is afforded at shorter wavelengths. Efficient sensor systems with multiple-wavelength (i.e. multi-spectral) imaging capability will enable both improved target-from-background discrimination capability and enhanced target characterization (shape, composition, temperature) beyond what is currently possible. The new multiplexed imaging system being developed at NPS is not restricted to IR wavelengths, but it is expected to have its most extensive uses in that portion of the electromagnetic (EM) spectrum.

2. Conventional Imaging Systems

The purpose of any image recording system is to generate some kind of permanent record of the spatial distribution of irradiances produced by a target scene. Prior to the advent of electronic cameras (television), virtually all camera systems relied upon opto-chemical technologies, such as photographic film and plates. Those technologies were effective across a broad range of wavelengths, from the very near IR to the x-ray region of the EM spectrum. But, they were useless at longer IR wavelengths, where

objects in the ambient environment radiate most strongly. This shortcoming continued throughout the early years of the television era, during which IR-sensitive vacuum tube sensor technology progressed very slowly.

The first significant advances in IR imaging technology occurred with the development of solid state IR photodetectors, particularly InSb, PbS, and HgCdTe devices. The detector systems based upon these devices were initially just simple, single pixel, discrete detectors. To record an image, these devices are typically scanned across the image plane in a pixel-by-pixel raster scan. The resulting electronic data can then be stored and processed via any means that is used for other raster scan technologies, such as conventional electron beam raster scanned television. This technique is the basis for scanning forward-looking infrared (FLIR) devices currently in wide use by the military for target acquisition/identification systems.

Solid state IR technology has made giant strides in the last two decades. Due to microfabrication methods developed by the microelectronics and integrated circuit industries, detector manufacturers can now make closely packed 2-D arrays of IR detectors with integrated read-out and signal processing electronics. These focal plane arrays (FPAs) remove the need for opto-mechanical scanning and greatly simplify the acquisition of an IR image. FPAs made from InSb, PtSi, and HgCdTe are being used in a wide variety of imaging systems, much as their visible wavelength counterparts, charge coupled devices (CCD), are in wide use at visible wavelengths.

However, attempts to make an FPA that works efficiently at long IR wavelengths have encountered a fundamental technical problem. Existing solid state detector technologies depend upon the familiar doped material band-gap characteristics of semiconductors (Dereniak and Crowe, 1984). While attempting to develop devices to operate at longer wavelengths (which corresponds to lower photon energies), it becomes physically impractical to use conventional solid state quantum detector physics; the required band gap energies are too small. There are several other technologies such as bolometers, heterodyne systems, and photofluxonic devices that do operate efficiently at

these longer wavelengths (Kadin et al, 1990; Dereniak and Crowe, 1984). Unfortunately, it is either impractical or impossible to configure any of these devices into densely packed FPAs. All of them are inherently single discrete detectors. Their exploitation in imaging systems requires a return to scanning techniques.

Conventional FLIR raster scanning technologies record information from only one image pixel at a time while ignoring the rest of the scene. When operating in wavelength regions where background photon shot noise is not severe (e.g. either at very long IR wavelengths or at wavelengths < 2.5 microns), this scanning inefficiency results in an overall signal-to-noise ratio (SNR) that it inferior to what is theoretically possible (Davis, 1994). A remedy to this problem was developed in the realm of IR spectroscopy approximately 25 years ago. Researchers found that a greatly enhanced SNR could be achieved in low background noise measurements using multiplexing techniques based on Fourier transforms. The resulting technologies are known collectively as Fourier transform spectroscopy and are now the standard method for obtaining IR spectroscopic measurements. The new imaging technology research and development project at NPS is also based upon multiplexing, but does not involve Fourier transforms.

3. The New Imaging Technique

The proposed, fully multiplexed imaging technique circumvents the weaknesses of traditional scanning methods by recording complete linear combinations of the desired pixel irradiances, instead of the individual pixel irradiances themselves. The measured quantities are a linear superposition, or transform, of the pixel irradiances. The linear combinations are chosen so that the transform coefficients comprise a complete orthogonal set of basis functions spanning the 2-D image plane. By scanning through sufficient linear combinations to permit the unambiguous inversion of the transform, the desired individual pixel irradiances can be recovered from the sequence of measured linear combinations of signals. Details of this method are found in the article by D. S. Davis (1994).

That article specifies several of the potential advantages of this approach over the traditional raster scanning FLIR systems. Among these advantages are:

- The Fellget advantage- Mentioned in the previous section, this refers to the situation where the sensor system's noise performance is limited by its own intrinsic detector noise level, rather than by source or background photon shot noise. The multiplexing approach spreads the noise around to all the pixels, diluting its effects, resulting in a significant improvement in overall image SNR.
- The throughput advantage- The multiplexed imaging sensor can be configured so that its optical apertures have geometries that are optimized to maximize the number of photons gathered from the target. This optimizes the statistically realizable noise figure of the detection process.
- Passive two beam background cancellation- By employing a two beam optical input (with one beam centered on the target and other reading background signals), it is straightforward to design a simple optical system that is sensitive to only the differences in the two image scenes. This provides automatic, first-order background signal cancellation and makes the sensor highly capable of selecting the target from the background common mode signal.
- Geometric versatility- This is closely related to the throughput advantage. Unlike conventional square matrix FPAs, the new multiplexing technique can be applied to a wide variety of 2-D geometrical shapes to accommodate different applications. This adaptability can be used to further enhance its sensitivity and ability to select specific targets in a cluttered scene.
- Radiometric consistency- With only one or two discrete detectors used, there will be no requirement for detector sensitivity recalibrations each time the system is powered up. When calibration is required, it will be significantly easier to calibrate a couple of robust discrete detectors than it is to calibrate a large FPA pixel-by-pixel.

Perhaps not all of these potential advantages will be fully realized in all possible applications of this developmental technology, but they should all contribute in varying degrees to the overall increase in system performance offered by this technique over current systems.

II. THEORETICAL FOUNDATION

A. WALSH SEQUENCY FUNCTIONS

The multiplexed imaging scheme being developed by Davis (1994) will make explicit use of a family of complete, orthogonal basis functions known as Walsh functions (Harmuth, 1977). A significant branch of applied mathematics called sequency theory (Harmuth, 1977; Beauchamp, 1984), has grown up around these functions. Walsh functions have several fundamental characteristics:

- They only take on the values of +1 and -1, and so are discontinuous.
- The number of zero crossings (sign changes) that a particular Walsh function makes is called its sequency, or order. The term sequency was coined by Harmuth (1977) as an analogy to frequency in trigonometric functions.
- The standard notation for a Walsh function of sequency n, in one variable x, is wal(n,x). For two variables, it is wal(n,x,y), etc. (see Fig. 1.).
- Walsh functions are mutually orthogonal, in the sense that

$$\int_{domain} wal(m,x)wal(n,x)dx = a\delta_{m,n} \qquad (1)$$

where a is a constant and δ is the conventional Kronecker δ symbol.

In two dimensions,

$$\iint_{domain} wal(m,x,y)wal(n,x,y)dxdy = a\delta_{m,n}. \qquad (2)$$

- The Walsh functions form a complete basis set. Any other function can be represented as a series expansion of Walsh functions as

$$f(x) = \sum_{n=0}^{\infty} c_n wal(n,x), \qquad (3)$$

with

$$c_n = \frac{1}{D}\int_0^D f(x)wal(n,x)dx \qquad (4)$$

where D is the width of the domain in x over which the expansion takes place. In two dimensions, D would be an area of the domain. This is a transform-inverse transform pair.

- Because they are discrete transforms, the Walsh function basis set is complete only for basis sets containing 0,1,...,N-1 members, where N is an integer power of two. This is a mathematical requirement. With $N=2^k$ (k being an integer), the discrete transform-inverse transform pair is (Harmuth, 1977):

$$f(x) = \sum_{n=0}^{N-1} c_n wal(n,x) \quad i = 0, 1, ..., N-1 \qquad (5)$$

and

$$c_n = \frac{1}{N} \sum_{i=0}^{N-1} f_i wal(n,x_i) \quad n = 0, 1, ..., N-1, \qquad (6)$$

where $f_i = f(x_i)$ and the x_i are sampled uniformly into N partitions of the domain.

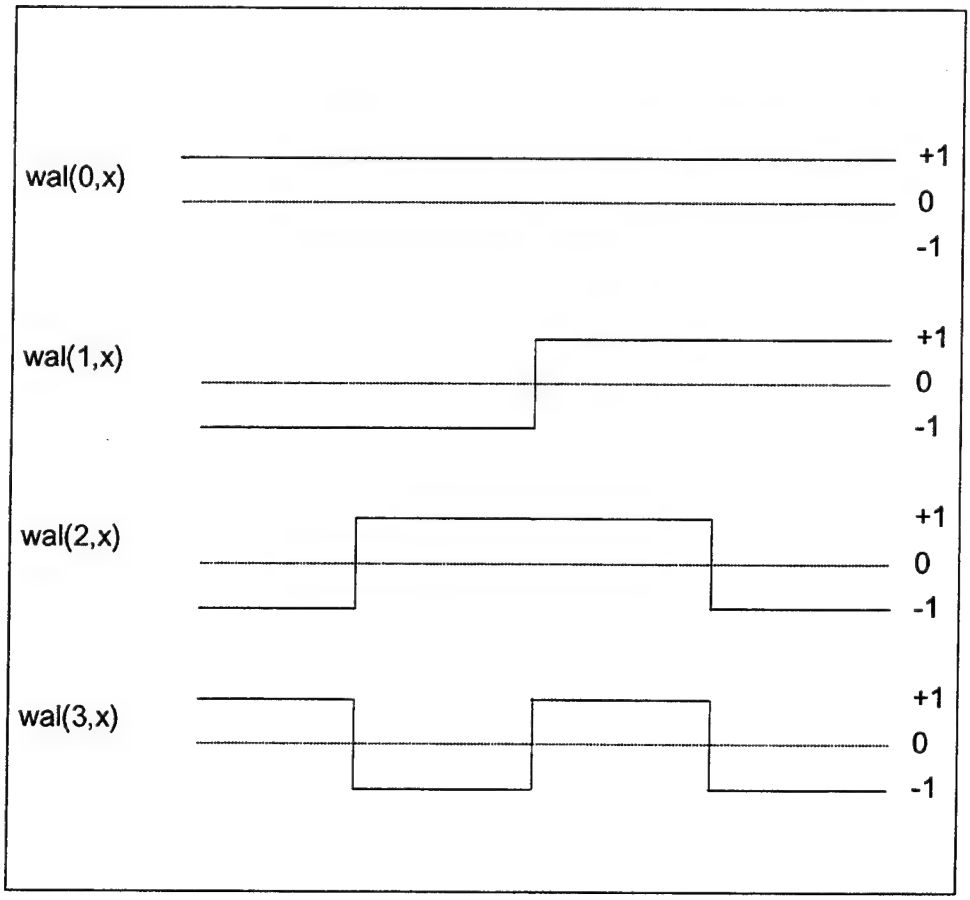

Fig. 1. The first four sequency-ordered Walsh functions

B. MULTIPLEXED IMAGING WITH WALSH FUNCTIONS

Davis's scheme for multiplexed imaging is based upon a novel technique for generating 2-D Walsh functions from 1-D Walsh functions using optical methods to produce a Kronecker product (Harmuth, 1977). The resulting 2-D Walsh basis set tiles (covers) the entire image plane. The sensor then records the sampled 2-D Walsh transform sequence of the irradiance distribution,

$$\Phi_n = \frac{1}{N} \sum_{i=0}^{N-1} E(x_i, y_i) wal(n, x_i, y_i) \qquad n = 0, 1, ..., N-1 \qquad (7)$$

rather than any individual image pixel irradiance, E_i . From the N measurements of Φ_n, the irradiances are recovered by inverse Walsh transformation. This thesis project attempts to determine if any usable target pattern recognition information is obvious in the spatial sequency spectral measurements Φ_n , before any data processing or inverse transforming takes place.

The Kronecker product imaging scheme depends upon the use of a pair of masks, each of which has a 1-D spatial sequency characteristic. These characteristics are represented by the mask sequencies shown along the bottom and left margins of Figure 2. Since the basic approach is 1-D, we chose to limit the thesis research to a subset of the general problem introduced above. How much pattern recognition information is expressed by a 1-D Walsh spatial sequency spectrum of an image? Does that spatial sequency spectrum contain useful information about the target's shape, regardless of image orientation, scale, and contrast?

C. HYPOTHESES AND PREDICTIONS

We can predict some of the behavior of spatial sequency spectra under conditions of target-background contrast reversal and variable scaling on the basis of the symmetry

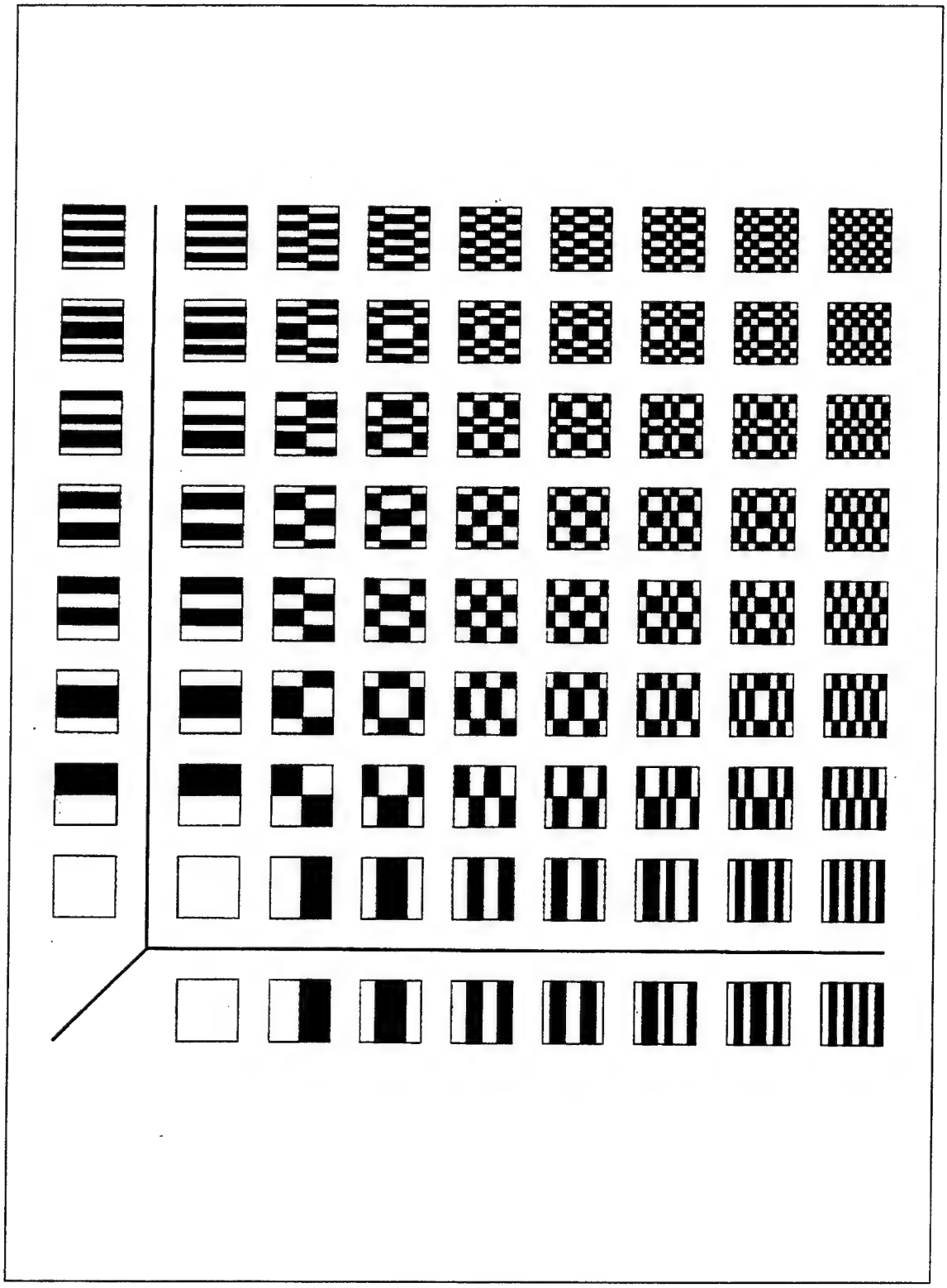

Fig. 2. Walsh function masks

properties of the Walsh basis functions themselves.. Other behaviors are not predictable, and have been explicitly simulated in numerical experiments as part of this research. One type of behavior that is predictable is how the spectra will change with contrast reversal (light-on-dark image complemented to a dark-on-light image). Suppose that the irradiances for a given scene range from 0 to E_{max} . The sequence of spectral samples will be

$$\Phi_n = \frac{1}{N}\sum_{i=0}^{N-1} E(x_i, y_i) wal(n, x_i, y_i), \qquad (8)$$

as before.

If scene contrast is complemented, such that black and white are reversed, a new set of spectral samples would appear

$$\Phi_n' = \frac{1}{N}\sum_{i=0}^{N-1} [E_{\max} - E(x_i, y_i)] wal(n, x_i, y_i)$$

$$= \frac{1}{N}\sum_{i=0}^{N-1} E_{\max} wal(n, x_i, y_i) - \frac{1}{N}\sum_{i=0}^{N-1} E(x_i y_i) wal(n, x_i, y_i)$$

$$= E_{\max} wal(0, x_i, y_i) - \Phi_n . \qquad (9)$$

Thus, the prediction from mathematical indicators are that the spectrum of the complemented image will be the negative of the original spectrum, plus a large spike at zero sequency due to the E_{max} term.

The effects of image scale changes on the resulting spectra can be approximated, but not predicted exactly. If an original image E(x) is magnified to become E(mx), the new spectrum would be

$$\Phi_n'' = \frac{1}{N}\sum_{i=0}^{N-1} E(mx_i) wal(n, x_i). \qquad (10)$$

At this point, it may seem that a change of variable to derive a simple transform scaling theorem as in Fourier analysis would be appropriate (Bracewell, 1965). But, that would not necessarily be valid mathematically. It would yield

$$\Phi_n'' \approx \frac{1}{N} \sum_{i=0}^{N-1} E(x_i) wal(n, \tfrac{x_i}{m}). \qquad (11)$$

Interpretation of this in terms of Φ_n is difficult. The difficulty arises from the strange, self similar (wavelet) behavior of the Walsh functions at different scales (Harmuth, 1977; Beauchamp, 1984). Generally, wal(j,x) and wal(j,x/m) are simply related only if m is an integer power of two. We can only assert that Equation (11) is approximately true for an arbitrary choice of m, so that magnification (or reduction) of an image will result in an approximately corresponding shrinkage (or expansion) of its sequency spectrum scale. If the scale change is an integer power of two, the relationship will be exact.

Reflection of an image about a bisector produces changes in the spatial sequency spectrum that are predictable. Walsh functions do exhibit some spatial symmetry that allows the effects of reflection to be calculated. For even n, wal(n,x) has even parity about the bisection of its domain. For odd n, wal(n,x) has odd parity. Any 1-D image, E(x), will consist of a sum of spatially even and odd parts, $E_e(x)$ and $E_0(x)$ (with the origin of the x axis at the bisector), such that

$$E_e = \tfrac{1}{2}[E(x) + E(-x)], \text{ and}$$

$$E_o = \tfrac{1}{2}[E(x) - E(-x)]. \qquad (12)$$

Its resulting spatial sequency spectrum would then be

$$\Phi_n = \frac{1}{N} \sum_{i=0}^{N-1} E(x_i) wal(n, x_i)$$

$$= \frac{1}{N} \sum_{i=0(even)}^{N-2} E_e(x_i) wal(n, x_i) + \frac{1}{N} \sum_{i=1(odd)}^{N-1} E_o(x_i) wal(n, x_i). \qquad (13)$$

The irradiance distribution of the reflected image is calculated by making the transformation x $\rightarrow$ -x. Thus, the reflected image's spatial sequency spectrum should be

$$\Phi_n''' = \frac{1}{N} \sum_{i=0(even)}^{N-2} E_e(-x_i) wal(n, -x_i) + \frac{1}{N} \sum_{i=1(odd)}^{N-1} E_o(-x_i) wal(n, -x_i)$$

$$= \frac{1}{N} \sum_{i=0(even)}^{N-2} E_e(x_i) wal(n, x_i) + \frac{1}{N} \sum_{i=1(odd)}^{N-1} (-1) E_o(x_i)(-1) wal(n, x_i)$$

$$= \frac{1}{N} \sum_{i=0(even)}^{N-2} E_e(x_i) wal(n, x_i) + \frac{1}{N} \sum_{i=1(odd)}^{N-1} E_o(x_i) wal(n, x_i)$$

$$= \Phi_n. \qquad (14)$$

Therefore, we predict that the spatial sequency spectrum will be invariant with respect to target reflection about the image bisector.

Finally, we can make no detailed predictions about behavior resulting from spatial translation of an image, or resulting from rotation in the Cartesian coordinate system. There is no analogy in sequency theory to the phase shift theorem in Fourier analysis. We made no attempt to explore this avenue further, though there are non-Cartesian geometries for which multiplexed imaging may be used for this type of analysis, (Davis, 1994).

III. EXPERIMENTAL PROCEDURE

A. GENERAL APPROACH

1. Outline

As stated in Chapter I, the goal of this thesis research has been the determination of the feasibility of using raw (i.e. spatial sequency spectral) data stream from the multiplexed imager to do target recognition. Most of the theoretical considerations that underlie this question were discussed in Chapter II.

Rather than attack the complete question posed above, we decided to address a more constrained issue as a first step : How much unique target morphology is expressed by a pair of geometrically orthogonal spatial sequency spectra of a simple image scene? This question is not an attempt to oversimplify the general problem. The new multiplexed imaging technique being developed by Davis makes explicit use of an encoding scheme that automatically records a pair of geometrically orthogonal spatial sequency spectra. The technique then tiles the entire image plane by means of an elegant mathematical construct known as the Kronecker product (Davis, 1994; Beauchamp, 1984; and Harmuth, 1977). Thus, this more restricted thesis problem is very relevant to the more general question.

The major steps involved in attacking the problem were:

- Decide the type of image format to use and what types of targets to image. We emphasized the selection of an assortment of targets that were either simple to analyze or were of potential military significance.
- Familiarization with the TIFF standard.
- Develop software to convert a conventional 2-D TIFF image file to a set of intrinsically 1-D data files that address the thesis problem.
- Develop software to convert the 1-D data files into spatial sequency spectrum form to simulate the output of the multiplexed imager.

Each of these steps is discussed in more detail below.

2. Computer Configuration

a. Hardware

The computer used for this experiment was an MSE 486DX2-66MHz with a Nanoa Flexscan F550iW monitor, 16 MB of RAM, dual disk drives (HD 3.5" and HD 5.25"), and a 510 MB hard drive. The printer was a Hewlett Packard Laserjet IIP. The charge coupled device (CCD) camera used to capture images was an EDC-1000 with a 192 (horizontal) x 165 (vertical) or 192 x 330 (interlaced) pixel distribution manufactured by the Electrim Corporation.

b. Software

Software provided with the EDC-1000 captured images, created TIFF files and enabled preliminary viewing of all TIFF files used in the experiment. Microsoft Quick C, Microsoft C 6.0, and Microsoft Visual C++ were all used at various stages of software development. Microsoft Excel provided the means to create most of the figures included in this thesis.

B. FILE FORMAT, FILE GENERATION, AND TARGETS

1. Image File Format

Before beginning data collection, it was necessary to choose a suitable image file format. The image file format needed to be readily available, widely used, and easily understood. The hardware/software configuration (EDC-1000 package mentioned above) used for recording the initial unprocessed image data, generates image files in a variety of standard formats. After considering our unconventional processing goals and the various common formats and their properties (Lindley, 1991), we chose the TIFF format due to its

extendibility, portability, and availability. The TIFF format is somewhat complex, but it is thoroughly documented.

2. Target Selection and Initial Image Creation

We chose a variety of objects as sample targets. For testing the transforming and manipulation code, we used simple, high contrast images commonly used to test and evaluate imaging system optical resolution. These are found in Appendix B, figures B-1, B-18, B-35, and B-52. These were displayed against white posterboard and recorded as TIFF files with the EDC-1000 camera and software. Next, we selected an assortment of more complex, military-relevant targets. After some trial-and-error experimentation, we selected a plastic model tank and a metal model helicopter. Both objects were displayed against a uniformly diffuse bright background. We used white posterboard, two 100 watt lamps, and four pound test fishing line to suspend the objects. We then recorded several images of each object from different perspectives and at different scales of magnification. After acquiring each image, it was displayed to verify its quality. Nine helicopter images and sixteen tank images entered our initial portfolio. After careful examination, we pared these down to five helicopter and thirteen tank images. The helicopter images are included in Appendix C and the tank images are in Appendix D. The elimination of some of the initial tank images resulted in some discontinuities in image sequence numbers. On the first pages of Appendices B-D, are descriptions of the TIFF images and their figure numbers.

C. TIFF EDUCATION

Learning about the structure of the TIFF files created by the camera software turned out to be a time-consuming process. An excellent reference (Lindley, 1991) details the structure of TIFF files. We used this information to create programs using Microsoft Quick C 2.5, Microsoft Visual C++, and Microsoft C 5.1 to learn about the internal structure of the TIFF image files. First, we wrote a program to extract image parameters

from the TIFF files. Next, we created a series of programs to extract and to display the images, to put them into an array in computer memory, and to display the image from the array. The memory requirements for the last step presented numerous roadblocks, and we never completed a fully working program to completely display a 2-D image. This did not present a significant obstacle, since only the user-processed images were of interest for the project. The ECM software proved adequate as a basic TIFF image display platform. From this series of programs, we were able to learn enough about the TIFF files to make some decisions regarding the overall project and to start writing the program required to process the data needed to conduct the core phases of the research.

D. DATA PROCESSING

A primary question of this thesis research was whether the 1-D spatial sequency spectra of an image contains sufficient information to permit straightforward identification of an object. We also sought answers to three subsidiary questions. First, what differences are there in comparing dark images against light backgrounds versus light images against dark backgrounds using spatial sequency spectra? Second, is there an obvious correlation between the spectra of a given object and its mirror image? Third, is there a simple scaling behavior in the spatial sequency spectra that follows the predictions of Chapter II?

The simple dark-on-light images in the TIFF files were processed in a straightforward fashion to address all of the above subsidiary questions. The answer to the more basic question would follow from the analysis of the others. The first subsidiary question was addressed by processing an image and its complement. Since the image was recorded in 8-bit binary format, creation of a complementary image was done with a pixel-by-pixel subtraction from 255 (Lindley, 1991), just as was explained in section II.C., Equation (9). The second question was addressed by having the software perform a reflection symmetry operation on the original image array. Image data files that were to retain horizontal information were reflected about a vertical bisector (column 96) retention

of vertical information required reflection about a horizontal bisector (row 165). This reflection was discussed previously in Section II.C., Equations (12) through (14). Images of the tank taken at different distances, but identical perspectives provided the needed data to answer the third (magnification scale) question, which earlier had been illustrated with Equations (10) and (11).

The processing software was written in ANSI standard C and is included in Appendix A. It was not designed for universal application, and is configured only for 192x330 image arrays. The program's operational sequence is:

- Open the TIFF file.
- Complement the image (if requested).
- Reflect the image (if requested).
- "Squash" the image, either horizontally or vertically (as directed).
- Write the squashed image to a new file.
- Perform the fast Walsh transform of the processed image to produce the spatial sequency spectrum.
- Write the spectrum data to a new file.

Image "squashing" is the creation of a 1-D image from a 2-D image. If we wanted to retain the horizontal spatial information, the 2-D input image had each of its rows averaged together column-by-column, producing a squashed 1-D image. The effect is similar to what you would expect if the object had been compressed vertically in a giant hydraulic press. For the retention of vertical information, compression was along the horizontal direction, on a row-by-row basis. Mathematically, the squashed versions of the images are obtained as follows:

$$f_{x_i} = \sum_{j=0}^{N} g(x_i, y_j), \text{ preserving horizontal information} \qquad (15)$$

and

$$f_{y_j} = \sum_{i=0}^{M} g(x_i, y_j), \text{ preserving vertical information} \qquad (16)$$

where,

$$f_{x_i,y_j} = g(x_i, y_j) \text{ with i = 0,..,N and j = 0, ..,M are the image} \qquad (17)$$

data of each pixel.

The final operation performed on the data for the spectrum files was needed to fulfill a requirement of Walsh functions. Complete Walsh basis sets require an integer power of two number of data samples. Our squashed 1-D data sets had either 192 or 330 samples. The data sets were padded with zeroes prior to Walsh transforming, resulting in either 256 or 512 samples. We did not apodize the data during this padding process, which resulted in some of the spectra coming out noisy-looking. This phenomenon will be discussed in the following chapter, as appropriate.

Since there were three questions (complementing, reflecting, and squashing direction) with two options each, there were eight variations of data files possible. Each variation produced two (transformed and squashed) data file types. Thus, the 22 TIFF files resulted in 352 data files. I decided on a mainly mnemonic system for naming the data files.

The data files have names of the form LNNLLL.txt, where L = letter and N = number. The first letter refers to **series**, either A (Air Force resolution pattern), R (general resolution pattern), T (tank), or H (helicopter). The numbers refer to the image's **sequence number** within the series, corresponding with the original TIFF files. The second letter is **processing category**, q (squashed) or p (Walsh transformed). The third letter denotes the **spatial information preservation direction**, h (horizontal) or v (vertical). The last letter denotes processing details as to whether the files was **complemented or reflected**, these are denoted by c, r, b (both), or n (neither). For example, T11phr.txt would be the 11th tank image that had been Walsh transformed horizontally after being reflected. I added the .txt file extension, because importing them into Excel as ASCII text files turned out to be the most convenient way to display them.

E. DATA DISPLAY

We wanted to display the contents of the files in as simple and meaningful a way as possible. A simple point line graph seemed to be the best choice. Since I was more familiar with Microsoft Excel for producing graphs than other software packages, that was my first choice. After much frustration, I finally arrived at a suitable figure format for displaying the data files. Once we decided on the proper figure formats and I created templates , figure creation went smoothly. While making the figures, I decided to keep the scaling as uniform as possible for convenient comparison. I set the vertical scale of the Walsh spectra figures at -2000 to 2000, but noticed the loss of data on some files. In order to keep as much detail as possible, yet also minimize data loss at the lower sequencies, I compromised and accepted two scales instead of one. Thus, some spectra figures have vertical scales of -5000 to 5000. I also chose to keep the vertical scales of the squashed data figures beginning at zero with the software automatically scaling the graph as appropriate. The result of this is that the figures displaying normal and reflected images are scaled differently than the figures displaying complemented and complemented-reflected images.

Three of the Walsh transformed data files turned out to be corrupted in some irretrievable manner. We attributed it to some machine numerical error or software bug. Due to a shortage of time, this problem was not pursued further. The three figures appearing in the appendices in their place are from an earlier chart production run with less flawed data files and are close approximations to what the graphs should look like. They are figures B-7 (A1phr), B-9 (A1phb), and D-7 (T1phr).

IV. RESULTS AND DISCUSSION

A. GENERAL COMMENTS

Once the graphs were all created, printed, and organized, the next task was to examine them to either verify or refute our hypotheses. We compared the spectra by overlaying them and holding them up to a strong light, and then estimating their degree of correlation, thus the percentages reported are the product of this visual inspection. Since the scope of this research was a first-order feasibility assessment we relied upon human observation and interpretation, leaving the more accurate computer cross-correlation of the spatial sequency spectra for follow-on work.

B. RESOLUTION TEST PATTERNS

Our examinations began with the relatively simple resolution charts. The TIFF images of these are included in Appendix B. The most basic of these is A2, an enlargement of one portion of a common US. Air Force resolution chart consisting of six horizontal bars. We first looked at the horizontally squashed figure, Fig. B-19. This figure looked exactly as we predicted, confirming that the horizontal squashing software seemed to work as expected. The spatial sequency spectrum, Fig. B-20, also met with predictions, depicting most activity at low sequency. We observed an interesting set of shapes right around the 32 sequency point, with a spiked dip followed by a spiked hump. The complemented horizontally squashed figure, Fig. B-21, again looked exactly as expected, confirming that the complementing portion of the software apparently functioned as designed. The next figure, Fig. B-22, was an exciting discovery. It looked like a mirror image of Fig. B-20 reflected about the zero amplitude axis! By turning the paper over and overlaying it on Fig. B-20, we saw that it was an exact match, except that the uncomplemented image had an extra spike at zero sequency! This verified the prediction of Section II.C. The horizontally squashed reflected image, Fig. B-23, was a mirror image

of Fig. B-19, reflected about its vertical bisector, again confirming that the manipulation software was working properly. The spatial sequency spectra, Fig. B-24, showed some correlation with Fig. B-20. When overlaid, we estimated (by eye) the correlation to be about 50%. This difference between the two spectra did not agree with predictions in II.C above that the spectra would be invariant with reflection about the image bisector. This lack of complete correlation requires further mathematical analysis to determine the degree of correlation with more precision than simple human observation is capable of. Another interesting observation was the lowering of the central axis of the spectra from the zero amplitude area to an amplitude of approximately -400. A comparison with the spatial sequency spectra of the complemented-reflected image again demonstrated an exact match except for a zero sequency spike.

Examination of the vertically squashed images, spectra, and permutations for A2, yielded similar results to the horizontal sequency figures, except that the uncomplemented figure and the reflected figure seemed to have a lot of noise added to the spectra. This phenomenon was mentioned in III. D. above. The noise is a predictable consequence of the abrupt edge and zero padding of the image data. It could be suppressed by the conventional techniques of apodization (Hecht, 1987; Bracewell, 1965). In any event, the problem is a computational artifact and will not appear in the raw data from the multispectral imaging system. The lines of the complemented and complemented-reflected spectra are clearly present in the noisy looking figures, as expected. By flipping over Fig. B-32 and overlaying it on Fig. B-28, we estimated more correlation between the spectra of the reflected image and the non reflected image than there appeared to be for the horizontal sequency case. This was good news, but without detailed numerical analysis, we cannot assign a real figure of merit to the result. Overlaying the original spectra and the complemented-reflected spectra also showed a good deal of correlation, but once again, it was difficult to estimate the amount.

A similar study of the remaining resolution test pattern images, A1, R1, and R2 yielded results similar to those of A2. In some instances, the central axis offset between

the normal image spectra and the reflected image spectra was not as large as the offset observed in A2, but there did appear to always be an offset and it was always in the negative direction. For image R1, the comparison between the normal vertical spectra, Fig. B-45, and its reflected image counterpart, Fig. B-49, clearly showed that even though the activity in the spectra was different, the location of that activity within the spectra was very similar.

C. HELICOPTERS

The resolution test pattern spectra study gave us some ideas about how to proceed with the rest of the spectra examination. Since the complementing of the images did yield predictable spectra, we chose to use the less noisy members of each pair of complements for our next stage of research. This reduced our comparisons by half. The earlier test pattern study also gave us some indications of what to look for when overlaying spectra. Since we had already compared spectra within sets (groups of spectra resulting from the permutations of a single TIFF image) we would largely confine our activity at this point to comparing spectra from different parent images, with occasional spot checking within image sets to confirm that the observations noted in IV. B. above were still valid.

To compare spectra, we overlaid them as before and used three criteria. We looked for how well the spikes in the two spectra matched in terms of direction (up or down), amplitude, and location.

We compared the spectra of the five helicopter images to each other in a variety of ways. We did always compare within a processing direction (horizontal sequencies to horizontal sequencies, vertical to vertical). First, we compared all the complemented image spectra to each other . Then we compared the complemented-reflected image spectra to each other. Next, we compared the complemented spectra to the complemented-reflected spectra. We estimated high correlation (greater than 75%) between H4 (Fig. C-52) and H5 (Fig. C-69) no matter how they were compared. This was

not surprising as the images are very similar. H1 (Fig. C-1) and H2 (Fig. C-18) showed medium correlation (estimated between 50 and 75%) with each other when complemented images were compared, but low correlation when the complemented image spectra of H1 was compared with the complemented-reflected image spectra of H2. H1 and H3 (Fig. C-35) agreed more than H1 and H2, as expected. Sometimes the correlation between the complemented image spectra and the complemented-reflected image spectra could be improved by flipping one of them over, but this was not always true. The results of these comparisons indicated that the more similar the parent images, the more similar the resulting spatial sequency spectra. It also was evident that reflecting the image did degrade correlation as observed earlier in the study of the resolution test patterns.

D. TANKS

The next step in this research involved comparing the tank image spectra to each other as the helicopter image spectra had been done and then comparing the helicopter image spectra with the tank image spectra. Besides the chance to compare the spectra of very different objects, the tank images presented a chance to test the hypothesis regarding the effects of image scaling on the resulting spatial sequency spectra. Figures D-1 (T1), D-171 (T13), D-188 (T14), and D-205 (T15) are virtually identical except in scale (magnification).

Comparisons of the tank spectra with each other yielded the same results as above. Similar images had similar spatial sequency spectra. T3 (Fig. D-18), T4 (Fig, D-35) and T10 (Fig. D-137) had similar, but not identical spectra, as did other images that were similar to each other.

Comparisons of the tank image spectra with the helicopter image spectra was confined to the comparison of tank-helicopter pairs where the parent images most closely resembled each other. Thus, T1 was compared with H1, T3 with H2, T11 (Fig. D-154) with H4, etc. These comparisons yielded the satisfying results that correlations between

the spatial sequency spectra of the tanks and helicopters were uniformly low to very low (estimated 49% and below).

Comparisons of the tanks at different scales did indicate that the predictions of III.C. were correct. A scale difference of approximately two and a half, between T1 and T15, did seem to result in a corresponding spreading out of spikes on their respective spatial sequency spectra.

E. SQUASHED IMAGE STUDIES

As an adjunct to the more interesting and potentially more important study of the spatial sequency spectra, we also examined and compared the squashed 1-D images for potential significance. After this study, it was obvious that given a horizontal-vertical 1-D pair of images, the object and its orientation in the parent image could be quickly deduced. To further confirm this, I had an assistant select twenty pairs of squashed, complemented image figures (a pair consisted of one graph of horizontal information and one graph of vertical information of an object), from the complete set of 176. The assistant hid the labels of the graphs and I attempted to identify the original TIFF file images from the graphs. I was able to correctly identify the object 95% of the time and the orientation of the object 45% of the time with either the horizontal or vertical information. With both horizontal and vertical information, I correctly identified orientation 85% of the time.

V. CONCLUSIONS AND RECOMMENDATIONS

A. CONCLUSIONS

The results of this research indicate that the use of spatial sequency spectra for automatic target recognition without further processing shows promise, but requires further study to validate or to refute its usefulness. Suggestions for carrying out these studies are found below.

The ease of identifying the target object with one set of squashed data is promising and indicates that the multiplexed imaging device can achieve target recognition with minimal processing of the raw data. The ability to recognize images with the squashed data in this experiment helps validates the possible usefulness of such an arrangement. A 1-D array should save significant bandwidth and storage space over a 2-D array.

B. RECOMMENDATIONS

We recommend further research to determine the answers to the following questions:

- How quantitative are the matches between the spatial sequency spectra of different targets? This is the key question that must be answered to determine if a spatial sequency database can be used for automated target recognition. The answer to this question will require a detailed, quantitative correlation analysis of spectra from a variety of objects (tanks, helicopters, planes, trucks, buildings, etc.).
- What are the fundamental limits on target spectral discrimination set by both temporal and spatial noise?
- What limitations on the recognition of military targets are imposed by nonuniform backgrounds and commonly used camouflage techniques?
- How much additional information will be provided by 2-D spatial sequency spectra over the 1-D spectra studied in this research?

Additional research, built upon the work described here, should be able to address these questions.

APPENDIX A: DATA PRODUCING PROGRAMS

1. TIFF FILE MANIPULATION PROGRAM

```
/*****************************************/
/* Read and manipulate TIFF files        */
/* Language:  ANSI  C                    */
/* Source file: filmkr.c                 */
/* Programmers: D. S. Davis & J. H. Davis */
/* Revision date: 22 Nov 94              */
/*****************************************/

#include <stdio.h>

#define FILE_NAME_LENGTH 24
#define DATA_ARRAY_LENGTH 512
#define TIFF_FILE_HEADER_LENGTH 150
#define TIFF_IMAGE_COLUMNS 192
#define TIFF_IMAGE_ROWS 330

void fast_walsh_transform (int, float *, int);

void main (void)
    { char image_file_name[FILE_NAME_LENGTH],
      squashed_image_file_name[FILE_NAME_LENGTH],
      spectrum_file_name[FILE_NAME_LENGTH], horiz_vert_mode,
      complement, reflect, scale;
     FILE * fp;
     int i, squashed_image_length, column, row, j, spectrum_length;
     unsigned char pixel;
     float data[DATA_ARRAY_LENGTH], scratch;
     printf ("\n\n\n\n\rEnter TIFF image file name, with path: ");
     gets (image_file_name);
     printf ("\n\rEnter squashed image file name, with path: ");
     gets (squashed_image_file_name);
     printf ("\n\rEnter output Walsh spectrum file name, with path: ");
     gets (spectrum_file_name);
     printf ("\n\rRetain horizontal or vertical sequencies ");
     printf ("(h or v) after squashing image? ");
     horiz_vert_mode = getchar ();
     getchar ();
```

```
 printf ("\n\rComplement black and white (y or n)? ");
 complement = getchar ();
 getchar ();
 printf ("\n\rReflect image (y or n)? ");
 reflect = getchar ();
 getchar ();
 printf ("\n\n\r");
 fp = fopen (image_file_name, "rb");
 for (i = 0; i < TIFF_FILE_HEADER_LENGTH; i ++)
  fread (& pixel, 1, 1, fp);
 if (horiz_vert_mode == 'h')
  { squashed_image_length = TIFF_IMAGE_COLUMNS;
   for (column = 0; column < TIFF_IMAGE_COLUMNS; column ++)
       data[column] = 0.0;
   for (row = 0; row < TIFF_IMAGE_ROWS; row ++)
       for (column = 0; column < TIFF_IMAGE_COLUMNS; column ++)
        { fread (& pixel, 1, 1, fp);
         if (complement == 'y')
          pixel = 255 - pixel;
         data[column] += (float) pixel / TIFF_IMAGE_ROWS; } }
 else if (horiz_vert_mode == 'v')
  { squashed_image_length = TIFF_IMAGE_ROWS;
   for (row = 0; row < TIFF_IMAGE_ROWS; row ++)
       { data[row] = 0.0;
        for (column = 0; column < TIFF_IMAGE_COLUMNS; column ++)
         { fread (& pixel, 1, 1, fp);
          if (complement == 'y')
              pixel = 255 - pixel;
          data[row] += (float) pixel; }
       data[row] /= TIFF_IMAGE_COLUMNS; } }
 fclose (fp);
 if (reflect == 'y')
  for (i = 0; i < squashed_image_length / 2; i ++)
   { j = squashed_image_length - i;
       scratch = data[i];
       data[i] = data[j];
       data[j] = scratch; }
 fp = fopen (squashed_image_file_name, "w");
 for (i = 0; i < squashed_image_length; i ++)
  fprintf (fp, "%f\n", data[i]);
 fclose (fp);
 spectrum_length = 1;
 while (spectrum_length < squashed_image_length)
```

```
  spectrum_length *= 2;
 for ( i = squashed_image_length; i < spectrum_length; i ++)
  data[i] = 0.0;
 fast_walsh_transform (spectrum_length, data, 0);
 fp = fopen (spectrum_file_name, "w");
 for (i = 0; i < spectrum_length; i ++)
  fprintf (fp, "%f\n", i, data[i]);
 fclose (fp);
 printf ("\n\n\n\n\r");
 return; }
```

2. WALSH TRANSFORM SUBPROGRAM

```
/*****************************************/
/* Walsh transform TIFF files            */
/* Language:  ANSI  C                    */
 /* Source file: walshxfm.c              */
 /* Programmers: D. S. Davis             */
 /* Revision date: 2 Nov 94              */
 /*****************************************/

  #include <stdio.h>

   void fast_walsh_transform (int, float *, int);
   int log2 (int);
   void bit_reversal_sort (int, int, float *);
   void decimation_in_sequency (int, int, float *);
   void scale_inverse_transform (int, float *);

   void fast_walsh_transform (int arraysize, float * data, int inverse)
       { int logbase2;
        logbase2 = log2 (arraysize);
        bit_reversal_sort (arraysize, logbase2, data);
        decimation_in_sequency (arraysize, logbase2, data);
        if (inverse)
          scale_inverse_transform (arraysize, data);
        return; }

   int log2 (int x)
       { int log;
        log = 0;
        while (x >>= 1)
```

```
    log ++;
  return log; }

void bit_reversal_sort (int arraysize, int logbase2, float * data)
  { int directindex, indexbuffer, reversedindex, bitnumber;
   float * datum1, * datum2, scratch;
   for (directindex = 0; directindex < arraysize; directindex ++)
    { indexbuffer = directindex;
     reversedindex = 0;
     for (bitnumber = 0; bitnumber < logbase2; bitnumber ++)
        { reversedindex <<= 1;
         reversedindex |= indexbuffer & 1;
         indexbuffer >>= 1; }
     if (directindex < reversedindex)
        { datum1 = data + directindex;
         datum2 = data + reversedindex;
         scratch = * datum1;
         * datum1 = * datum2;
         * datum2 = scratch; }}
  return; }

void decimation_in_sequency (int arraysize, int logbase2, float * data)
  { int blocksize, stage, toggle, node1start, node2start, node2, node1;
   float * datum1, * datum2, scratch;
   blocksize = arraysize / 2;
   for (stage = 0; stage < logbase2; stage ++)
    { toggle = 0;
     node1start = 0;
     while (node1start < arraysize)
        { node2start = node1start + blocksize;
         node2 = node2start;
         if (toggle)
          for (node1 = node1start; node1 < node2start; node1 ++)
           { datum1 = data + node1;
             datum2 = data + node2;
             printf ("\n\r%d   %d   %d   %f   %f", stage,
              node1, node2, * datum1, * datum2);
             scratch = * datum1;
             * datum1 -= * datum2;
             * datum2 += scratch;
             node2 ++; }
        else
         for (node1 = node1start; node1 < node2start; node1 ++)
```

```
                { datum1 = data + node1;
                    datum2 = data + node2;
                    printf ("\n\r%d   %d   %d   %f   %f", stage,
                      node1, node2, * datum1, * datum2);
                    scratch = * datum1;
                    * datum1 += * datum2;
                    * datum2 = scratch - * datum2;
                    node2 ++; }
              toggle = ! toggle;
              node1start = node2; }
          blocksize /= 2; }
      return; }

void scale_inverse_transform (int arraysize, float * data)
    { float scalefactor;
      int index;
      scalefactor = 1.0 / arraysize;
      for (index = 0; index < arraysize; index ++)
        * (data + index) *= scalefactor;
      return; }
```

APPENDIX B: TEST PATTERNS

This is the first of the image-graph appendices. Each image is followed by the graphs of its corresponding data files and hence each image is part of a nine page packet. The first page of each packet contains the image and the following pages display the graphs, two per page. Each page has a graph of a squashed image and the resulting Walsh transform of that squashed image. Images squashed to maintain horizontal sequencies are first, followed by vertical sequencies. Each horizontal and vertical set has a normal, complemented, reflected, and combination complemented and reflected data graph.

Within this appendices the packets are:

( ) = data file prefixes corresponding to that particular image

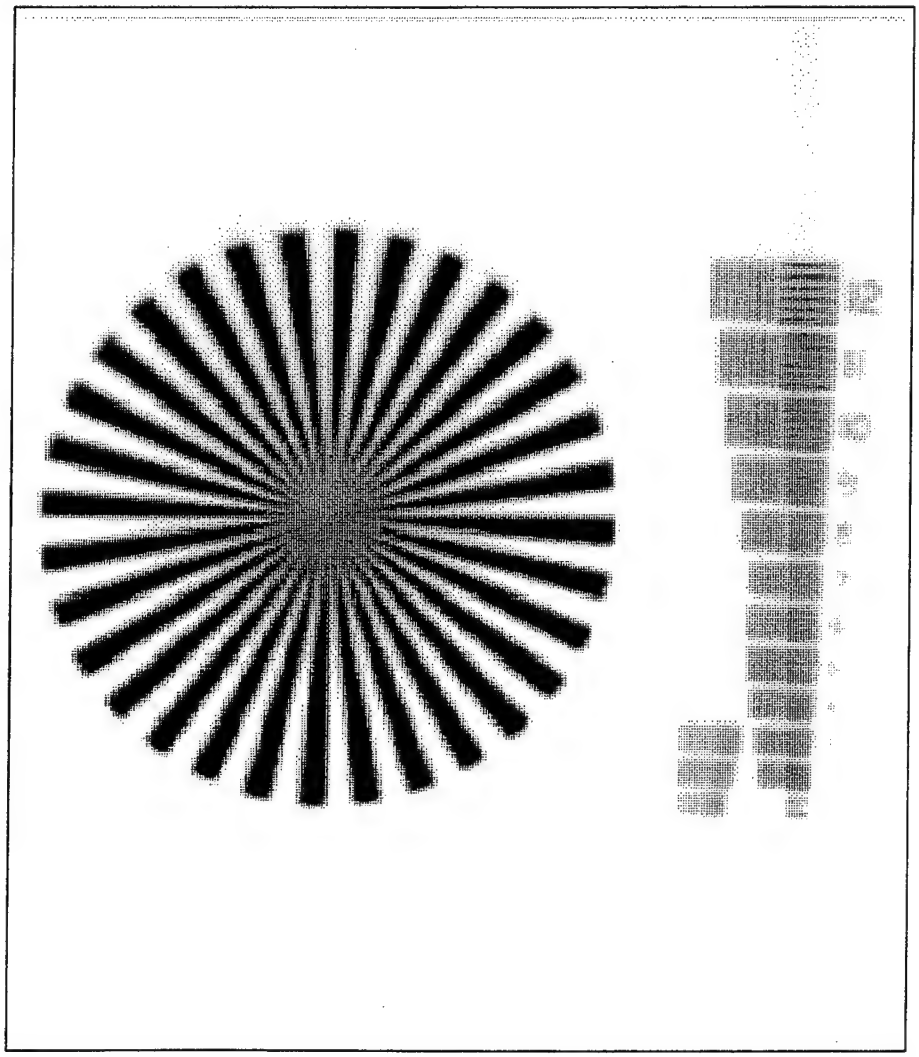

Fig. B-1. A1, an Air Force test pattern

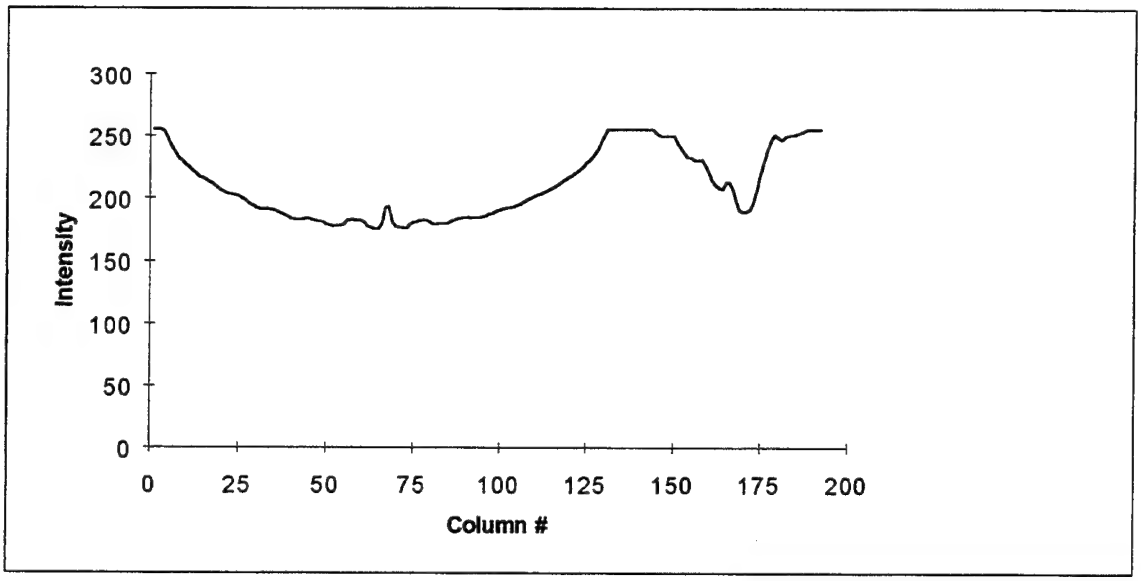

Fig. B-2. A1 squashed to preserve horizontal sequencies

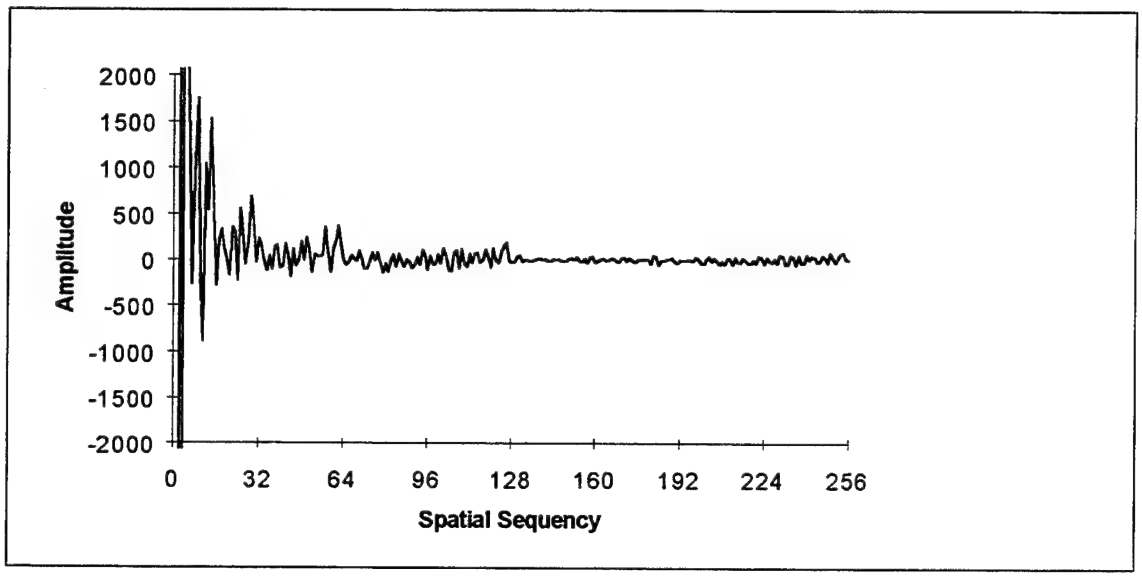

Fig. B-3. Walsh transform of Fig. B-2

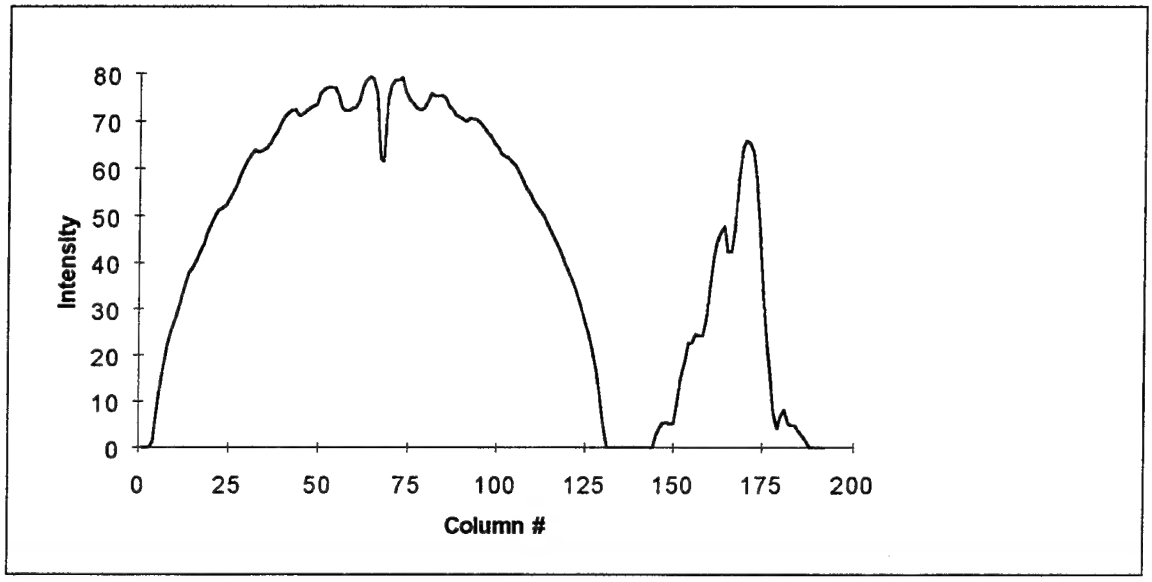

Fig. B-4. Complement of A1 squashed to preserve horizontal sequencies

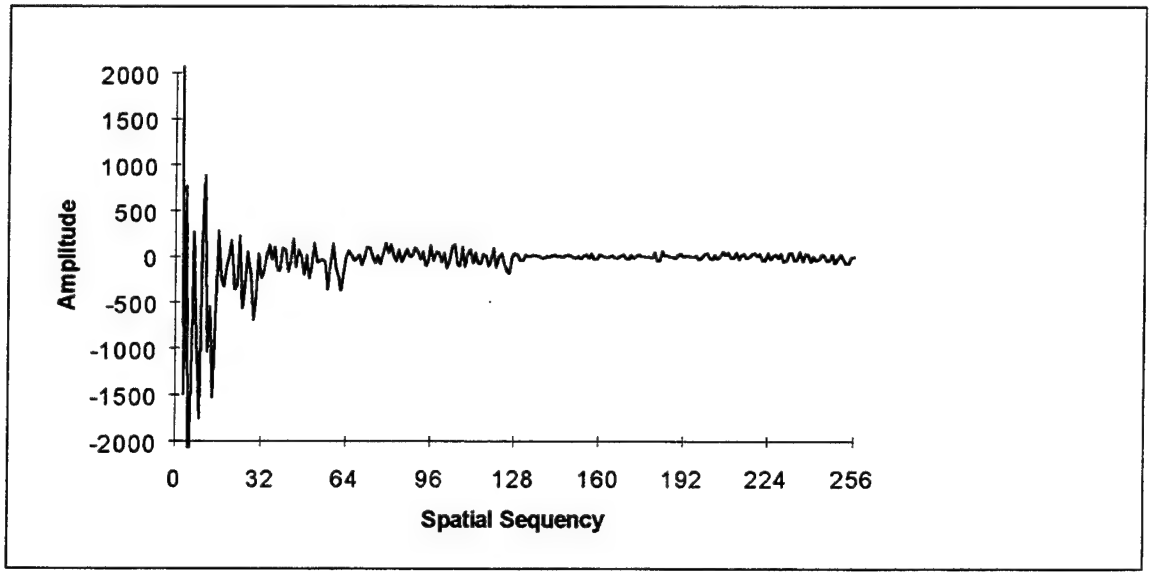

Fig. B-5. Walsh transform of Fig. B-4

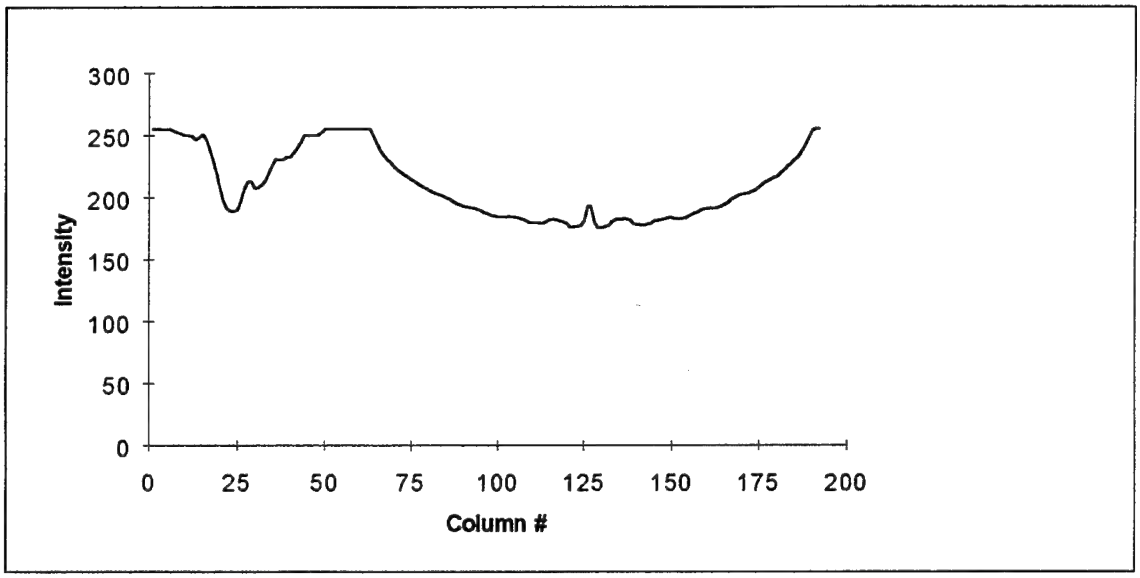

Fig. B-6. Reflection of A1 squashed to preserve horizontal sequencies

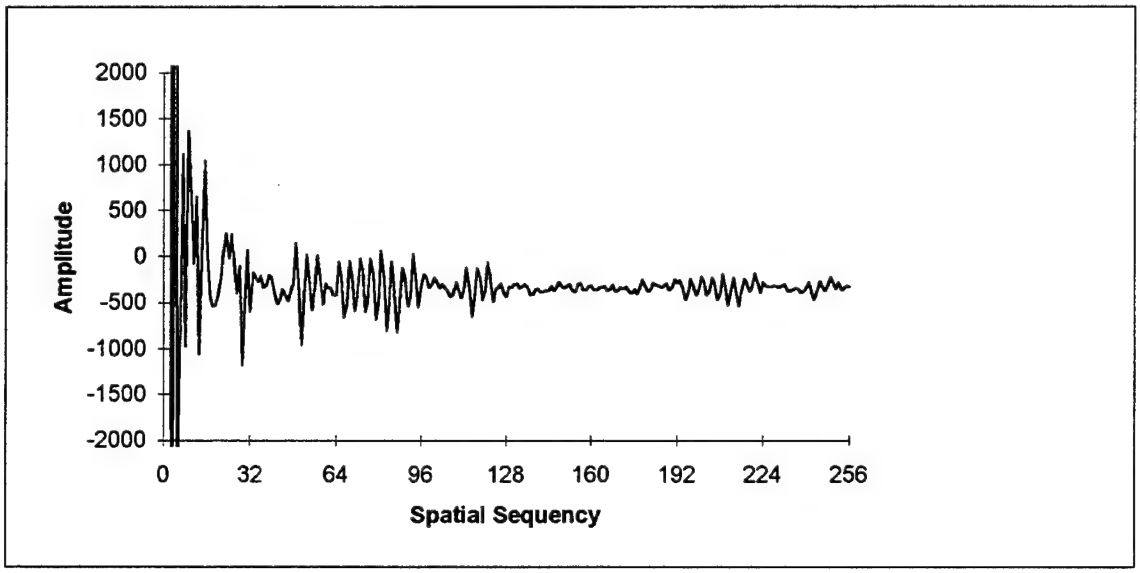

Fig. B-7. Walsh transform of Fig. B-6

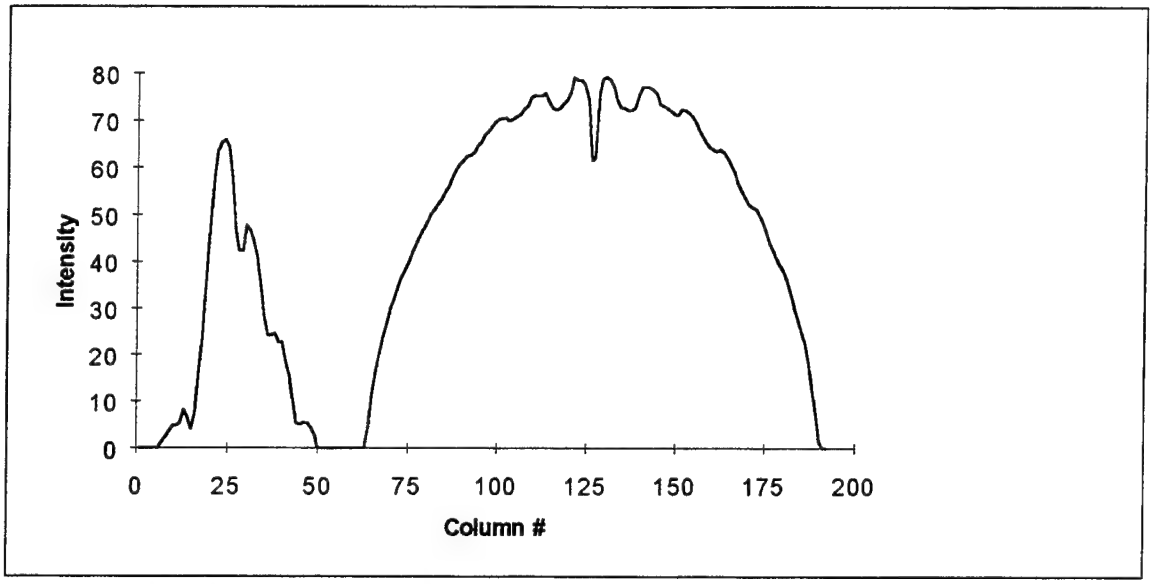

Fig. B-8. Complemented reflection of A1 squashed to preserve horizontal sequencies

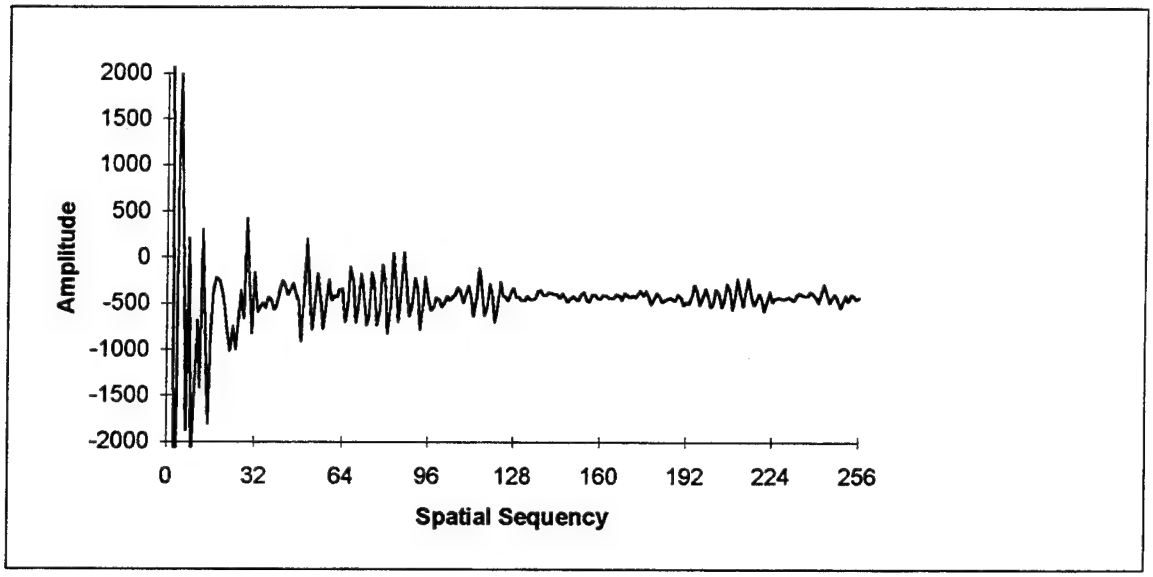

Fig. B-9. Walsh transform of Fig. B-8

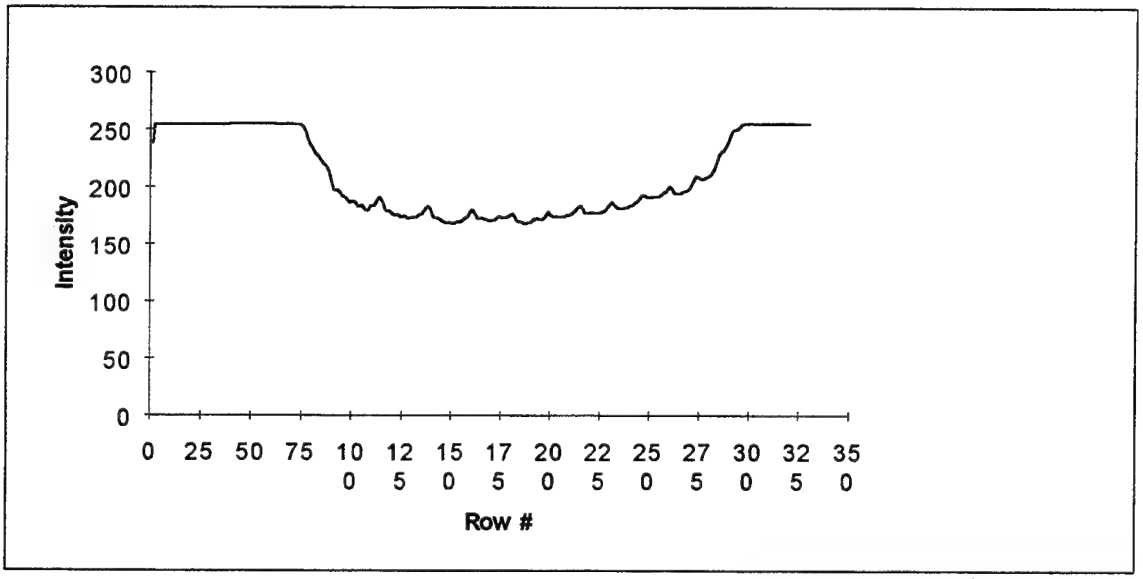

Fig. B-10. A1 squashed to preserve vertical sequencies

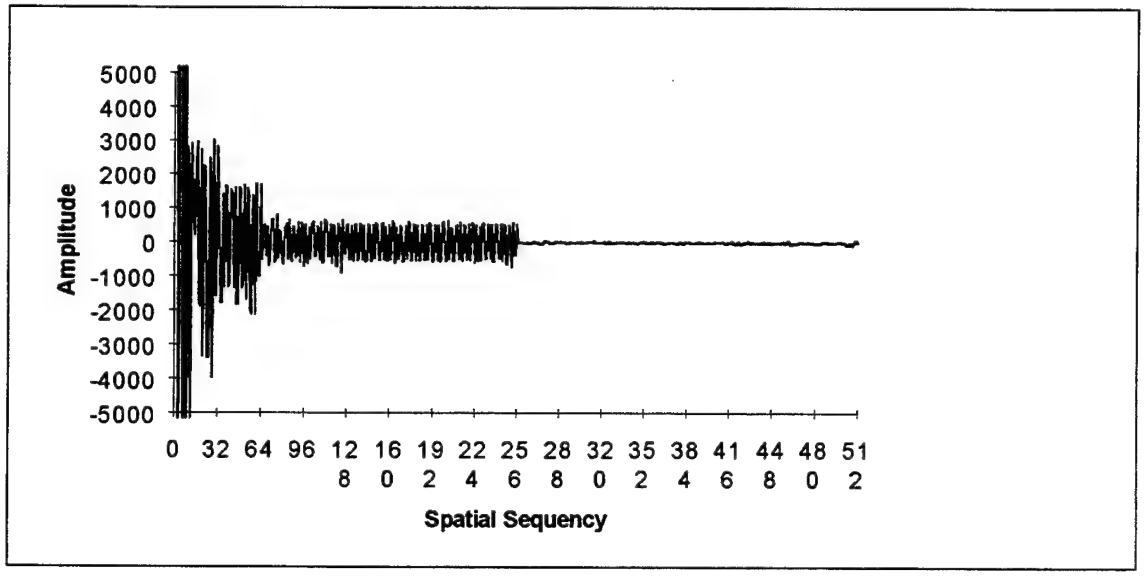

Fig. B-11. Walsh transform of Fig. B-10

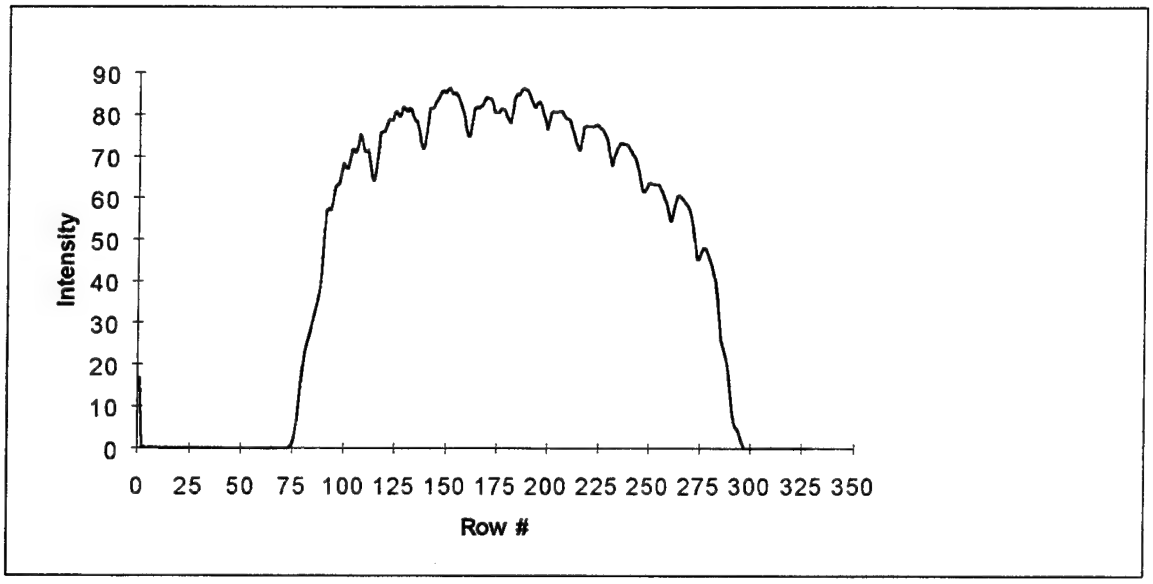

Fig. B-12. Complement of A1 squashed to preserve vertical sequencies

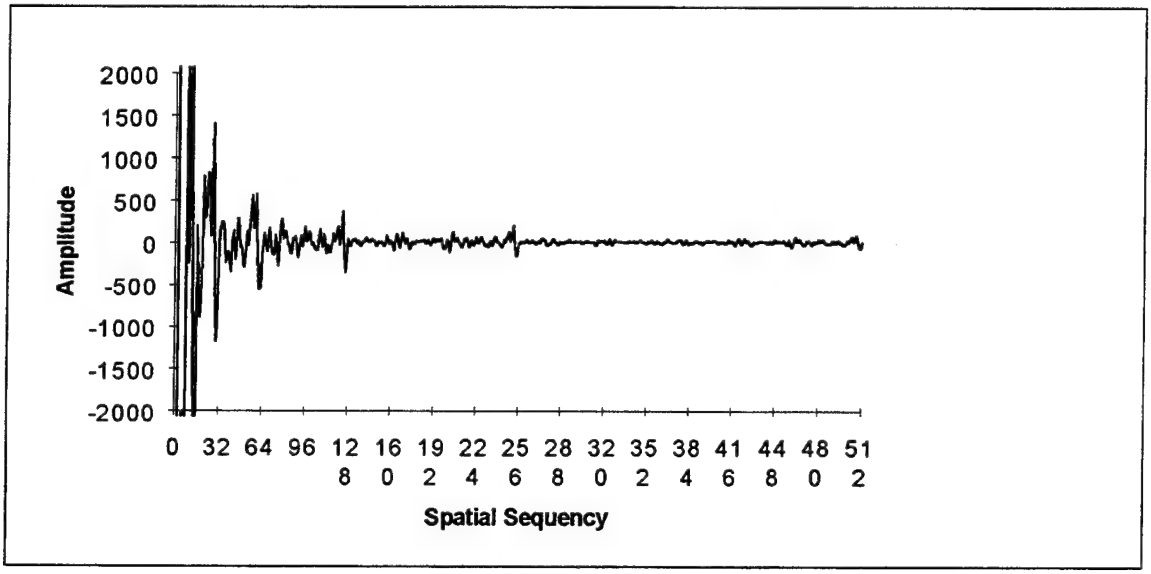

Fig. B-13. Walsh transform of Fig. B-12

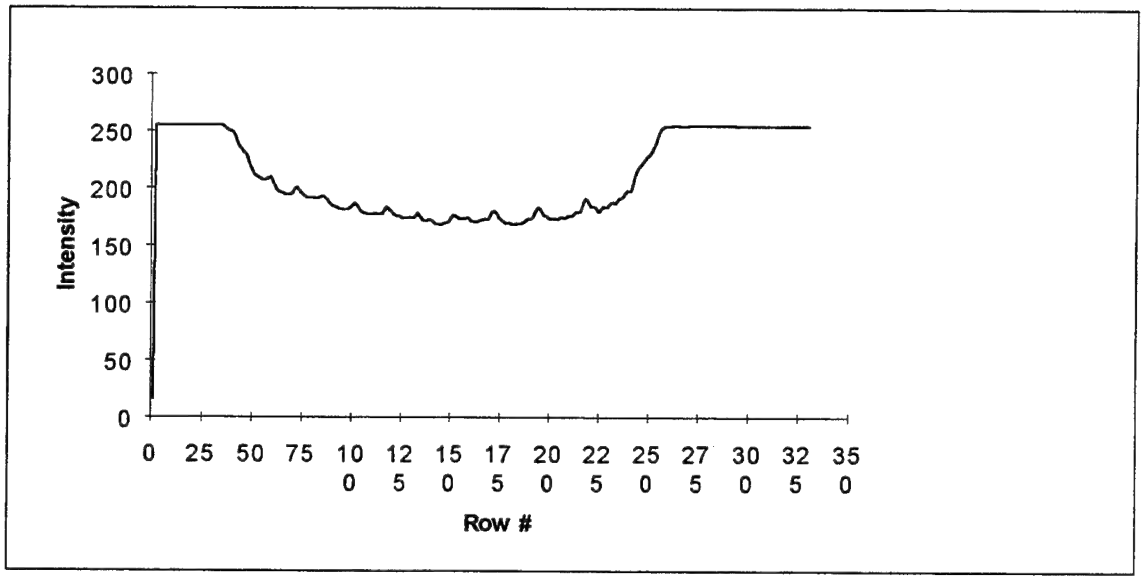

Fig. B-14. Reflection of A1 squashed to preserve vertical sequencies

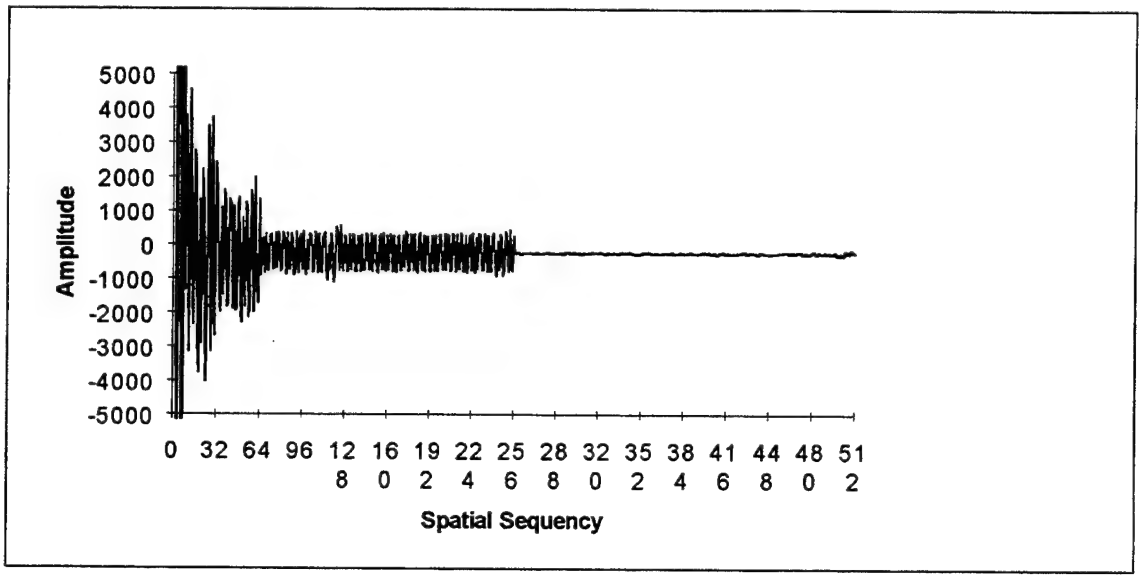

Fig. B-15. Walsh transform of Fig. B-14

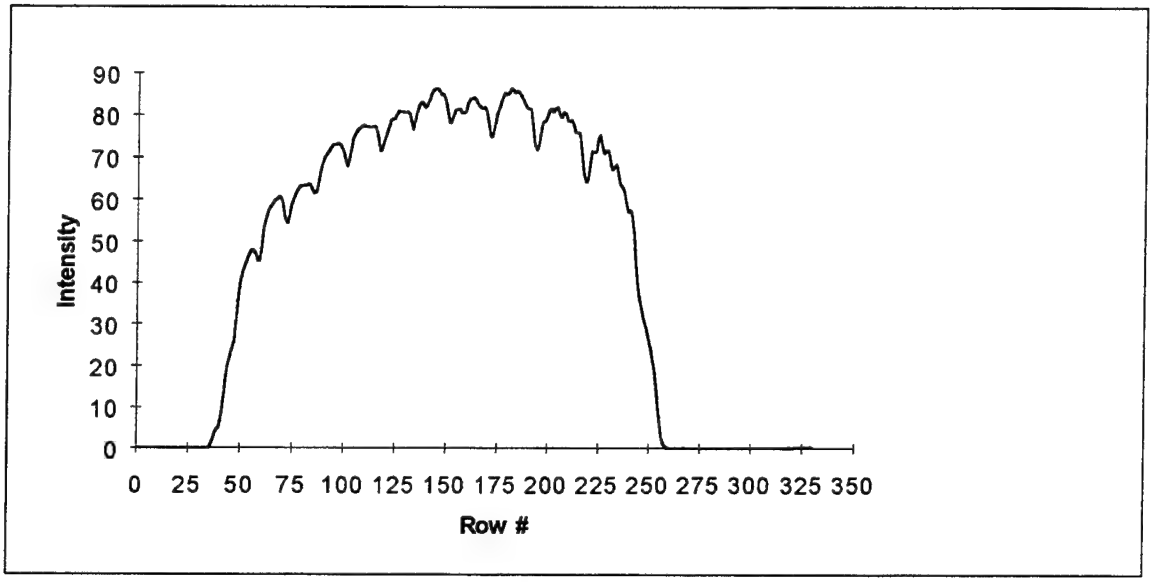

Fig. B-16. Complemented reflection of A1 squashed to preserve vertical sequencies

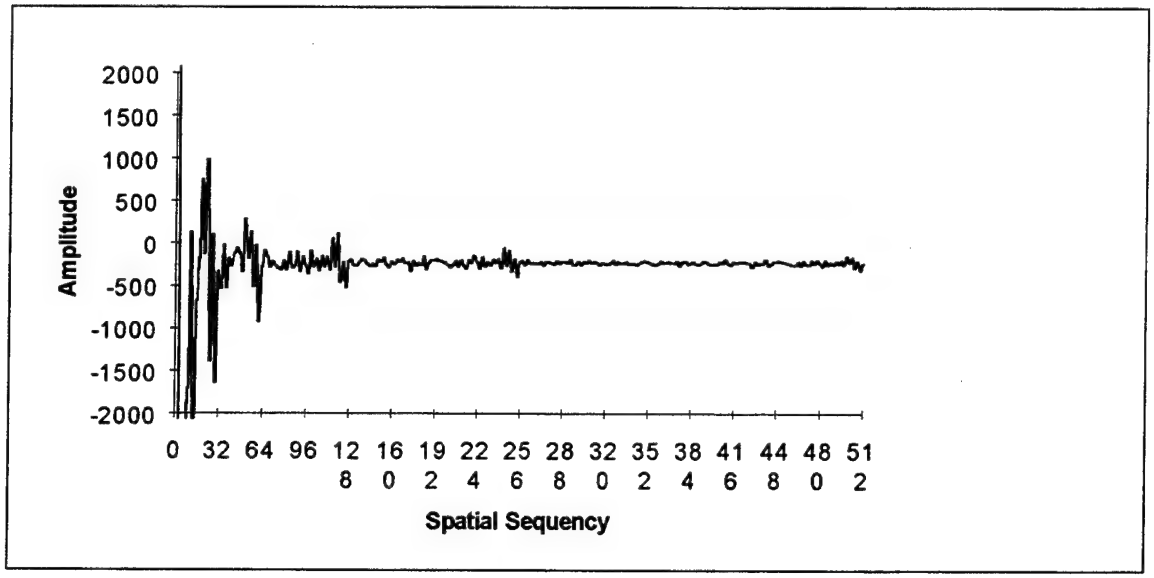

Fig. B-17. Walsh transform of Fig. B-16

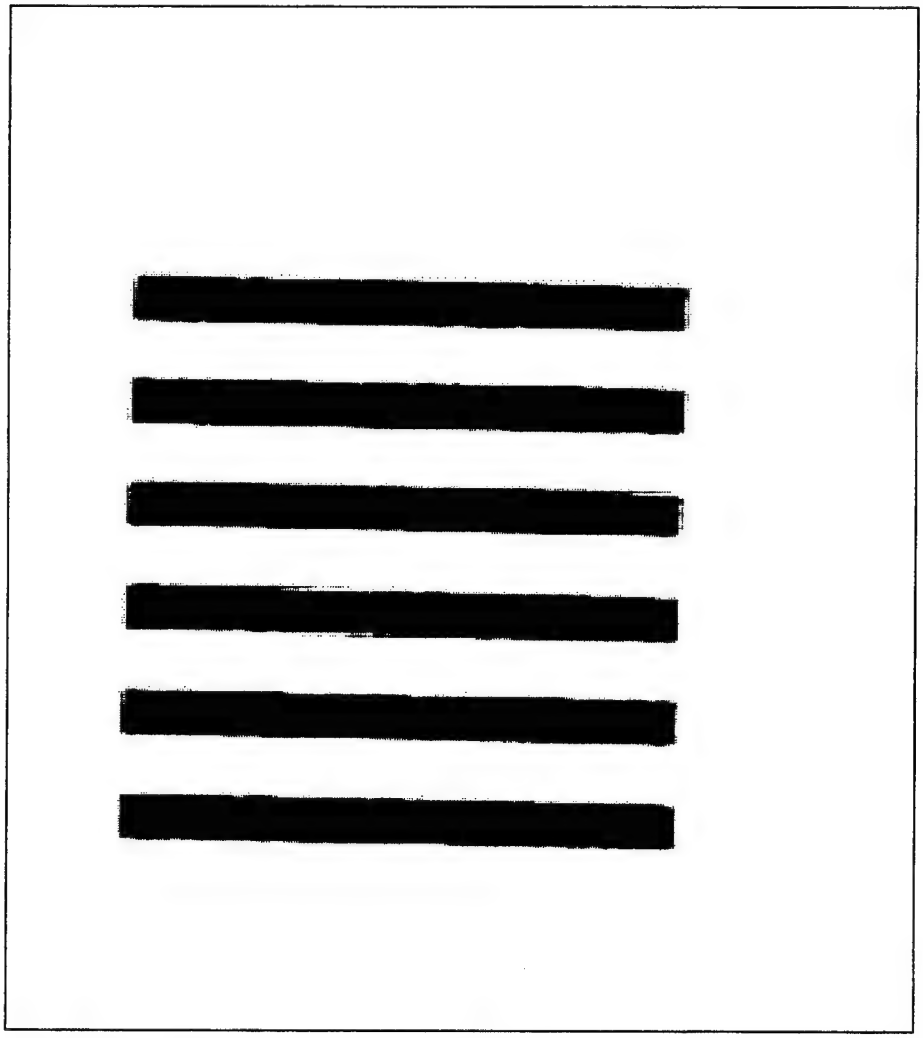

Fig. B-18. A2, enlarged portion of A1

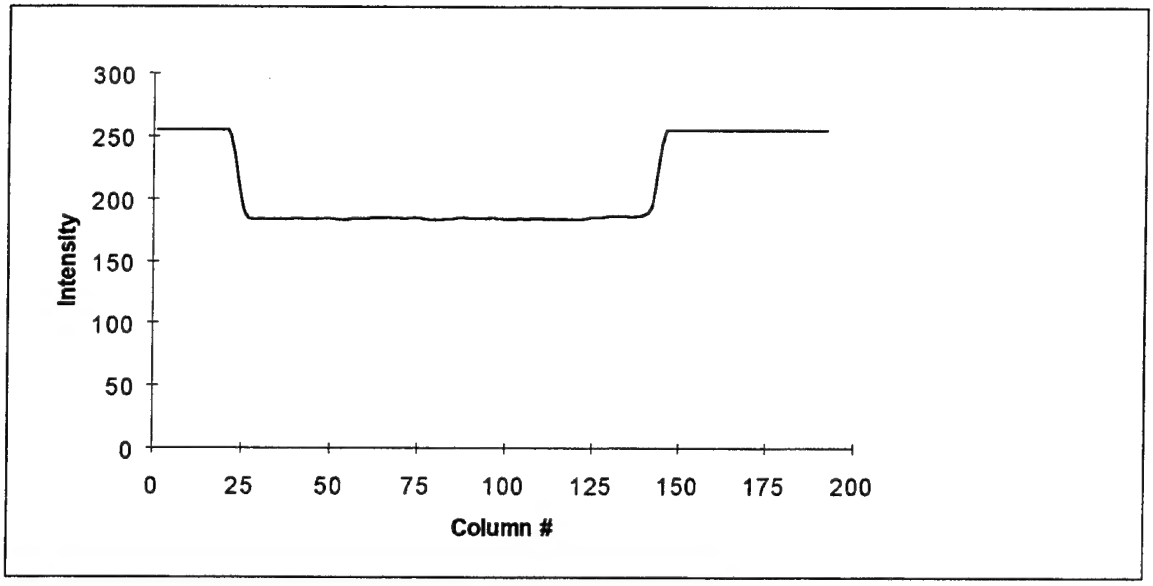

Fig. B-19. A2 squashed to preserve horizontal sequencies

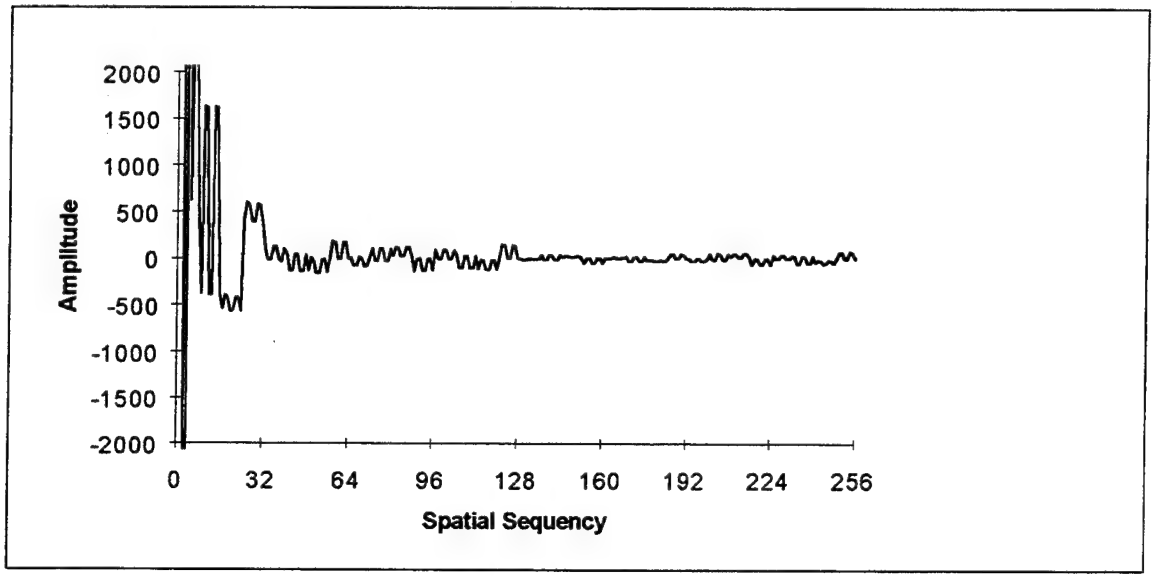

Fig. B-20. Walsh transform of Fig. B-19

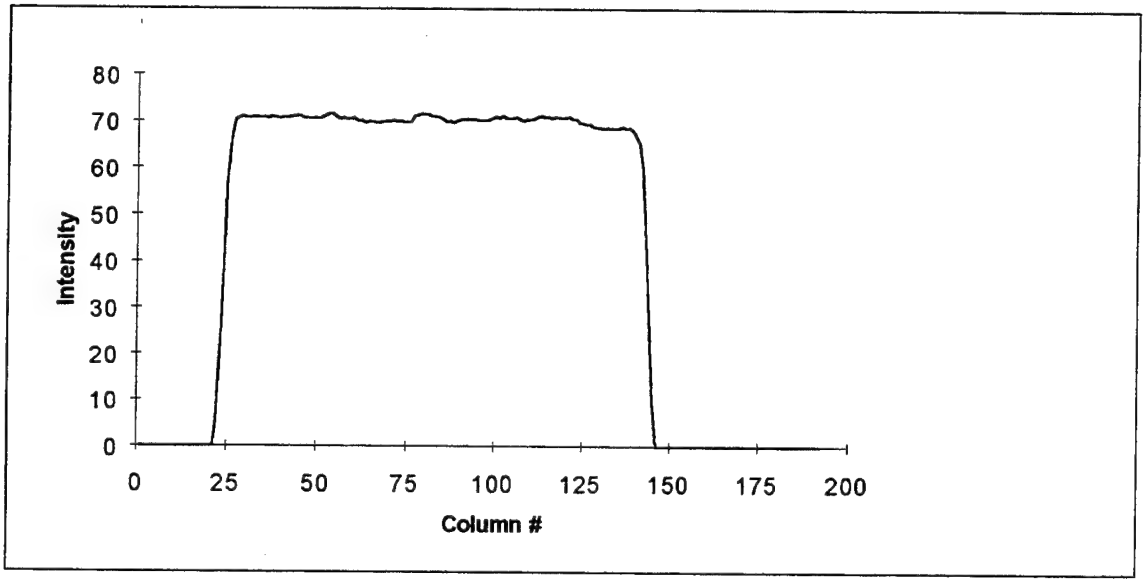

Fig. B-21. Complement of A2 squashed to preserve horizontal sequencies

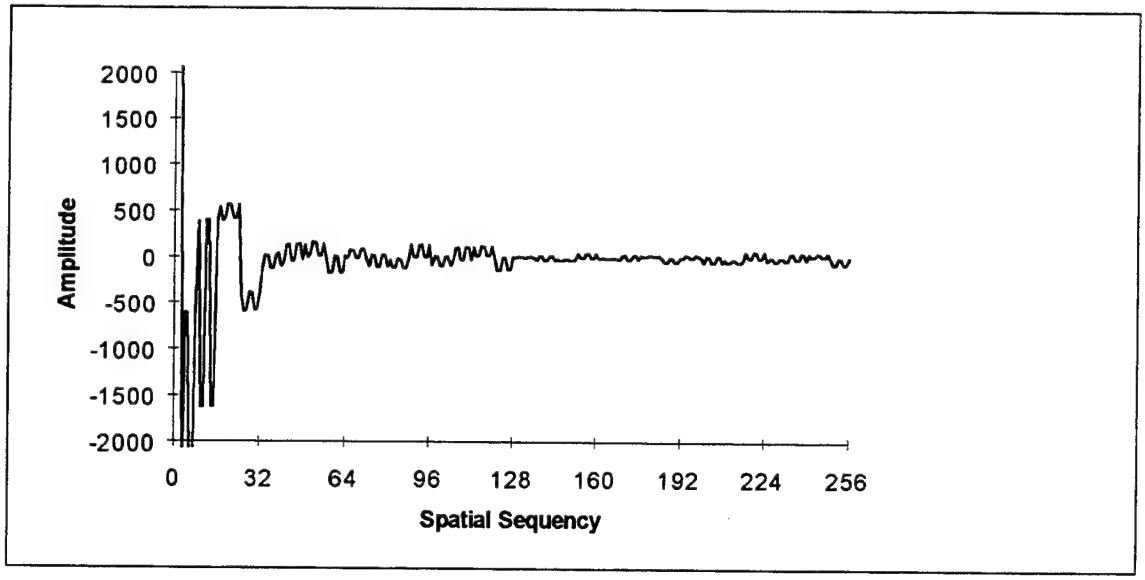

Fig. B-22. Walsh transform of Fig. B-21

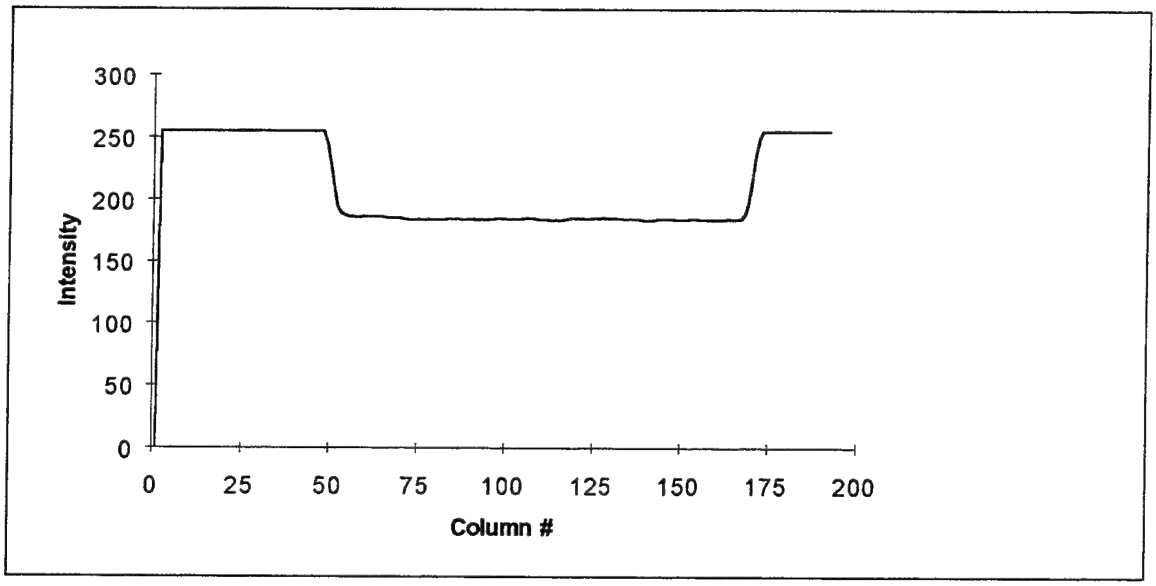

Fig. B-23. Reflection of A2 squashed to preserve horizontal sequencies

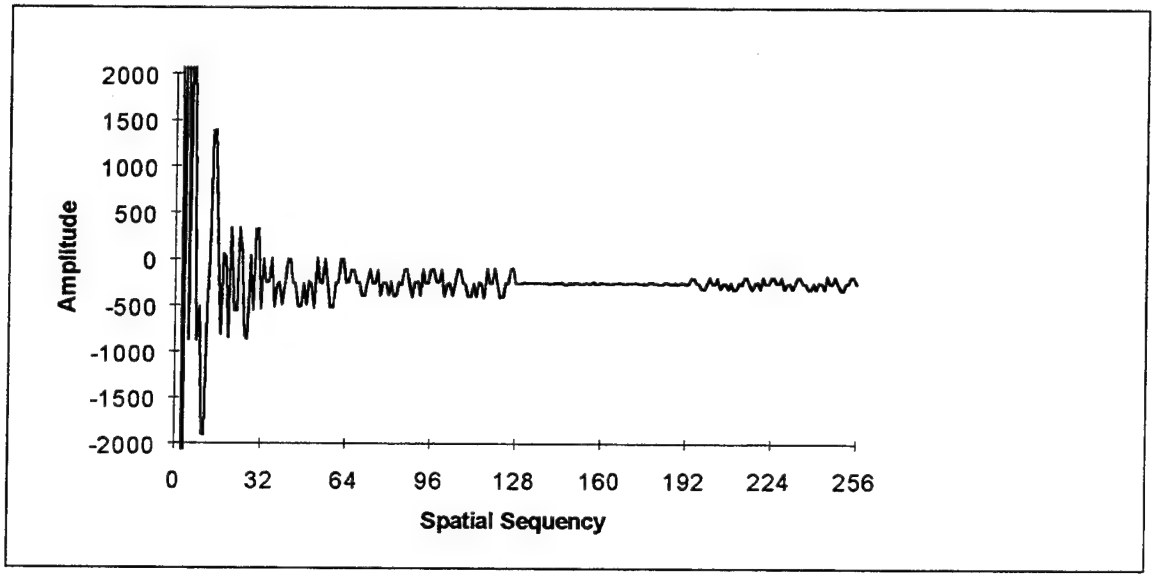

Fig. B-24. Walsh transform of Fig. B-23

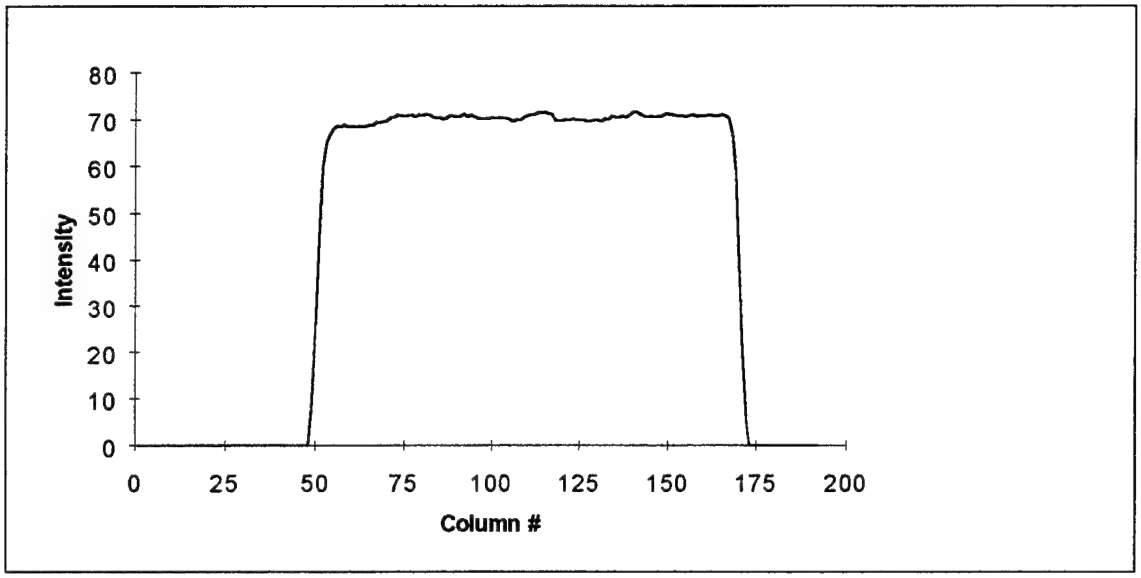

Fig. B-25. Complemented reflection of A2 squashed to preserve horizontal sequencies

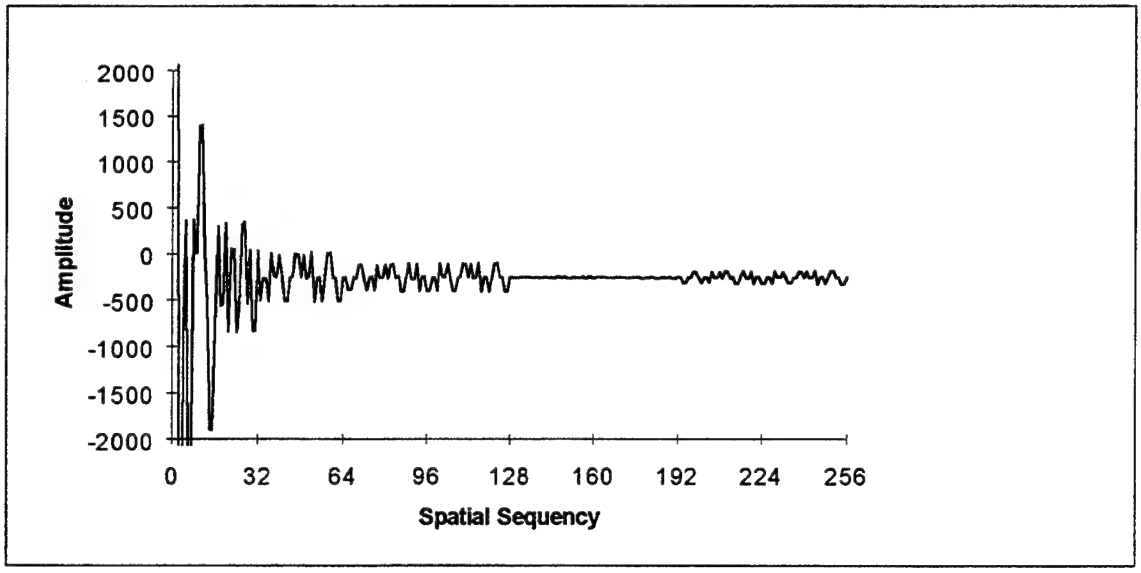

Fig. B-26. Walsh transform of Fig. B-25

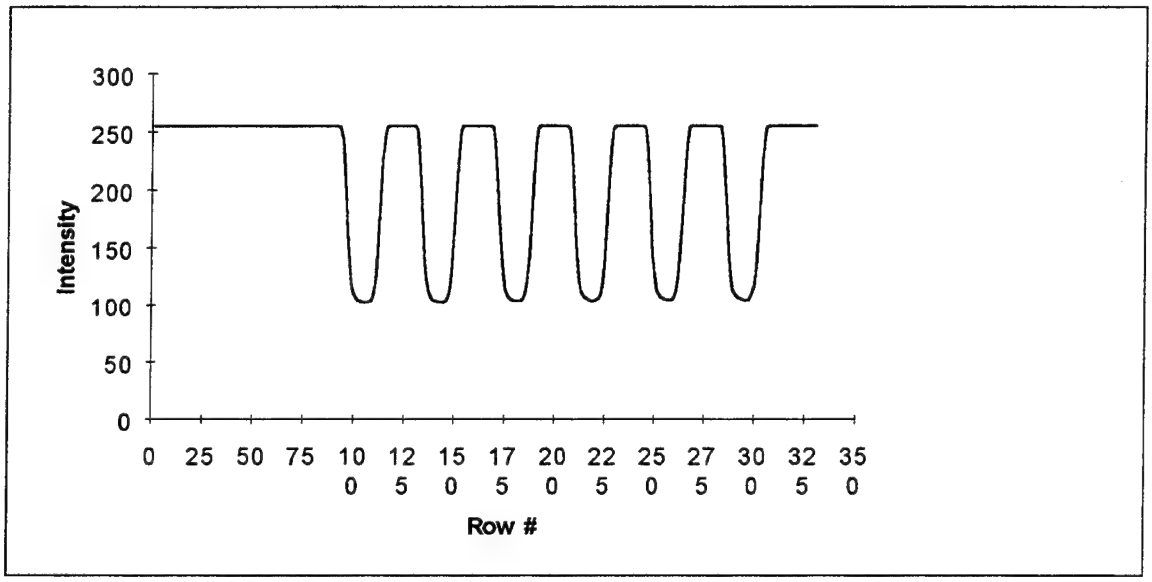

Fig. B-27. A2 squashed to preserve vertical sequencies

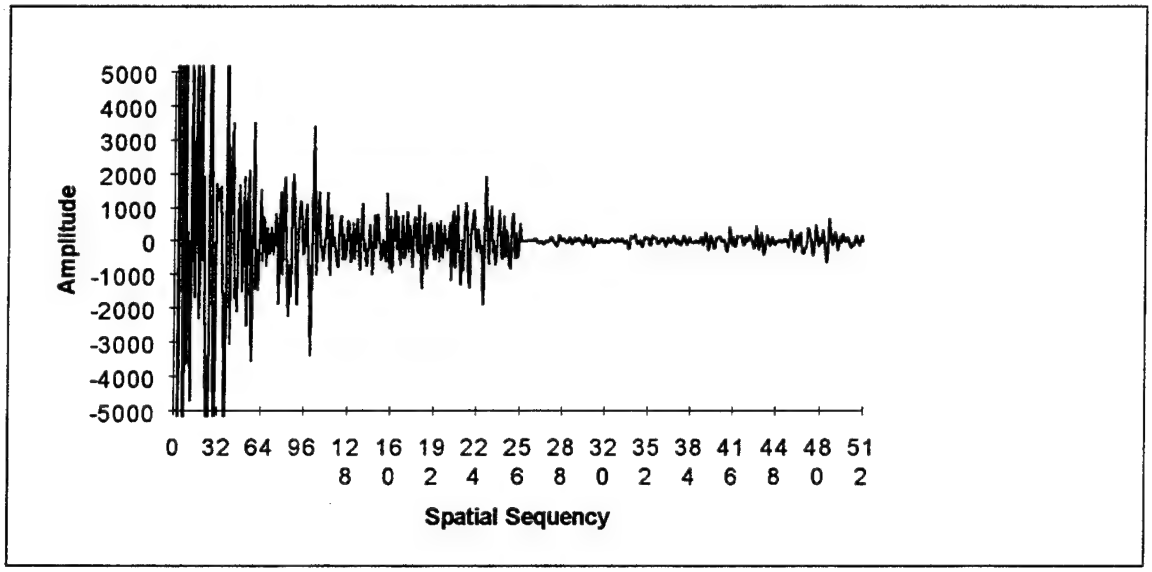

Fig. B-28. Walsh transform of Fig. B-27

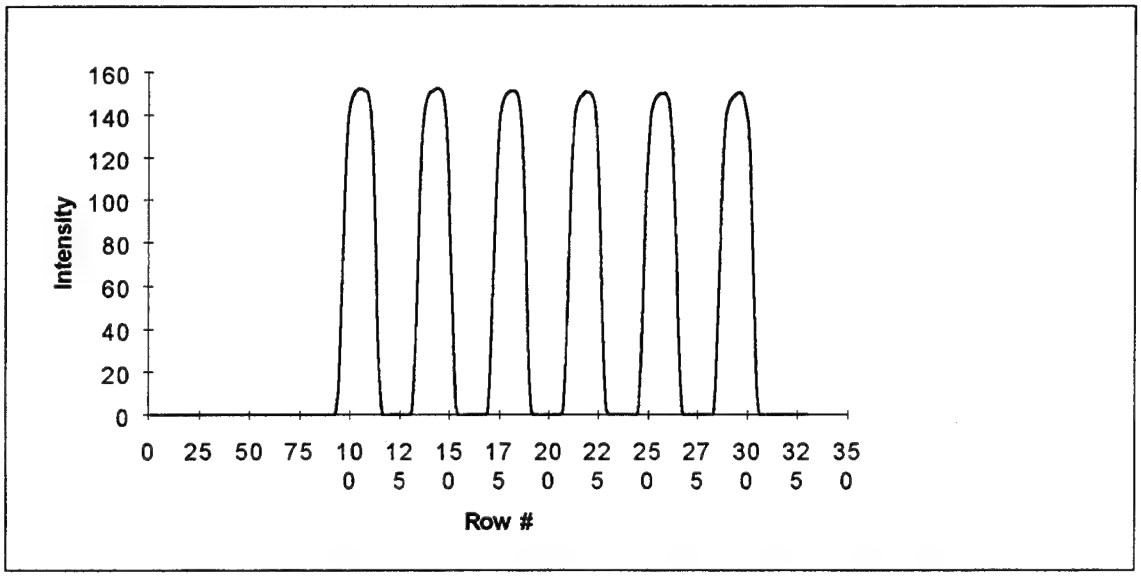

Fig. B-29. Complement of A2 squashed to preserve vertical sequencies

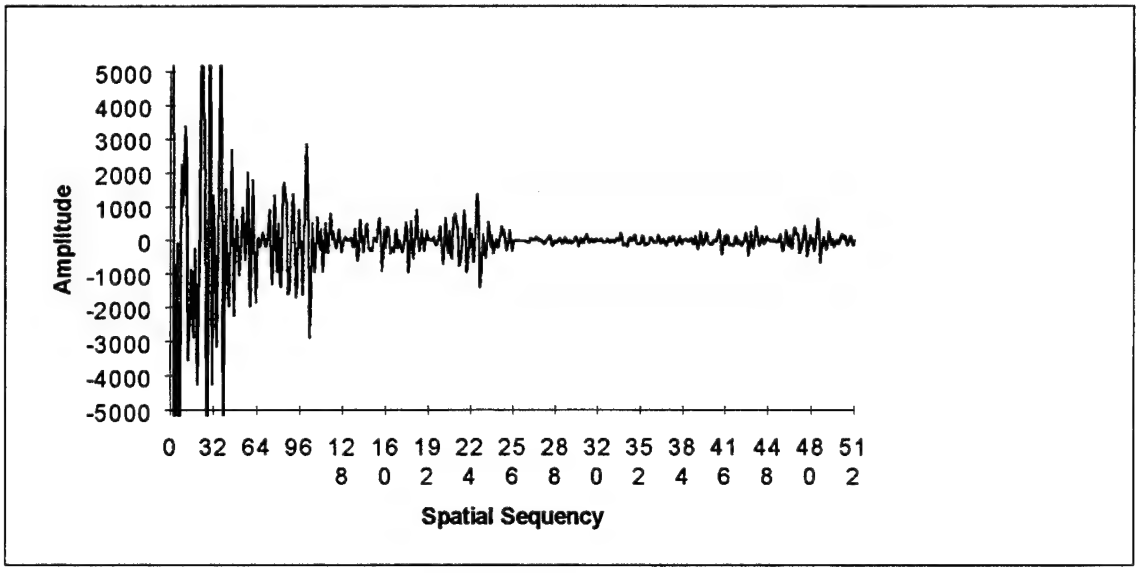

Fig. B-30. Walsh transform of Fig. B-29

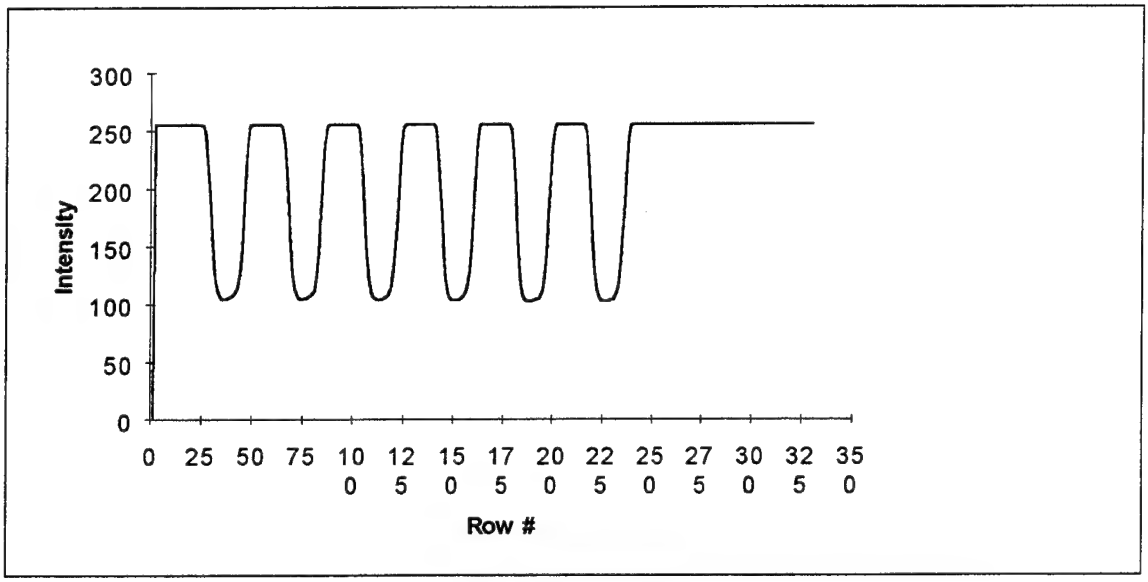

Fig. B-31. Reflection of A2 squashed to preserve vertical sequencies

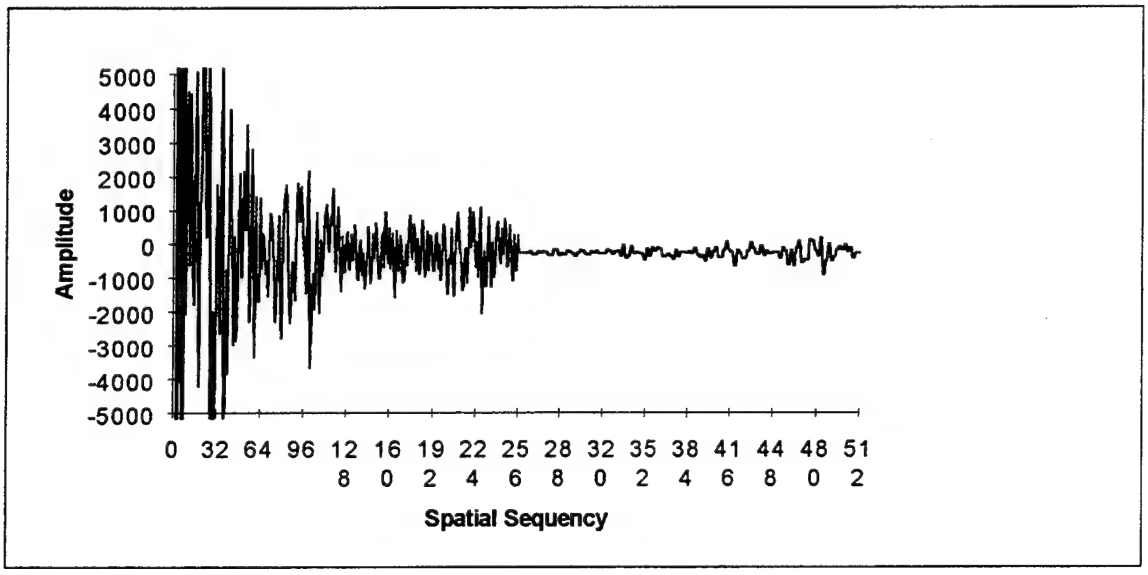

Fig. B-32. Walsh transform of Fig. B-31

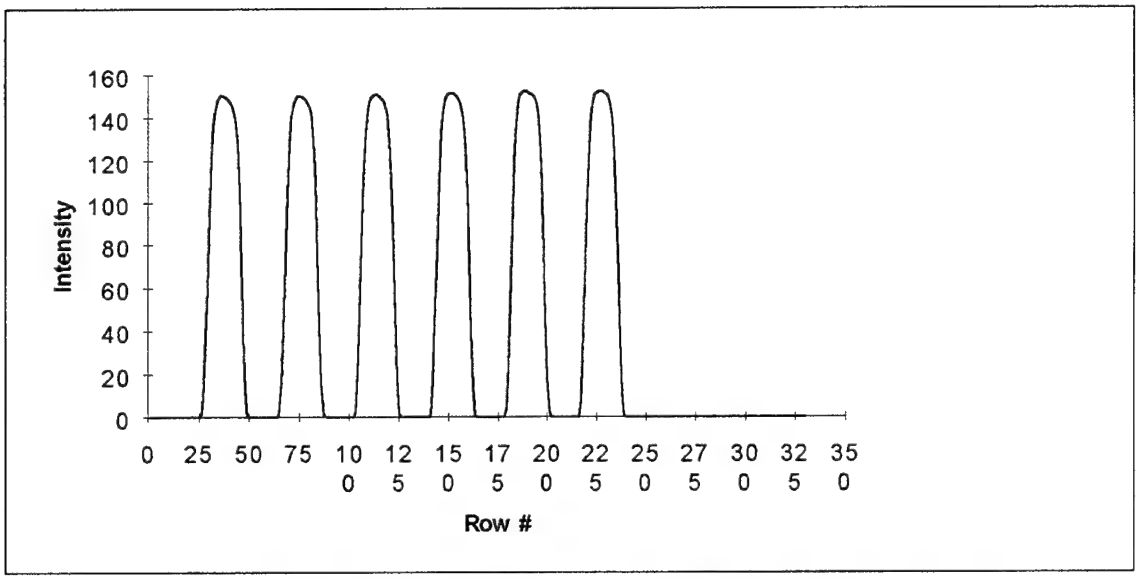

Fig. B-33. Complemented reflection of A2 squashed to preserve vertical sequencies

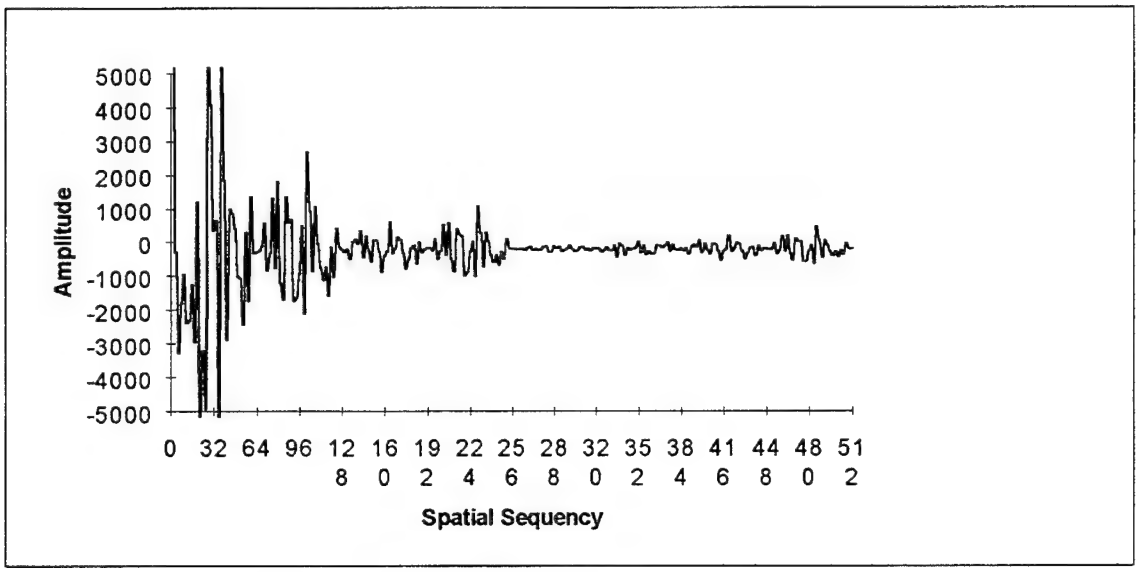

Fig . B-34. Walsh transform of Fig. B-33

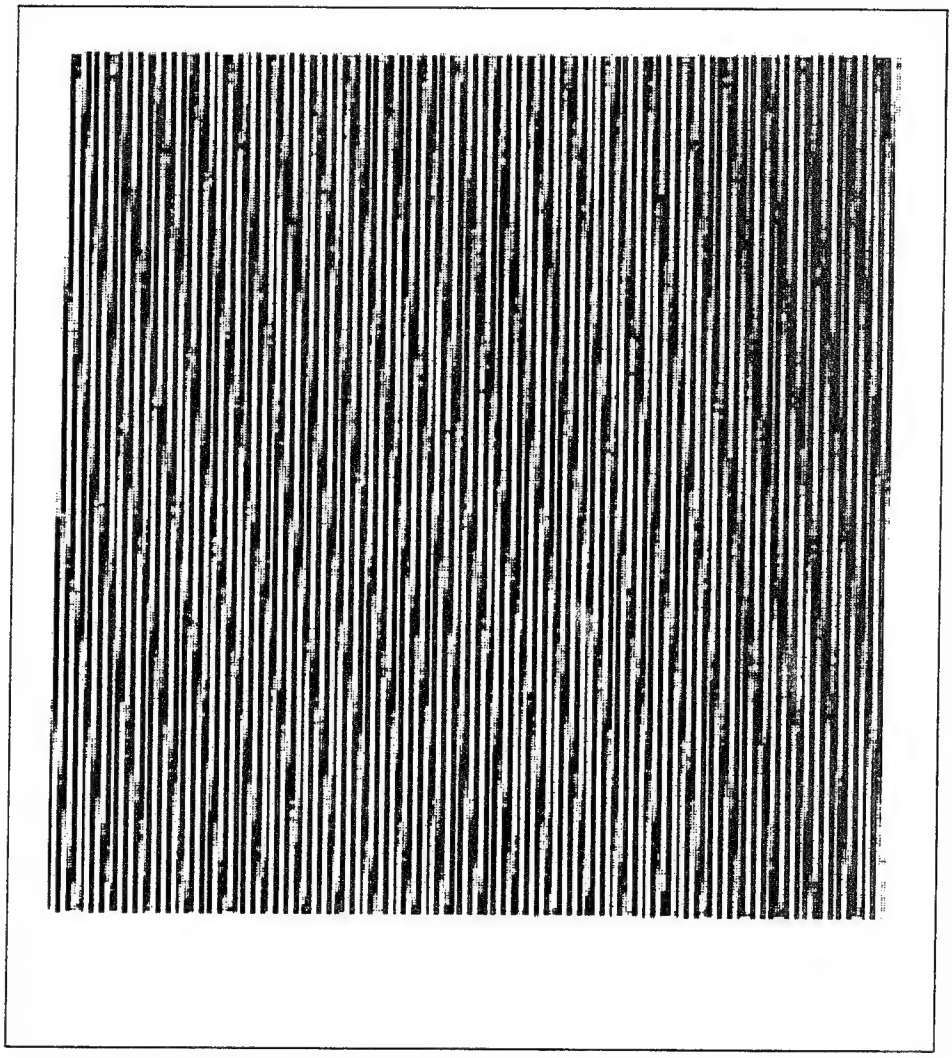

Fig. B-35. R1, closely spaced vertical lines

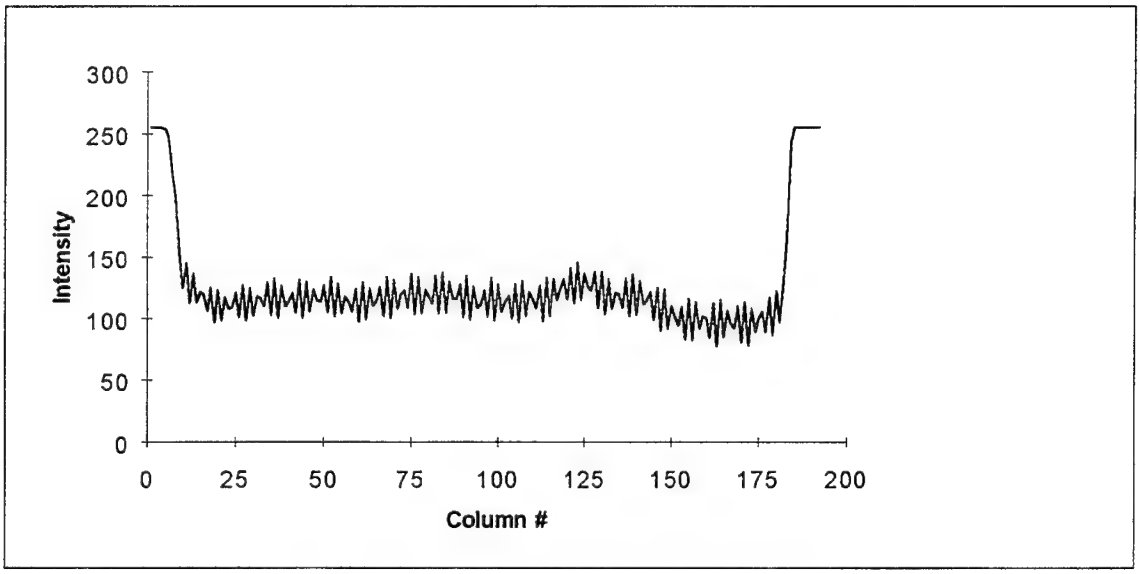

Fig. B-36. R1 squashed to preserve horizontal sequencies

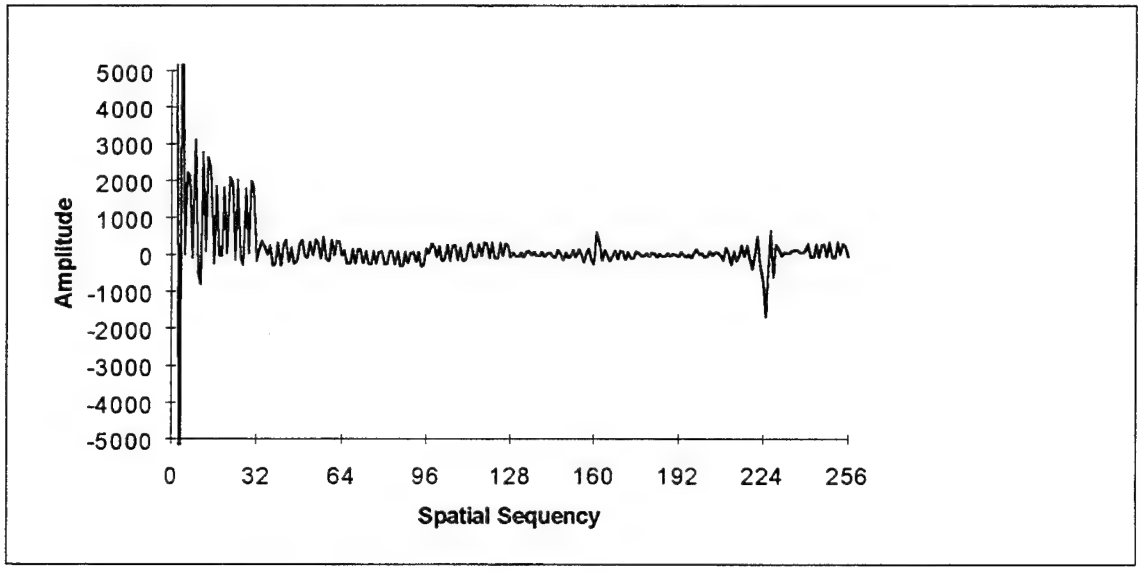

Fig. B-37. Walsh transform of Fig. B-36

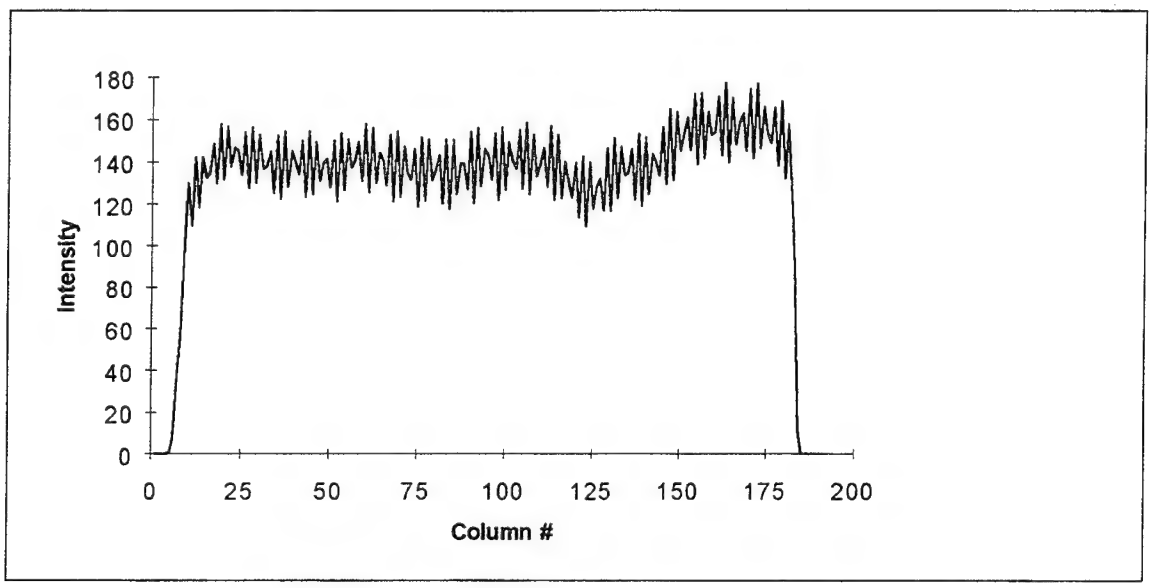

Fig. B-38. Complement of R1 squashed to preserve horizontal sequencies

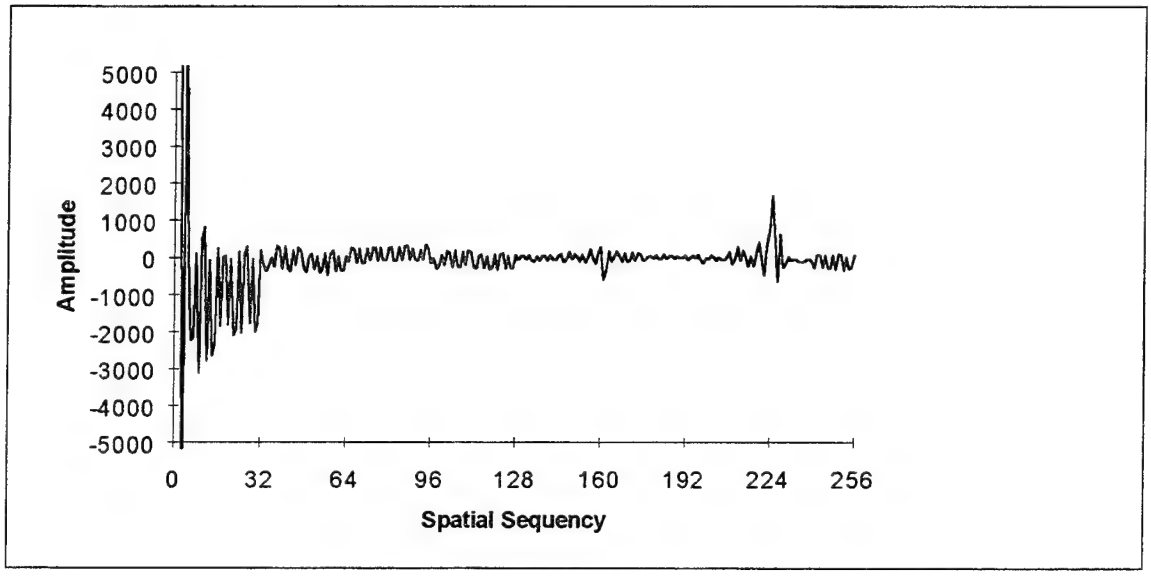

Fig. B-39. Walsh transform of Fig. B-38

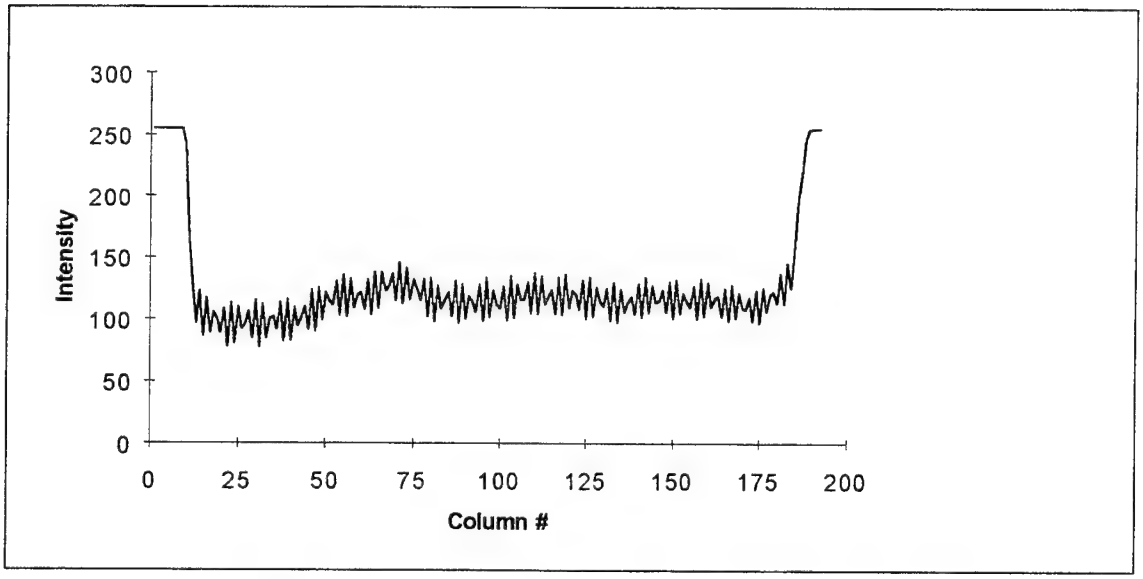

Fig. B-40. Reflection of R1 squashed to preserve horizontal sequencies

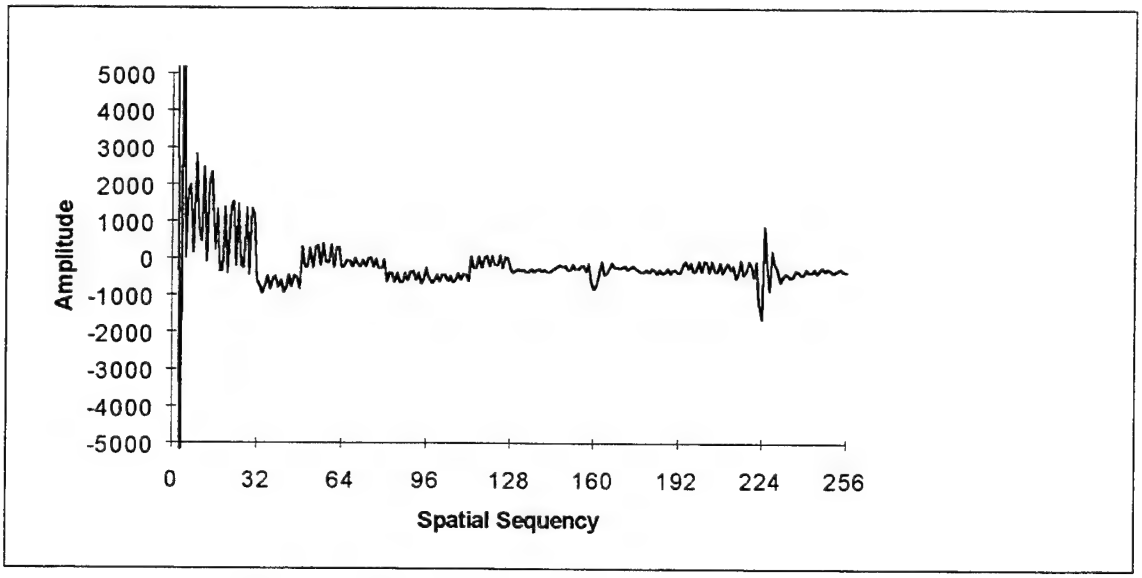

Fig. B-41. Walsh transform of Fig. B-40

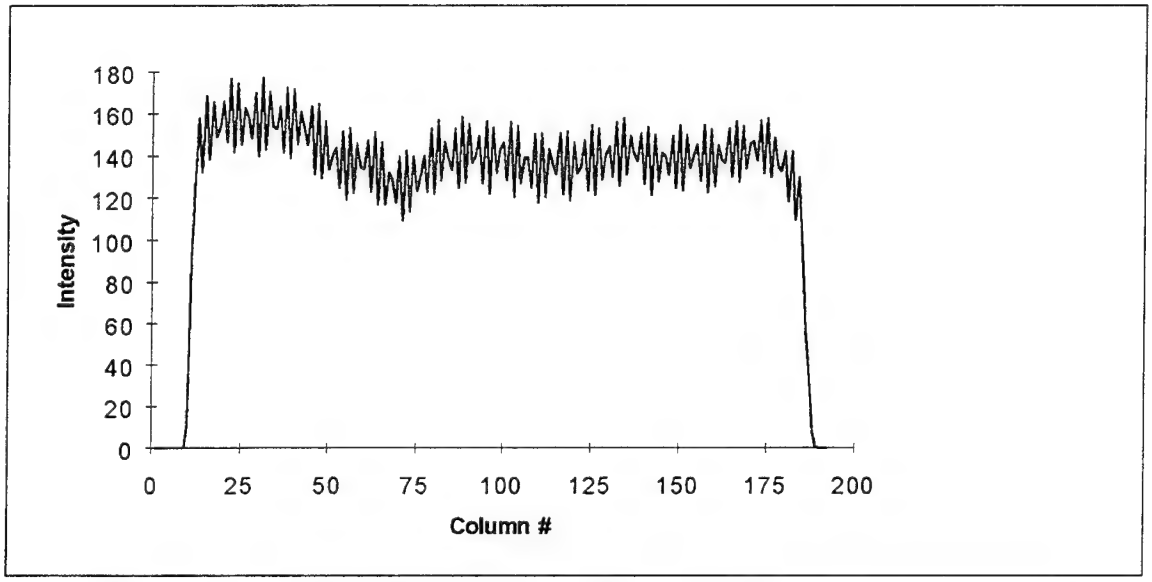

Fig. B-42. Complemented reflection of R1 squashed to preserve horizontal sequencies

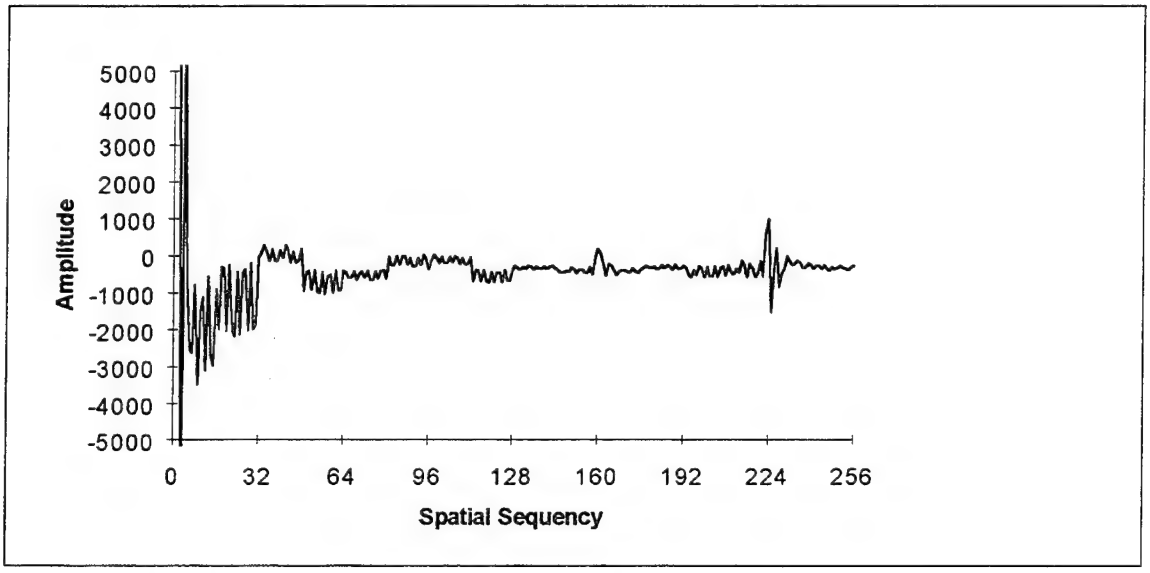

Fig. B-43. Walsh transform of Fig. B-42

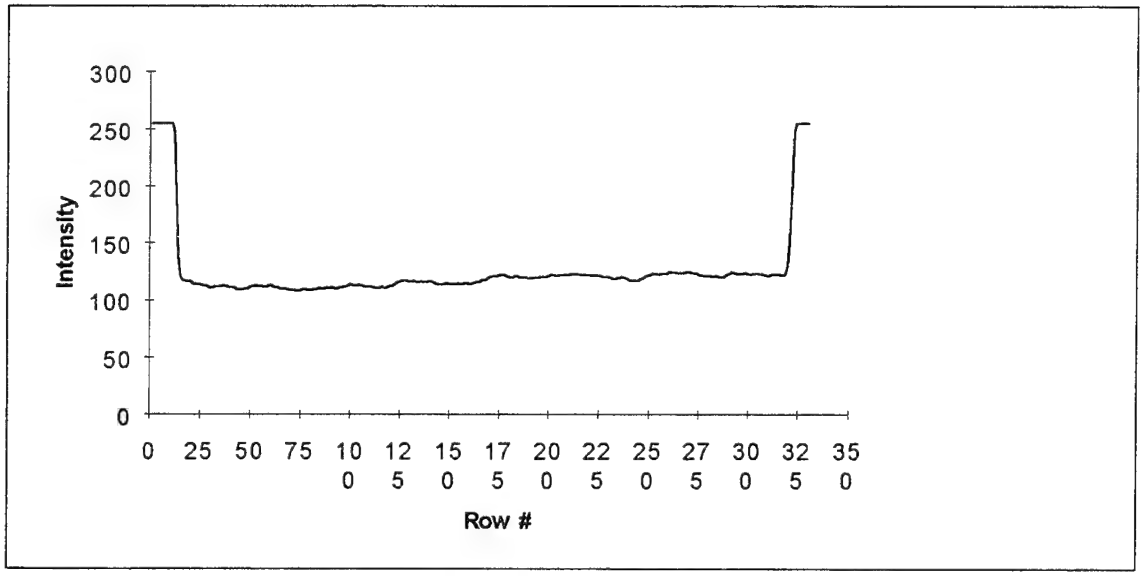

Fig. B-44. R1 squashed to preserve vertical sequencies

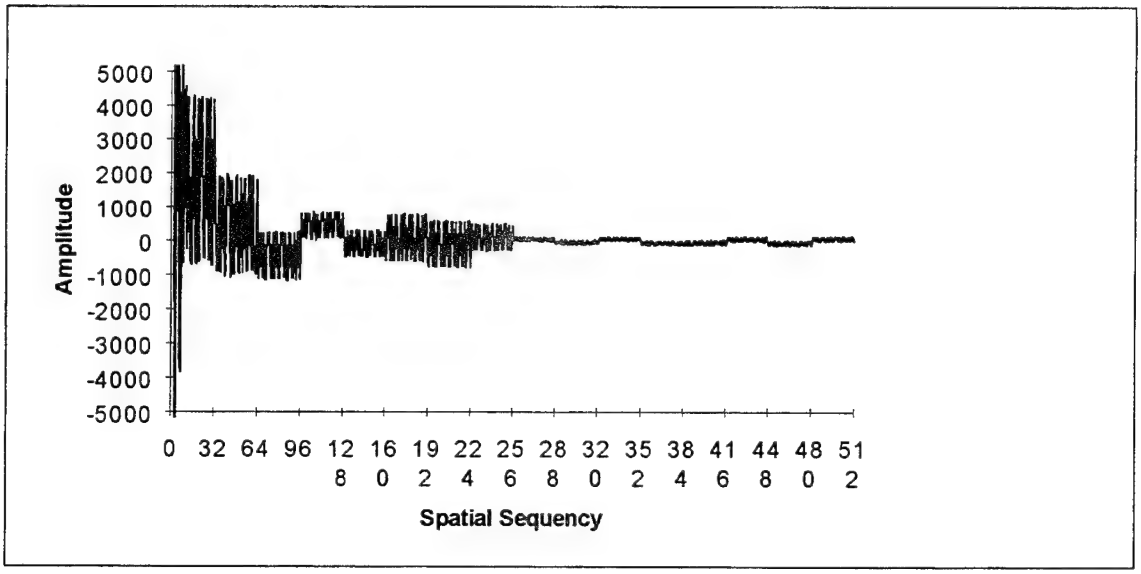

Fig. B-45. Walsh transform of Fig. B-44

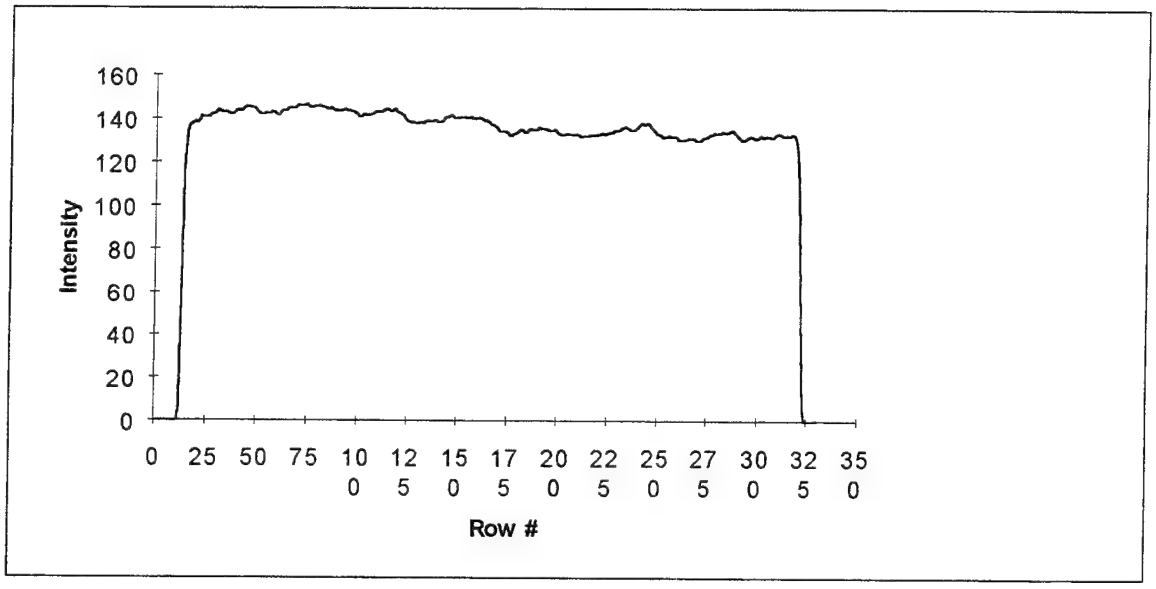

Fig. B-46. Complement of R1 squashed to preserve vertical sequencies

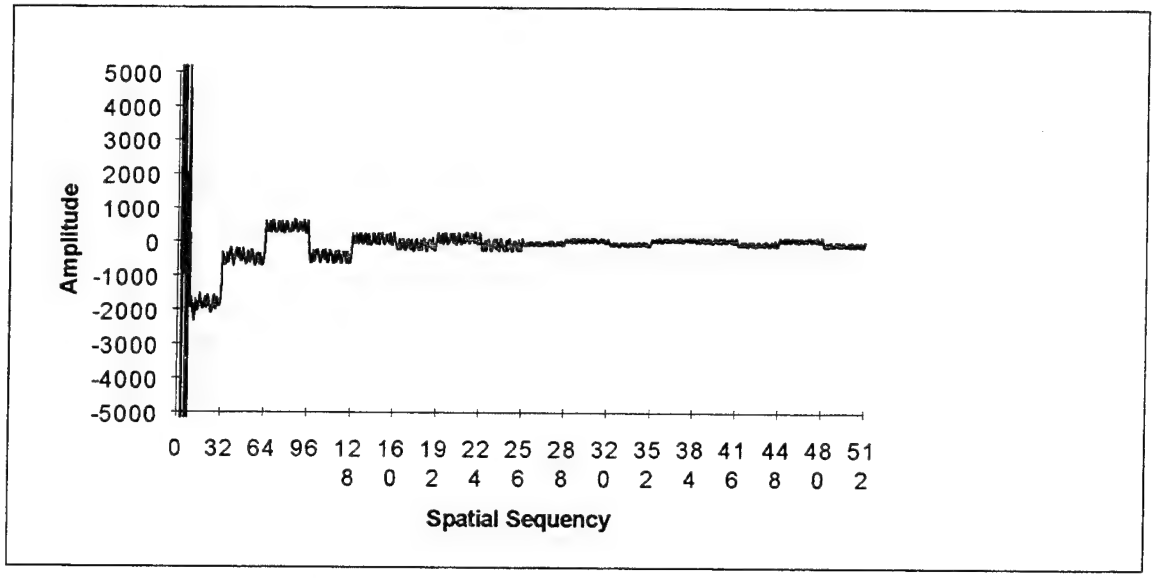

Fig B-47. Walsh transform of Fig. B-46

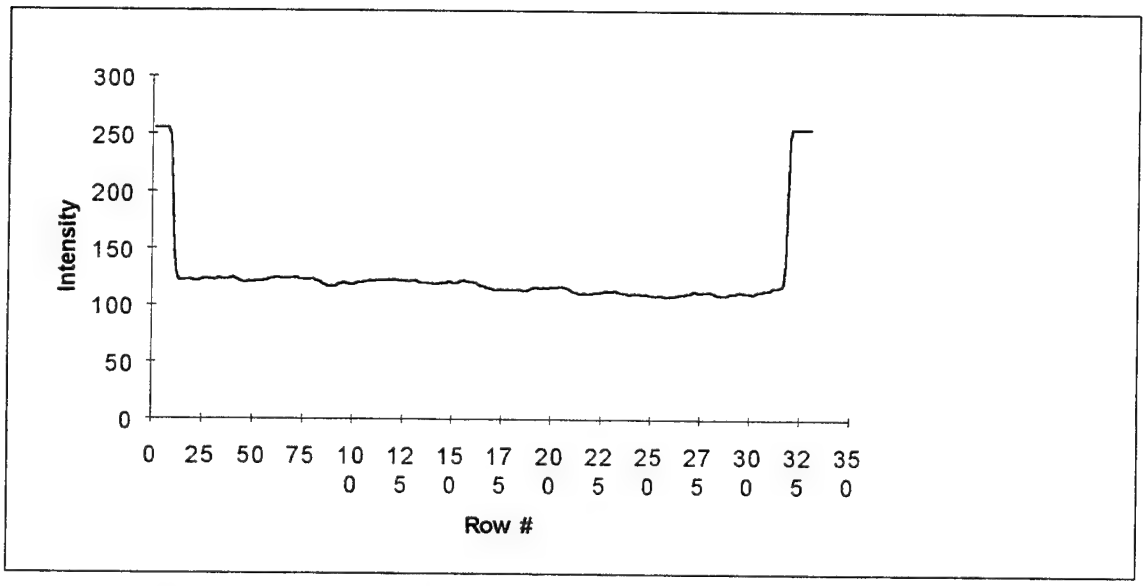

Fig. B-48 Reflection of R1 squashed to preserve vertical sequencies

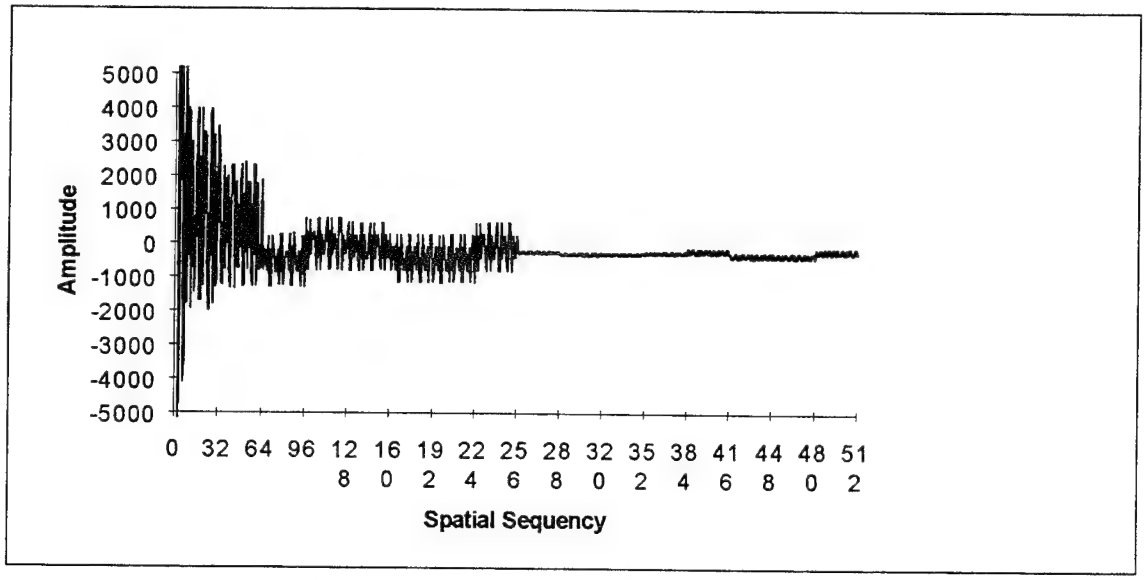

Fig. B-49. Walsh transform of Fig. B-48

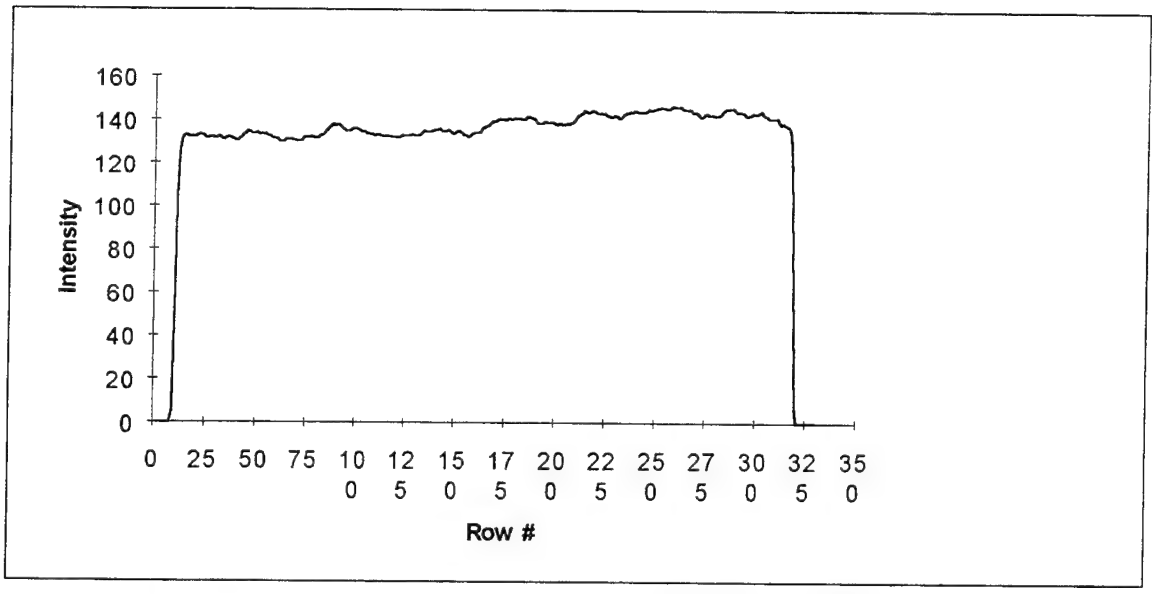

Fig. B-50. Complemented reflection of R1 squashed to preserve vertical sequencies

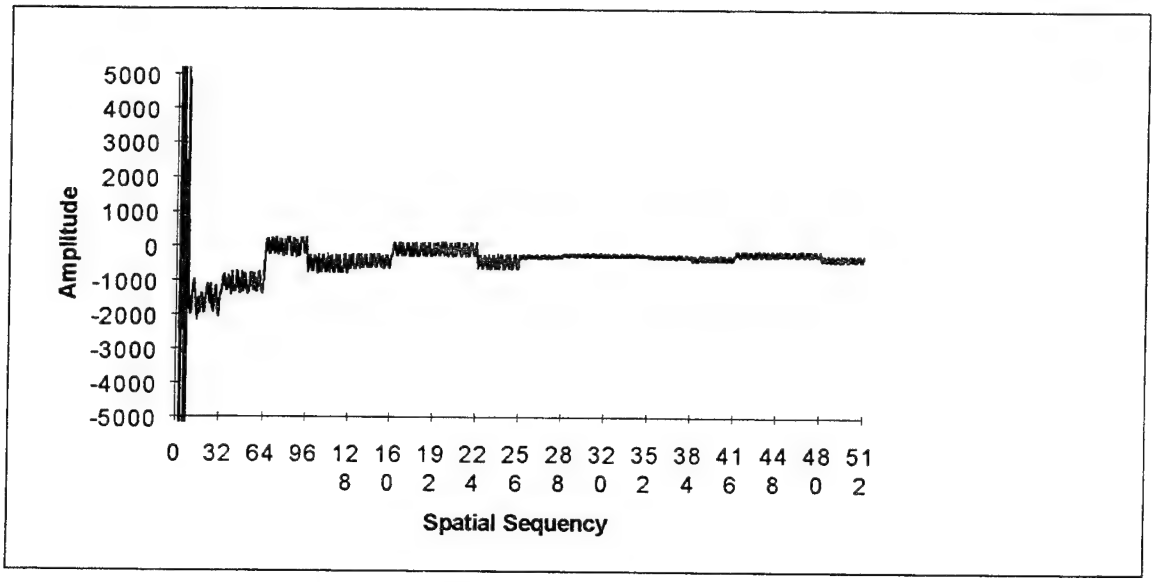

Fig. B-51. Walsh transform of Fig. B-50

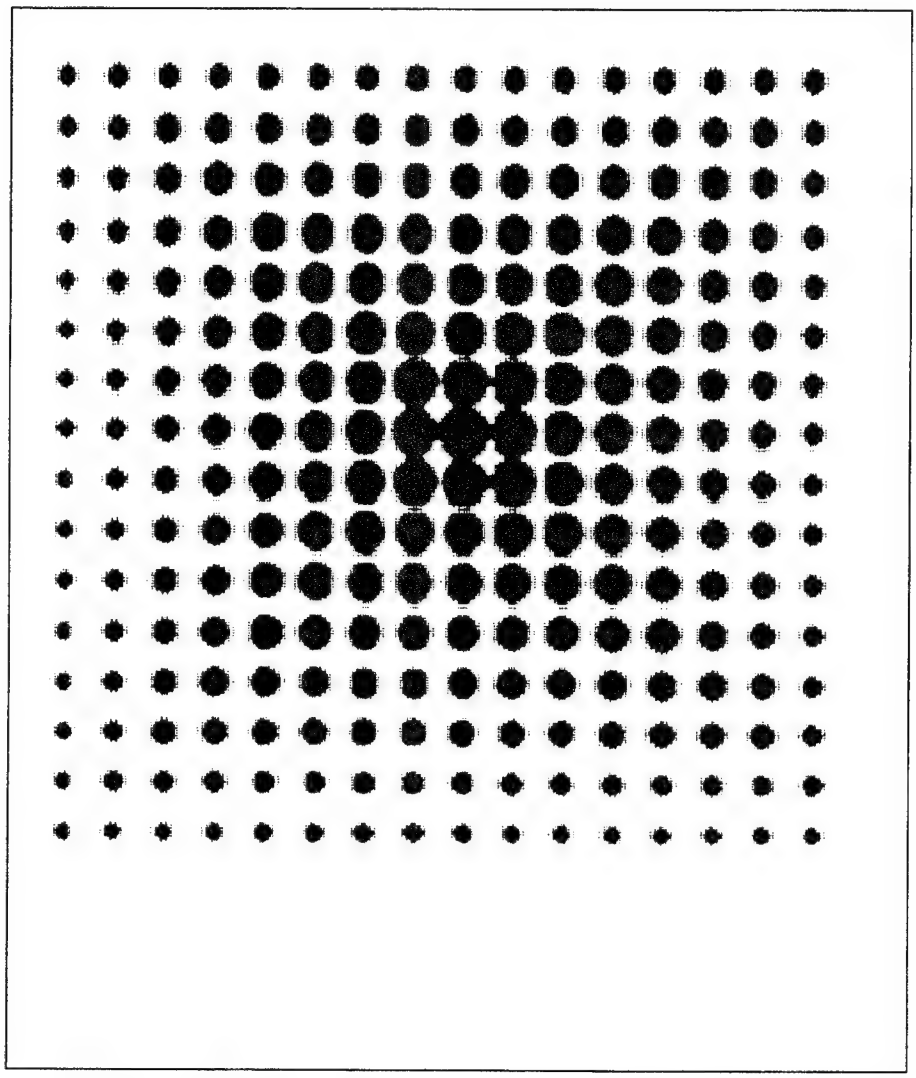

Fig. B-52. R2, test pattern of spots in different sizes

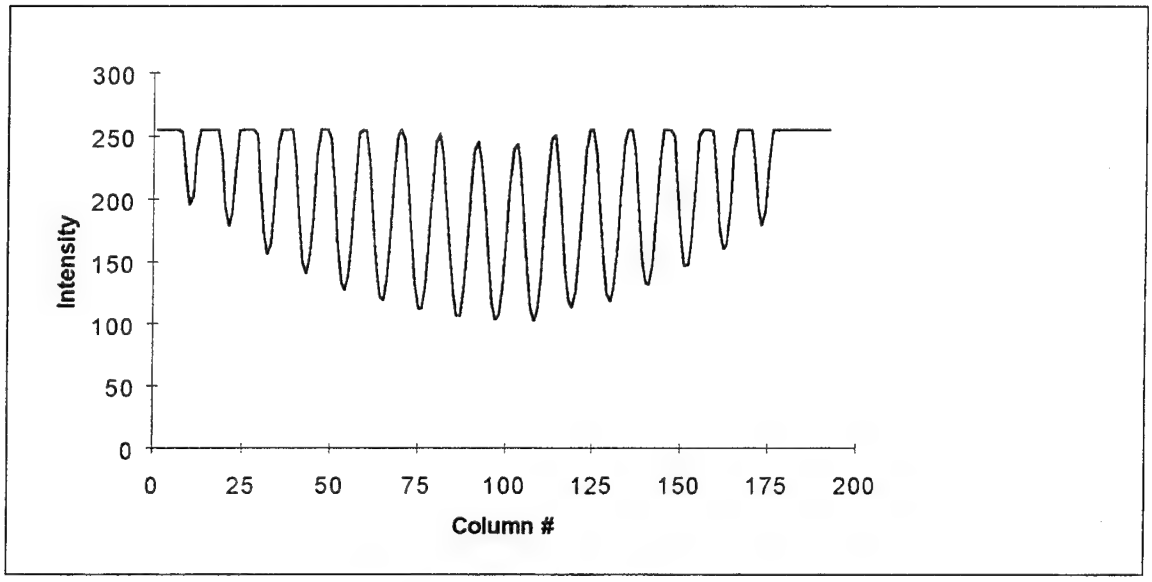

Fig. B-53. R2 squashed to preserve horizontal sequencies

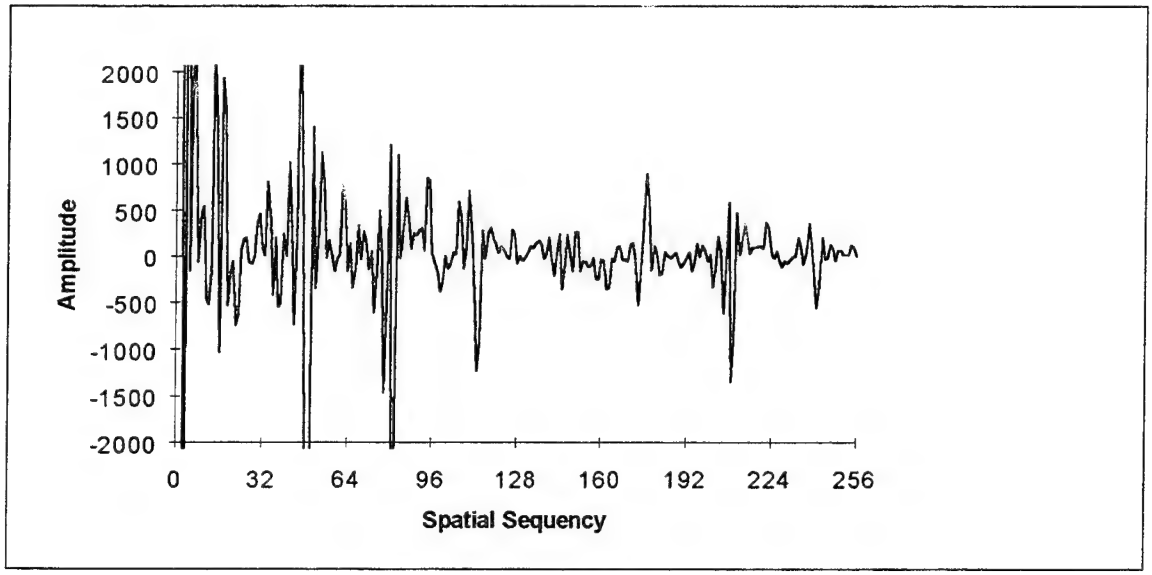

Fig. B-54. Walsh transform of Fig. B-53

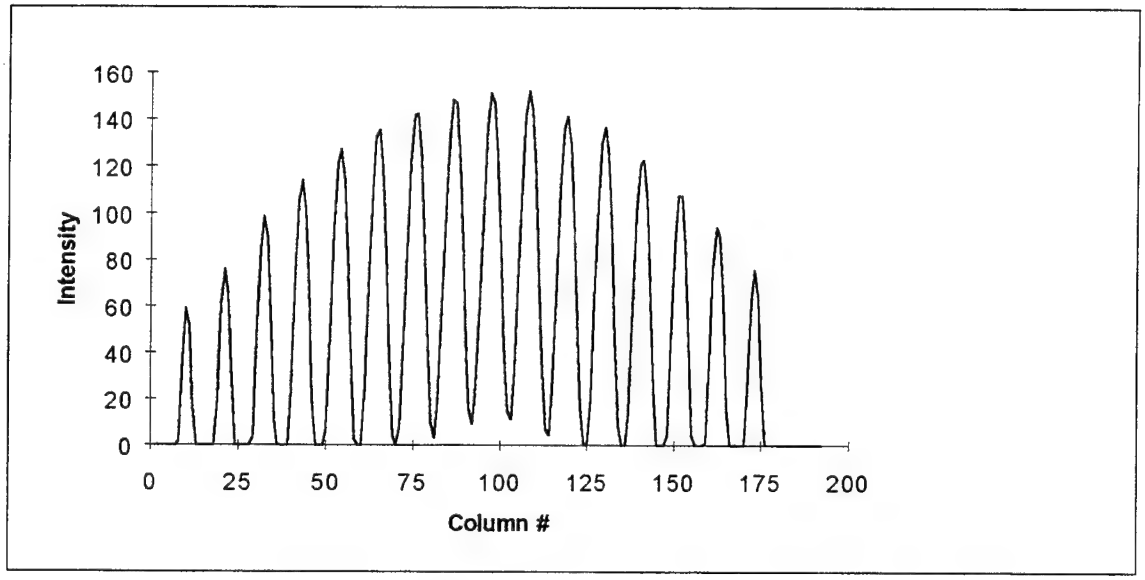

Fig. B-55. Complement of R2 squashed to preserve horizontal sequencies

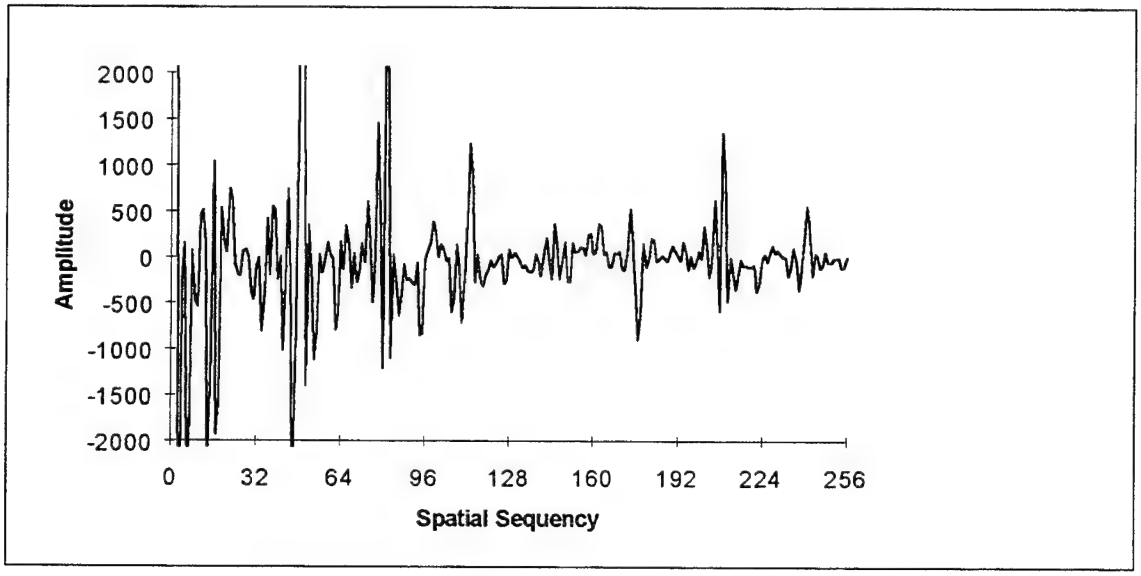

Fig. B-56. Walsh transform of Fig. B-55

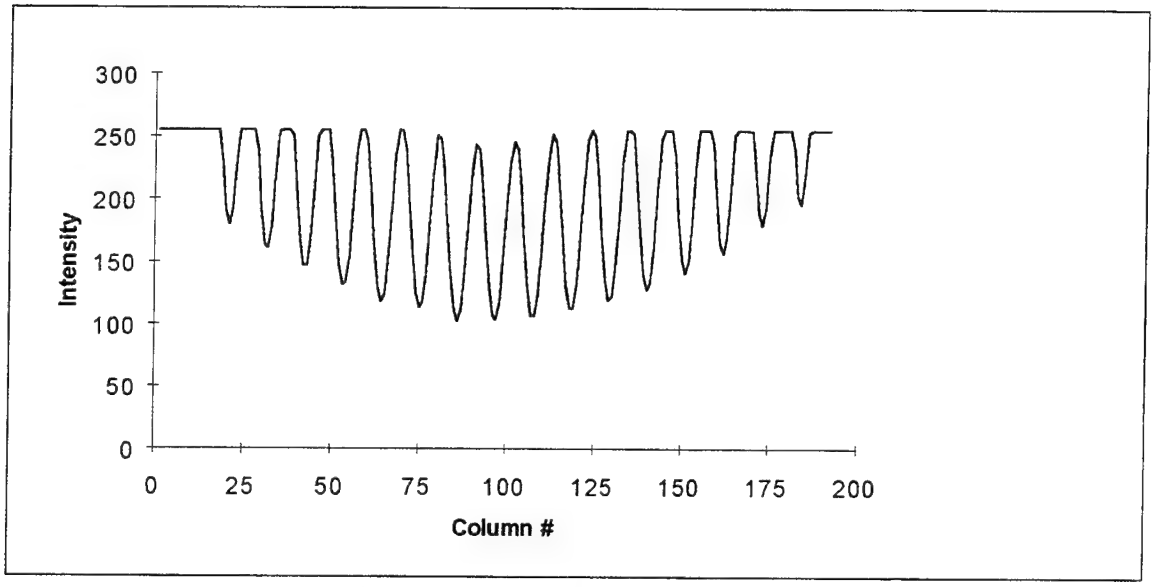

Fig. B-57. Reflection of R2 squashed to preserve horizontal sequencies

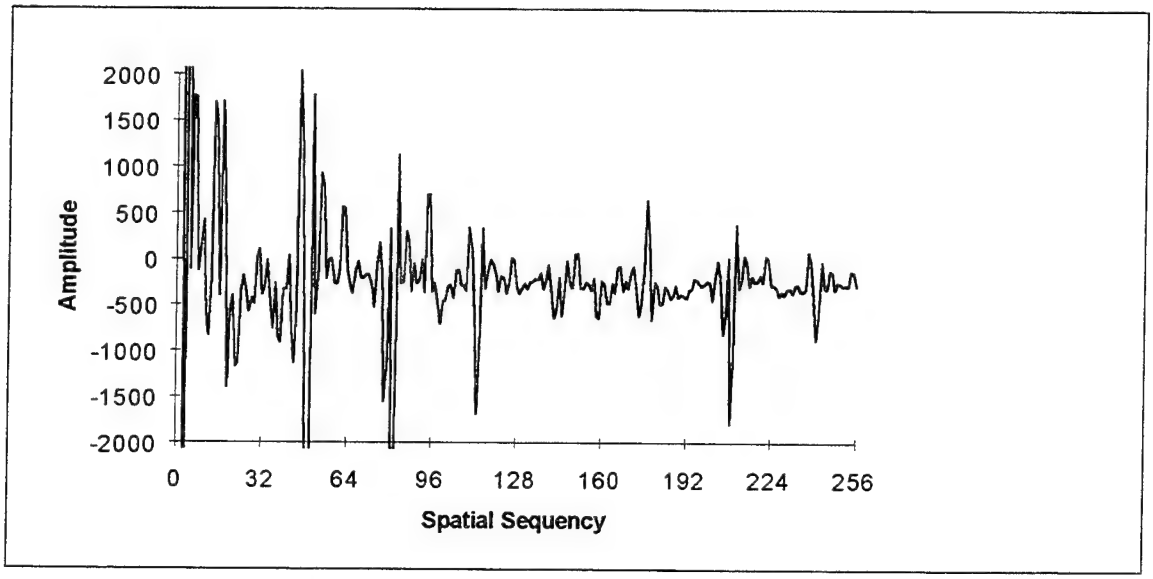

Fig. B-58. Walsh transform of Fig. B-57

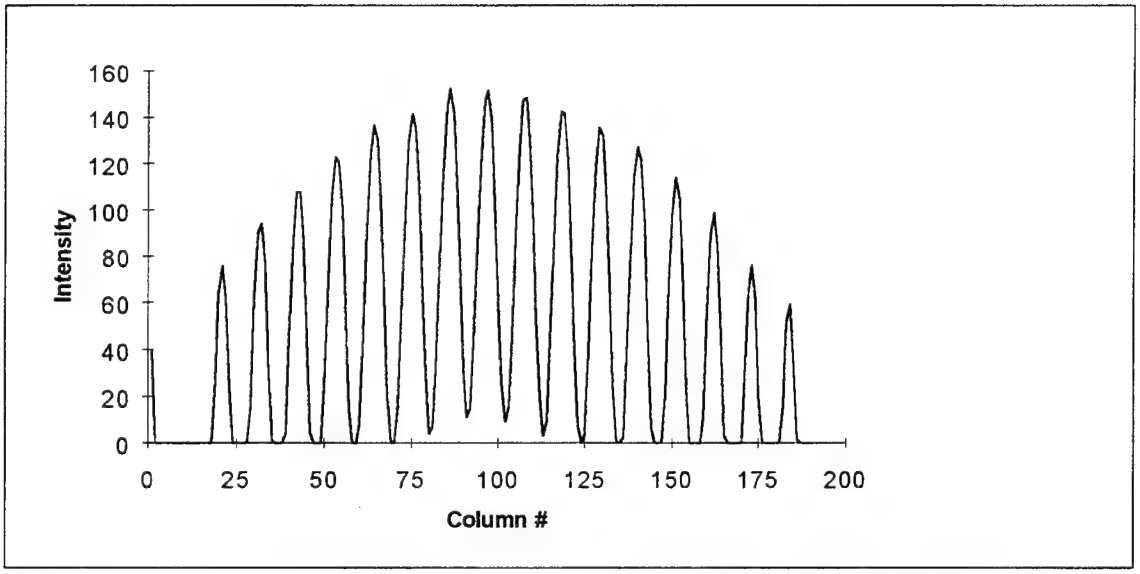

Fig. B-59. Complemented reflection of R2 squashed to preserve horizontal sequencies

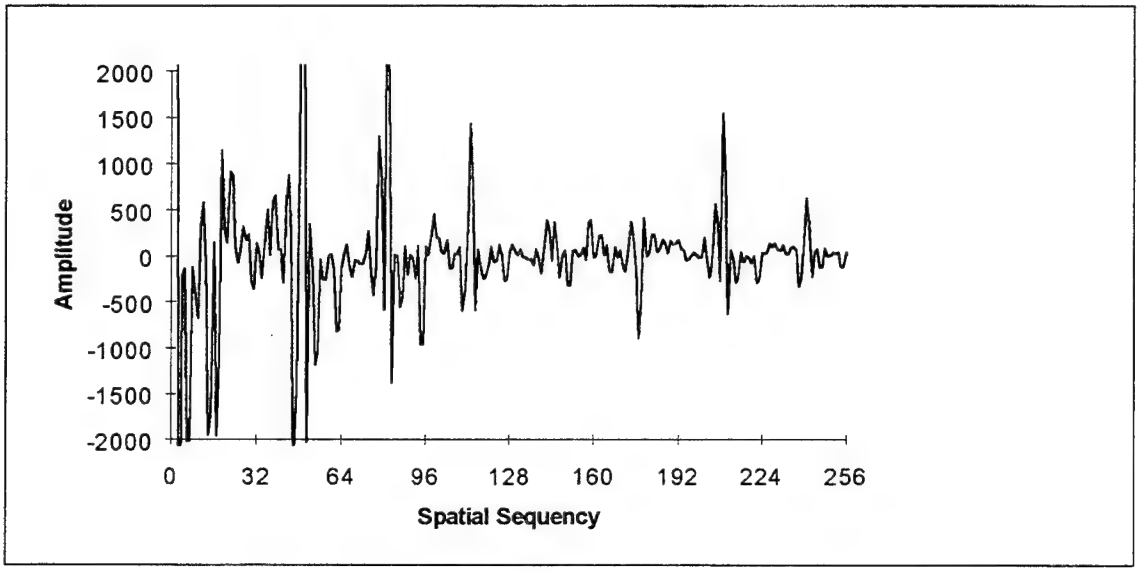

Fig. B-60. Walsh transform of Fig. B-59

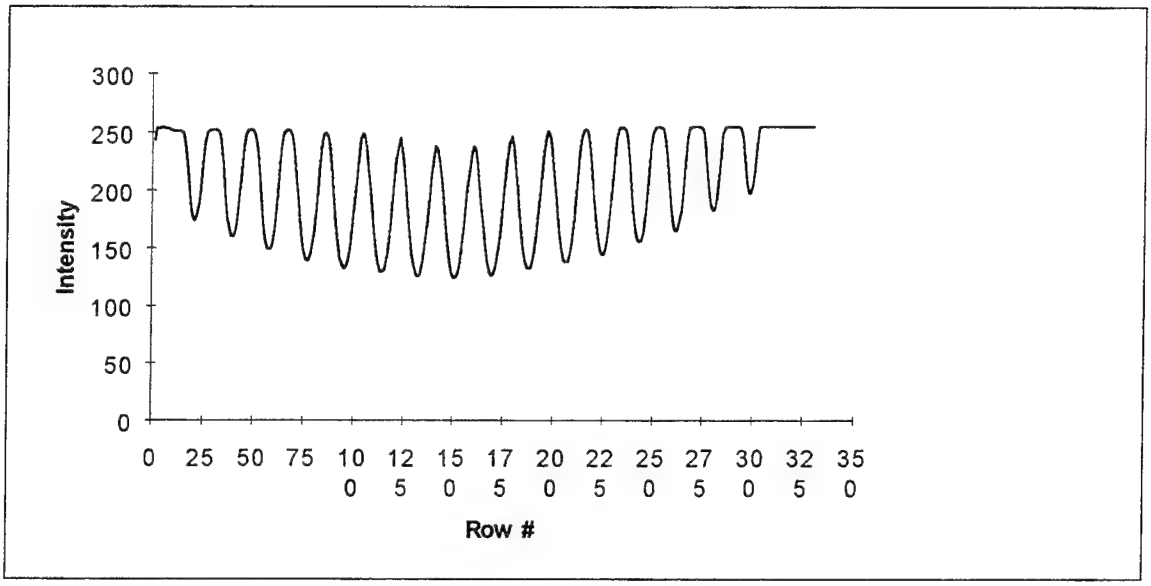

Fig. B-61. R2 squashed to preserve vertical sequencies

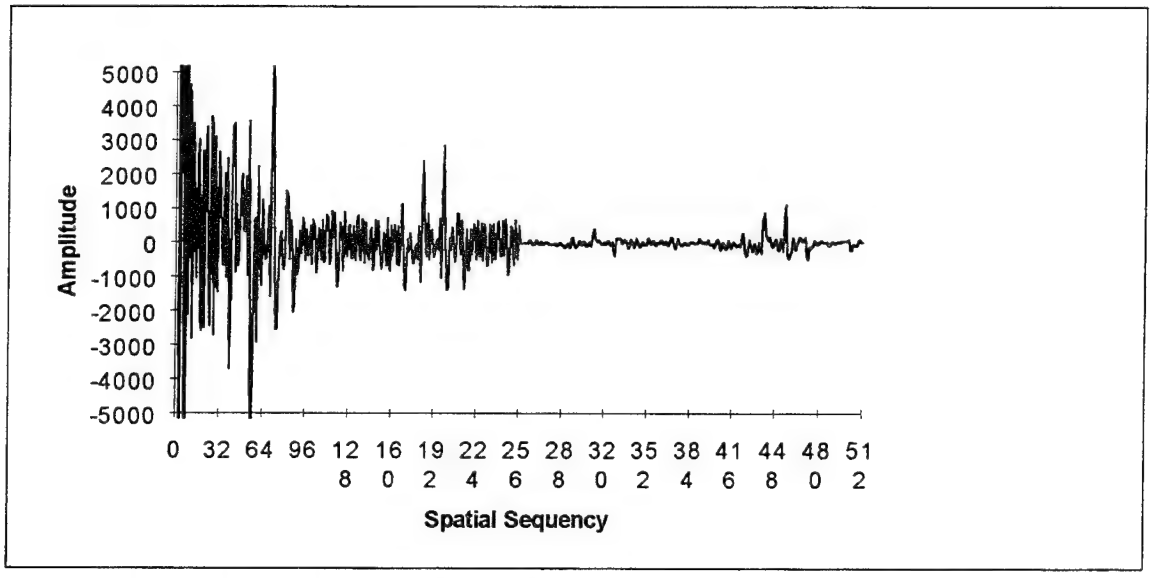

Fig. B-62. Walsh transform of Fig. B-61

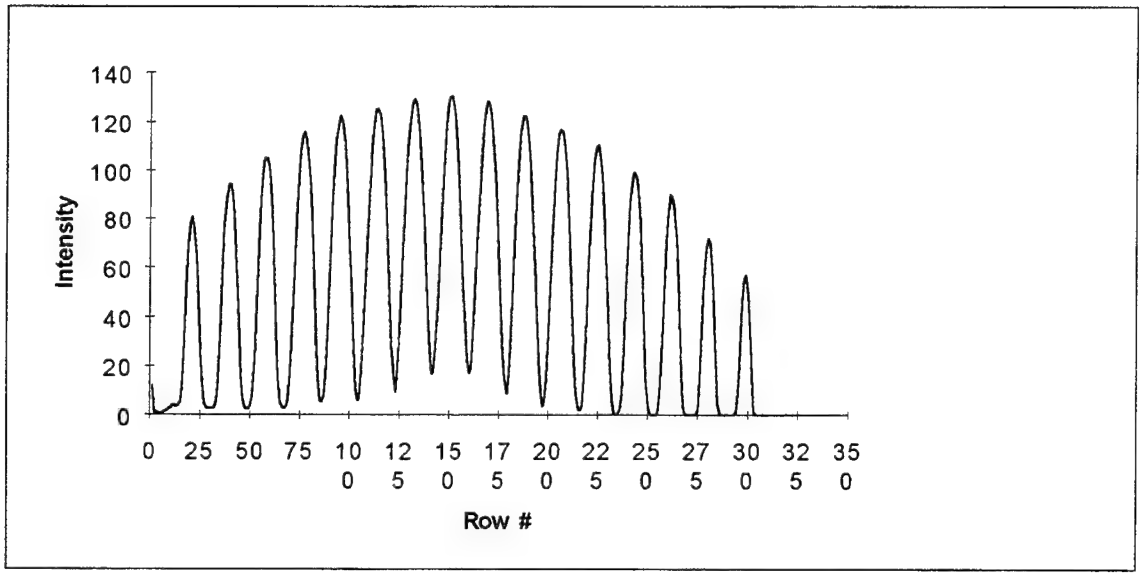

Fig. B-63. Complement of R2 squashed to preserve vertical sequencies

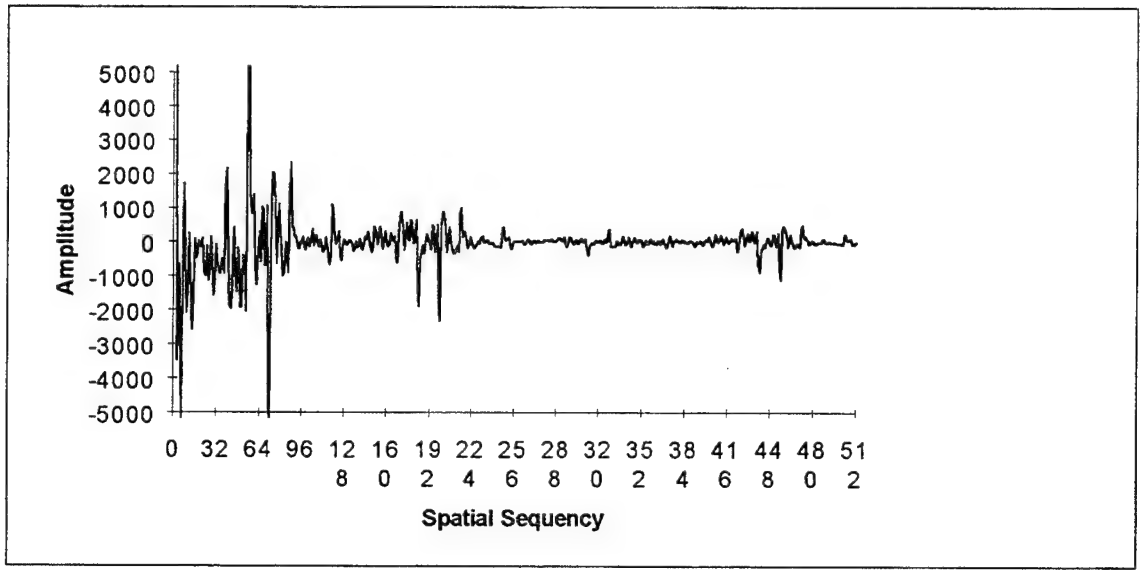

Fig. B-64. Walsh transform of Fig. B-63

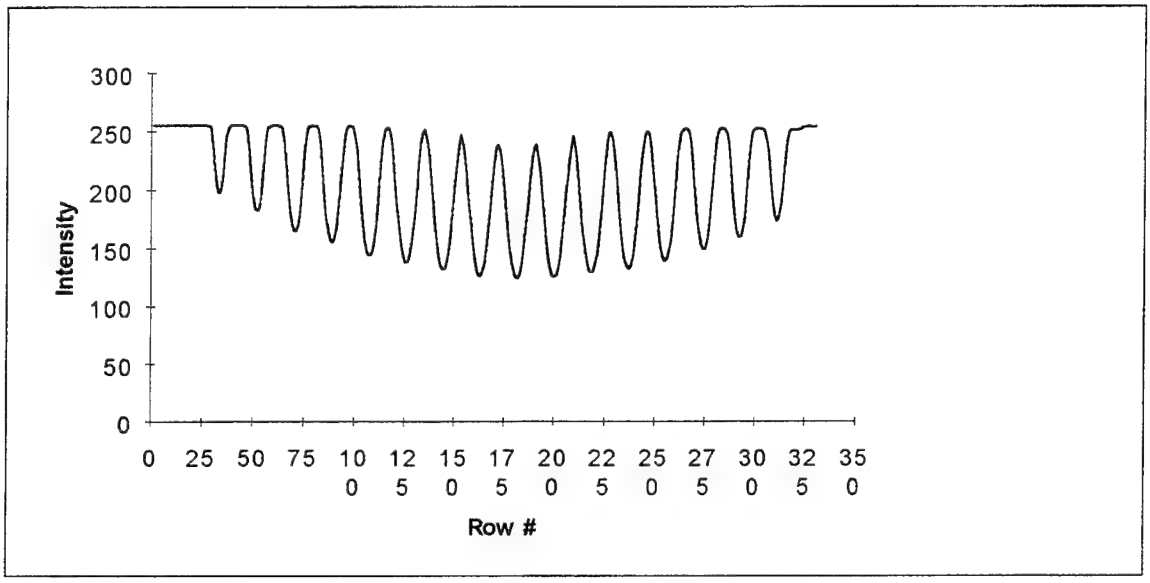

Fig. B-65. Reflection of R2 squashed to preserve vertical sequencies

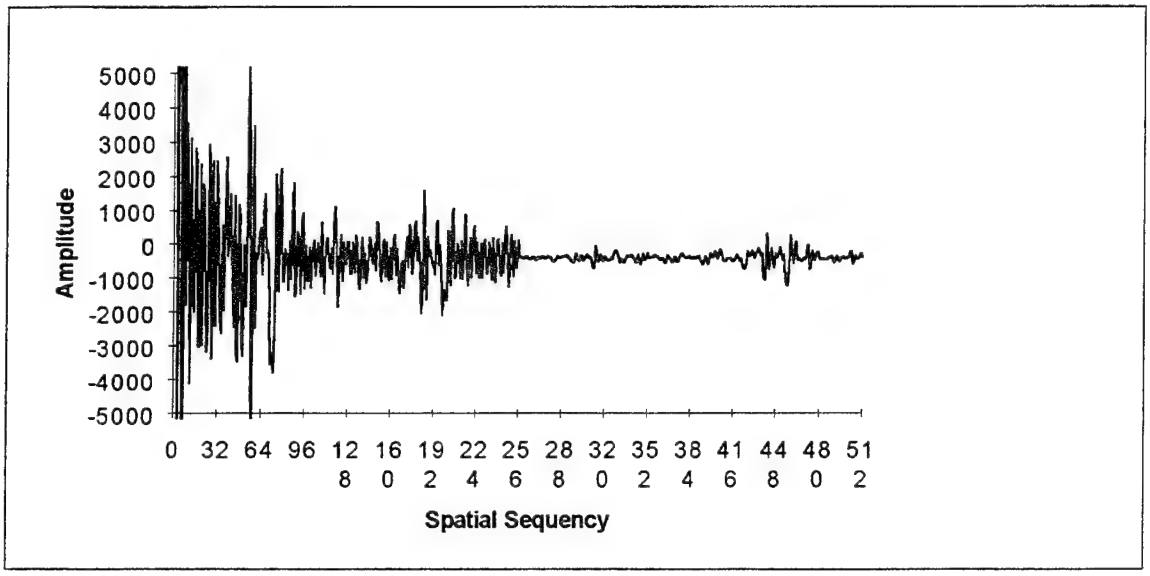

Fig. B-66. Walsh transform of Fig. B-65

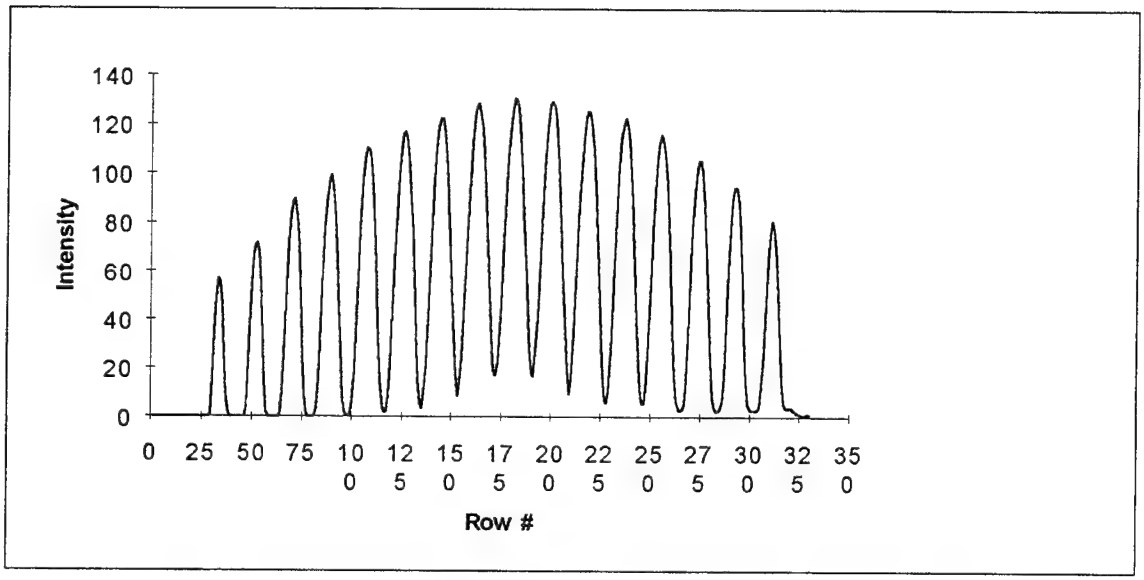

Fig. B-67 Complemented reflection of R2 squashed to preserve vertical sequencies

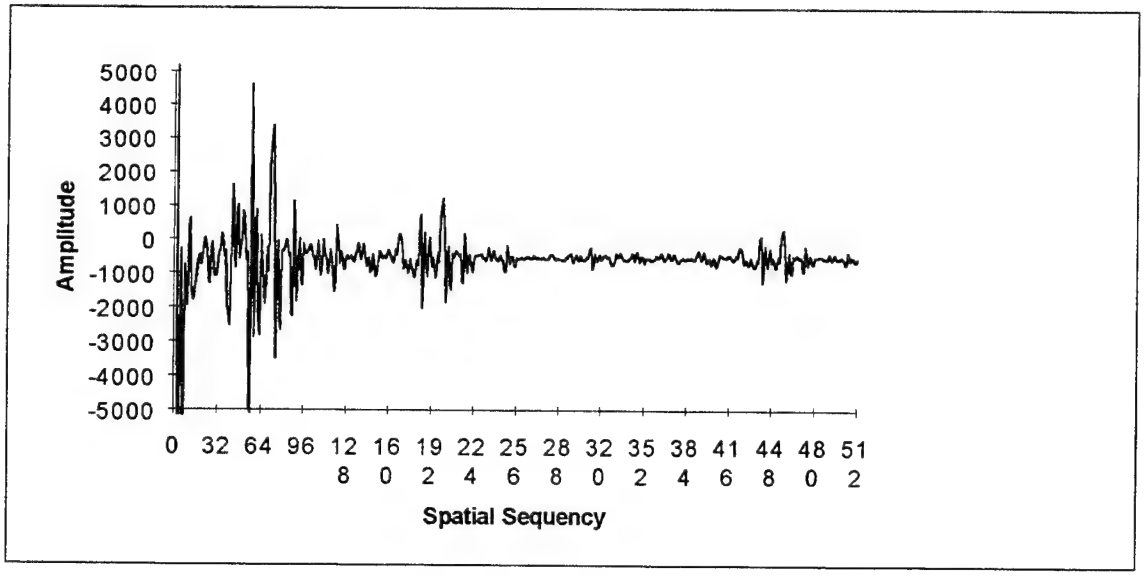

Fig. B-68. Walsh transform of Fig. B-67

APPENDIX C: HELICOPTERS

This appendix is organized like the previous one, but with five different images of a helicopter. Within this appendix are:

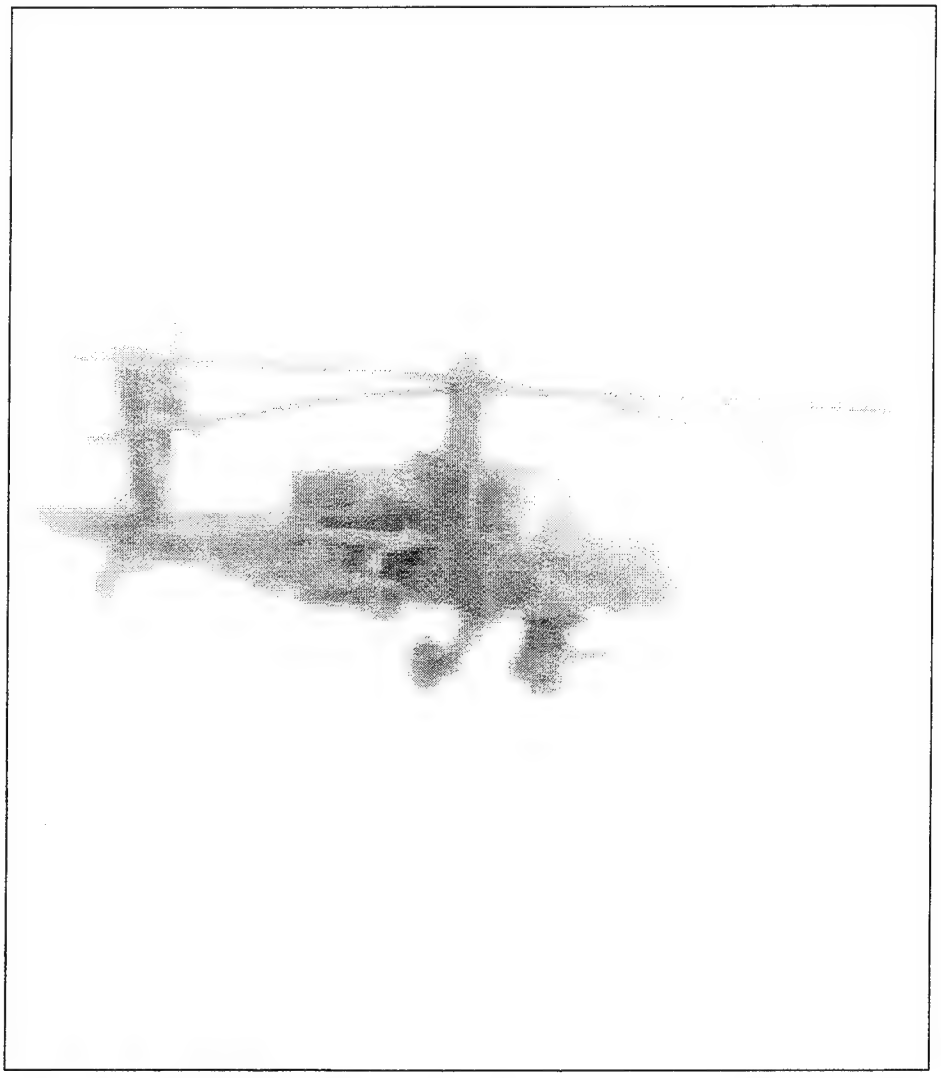

Fig. C-1. H1

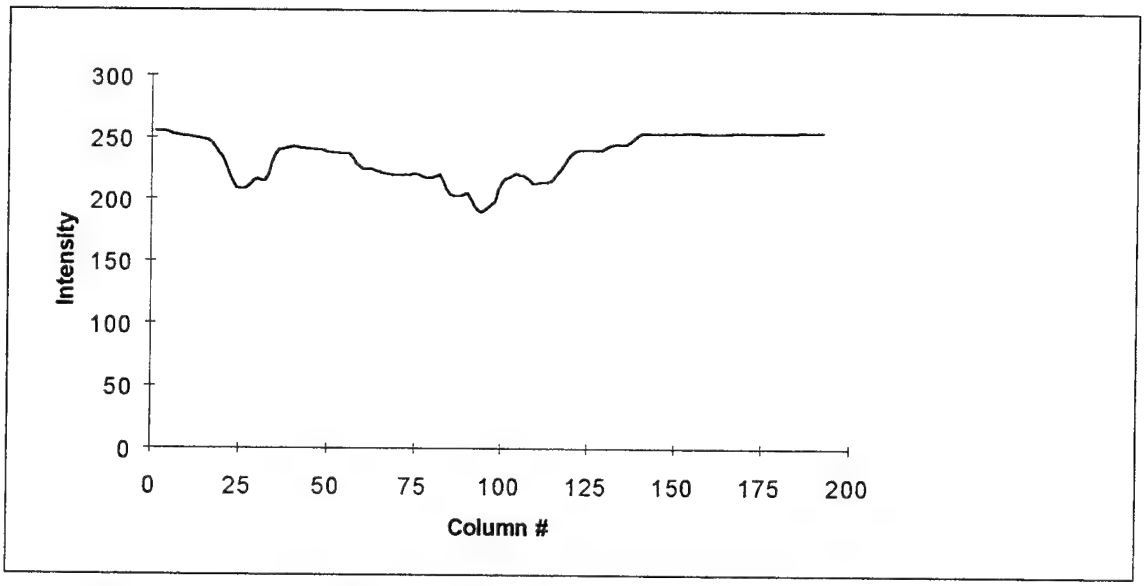

Fig. C-2. H1 squashed to preserve horizontal sequencies

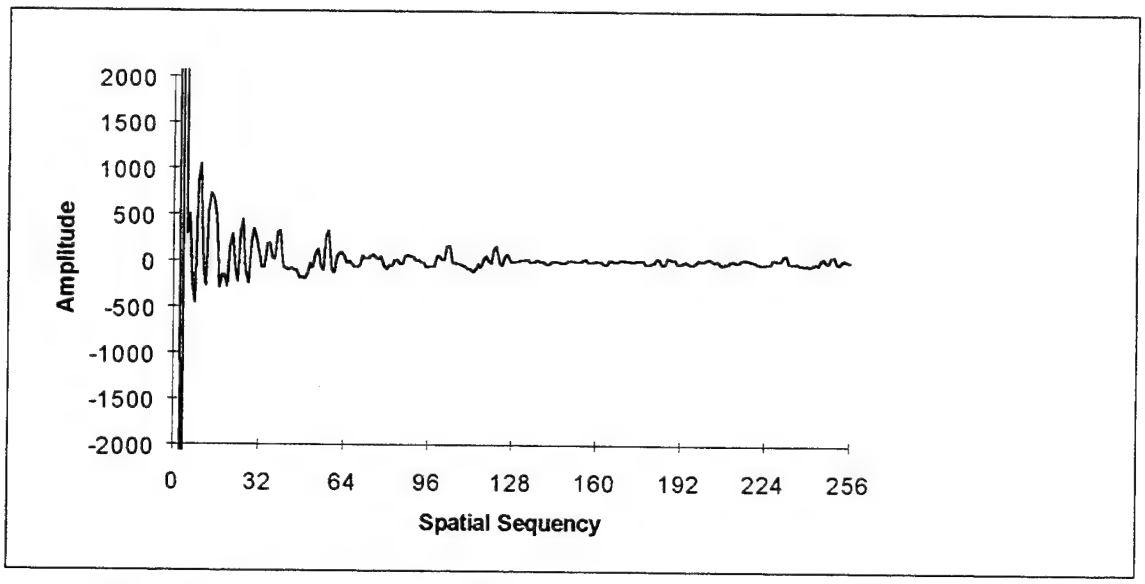

Fig. C-3. Walsh transform of Fig. C-2

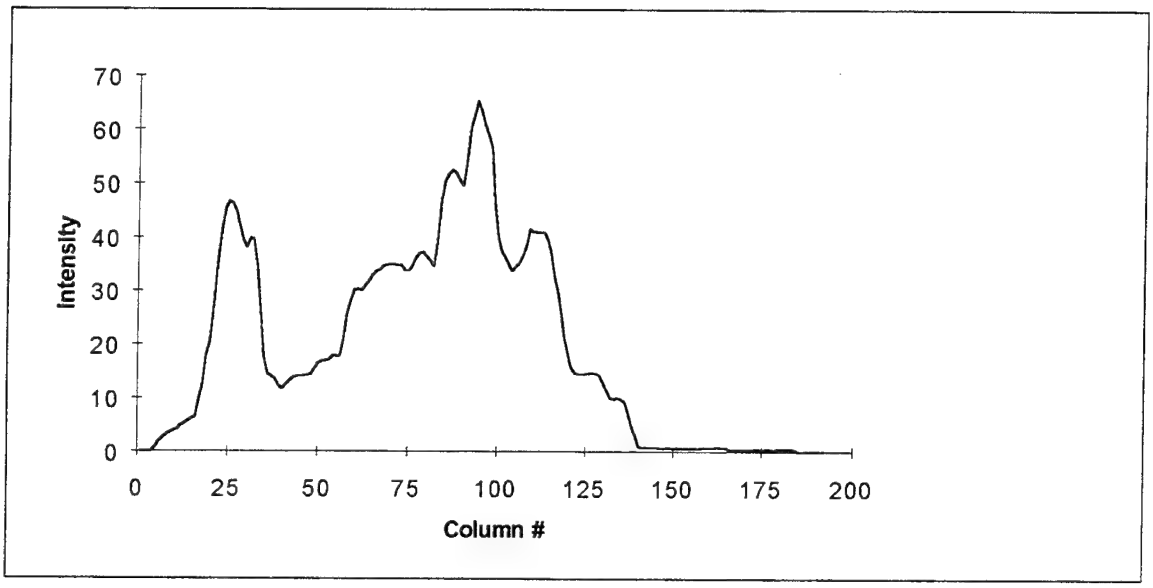

Fig. C-4. Complement of H1 squashed to preserve horizontal sequencies

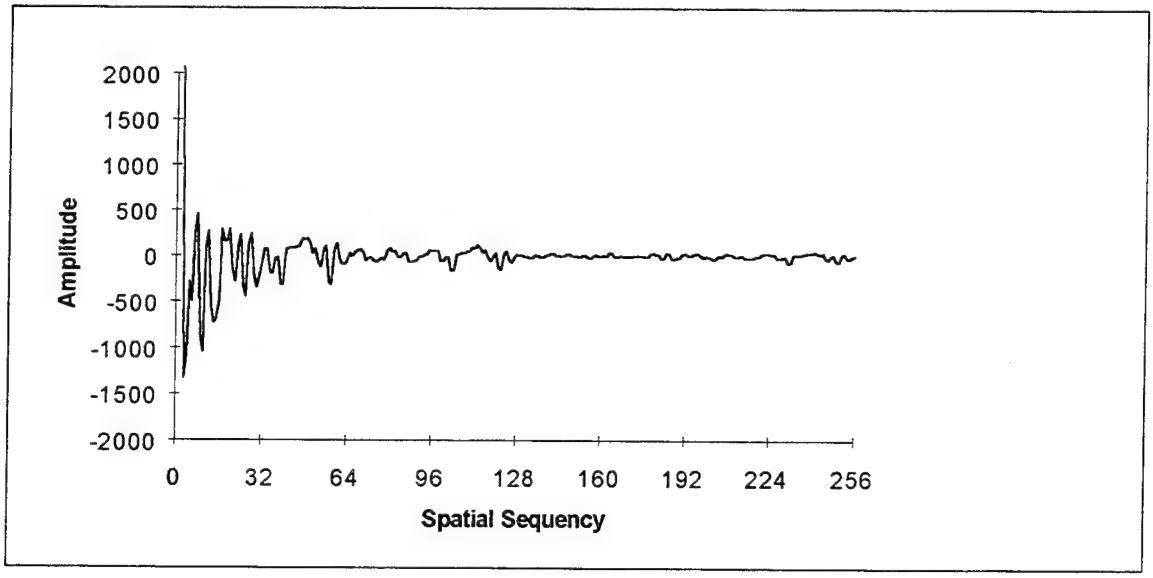

Fig. C-5. Walsh transform of Fig. C-4

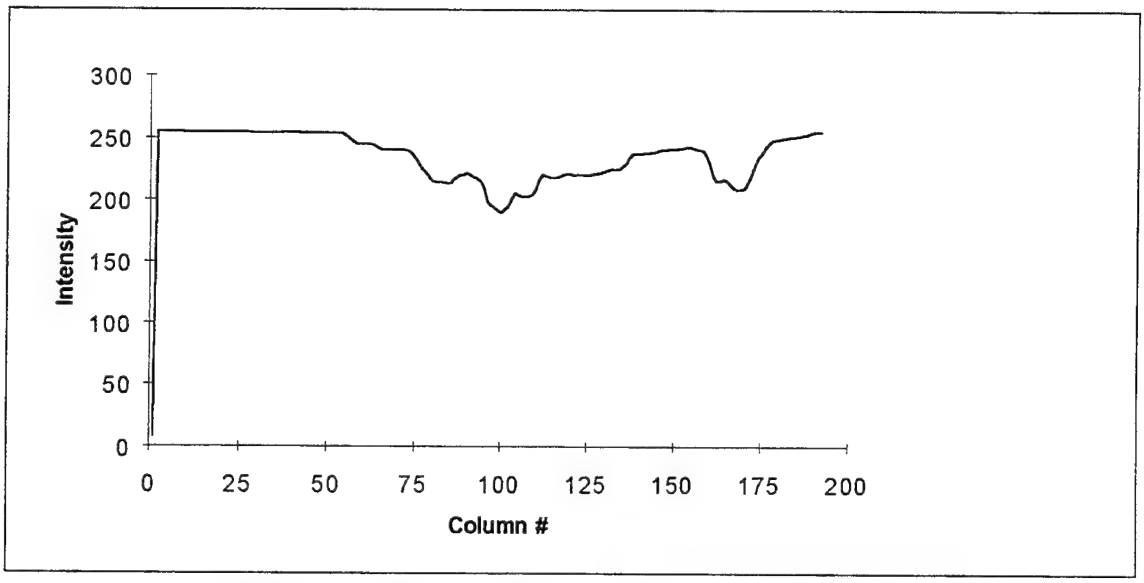

Fig. C-6. Reflection of H-1 squashed to preserve horizontal sequencies

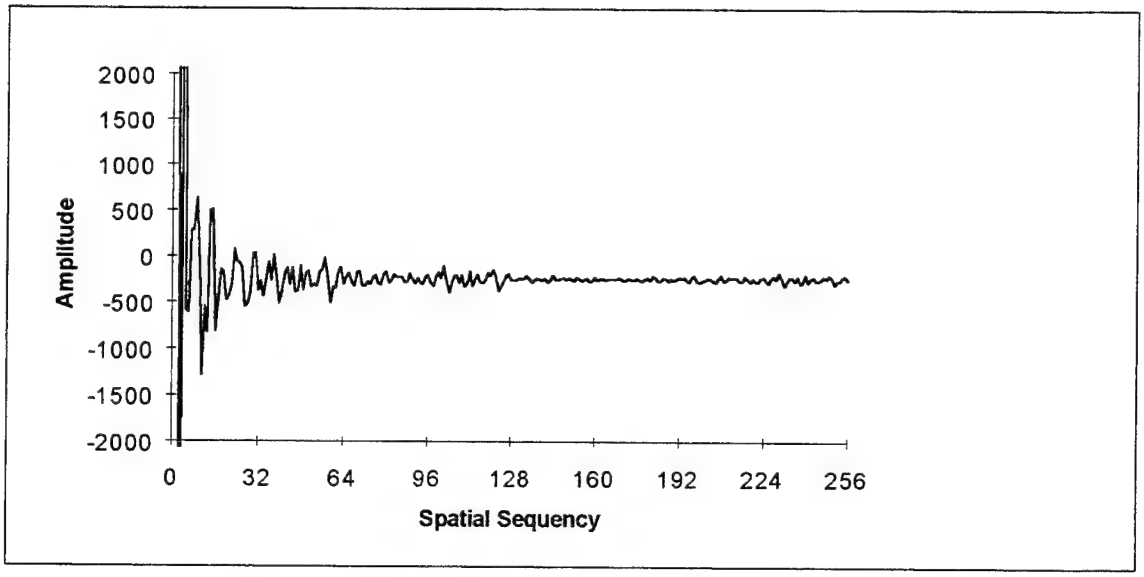

Fig. C-7. Walsh transform of Fig. C-6

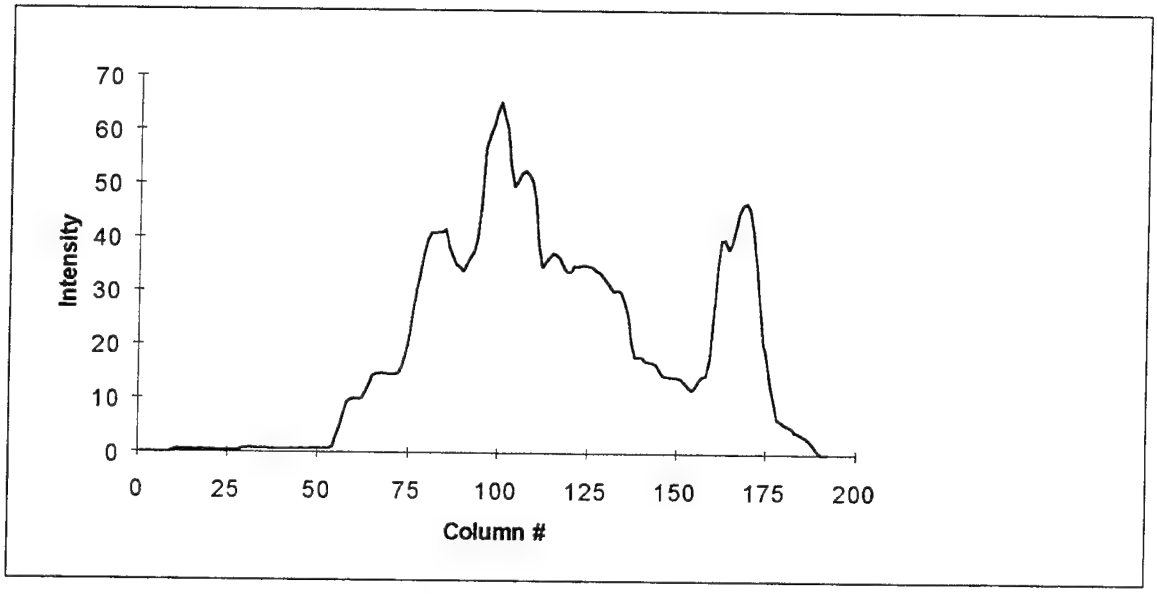

Fig. C-8. Complemented reflection of H1 squashed to preserve horizontal sequencies

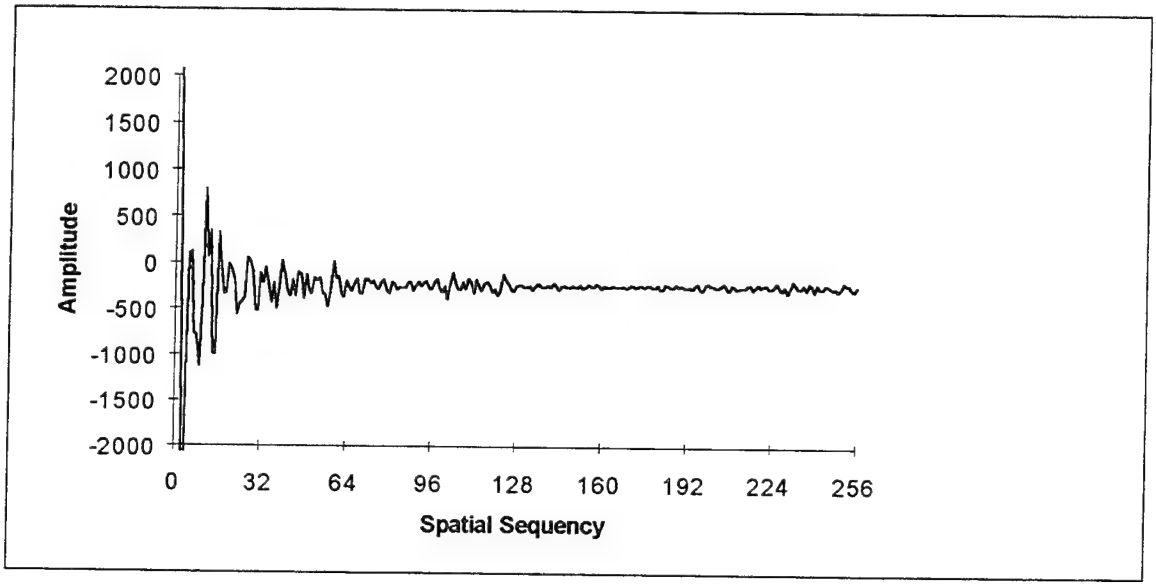

Fig. C-9. Walsh transform of Fig. C-8

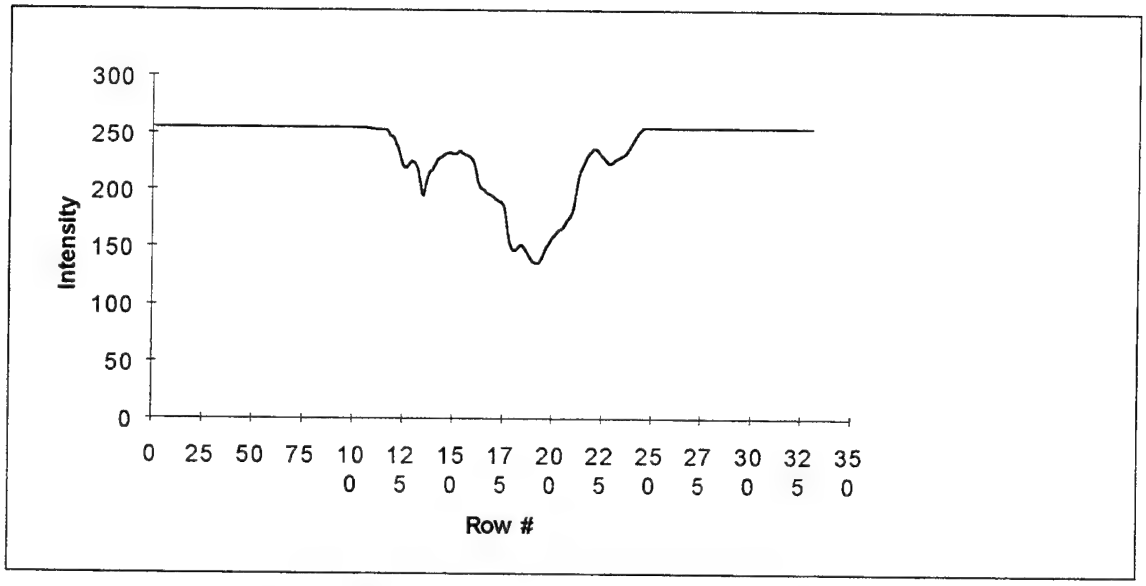

Fig. C-10. H1 squashed to preserve vertical sequencies

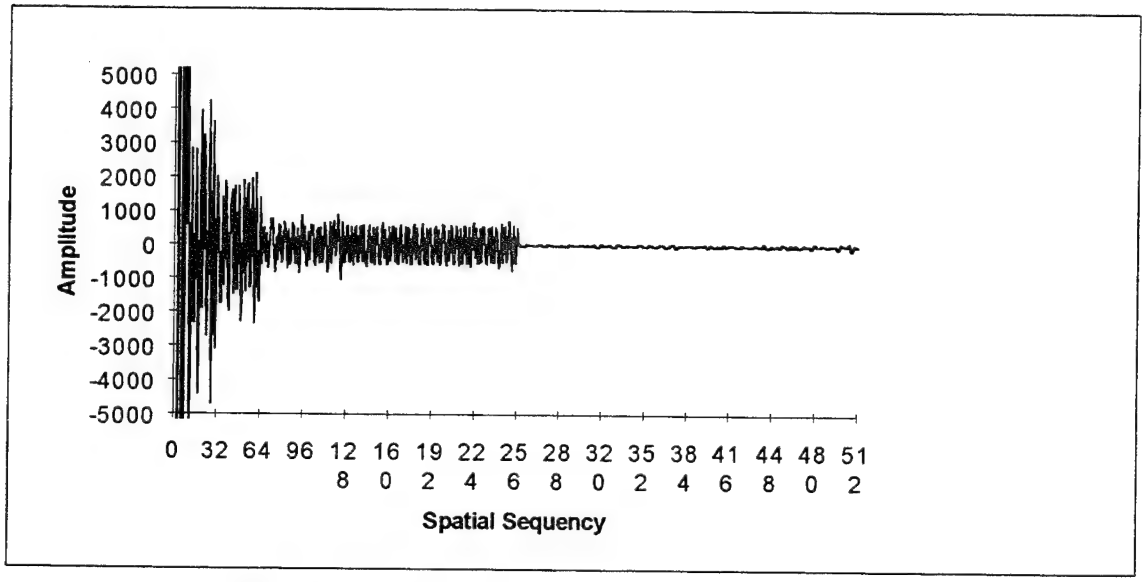

Fig. C-11. Walsh transform of Fig. C-10

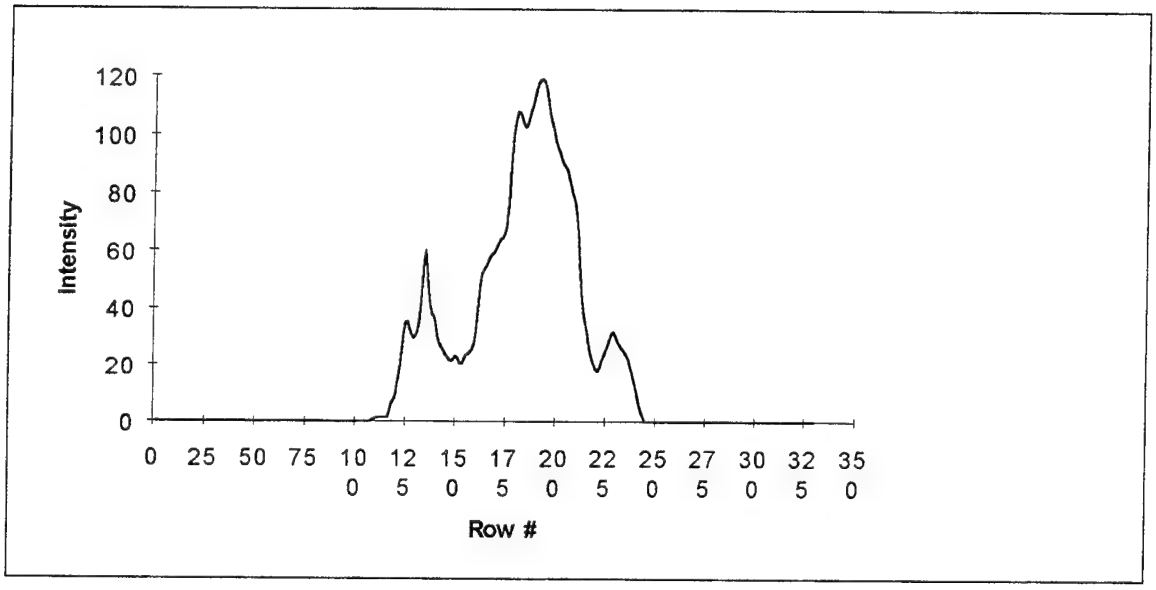

Fig. C-12. Complement of H1 squashed to preserve vertical sequencies

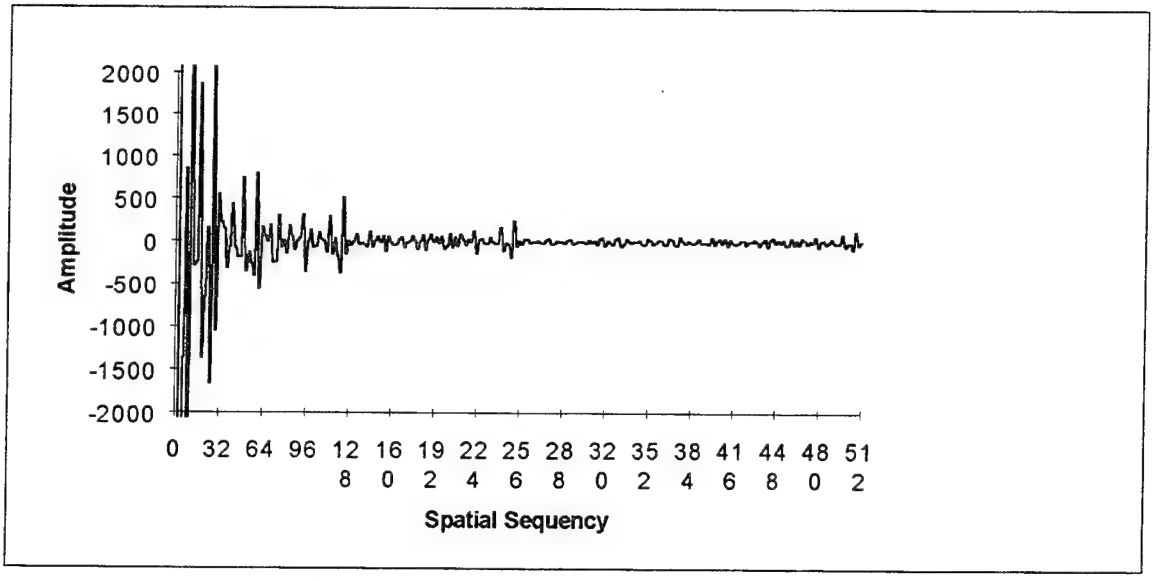

Fig. C-13. Walsh transform of Fig. C-12

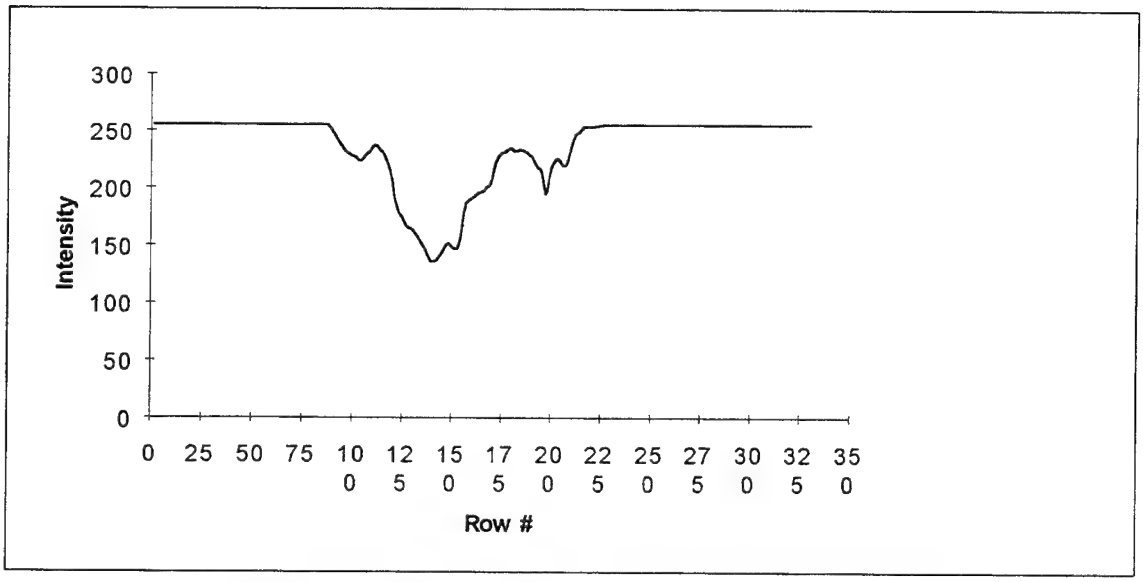

Fig. C-14. Reflection of H1 squashed to preserve vertical sequencies

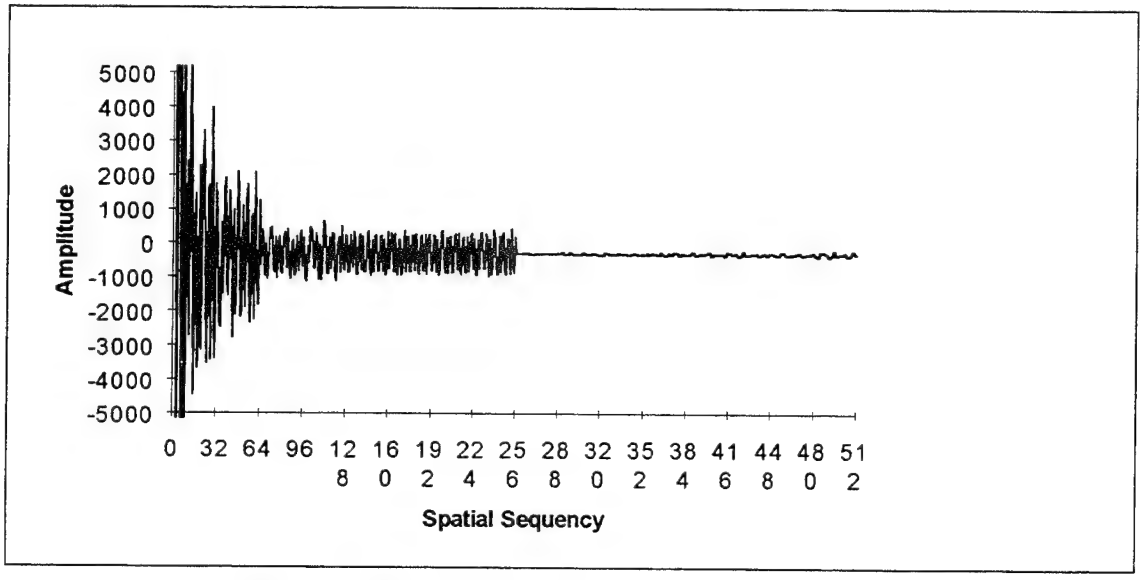

Fig. C-15. Walsh transform of Fig. C-14

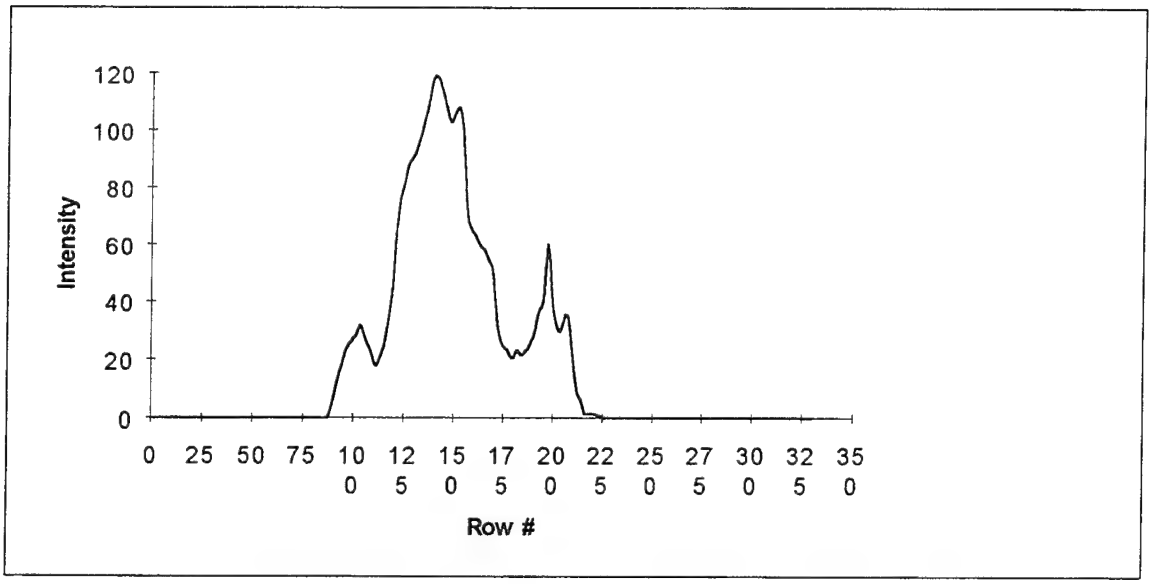

Fig. C-16. Complemented reflection of H1 squashed to preserve vertical sequencies

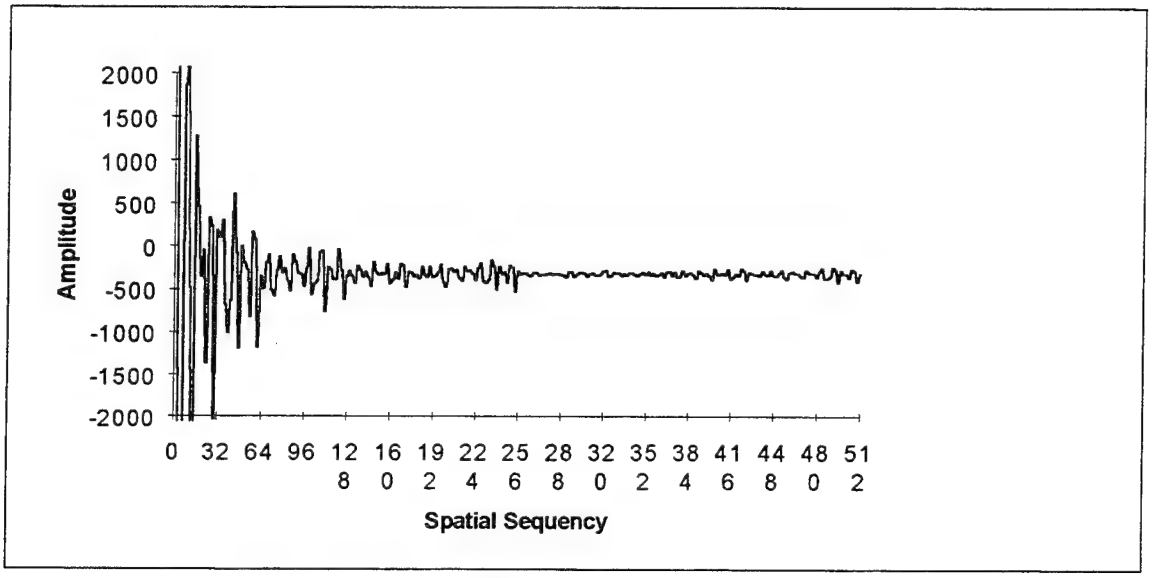

Fig. C-17. Walsh transform of Fig. C-16

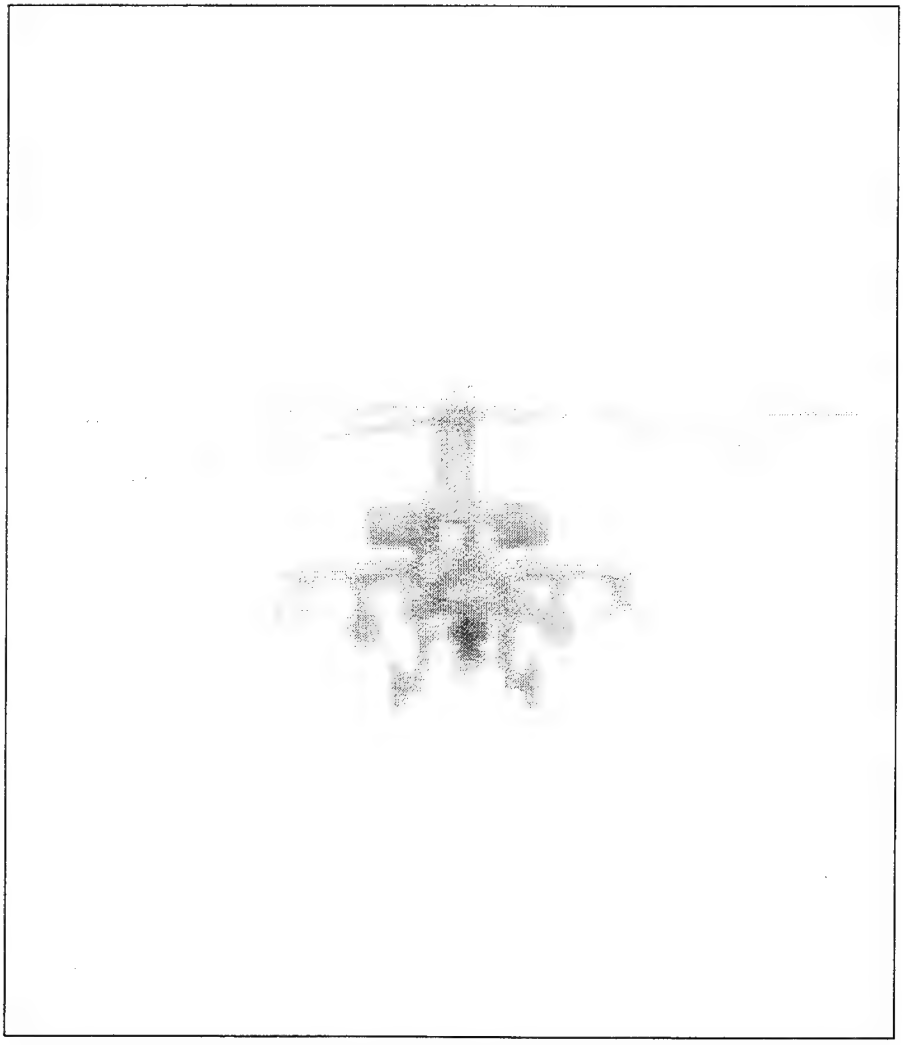

Fig C-18. H2

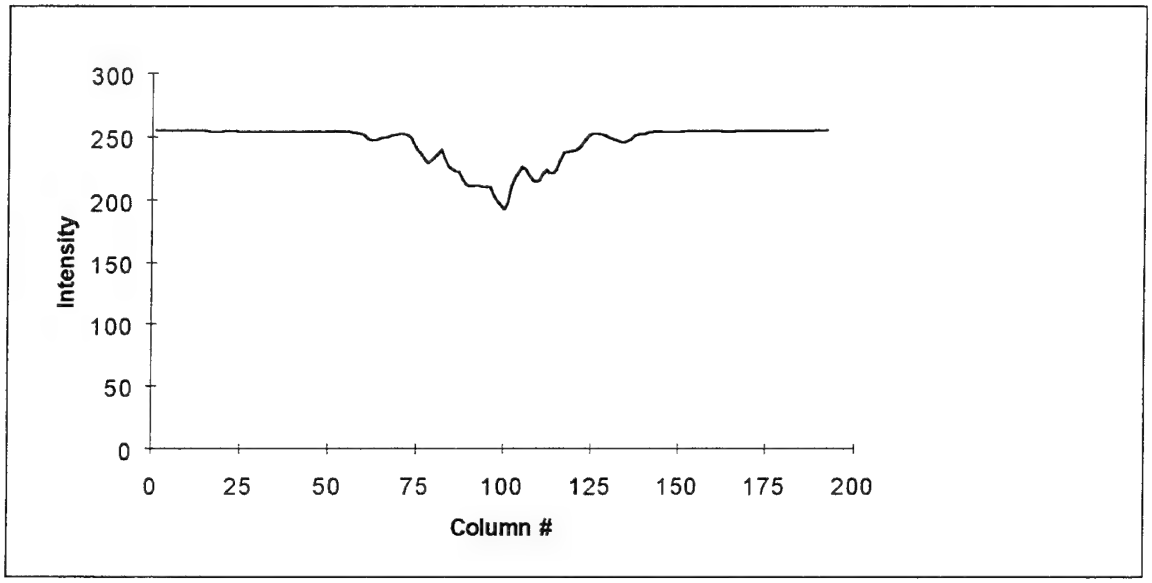

Fig. C-19. H2 squashed to preserve horizontal sequencies

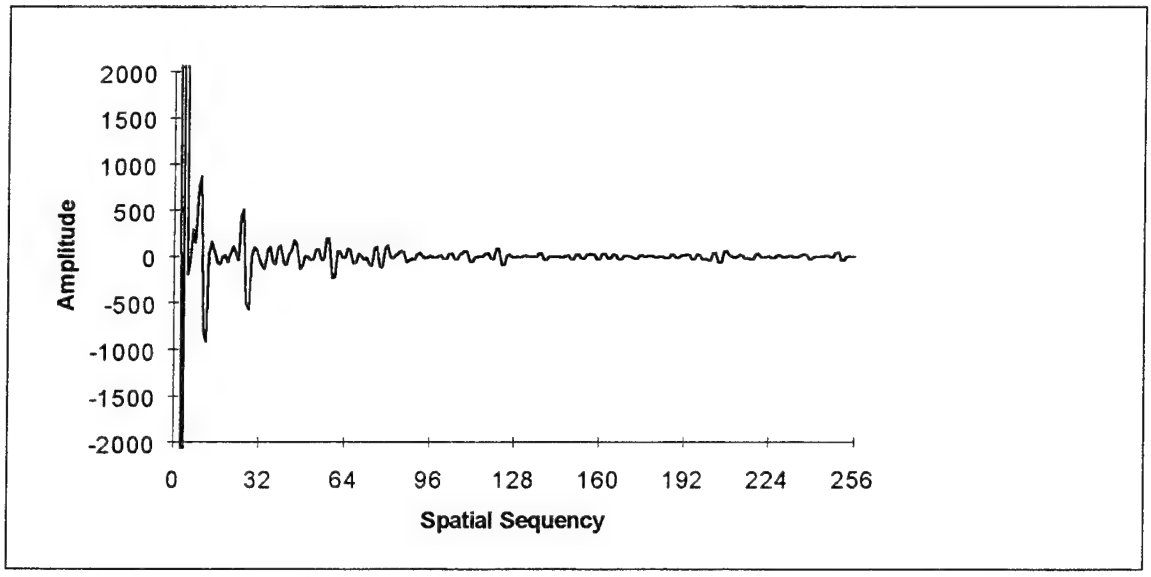

Fig. C-20. Walsh transform of Fig. C-19

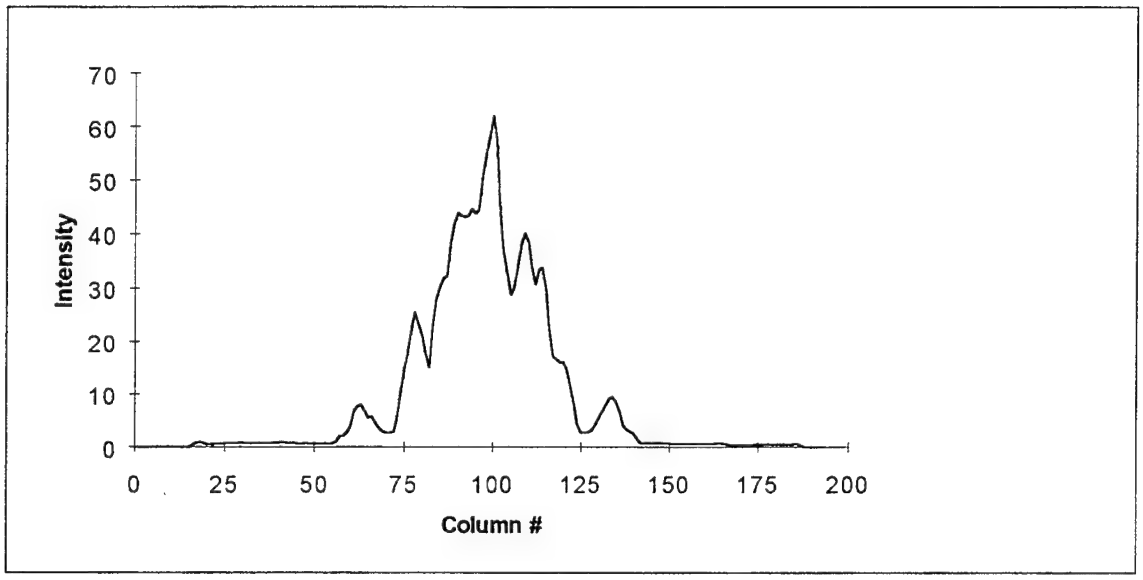

Fig. C-21. Complement of H2 squashed to preserve horizontal sequencies

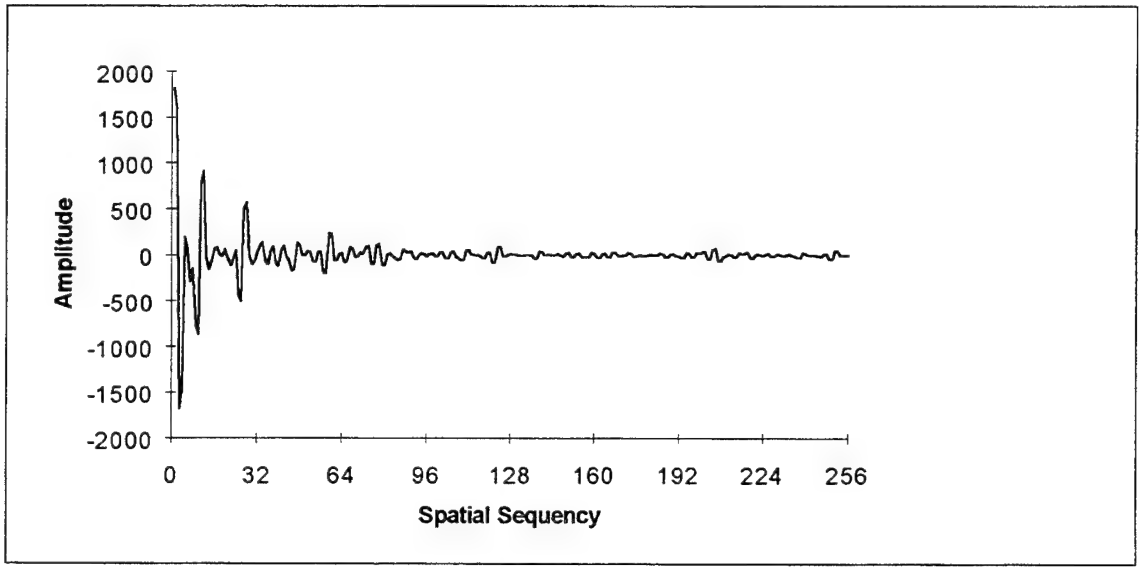

Fig. C-22. Walsh transform of Fig. C-21

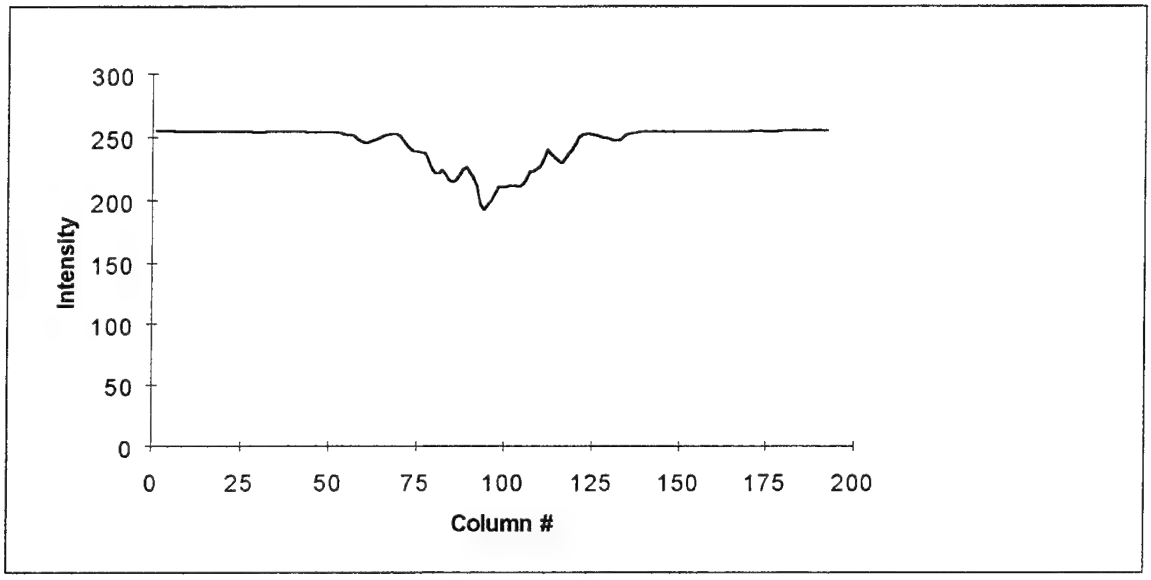

Fig. C-23. Reflection of H2 squashed to preserve horizontal sequencies

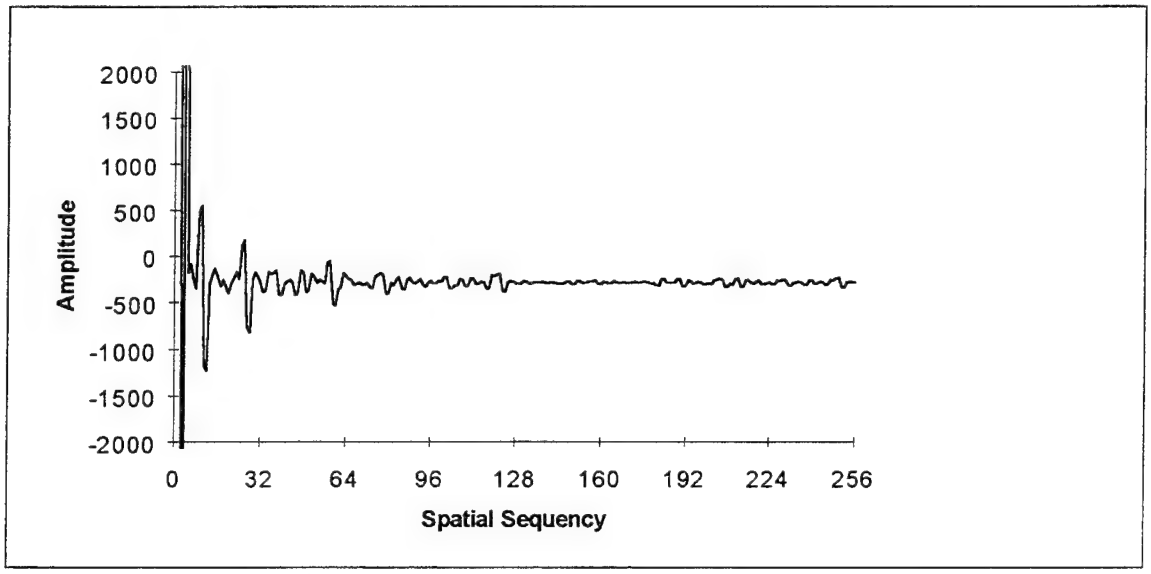

Fig. C-24. Walsh transform of Fig. C-23

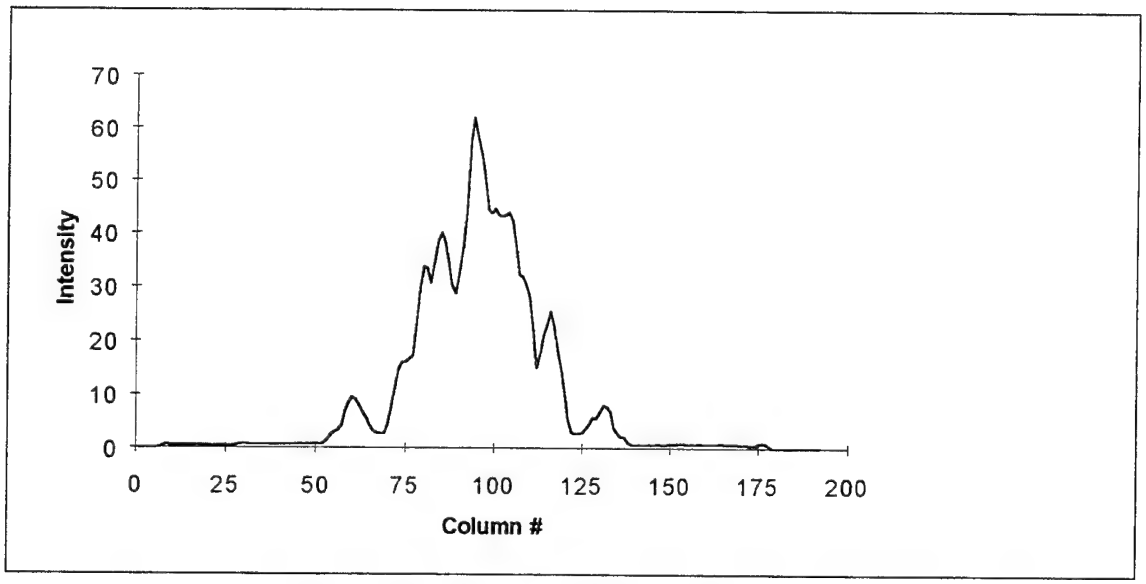

Fig. C-25. Complemented reflection of H2 squashed to preserve horizontal sequencies

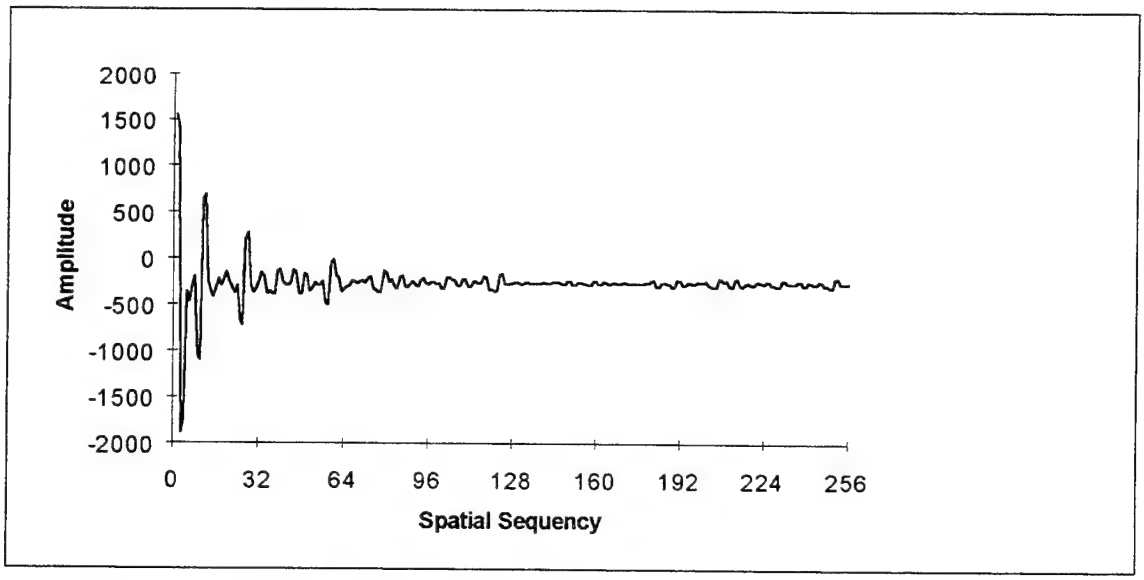

Fig. C-26. Walsh transform of Fig. C-25

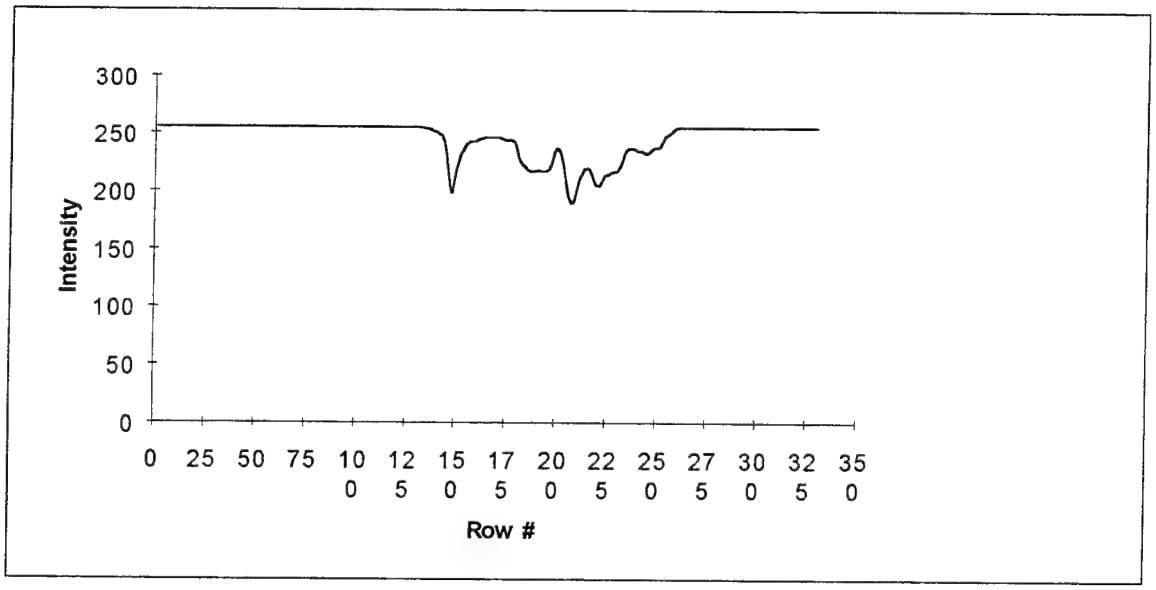

Fig. C-27. H2 squashed to preserve vertical sequencies

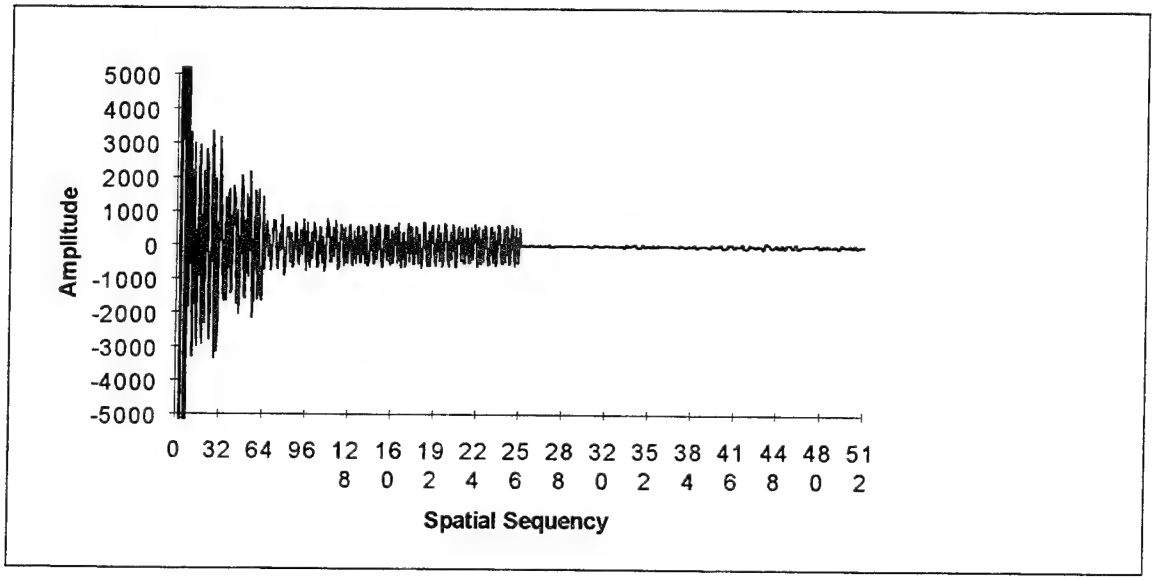

Fig. C-28. Walsh transform of Fig. C-27

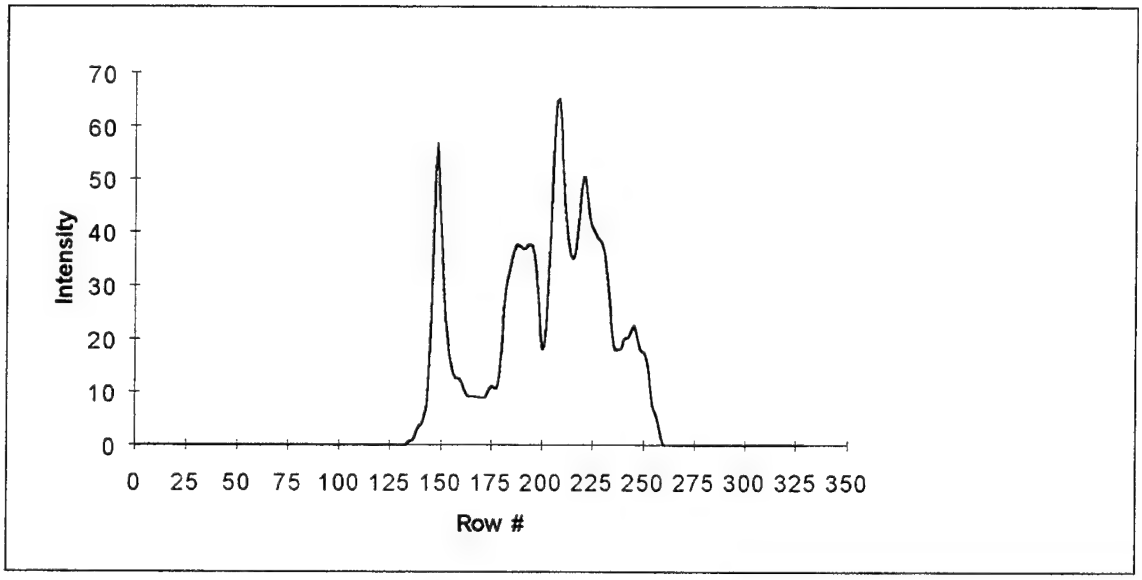

Fig. C-29. Complement of H2 squashed to preserve vertical sequencies

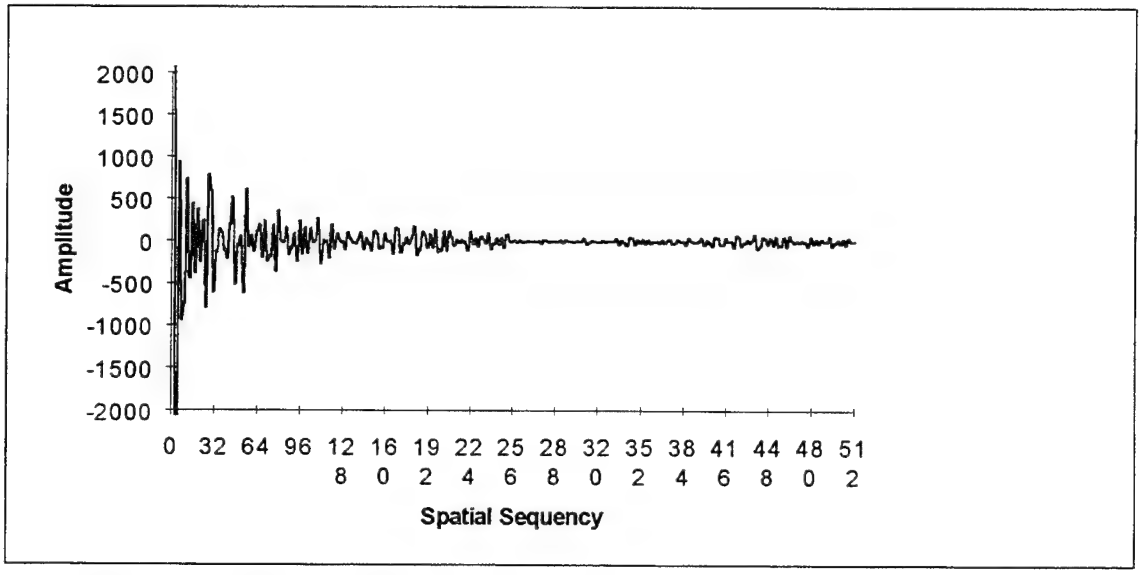

Fig. C-30. Walsh transform of Fig. C-29

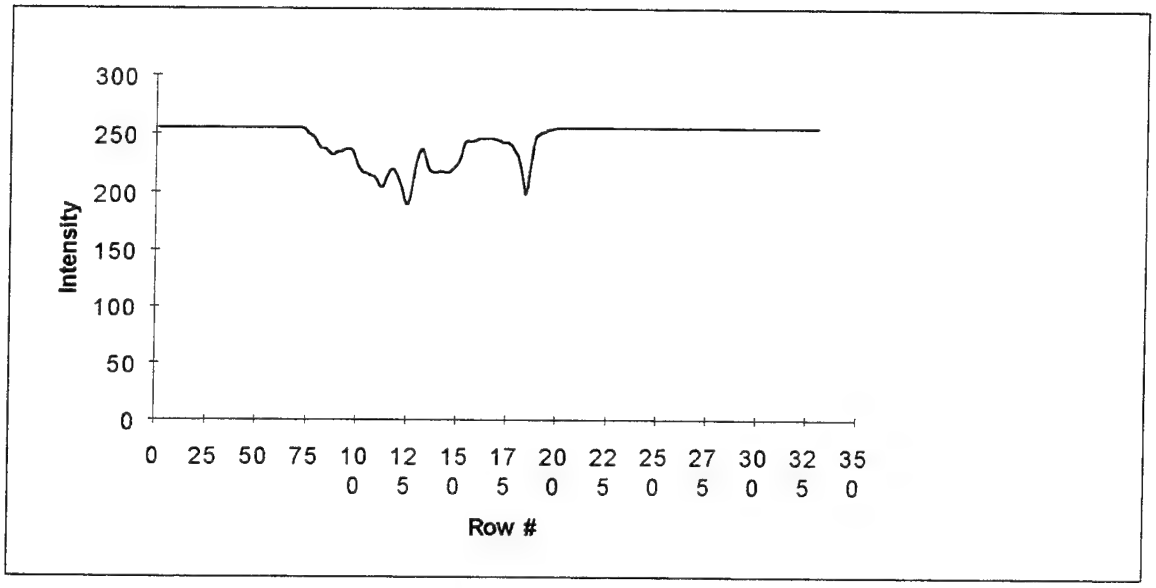

Fig. C-31. Reflection of H2 squashed to preserve vertical sequencies

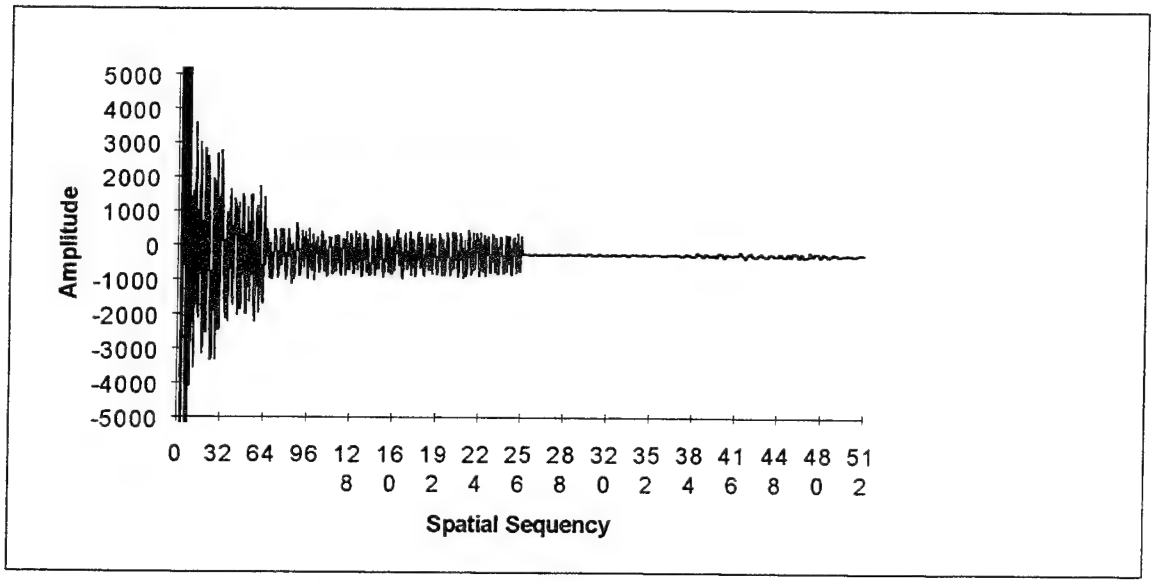

Fig. C-32. Walsh transform of Fig. C-31

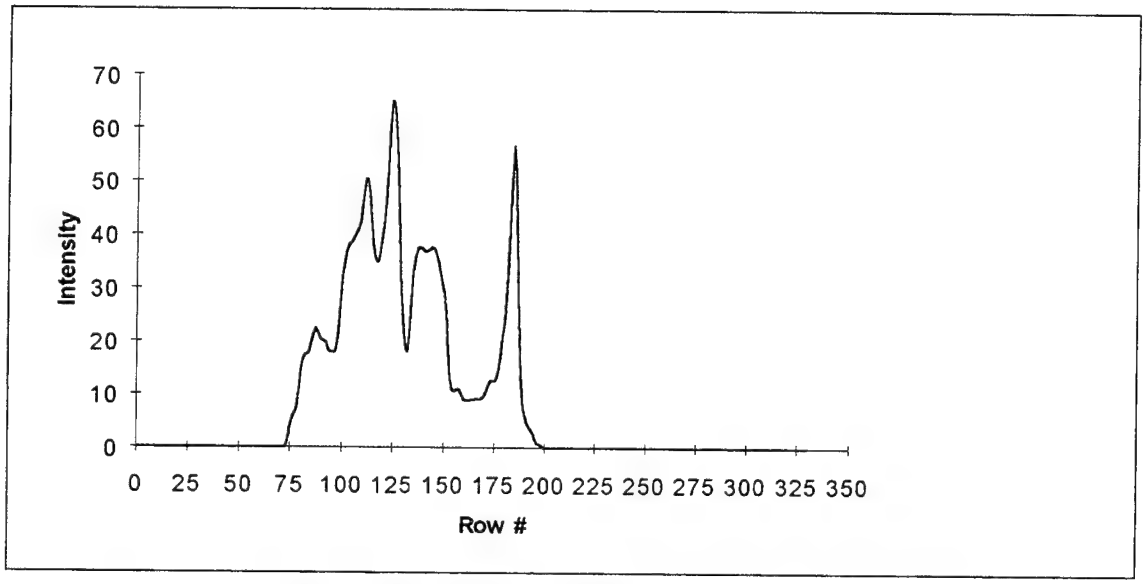

Fig. C-33. Complemented reflection of H2 squashed to preserve vertical sequencies

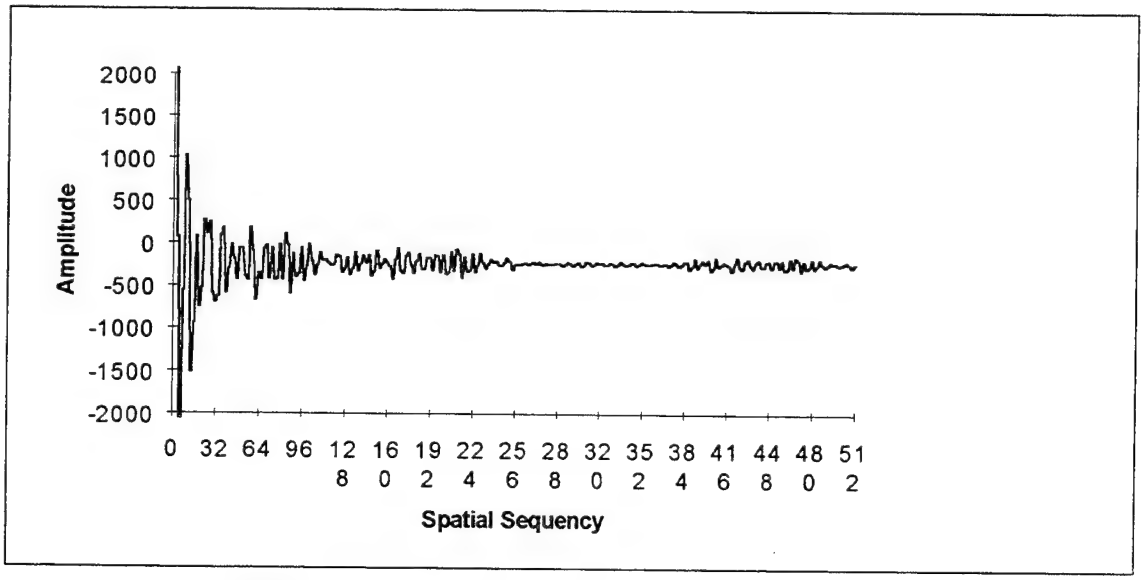

Fig. C-34. Walsh transform of Fig. C-33

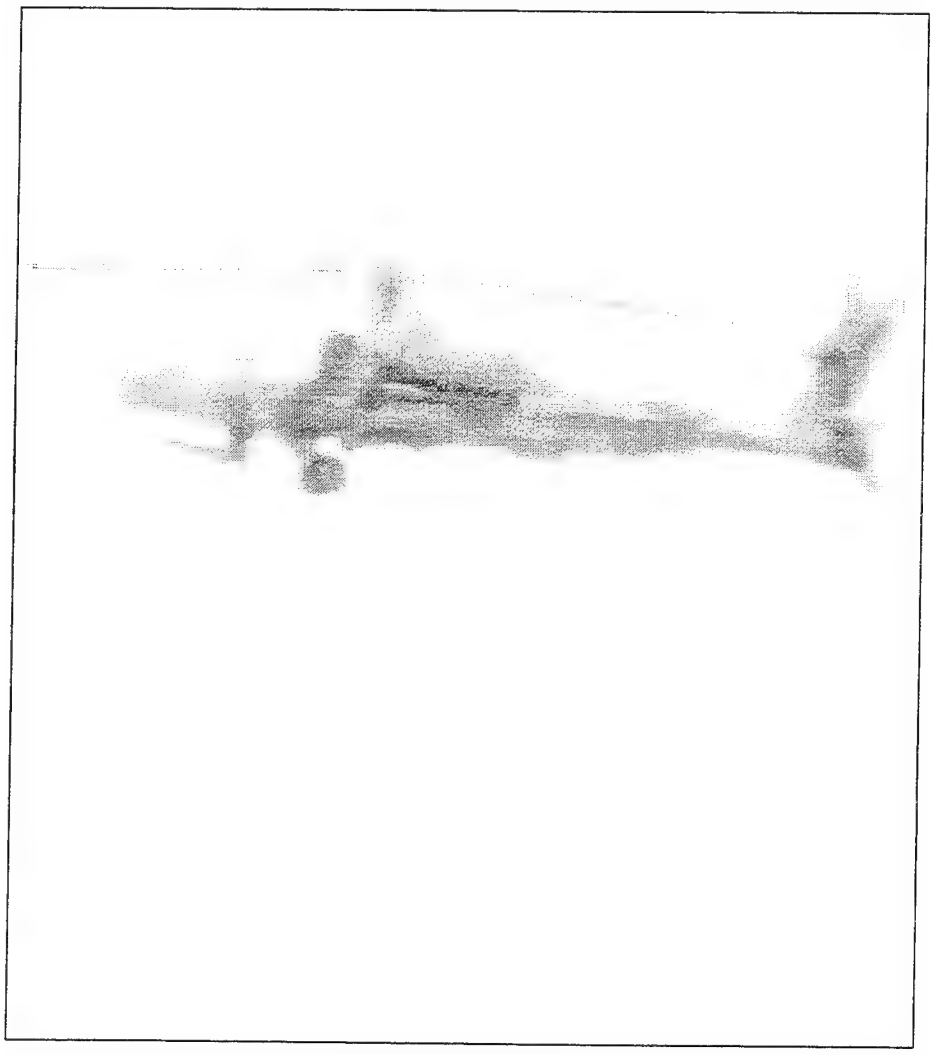

Fig. C-35. H3

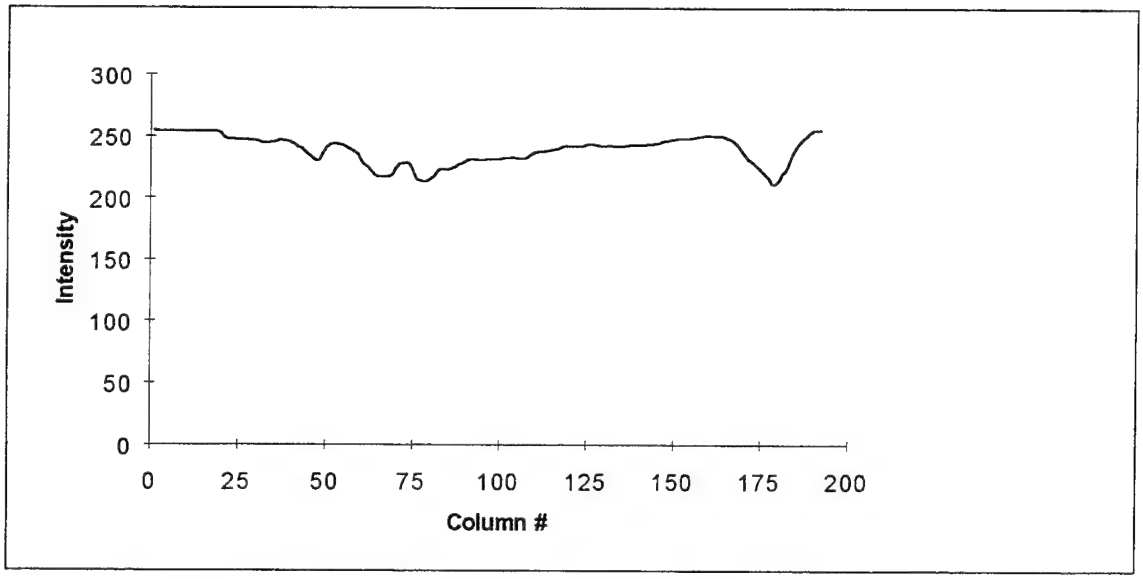

Fig. C-36. H3 squashed to preserve horizontal sequencies

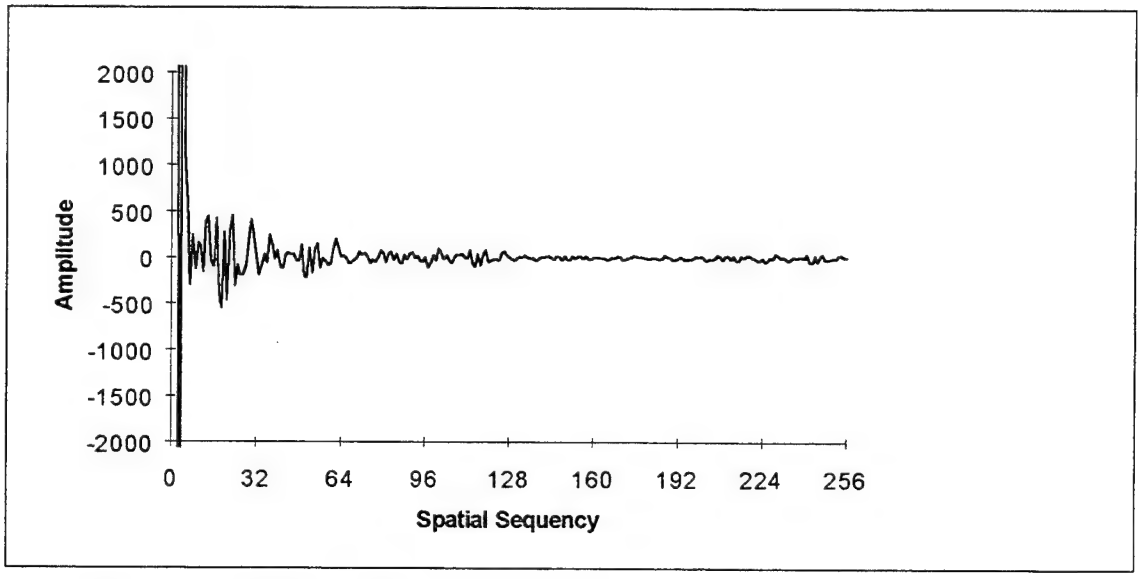

Fig. C-37. Walsh transform of Fig. C-36

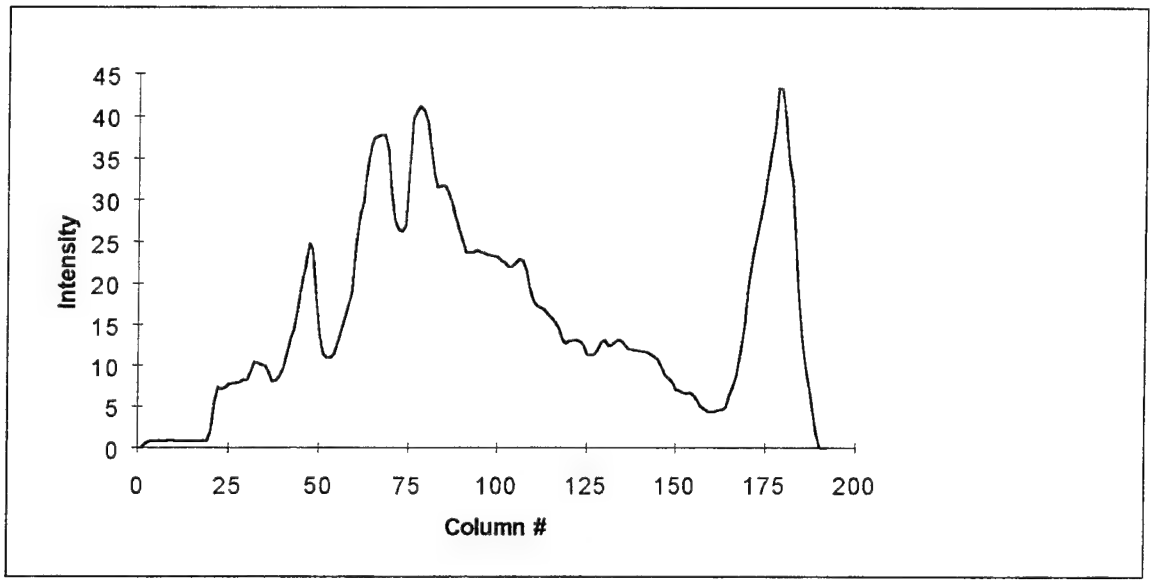

Fig. C-38. Complement of H3 squashed to preserve horizontal sequencies

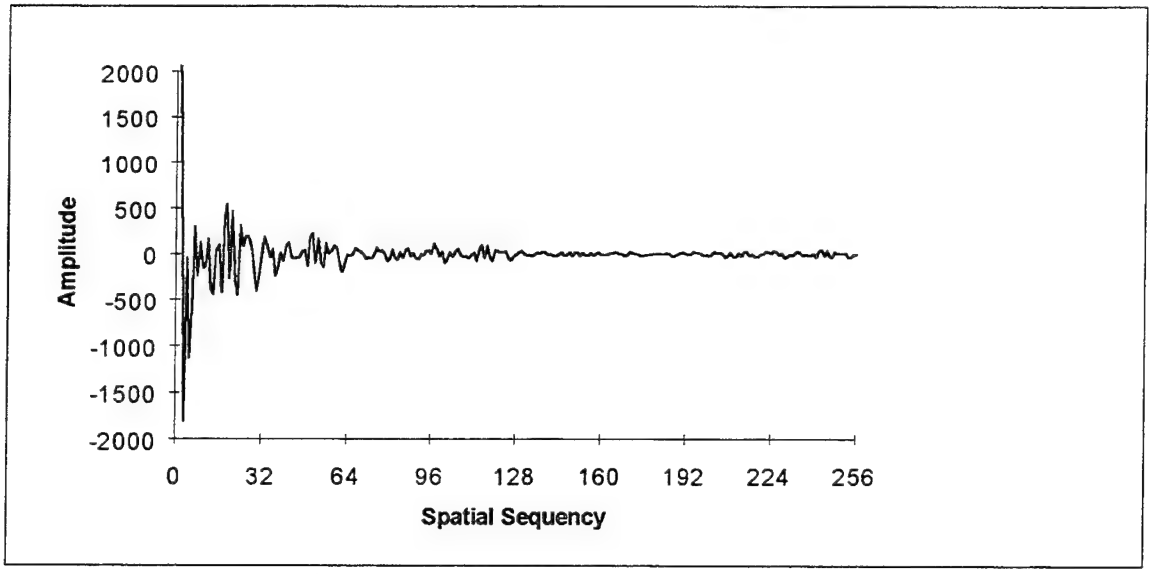

Fig. C-39. Walsh transform of Fig. C-38

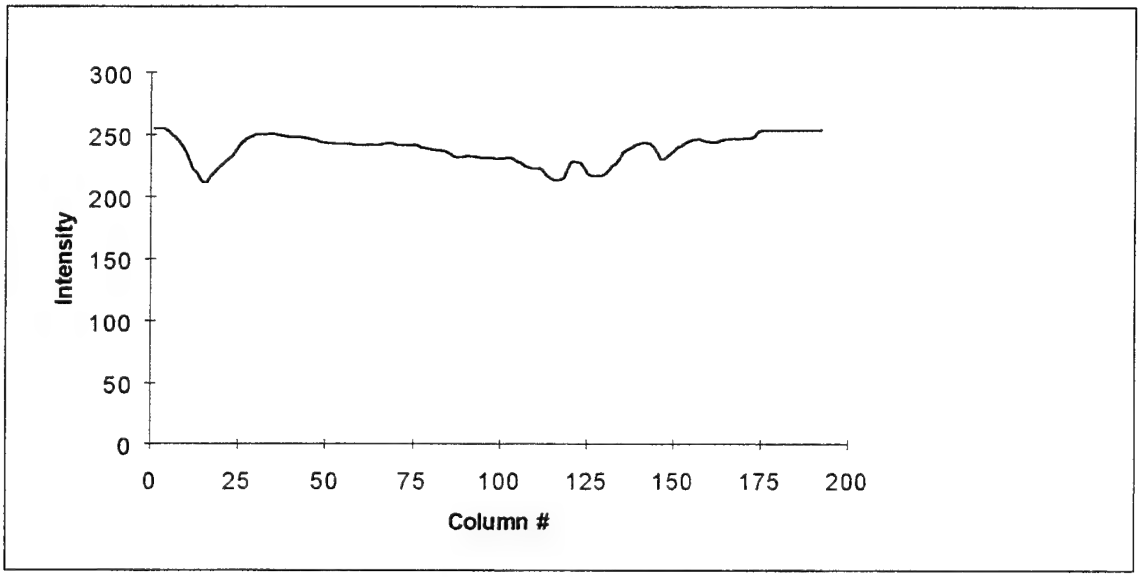

Fig. C-40. Reflection of H3 squashed to preserve horizontal sequencies

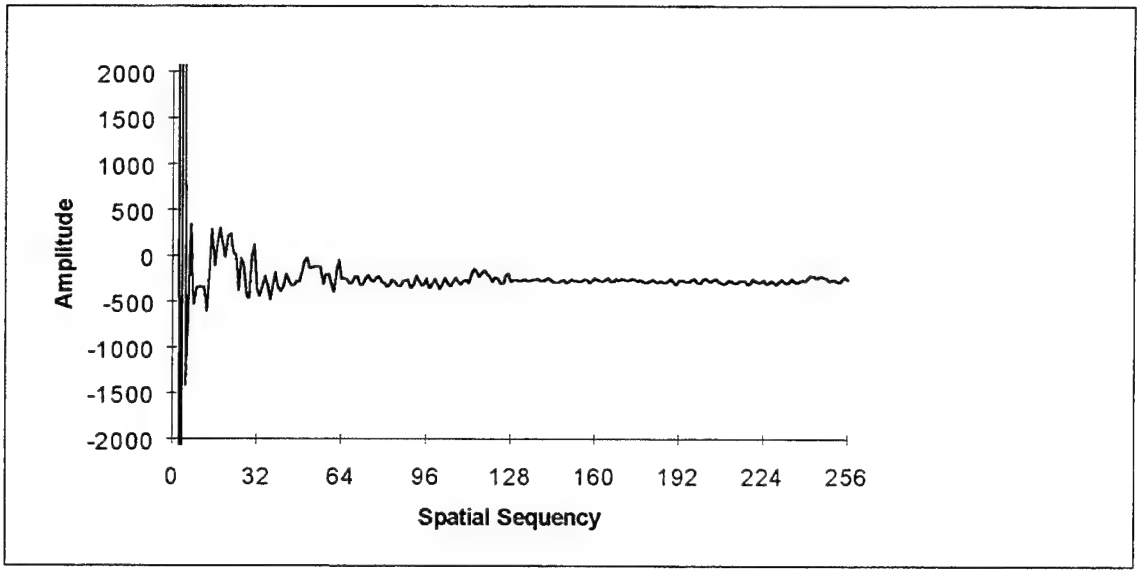

Fig. C-41. Walsh transform of Fig. C-40

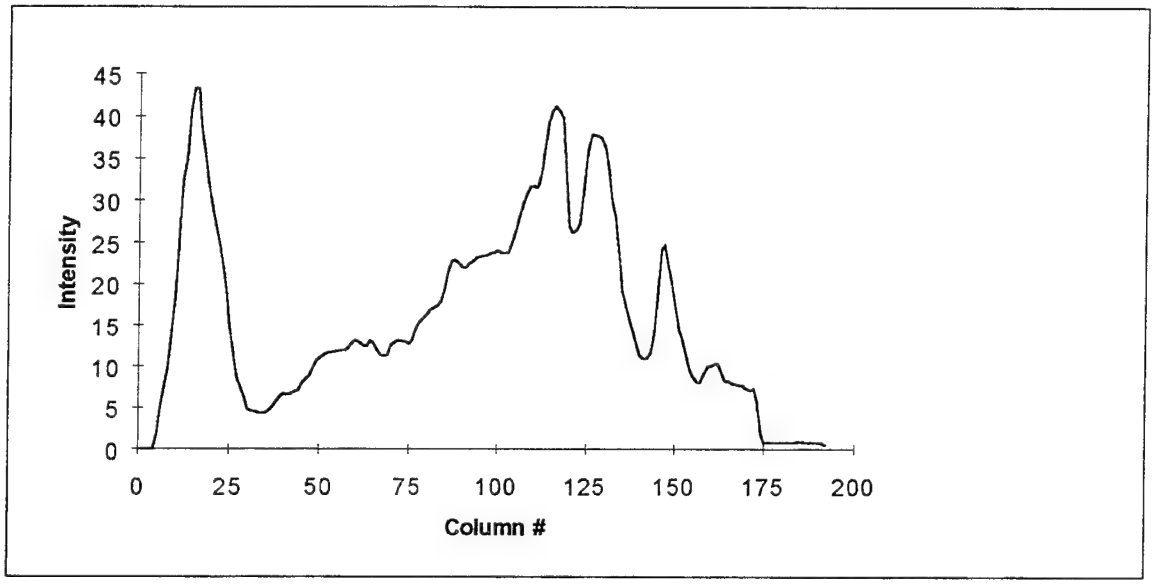

Fig. C-42. Complemented reflection of H3 squashed to preserve horizontal sequencies

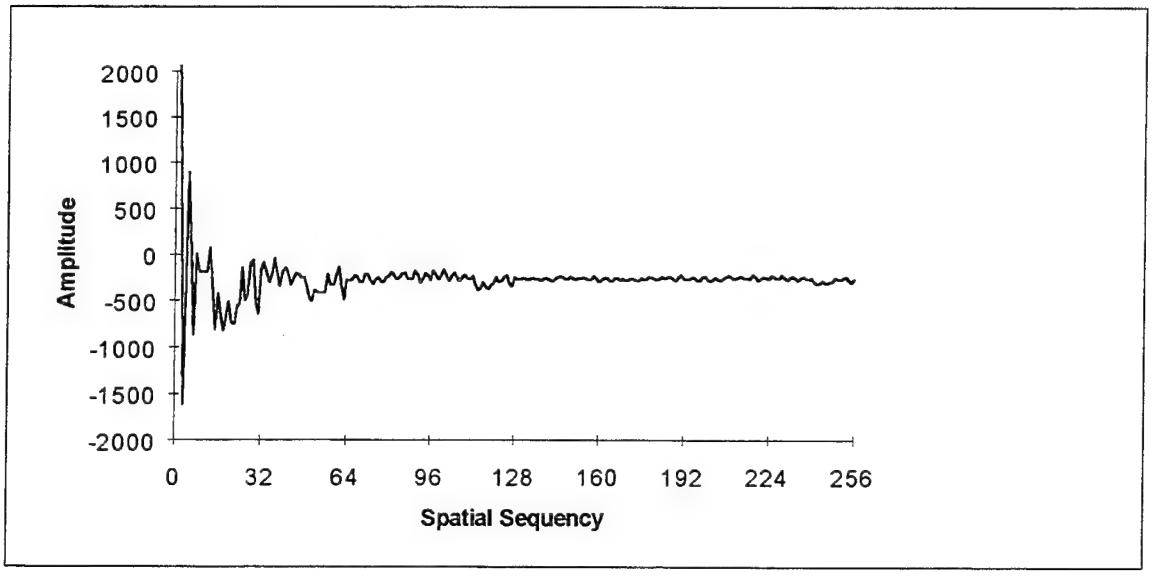

Fig. C-43. Walsh transform of Fig. C-42

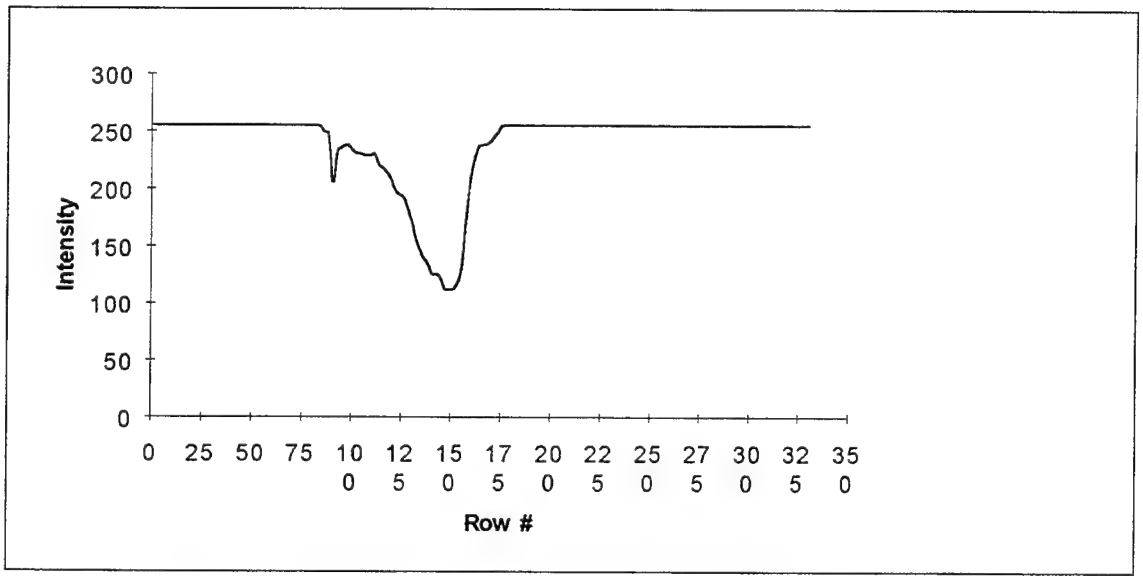

Fig. C-44. H3 squashed to preserve vertical sequencies

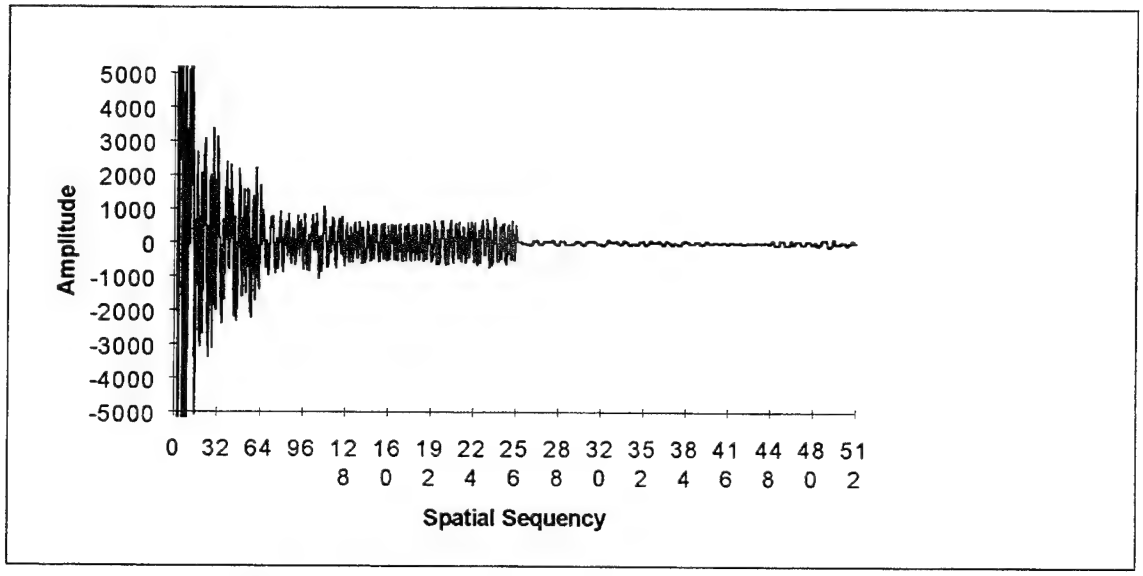

Fig. C-45. Walsh transform of Fig. C-44

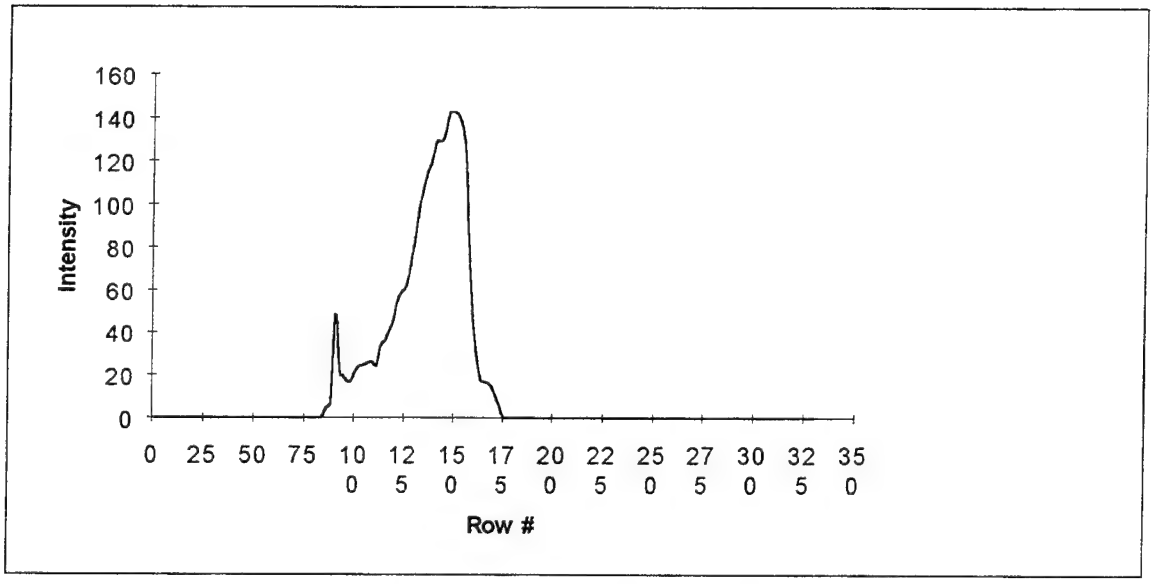

Fig. C-46. Complement of H3 squashed to preserve vertical sequencies

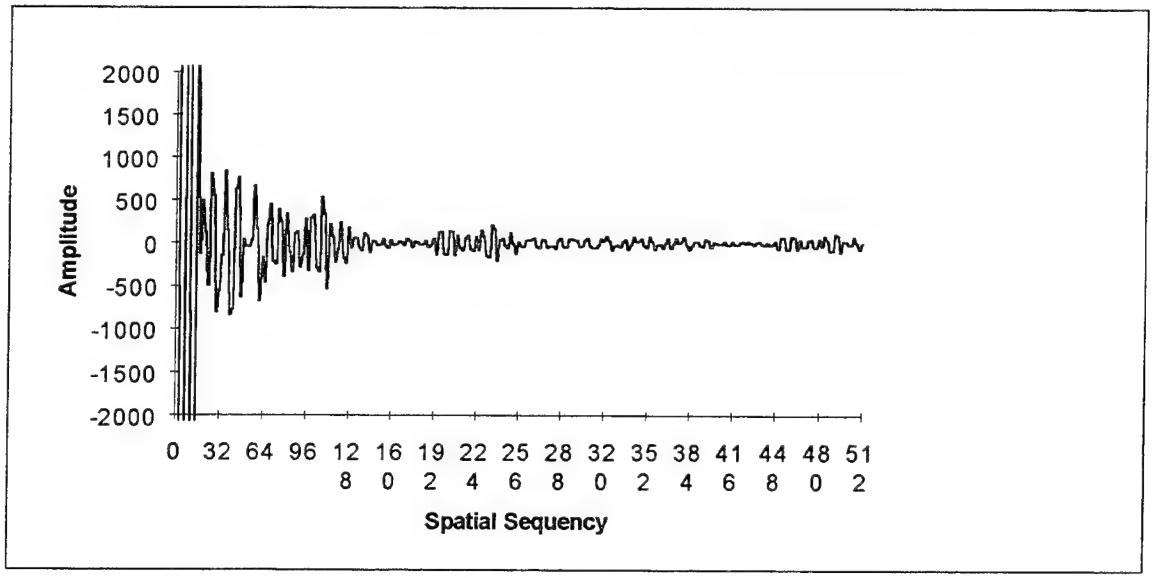

Fig. C-47. Walsh transform of Fig. C-46

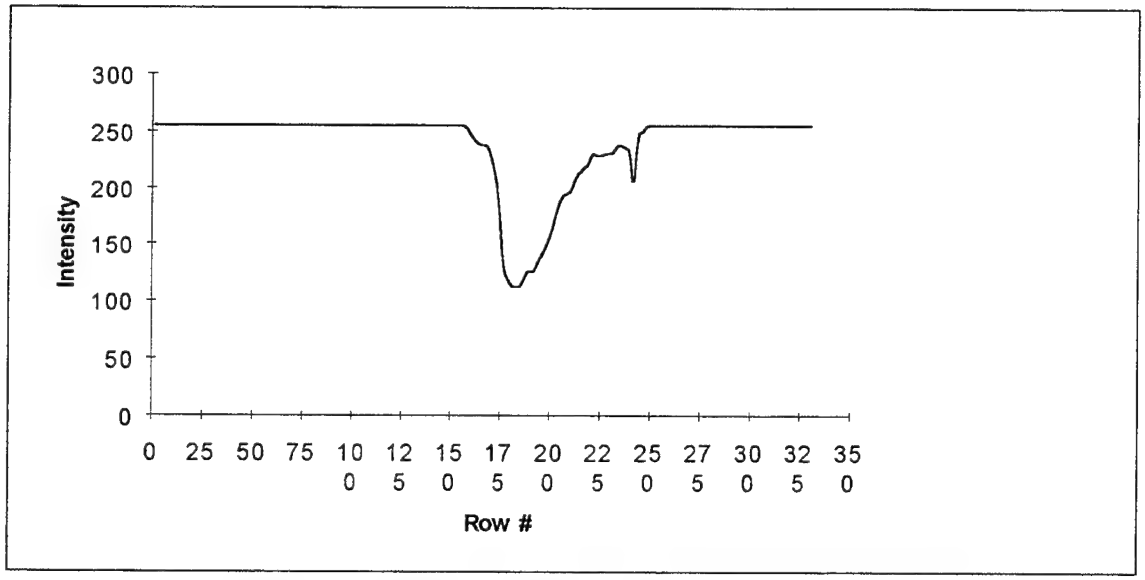

Fig. C-48. Reflection of H3 squashed to preserve vertical sequencies

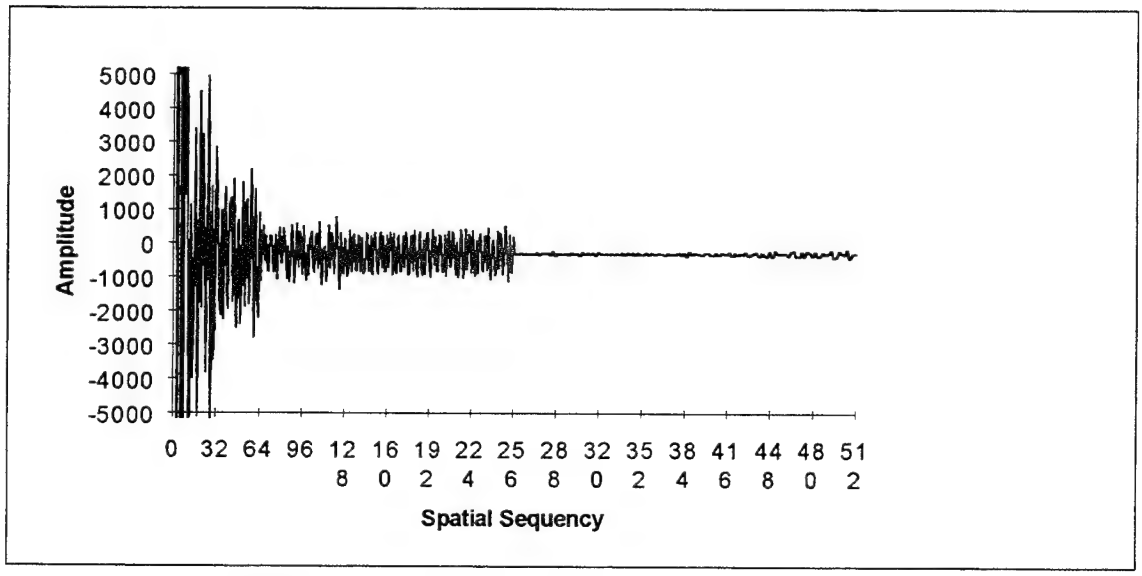

Fig. C-49. Walsh transform of Fig. C-48

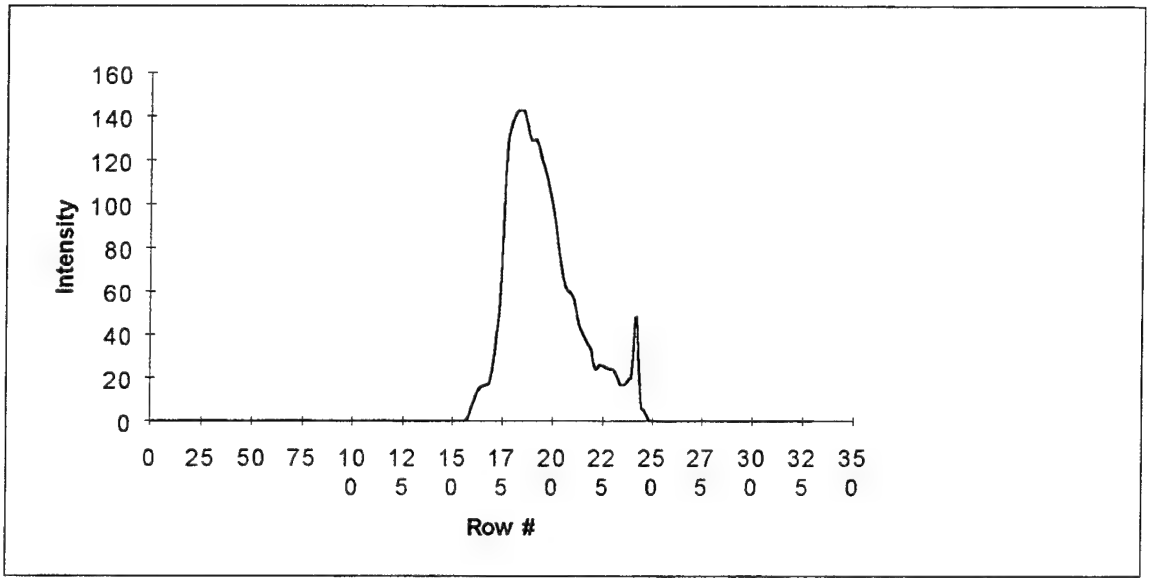

Fig. C-50. Complemented reflection of H3 squashed to preserve vertical sequencies

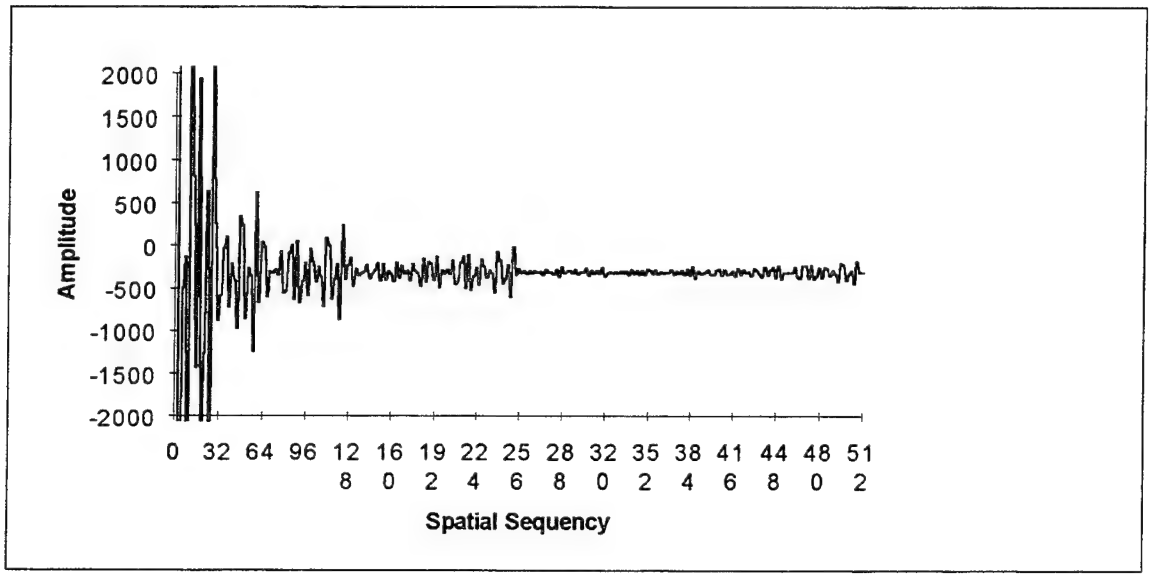

Fig. C-51. Walsh transform of Fig. C-50

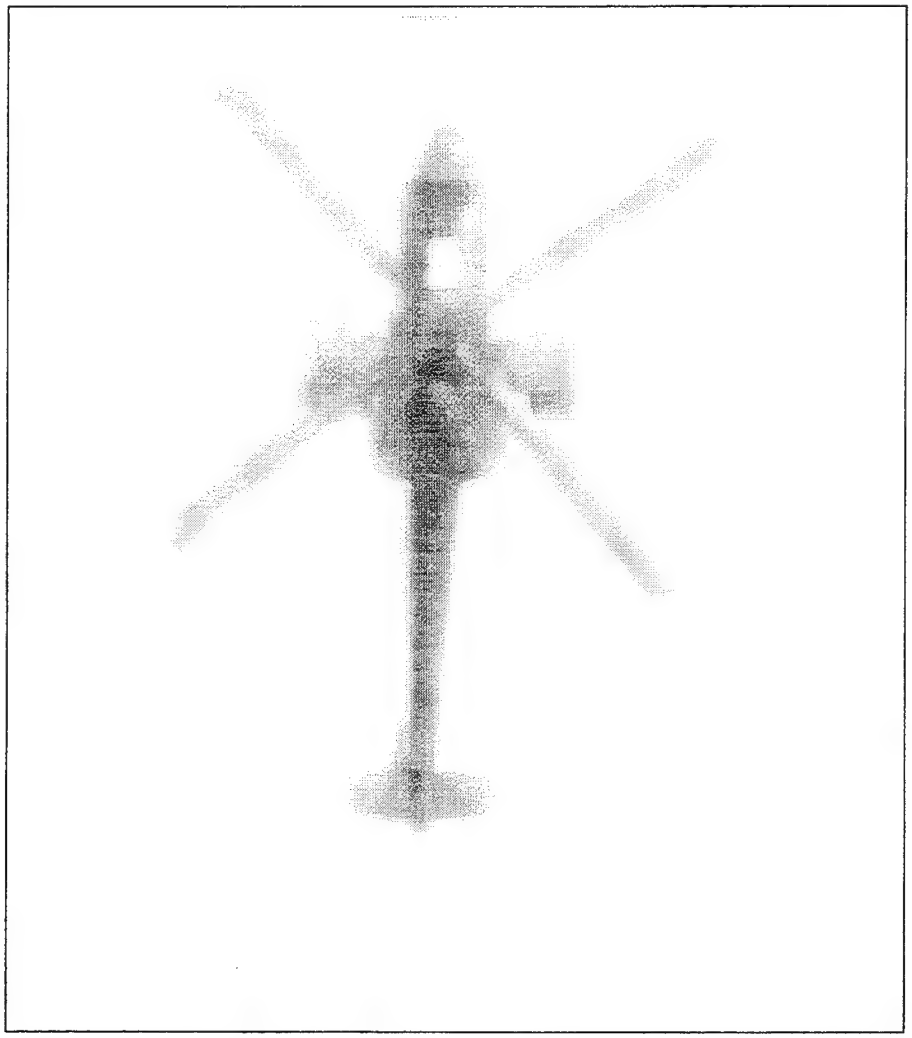

Fig. C-52. H4

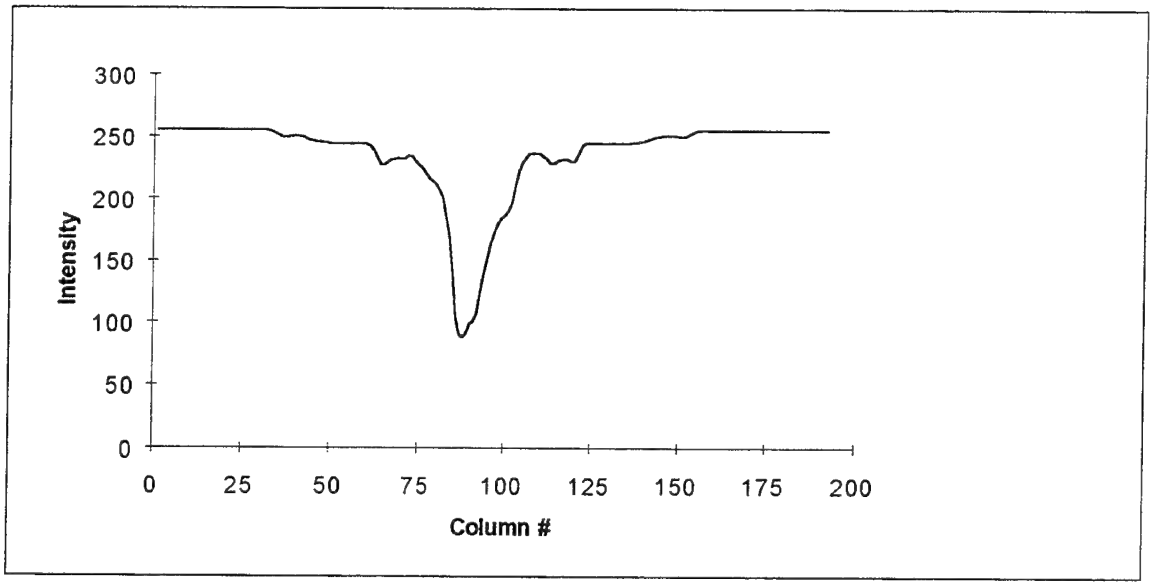

Fig. C-53. H4 squashed to preserve horizontal sequencies

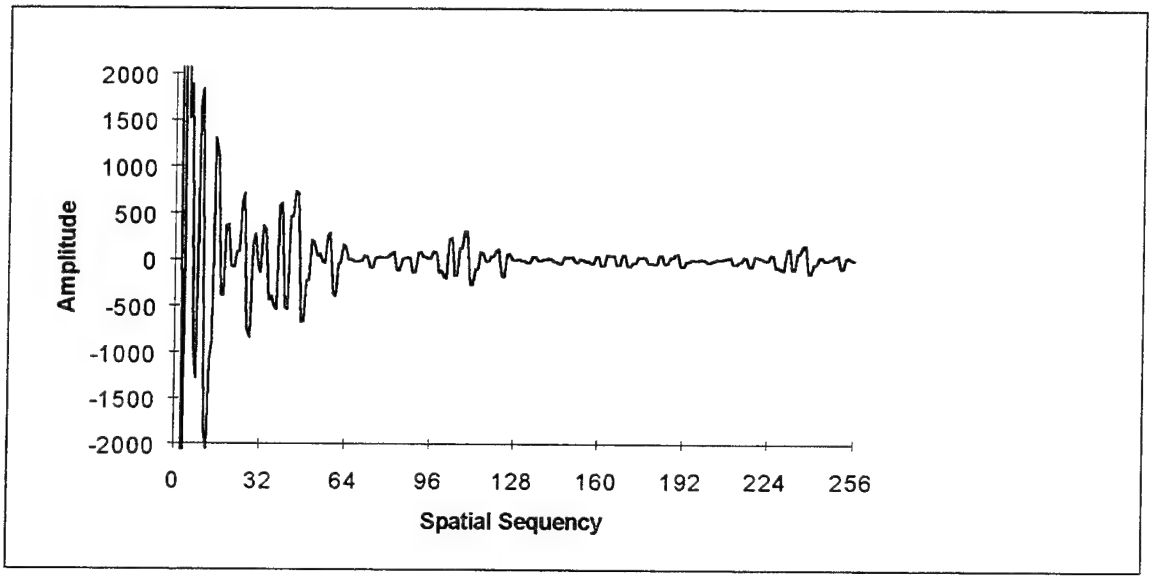

Fig. C-54. Walsh transform of Fig. C-53

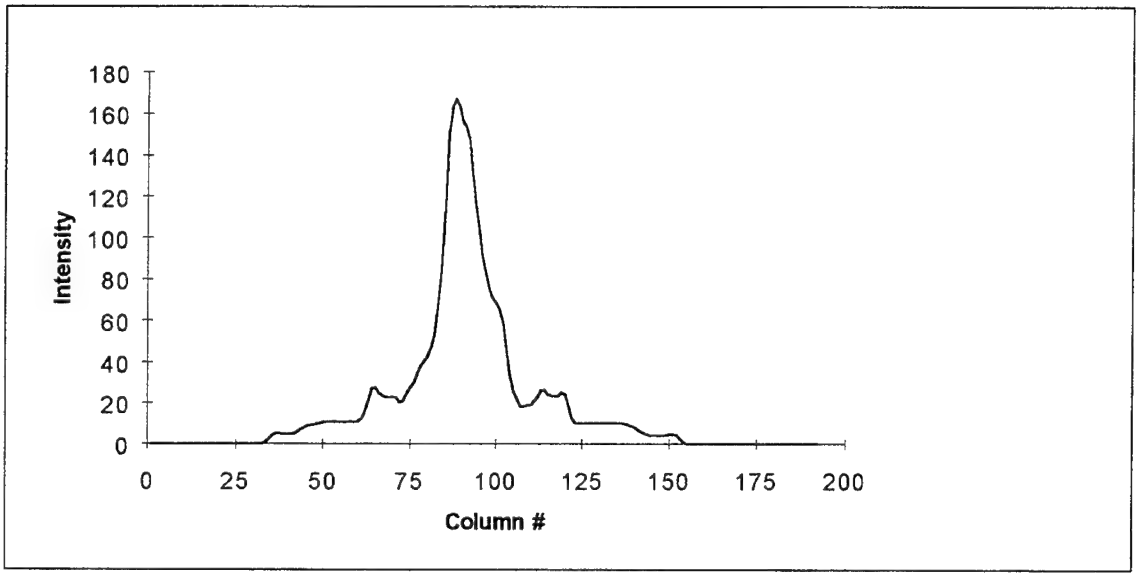

Fig. C-55. Complement of H4 squashed to preserve horizontal sequencies

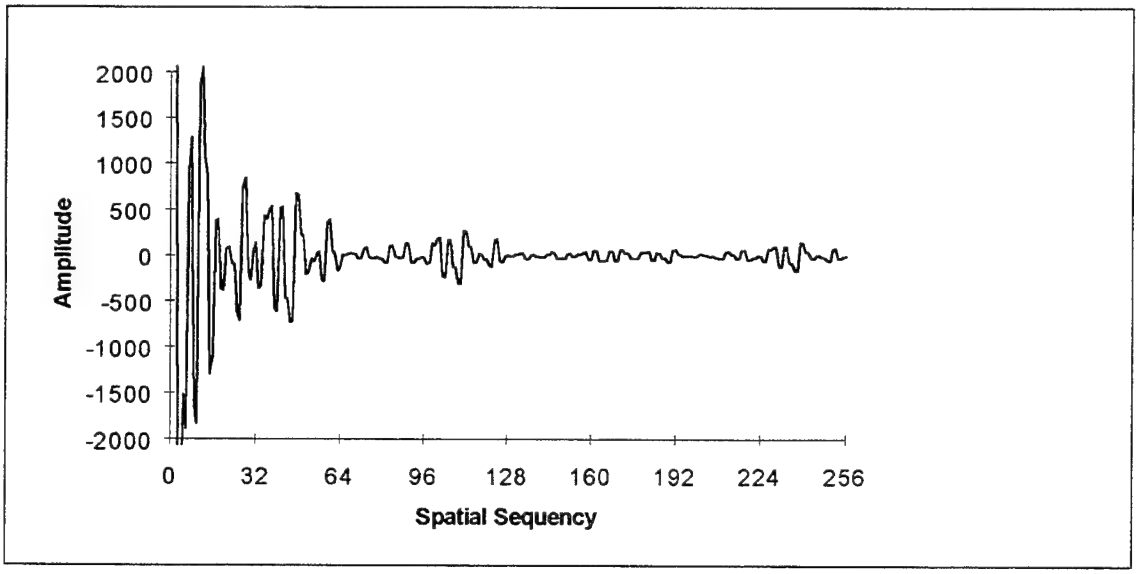

Fig. C-56. Walsh transform of Fig. C-55

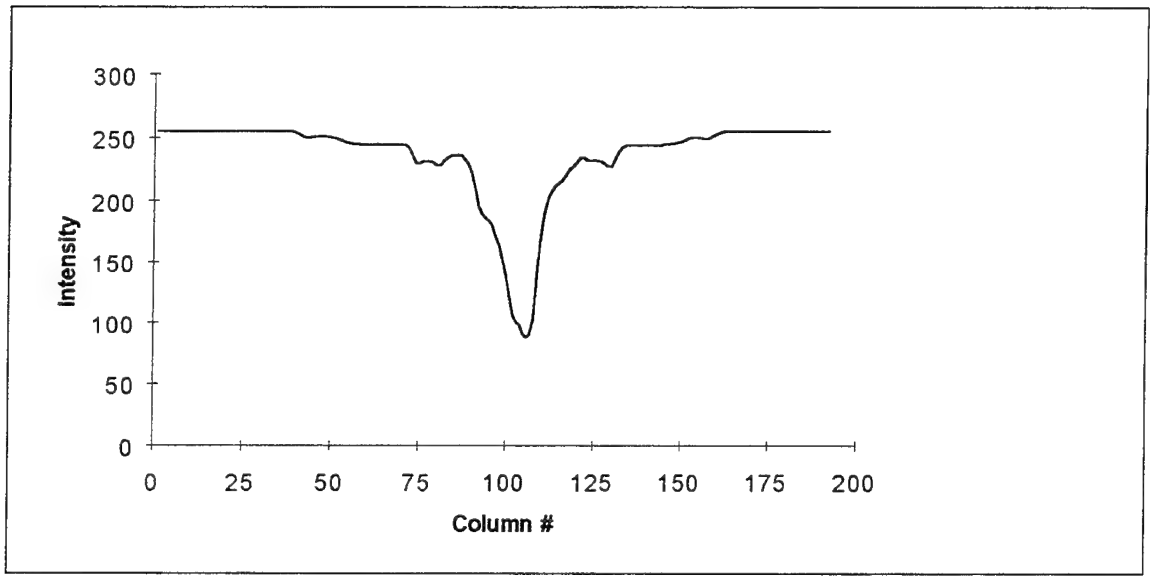

Fig. C-57. Reflection of H4 squashed to preserve horizontal sequencies

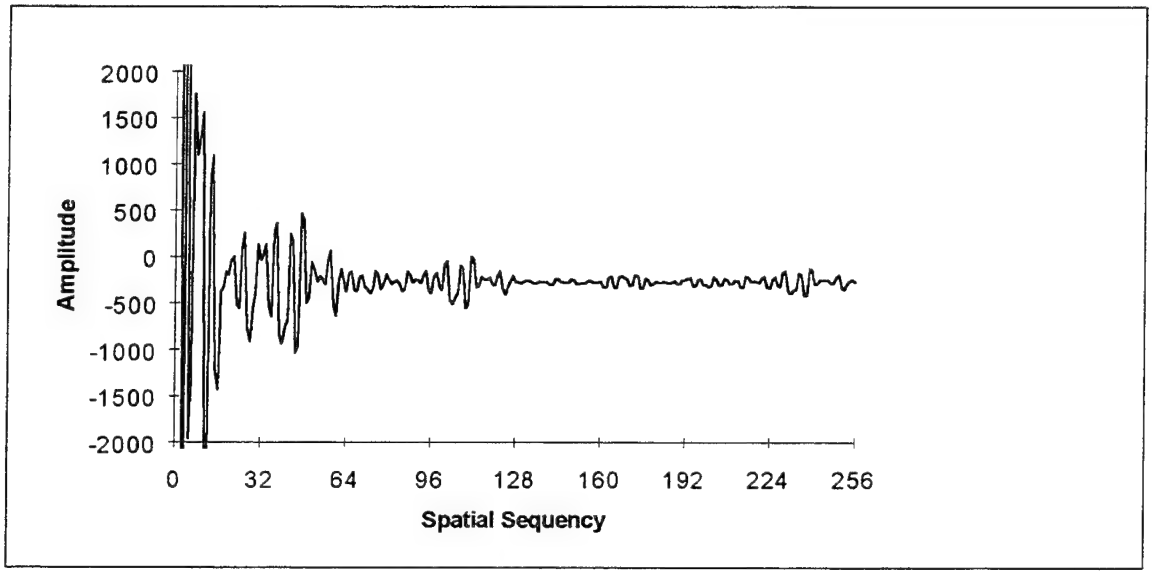

Fig. C-58. Walsh transform of Fig. C-57

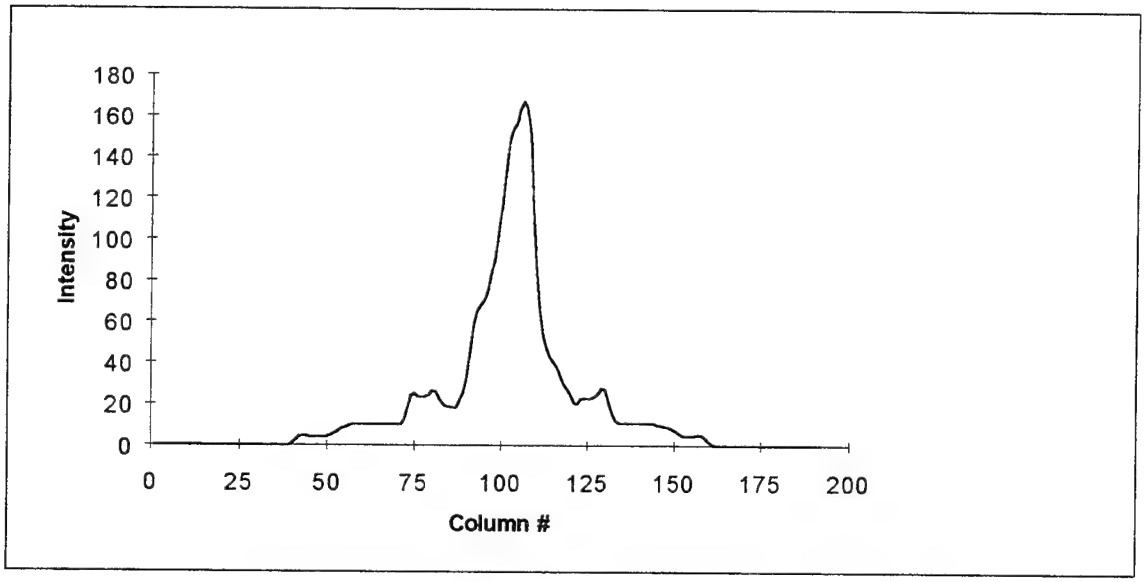

Fig. C-59. Complemented reflection of H4 squashed to preserve horizontal sequencies

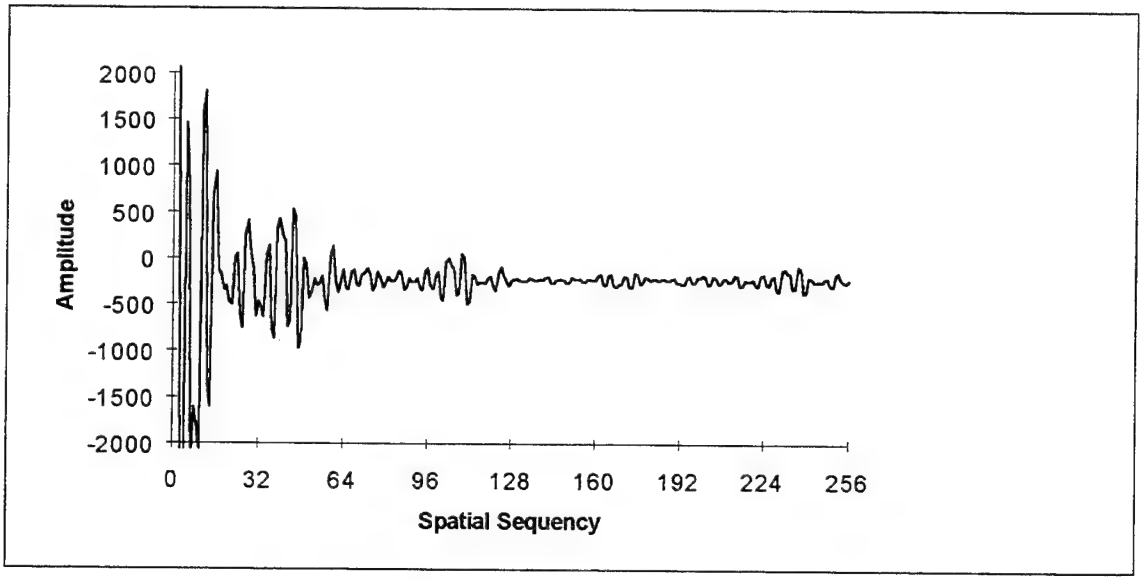

Fig. C-60. Walsh transform of Fig. C-59

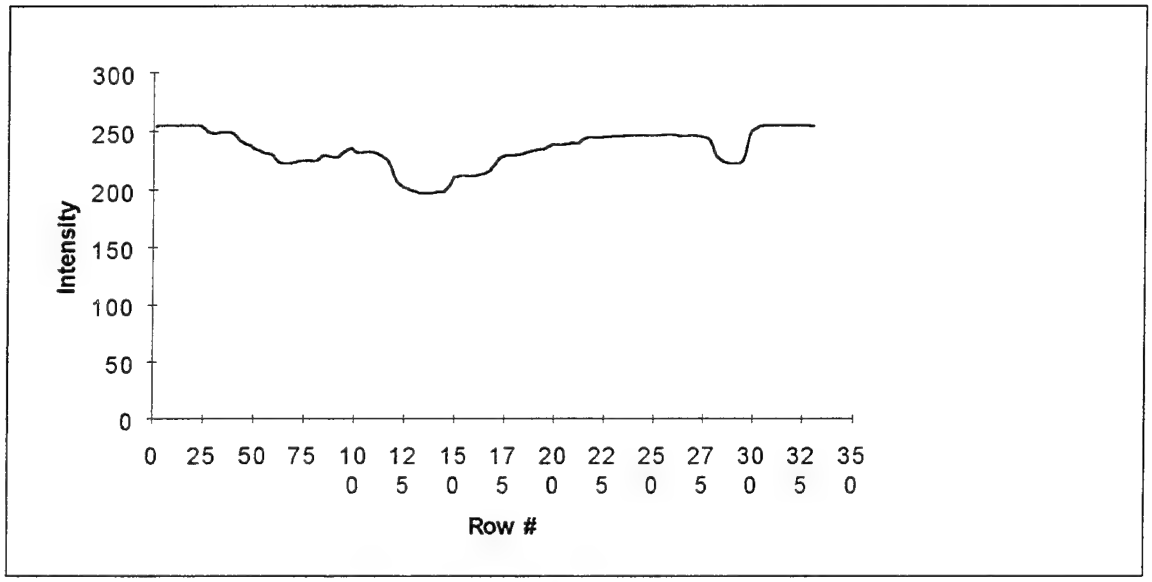

Fig. C-61. H4 squashed to preserve vertical sequencies

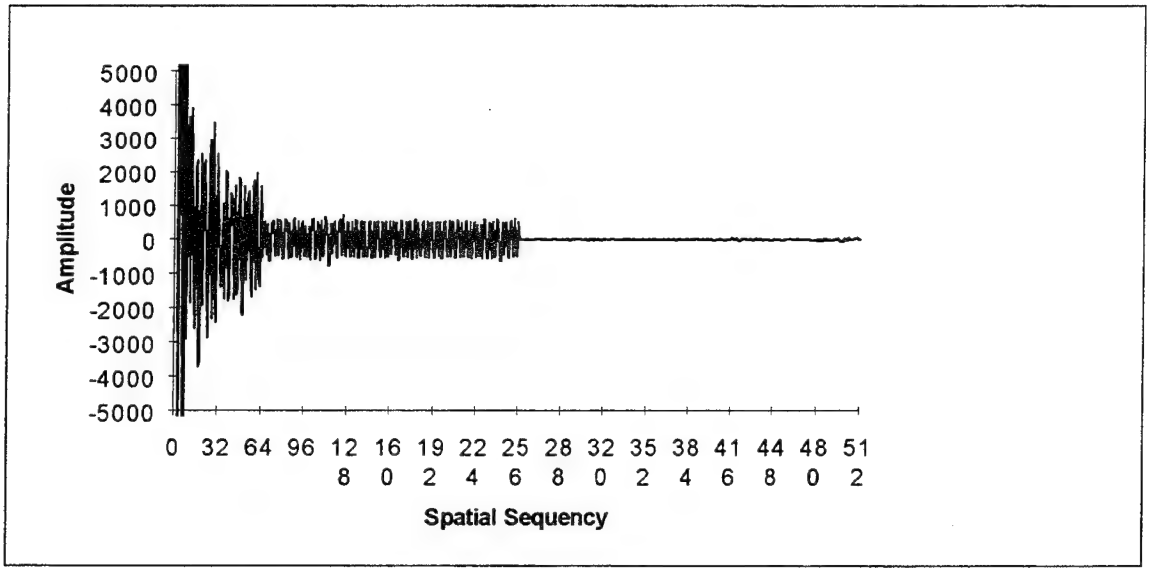

Fig. C-62. Walsh transform of Fig. C-61

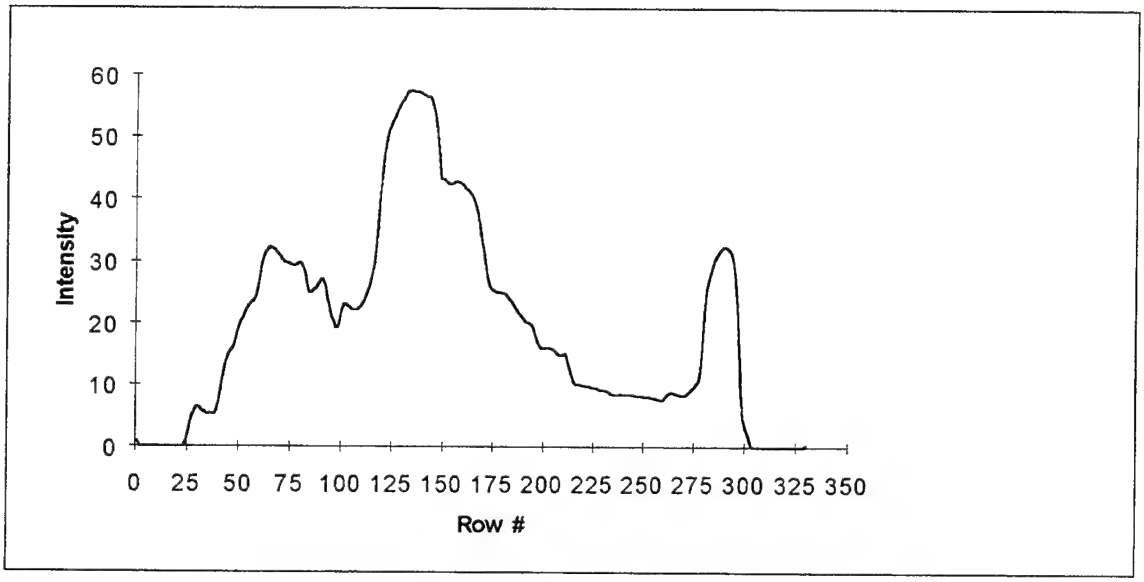

Fig. C-63. Complement of H4 squashed to preserve vertical sequencies

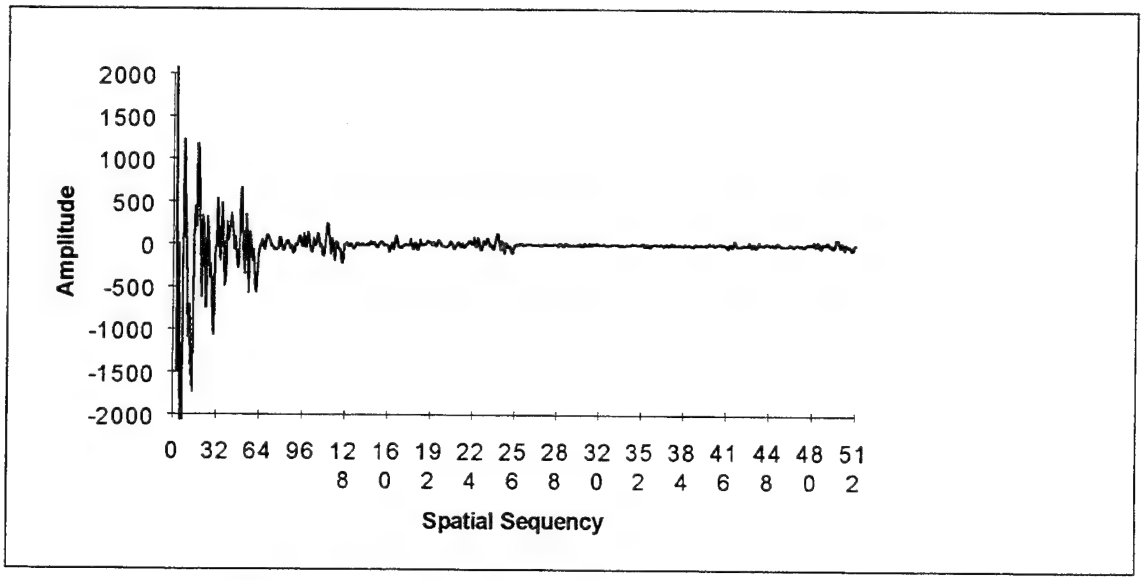

Fig. C-64. Walsh transform of Fig. C-63

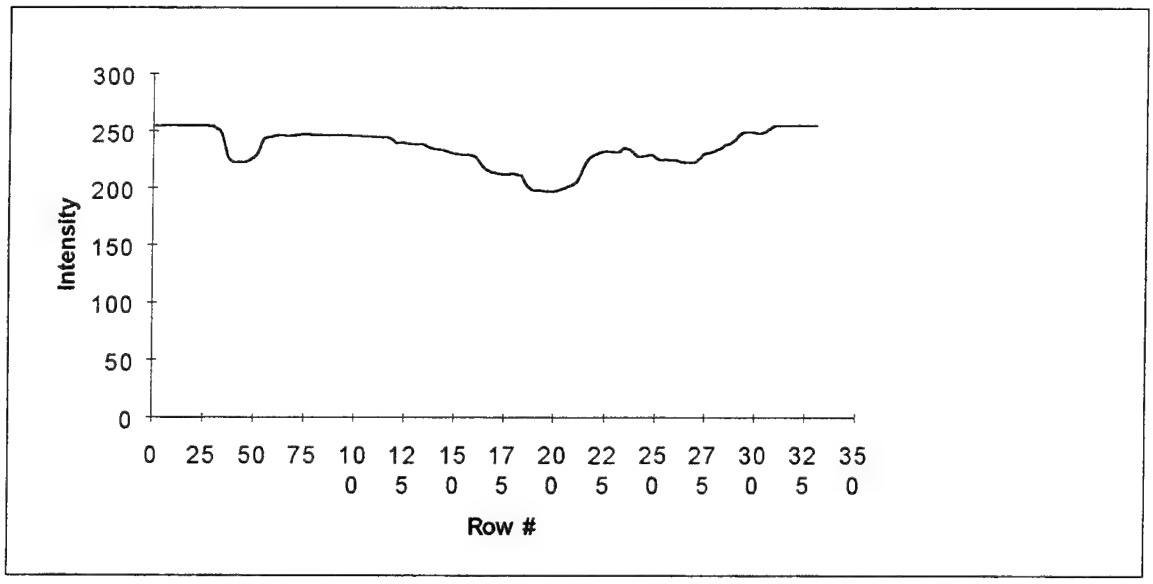

Fig. C-65. Reflection of H4 squashed to preserve vertical sequencies

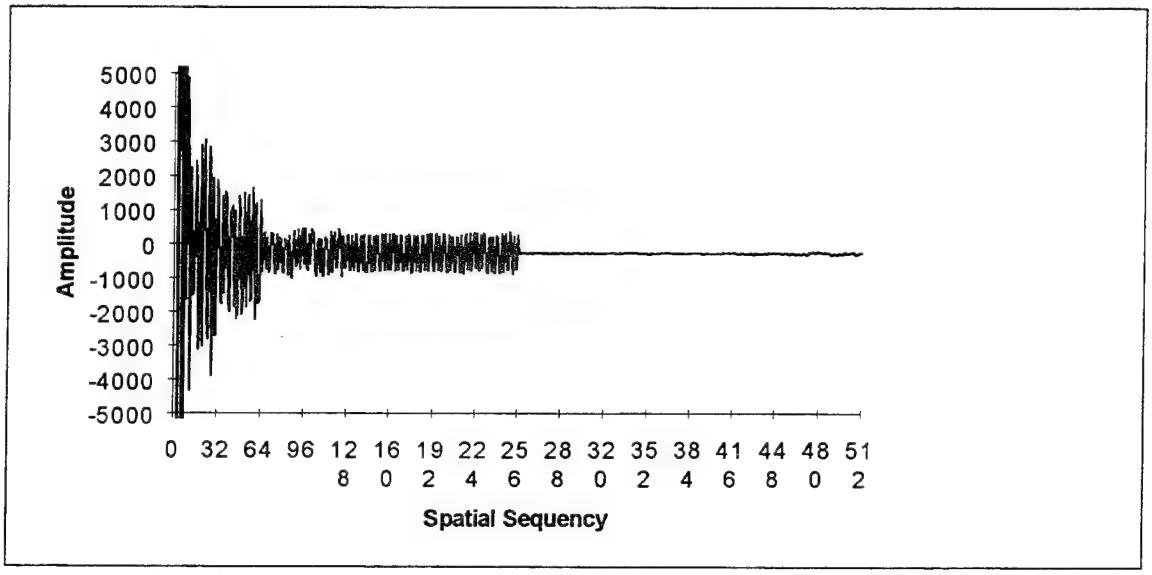

Fig. C-66. Walsh transform of Fig. C-65

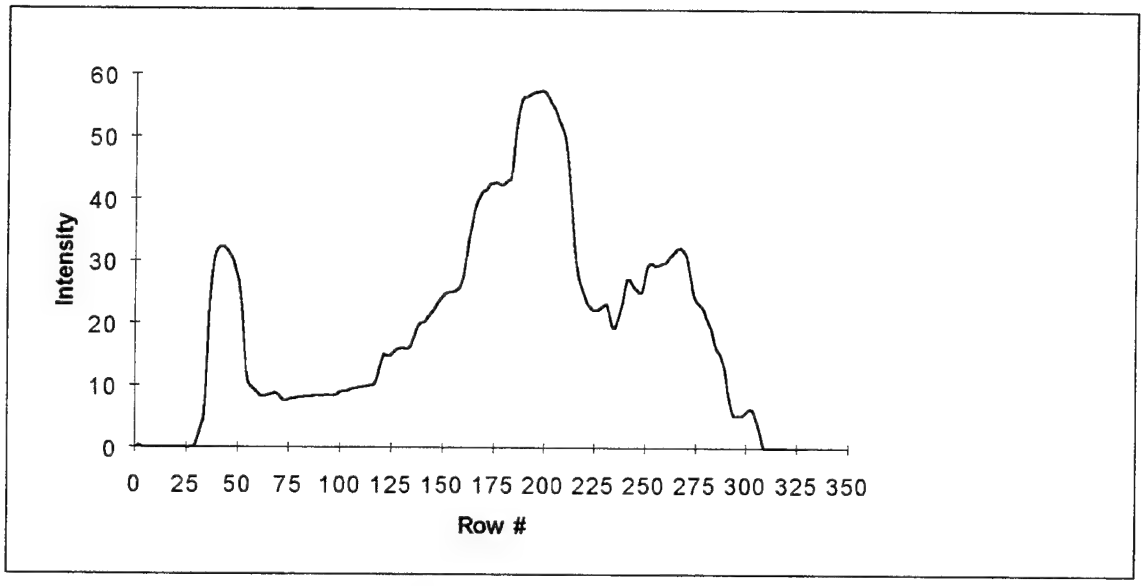

Fig. C-67. Complemented reflection of H4 squashed to preserve vertical sequencies

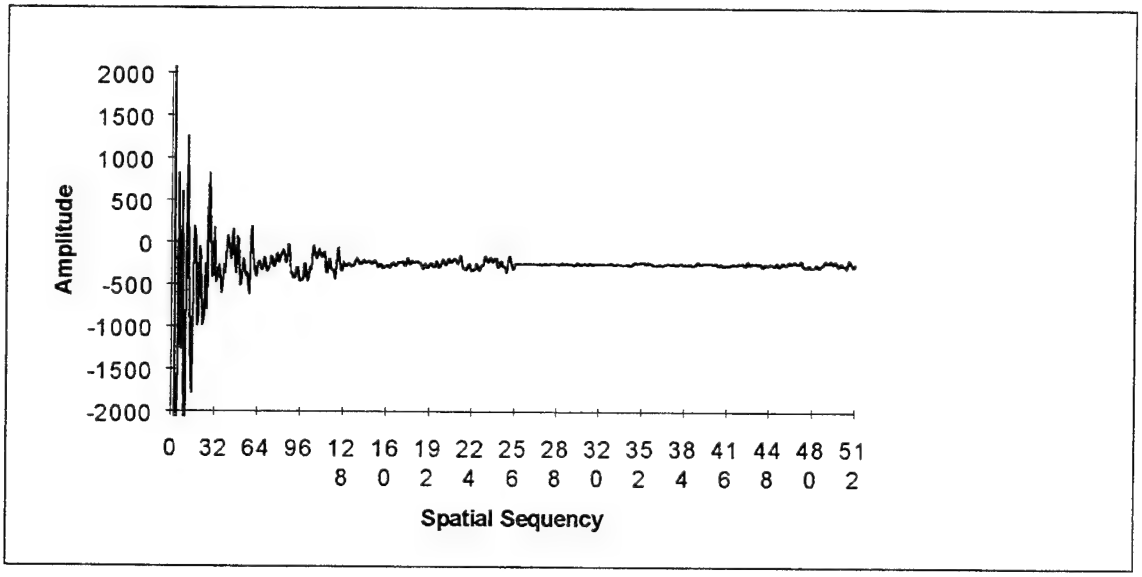

Fig. C-68. Walsh transform of Fig. C-67

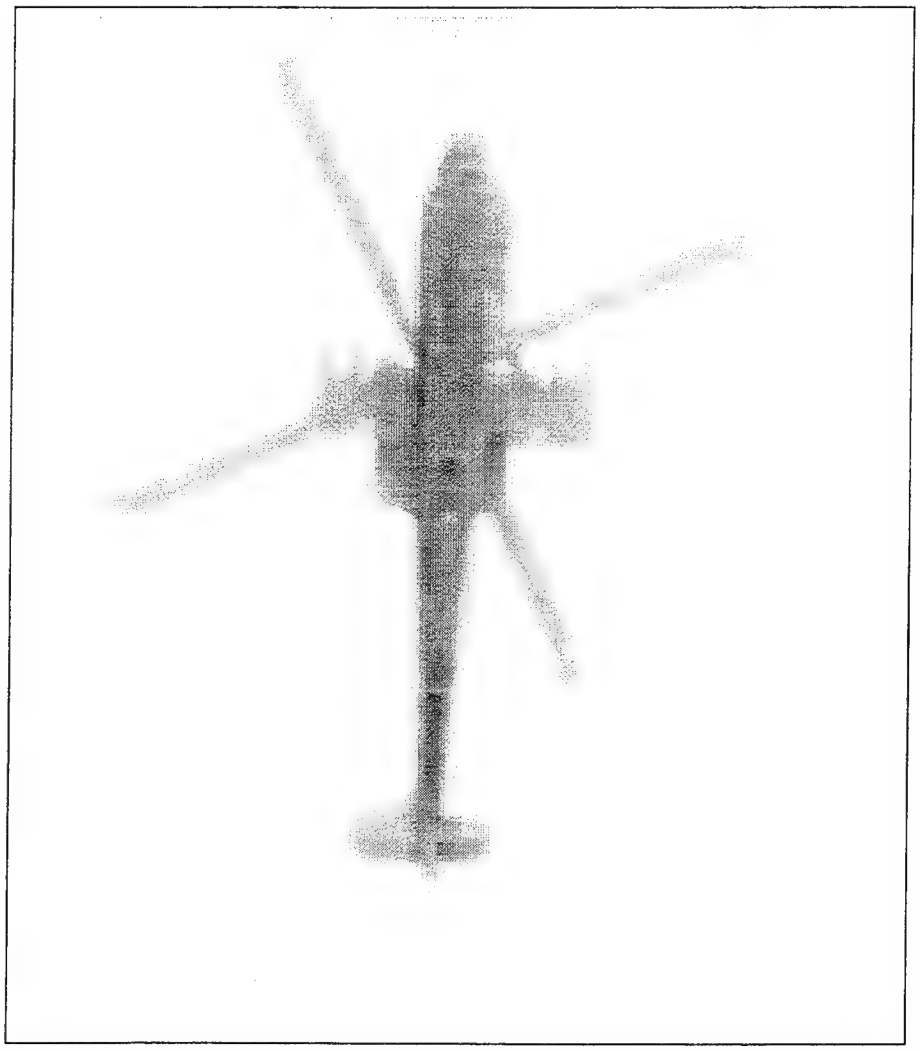

Fig. C-69. H5

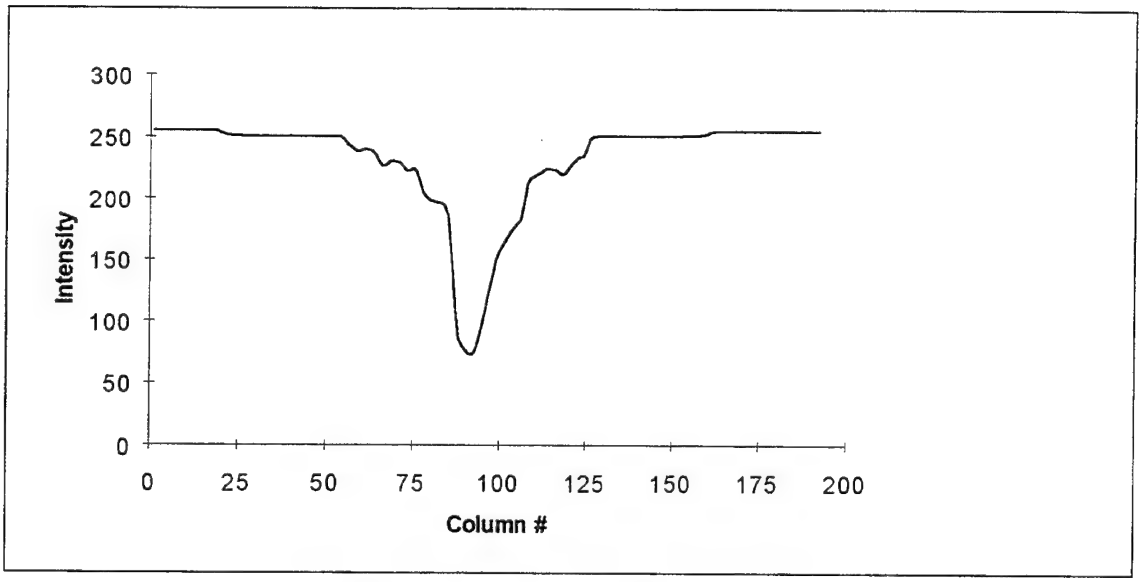

Fig. C-70. H5 squashed to preserve horizontal sequencies

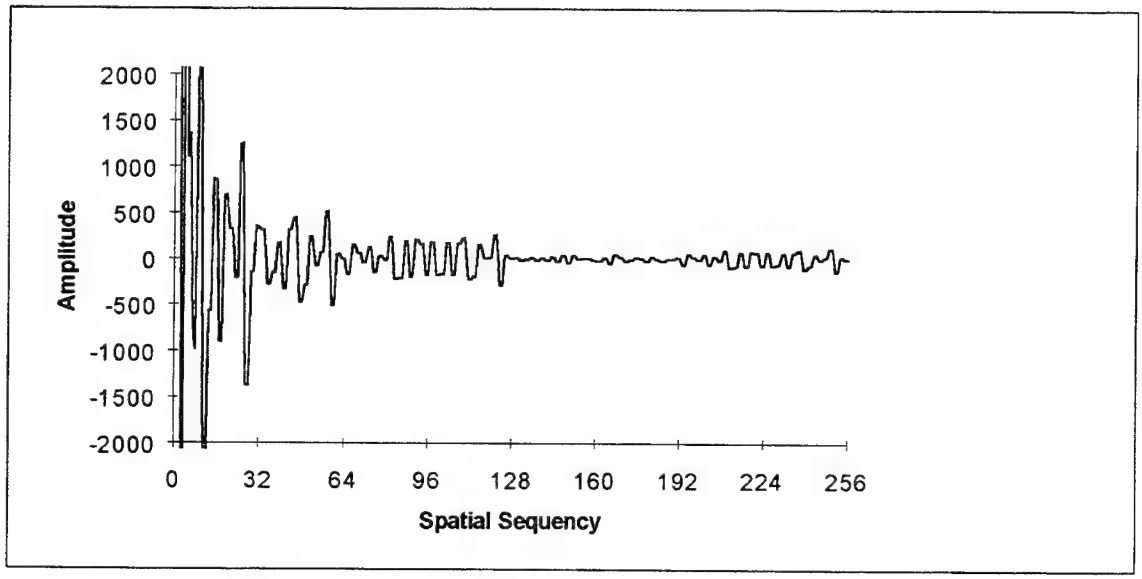

Fig. C-71. Walsh transform of Fig. C-70

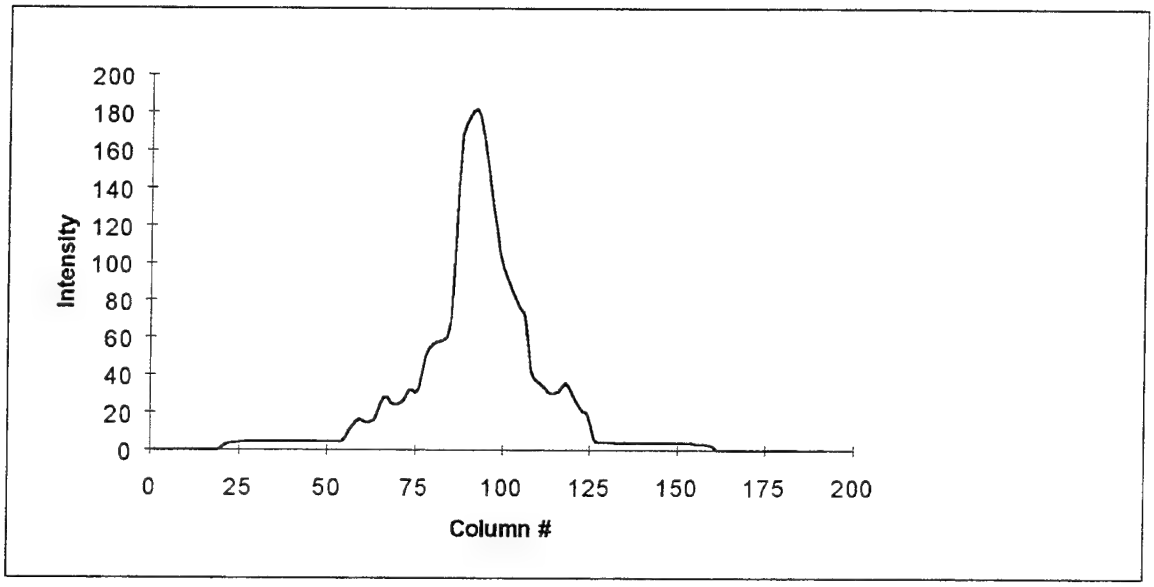

Fig. C-72. Complement of H5 squashed to preserve horizontal sequencies

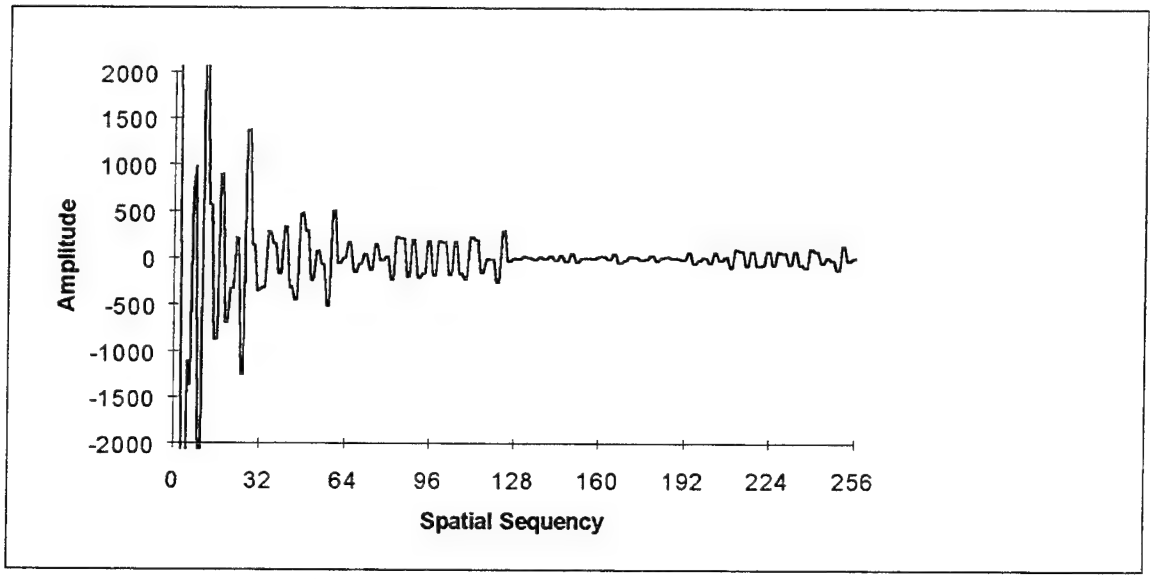

Fig. C-73. Walsh transform of Fig. C-72

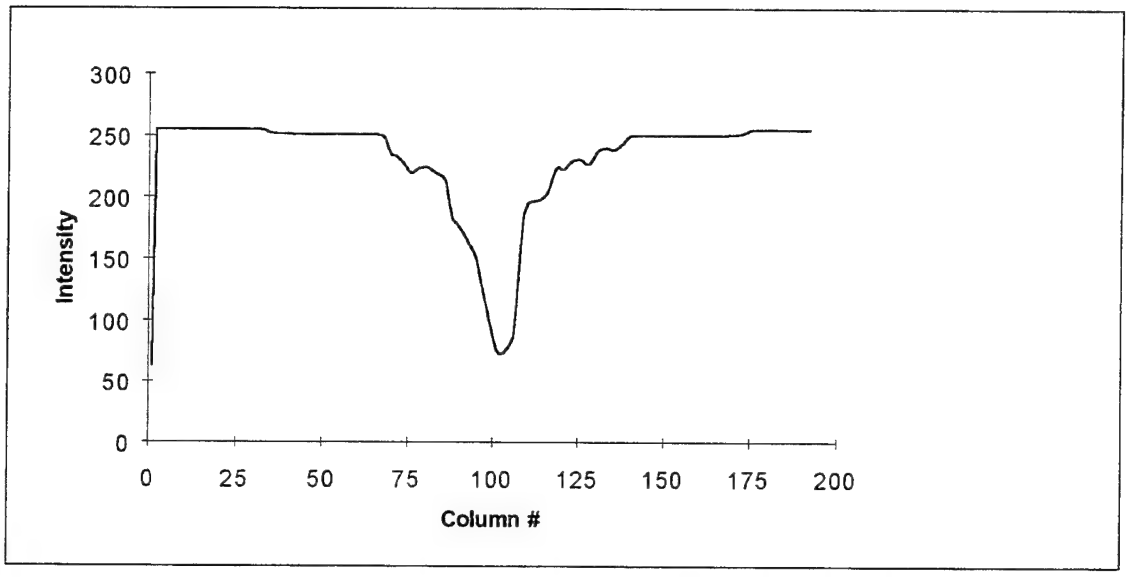

Fig. C-74. Reflection of H5 squashed to preserve horizontal sequencies

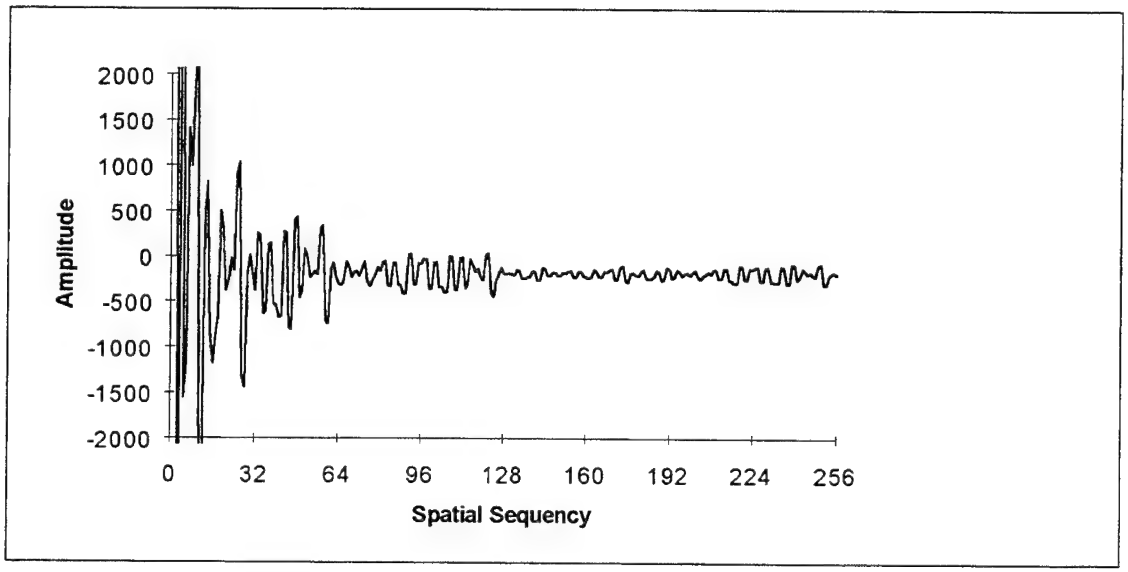

Fig. C-75. Walsh transform of Fig. C-74

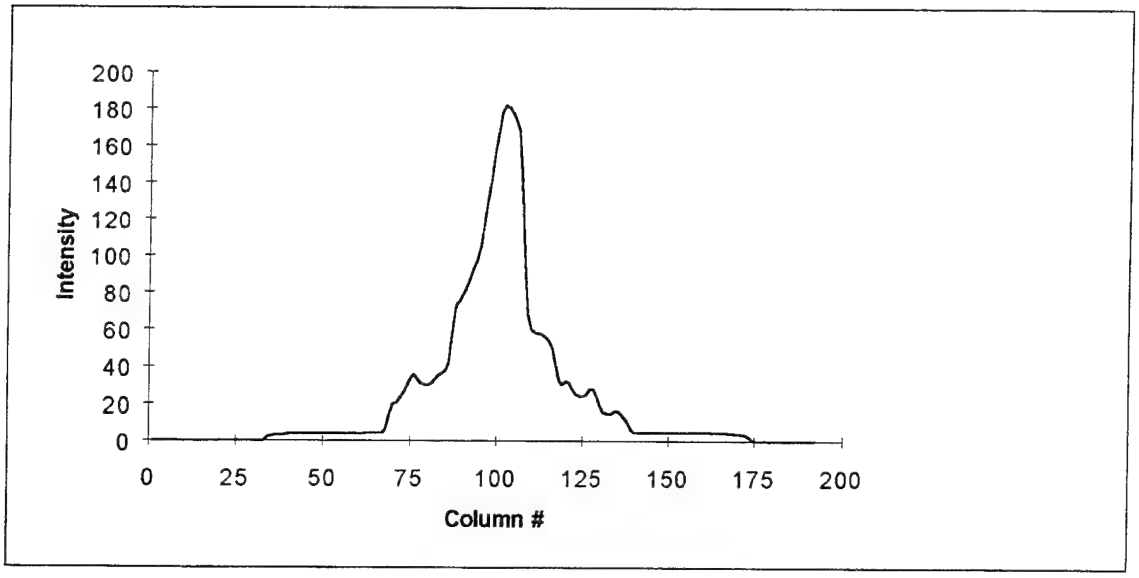

Fig. C-76. Complemented reflection of H5 squashed to preserve horizontal sequencies

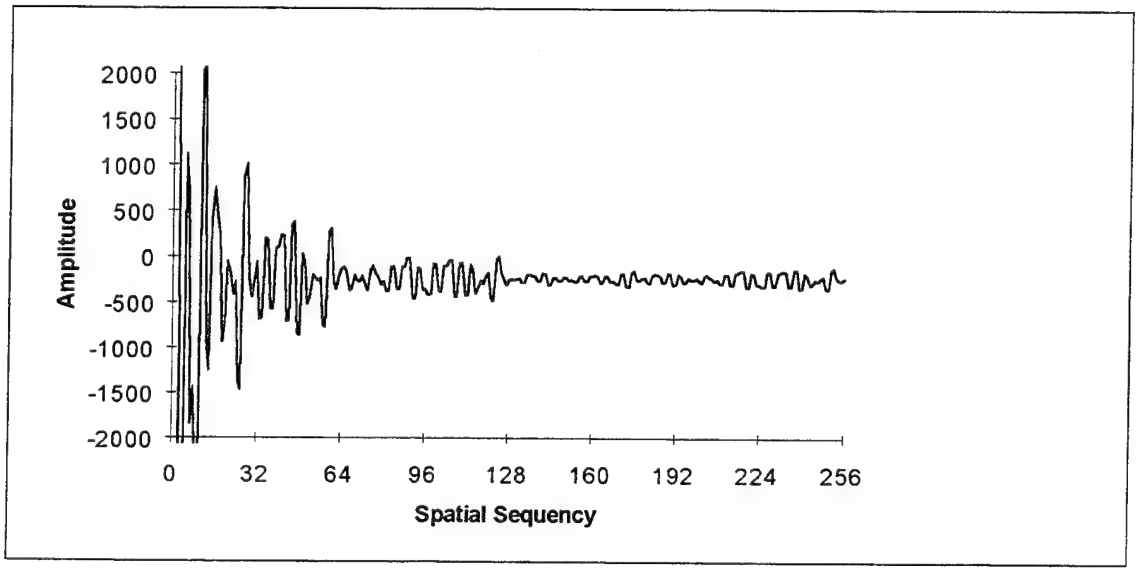

Fig. C-77. Walsh transform of Fig. C-76

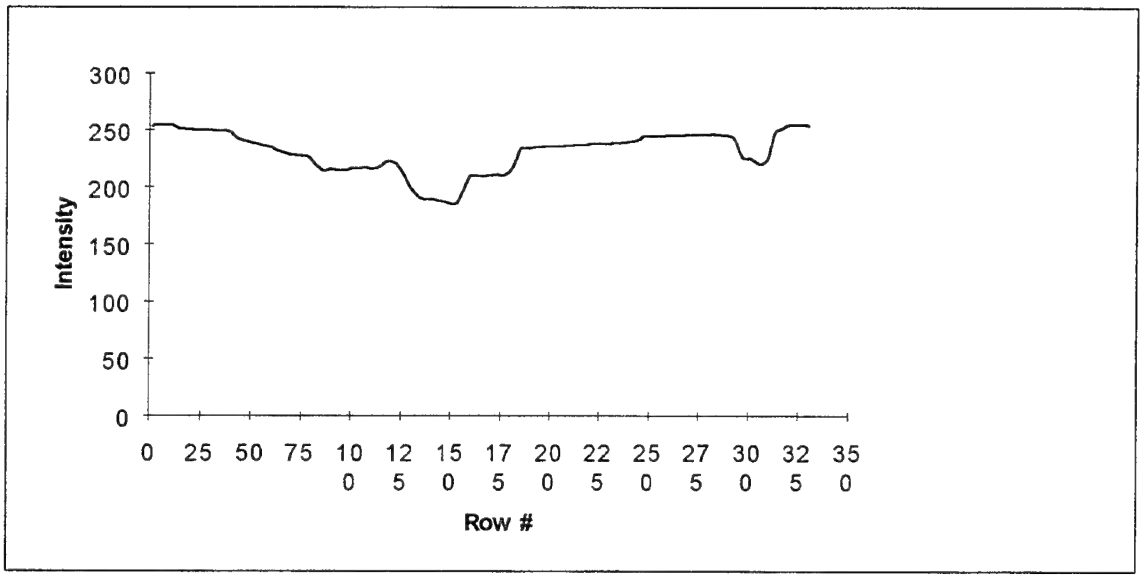

Fig. C-78. H5 squashed to preserve vertical sequencies

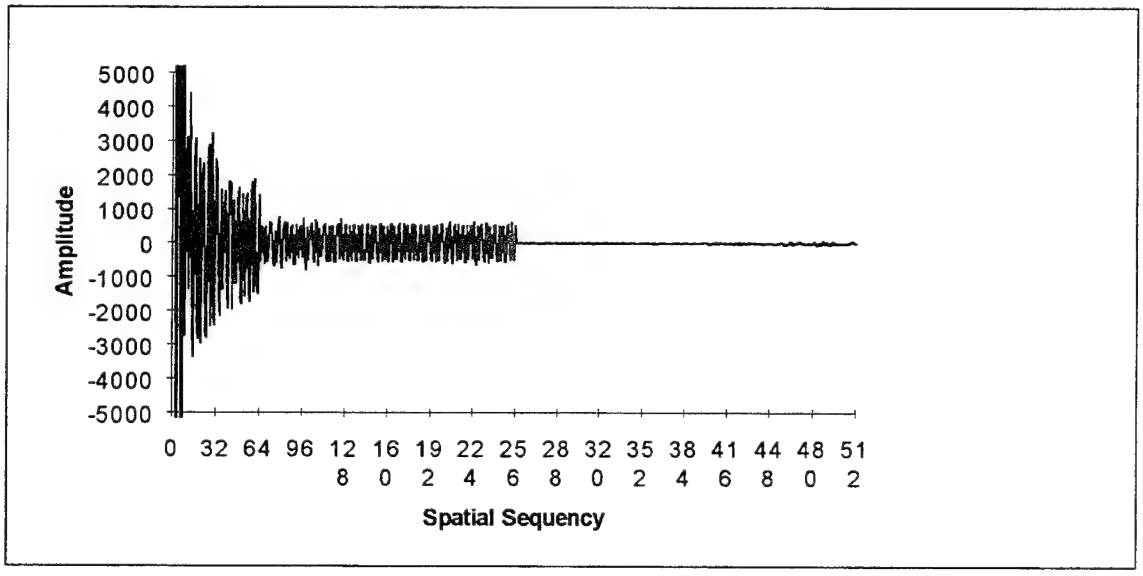

Fig. C-79. Walsh transform of Fig. C-78

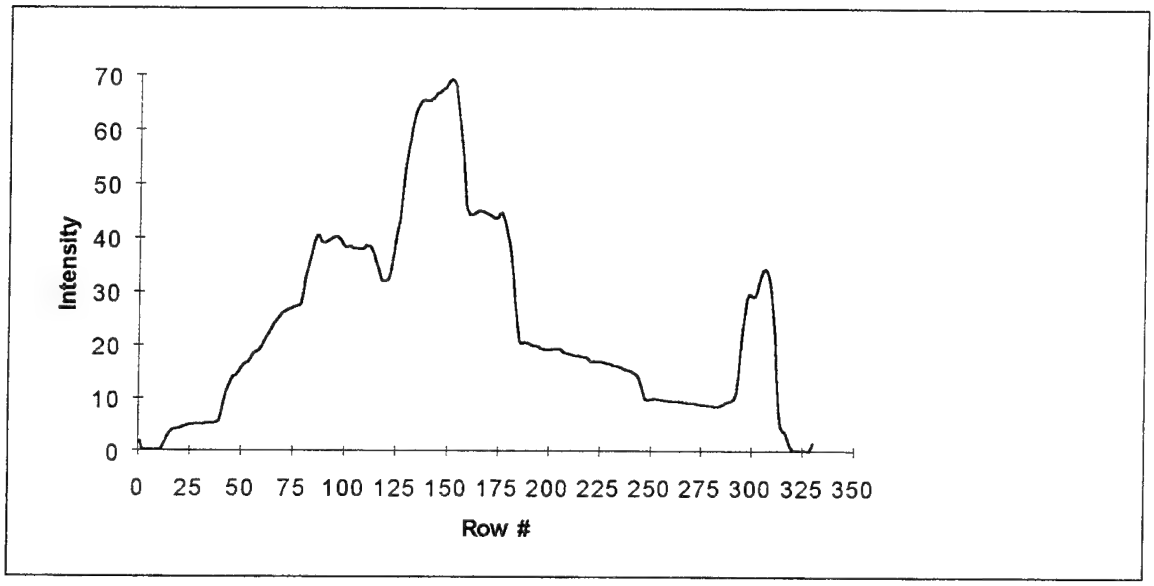

Fig. C-80. Complement of H5 squashed to preserve vertical sequencies

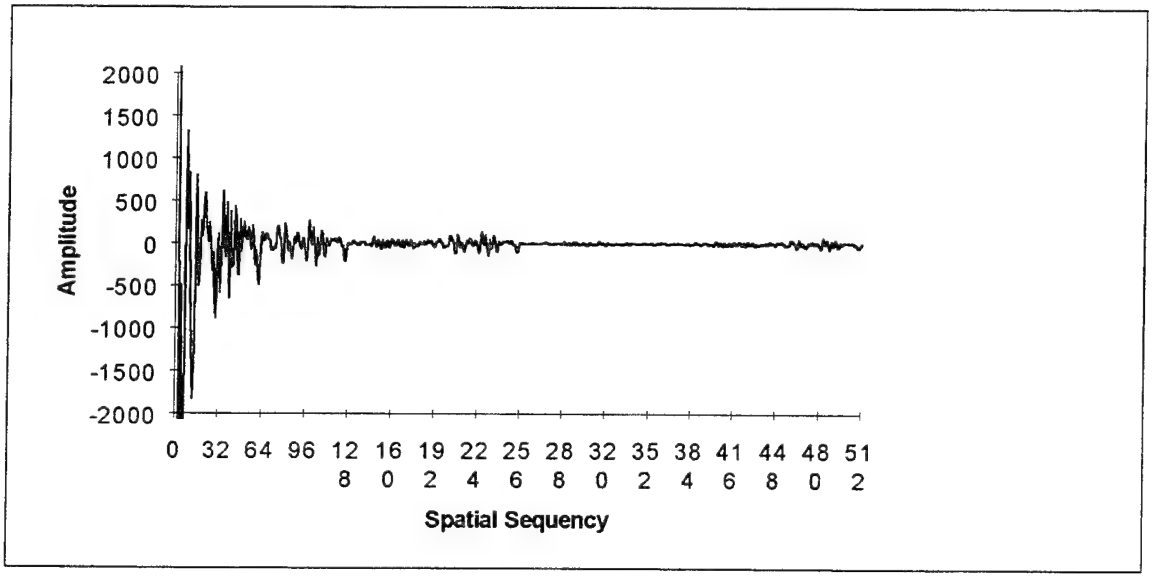

Fig. C-81. Walsh transform of Fig. C-80

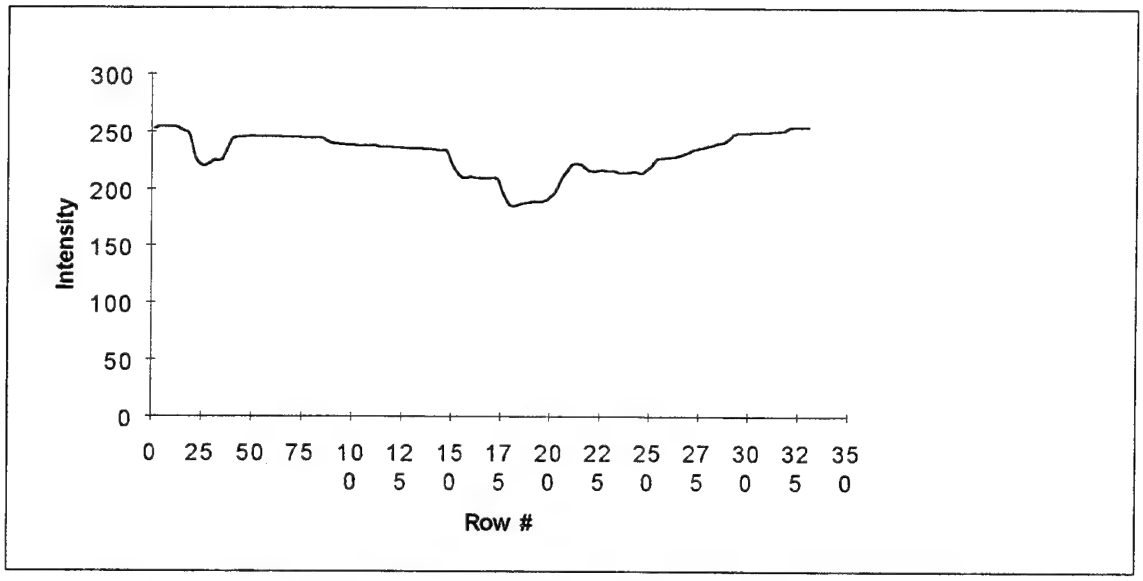

Fig. C-82. Reflection of H5 squashed to preserve vertical sequencies

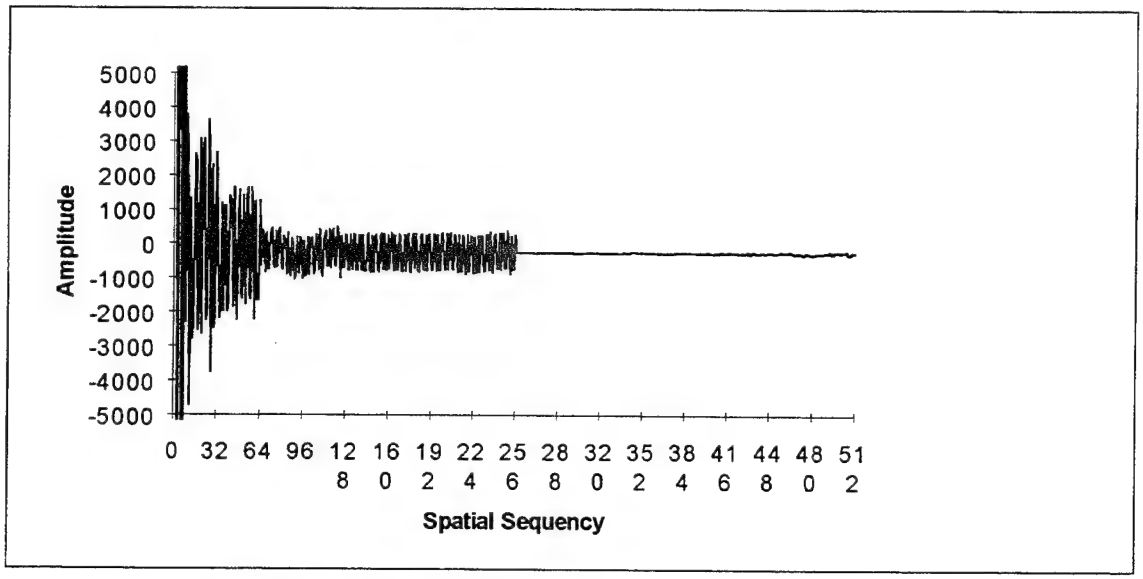

Fig. C-83. Walsh transform of Fig. C-82

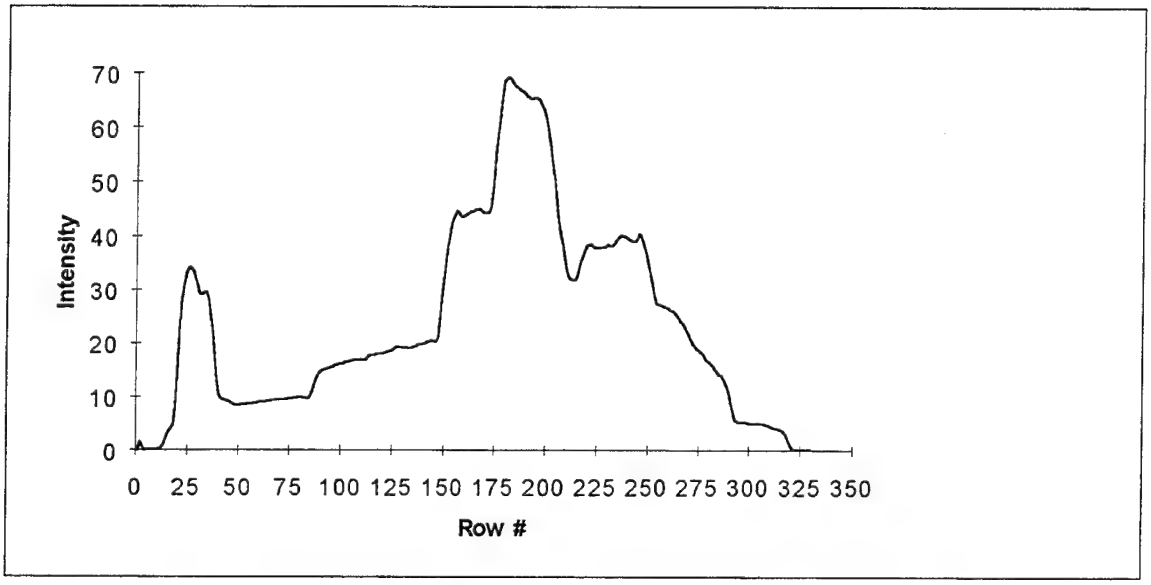

Fig. C-84. Complemented reflection of H5 squashed to preserve vertical sequencies

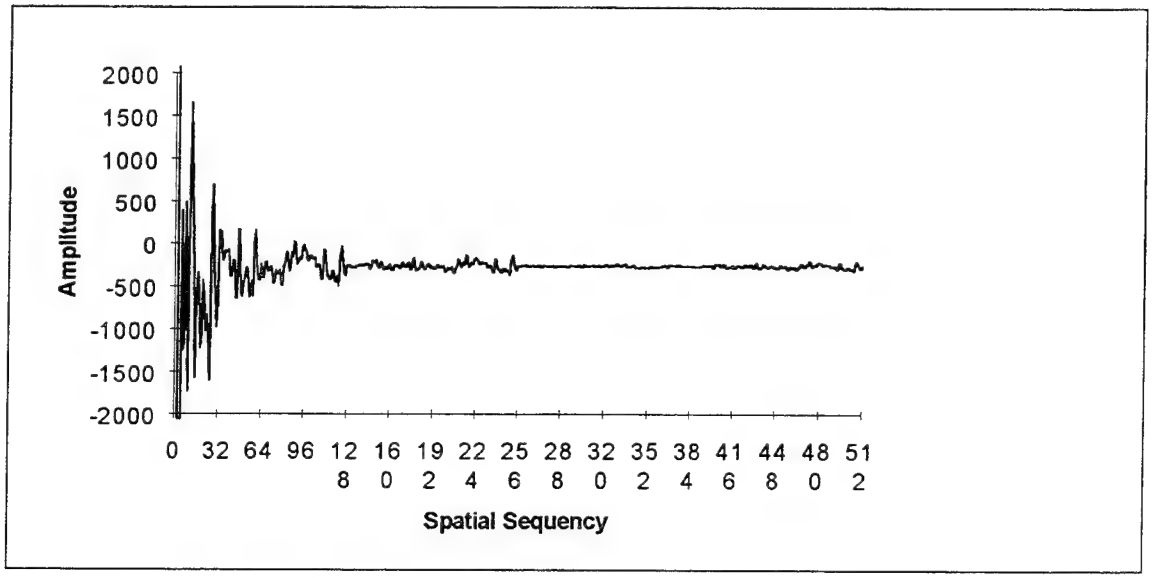

Fig. C-85. Walsh transform of Fig. C-85

APPENDIX D: TANKS

This appendix contains image packets for the following thirteen tank images:

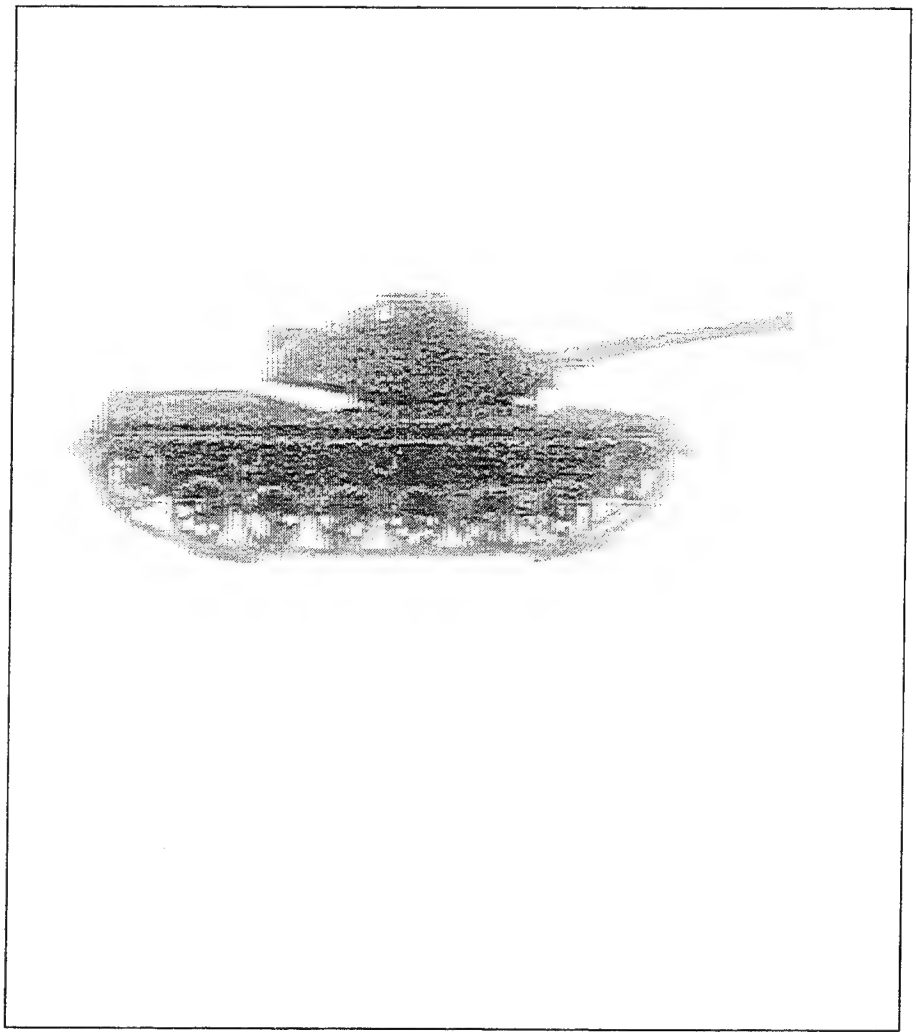

Fig. D-1. T1

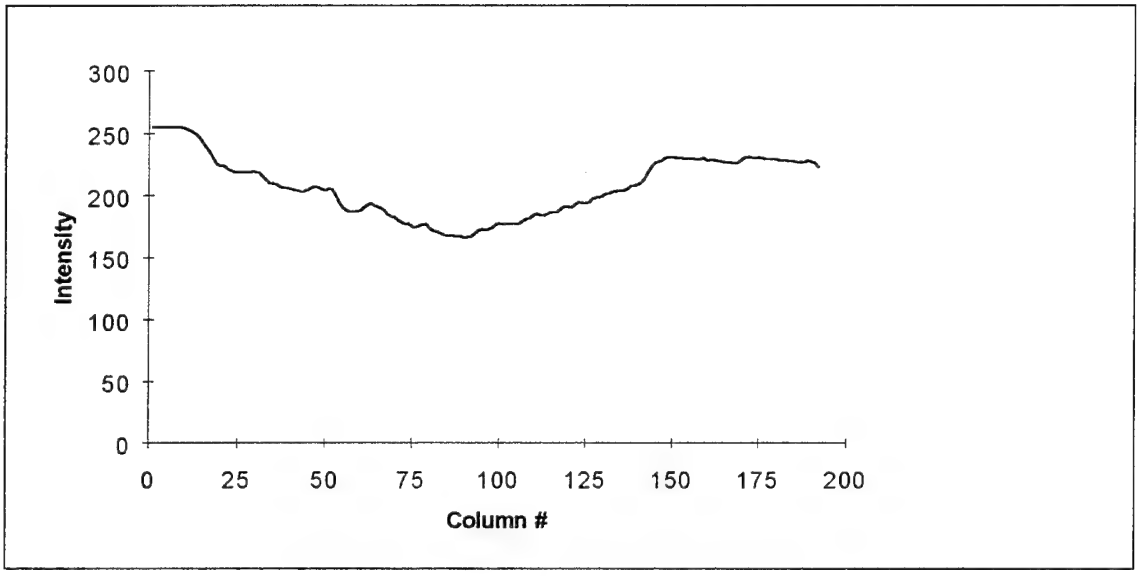

Fig. D-2. T1 squashed to preserve horizontal sequencies

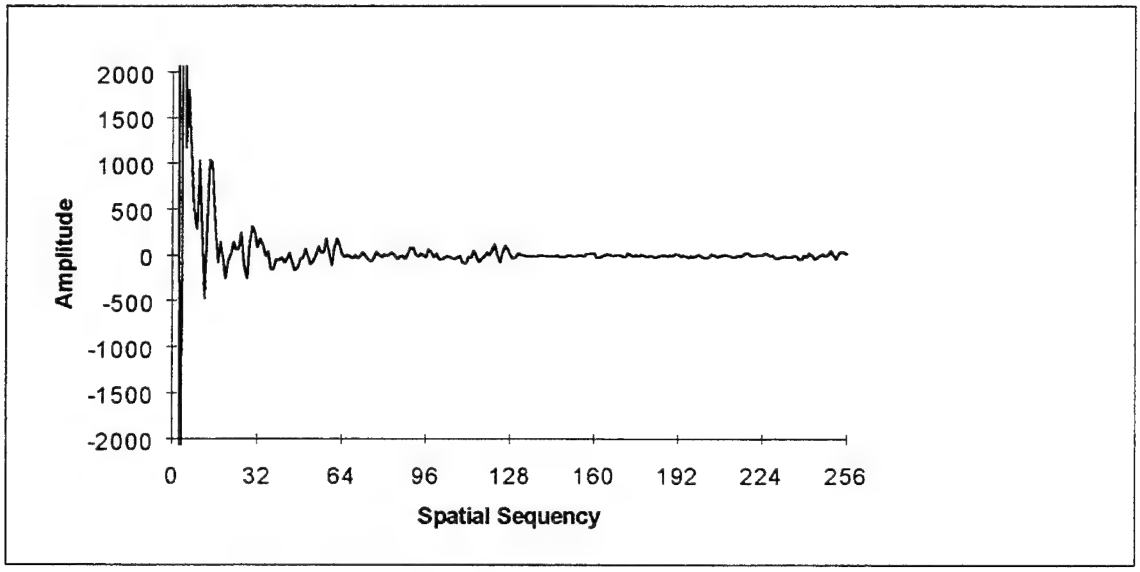

Fig. D-3. Walsh transform of Fig. D-2

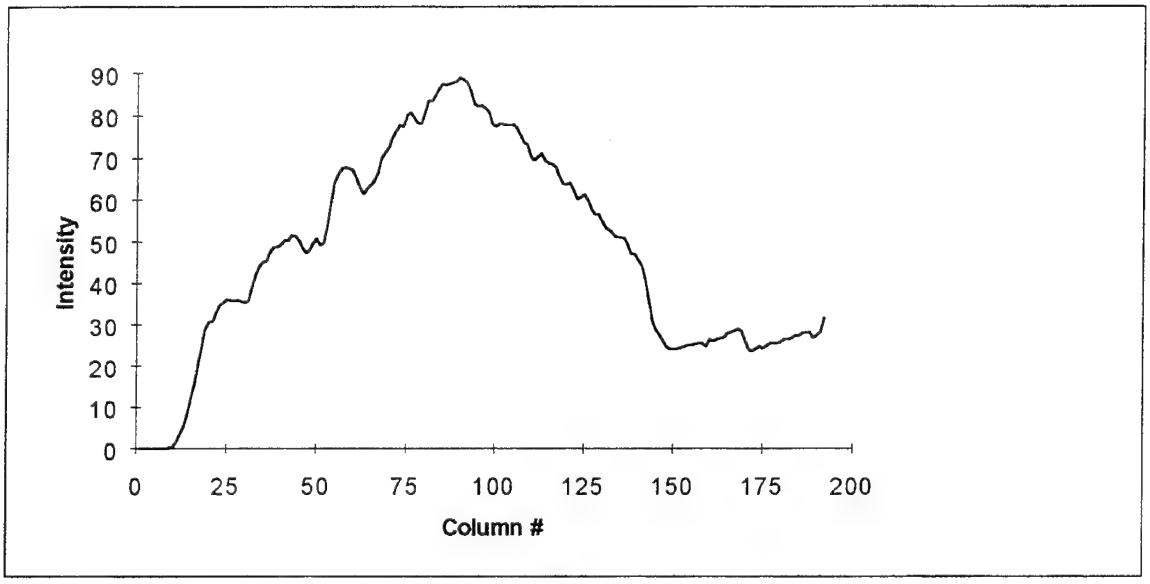

Fig. D-4. Complement of T1 squashed to preserve horizontal sequencies

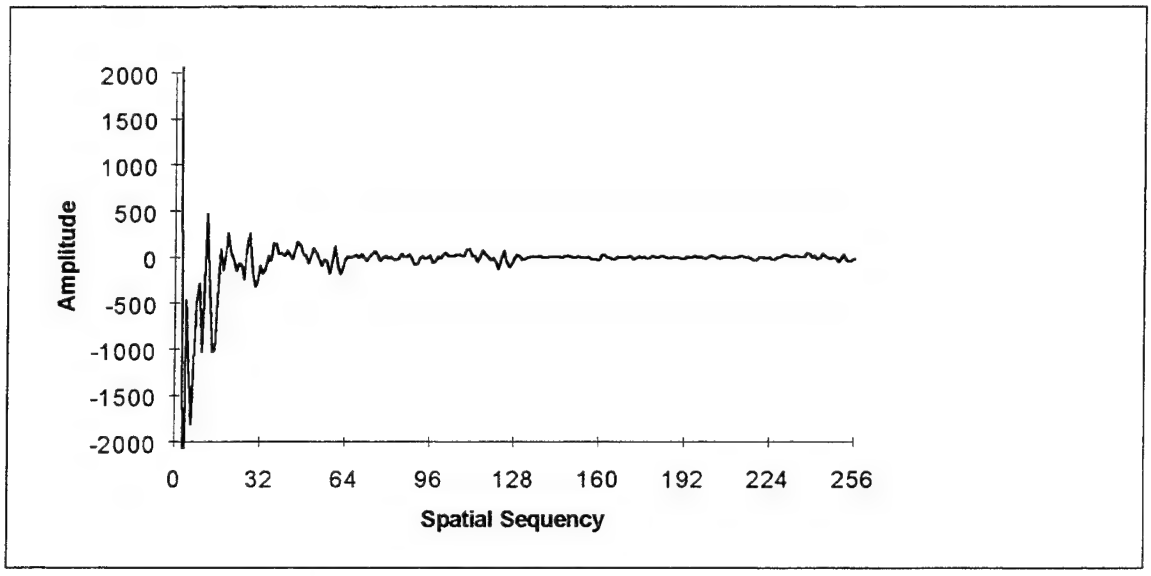

Fig. D-5. Walsh transform of Fig. D-4

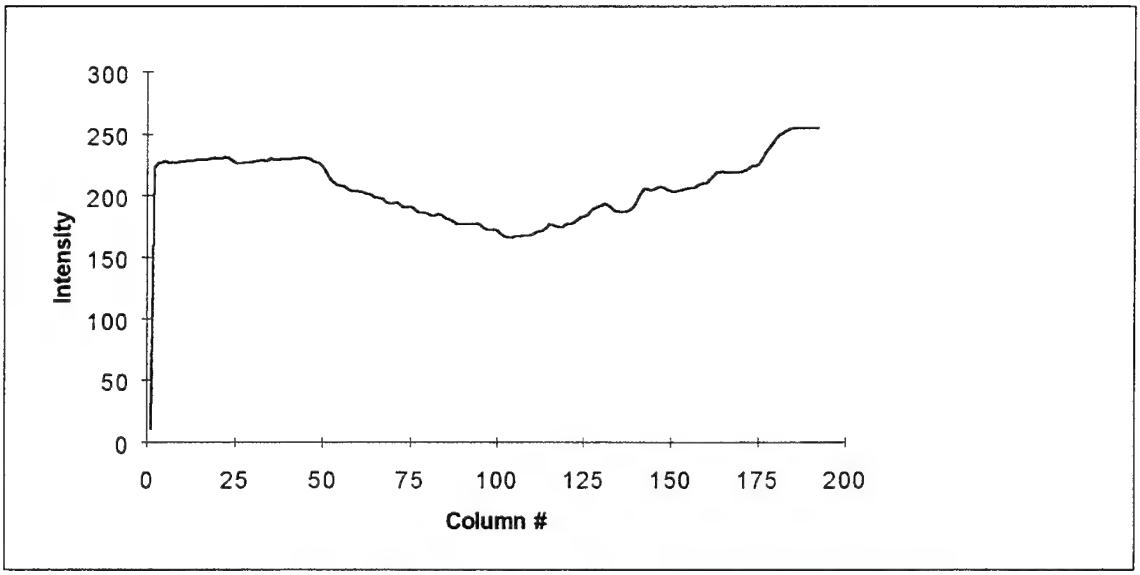

Fig. D-6. Reflection of T1 squashed to preserve horizontal sequencies

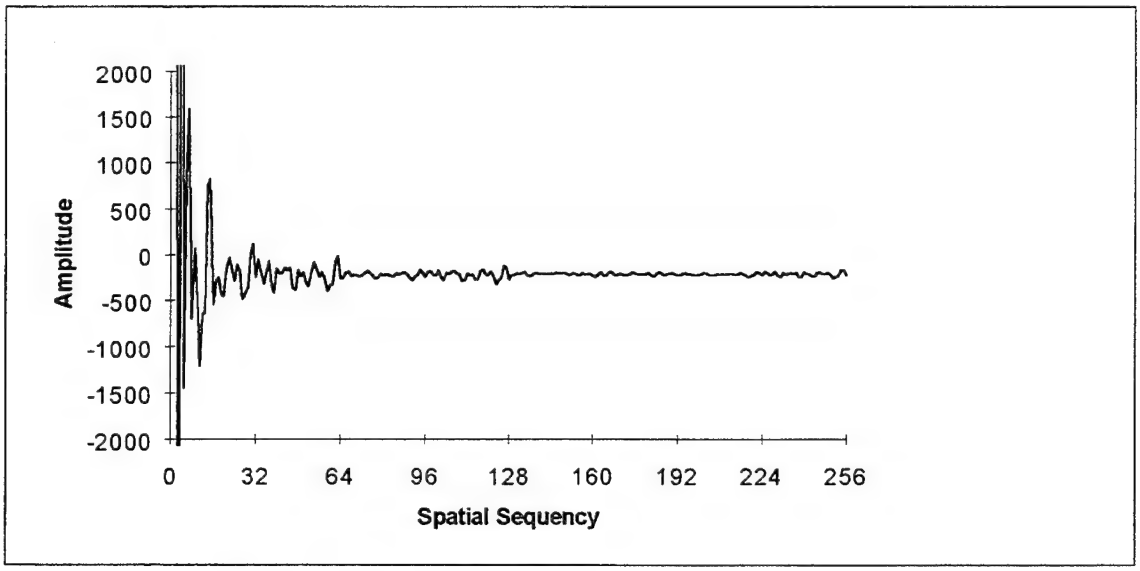

Fig. D-7. Walsh transform of Fig. D-6

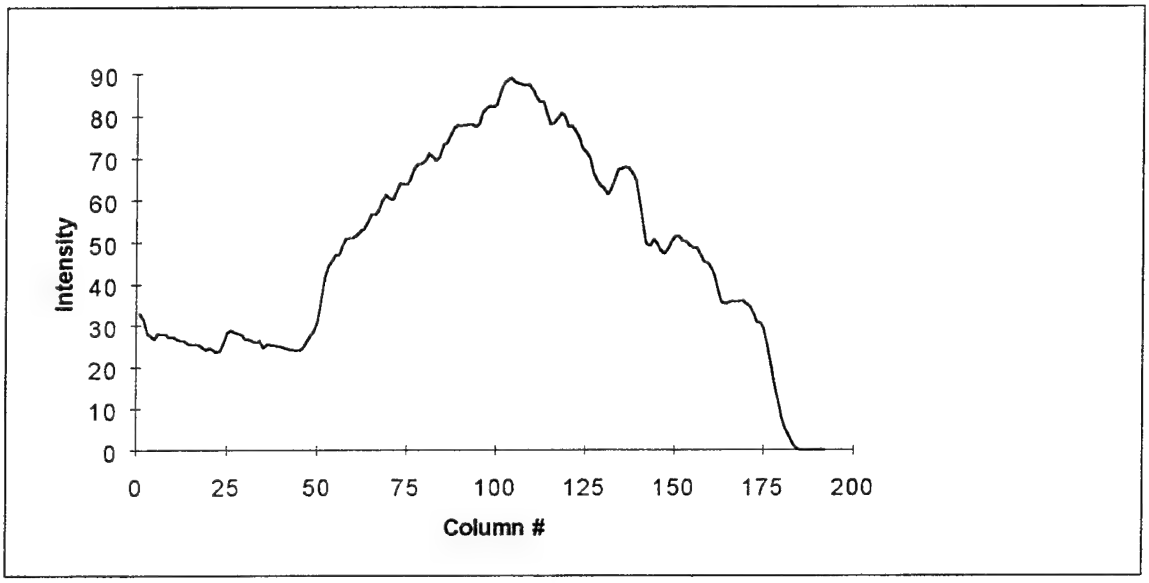

Fig. D-8. Complemented reflection of T1 squashed to preserve horizontal sequencies

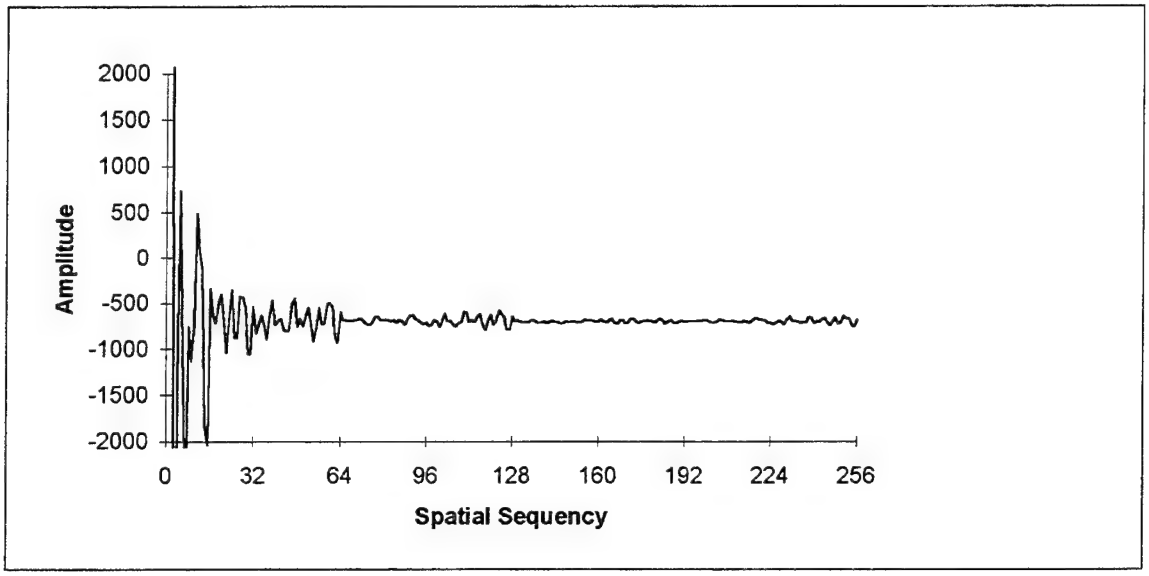

Fig. D-9. Walsh transform of Fig. D-8

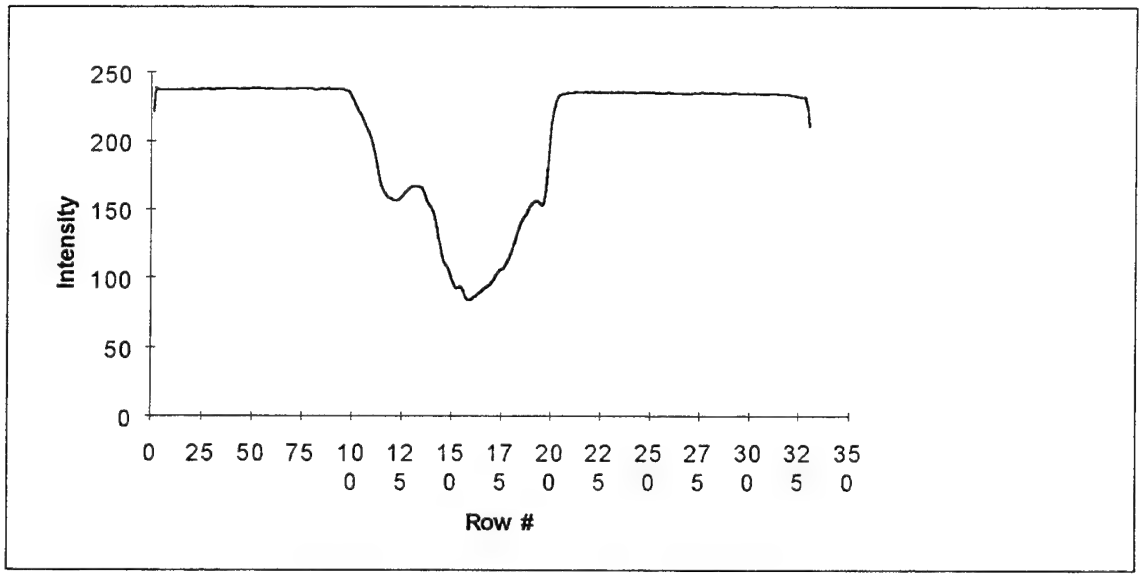

Fig. D-10. T1 squashed to preserve vertical sequencies

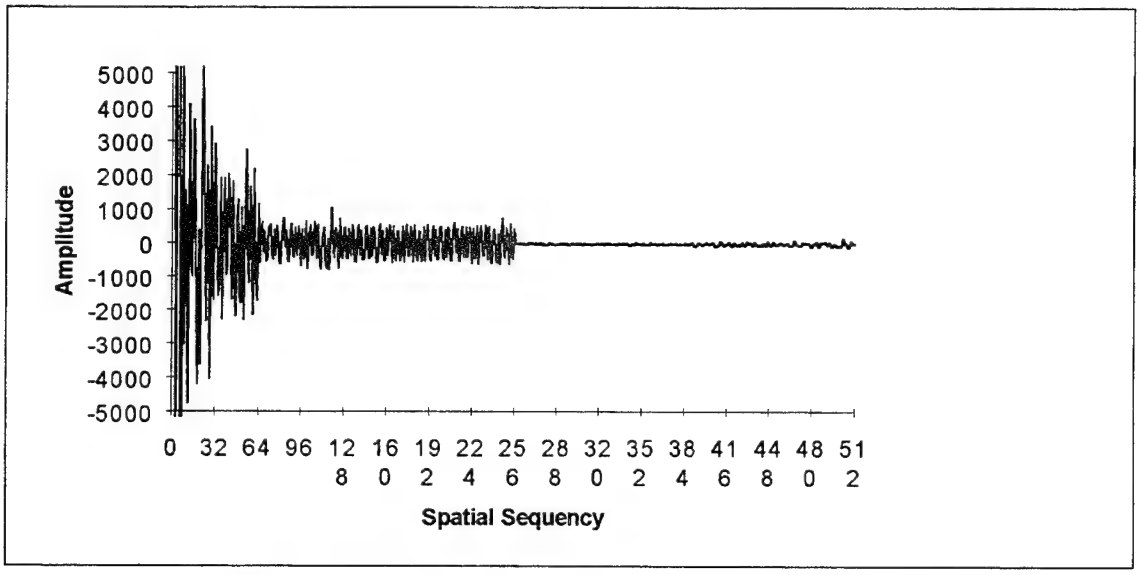

Fig. D-11. Walsh transform of Fig. D-10

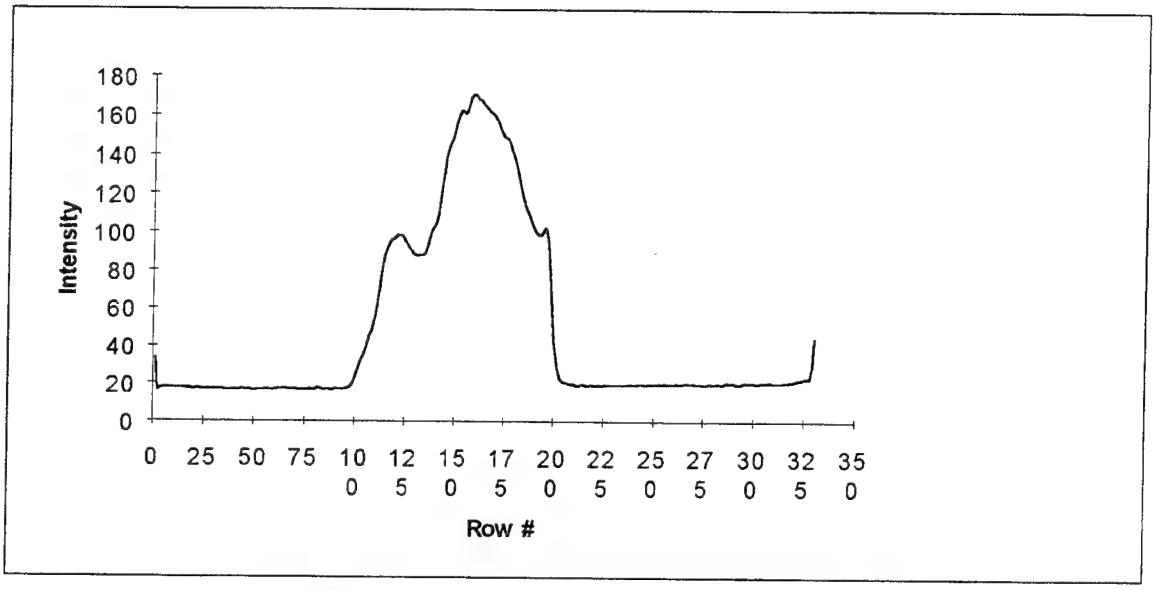

Fig. D-12. Complement of D-1 squashed to preserve vertical sequencies

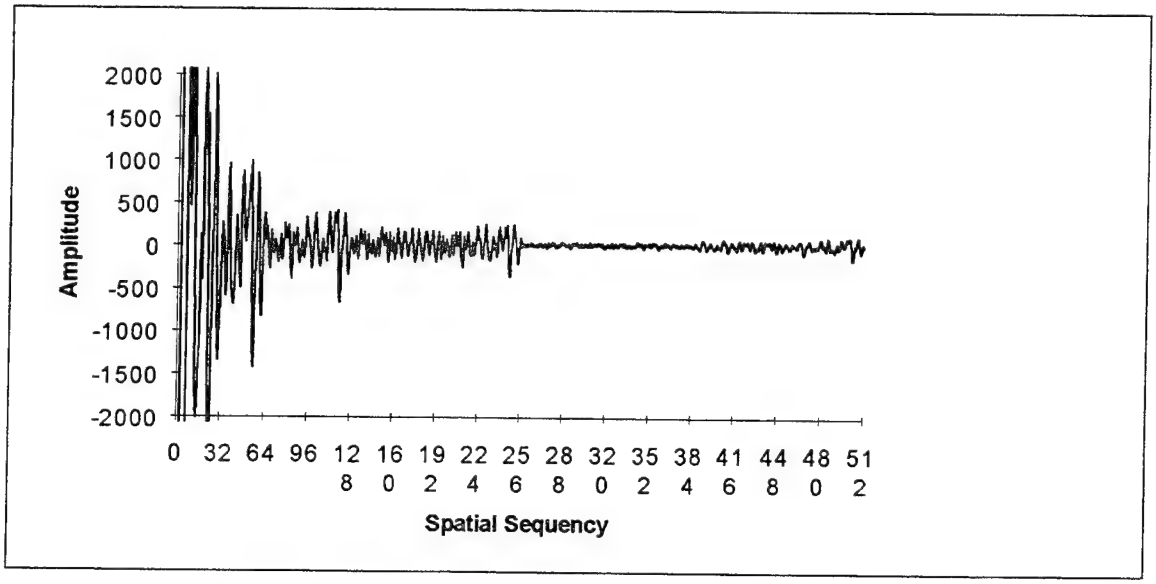

Fig. D-13. Walsh transform of Fig. D-12

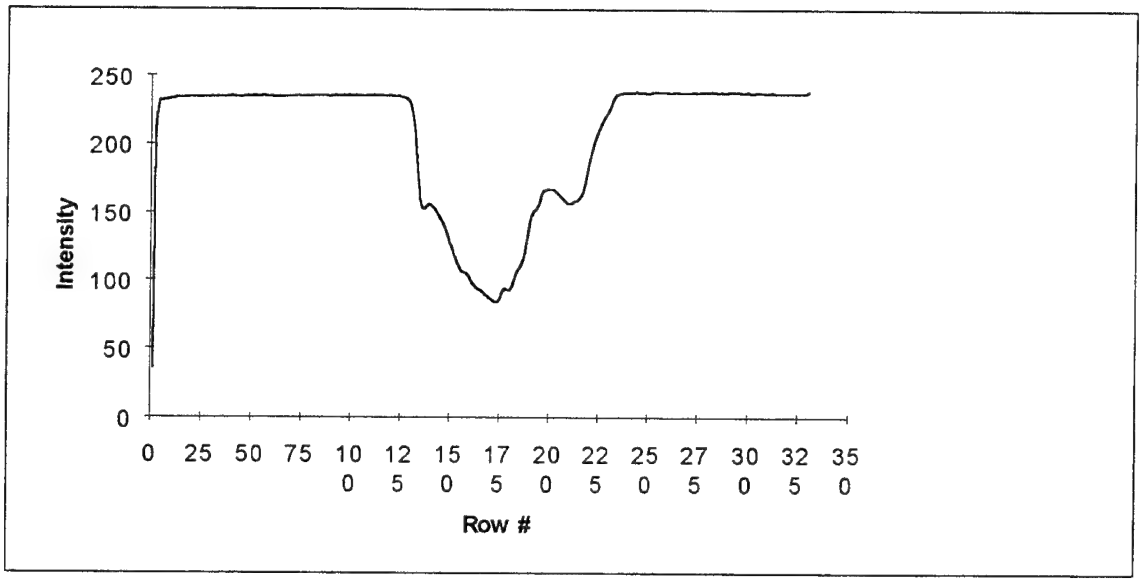

Fig. D-14. Reflection of T1 squashed to preserve vertical sequencies

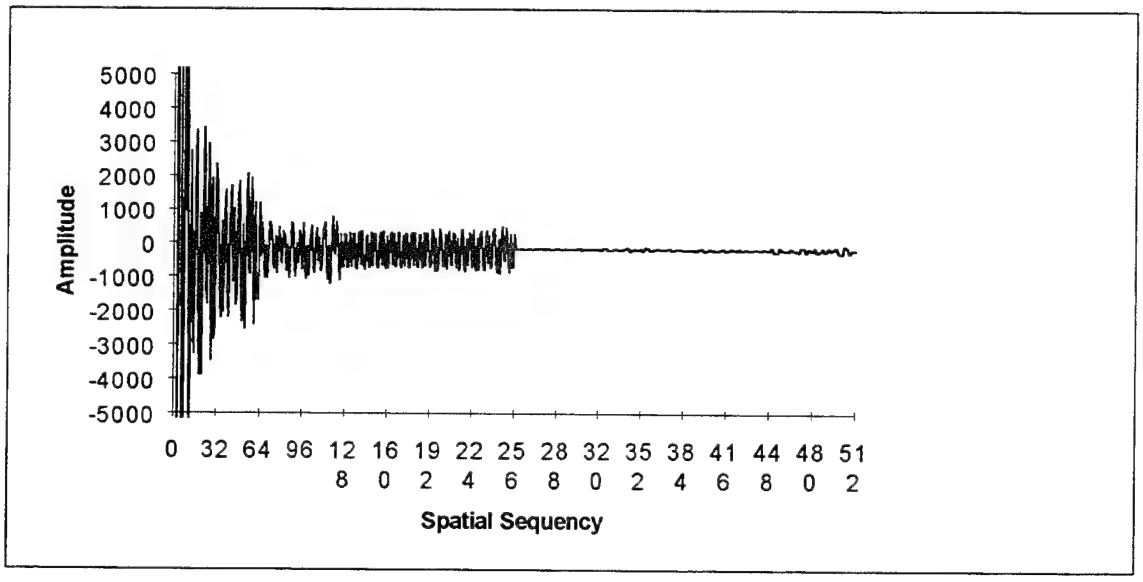

Fig. D-15. Walsh transform of Fig. D-14

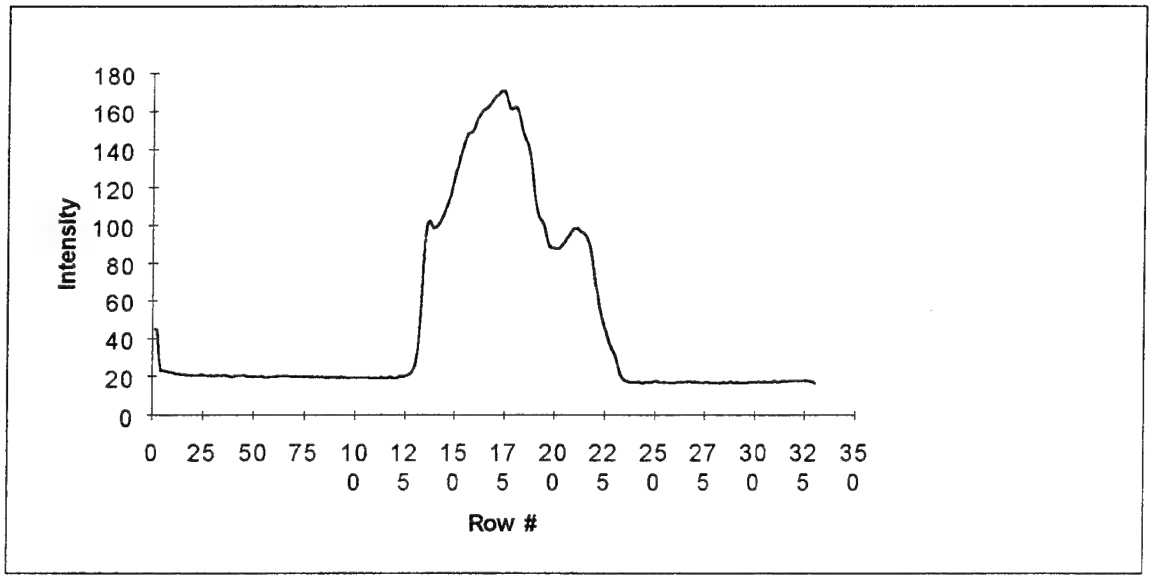

Fig. D-16. Complemented reflection of T1 squashed to preserve vertical sequencies

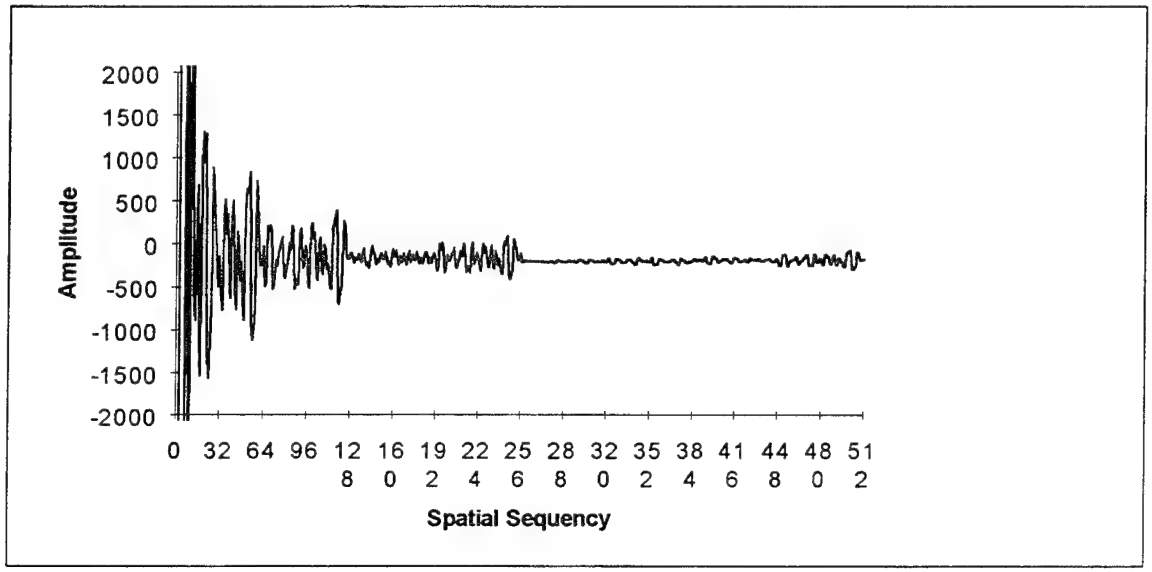

Fig. D-17. Walsh transform of Fig. D-16

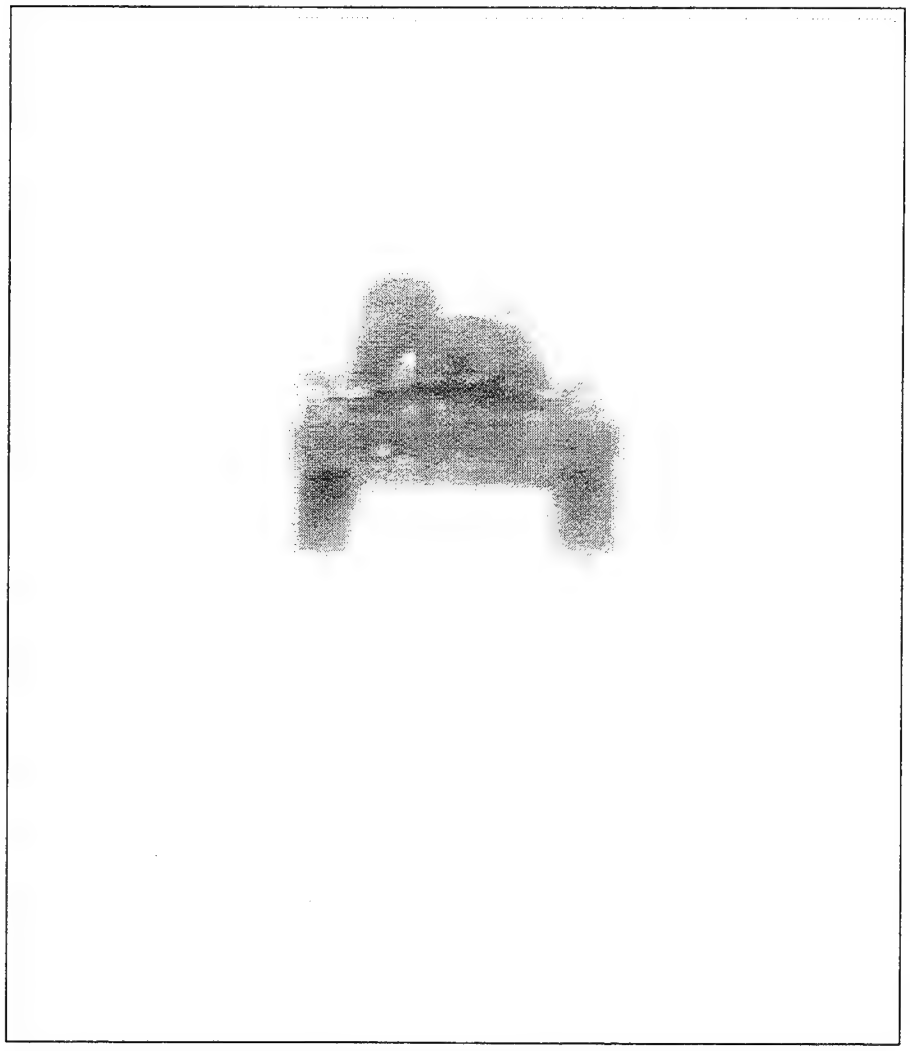

Fig. D-18. T3

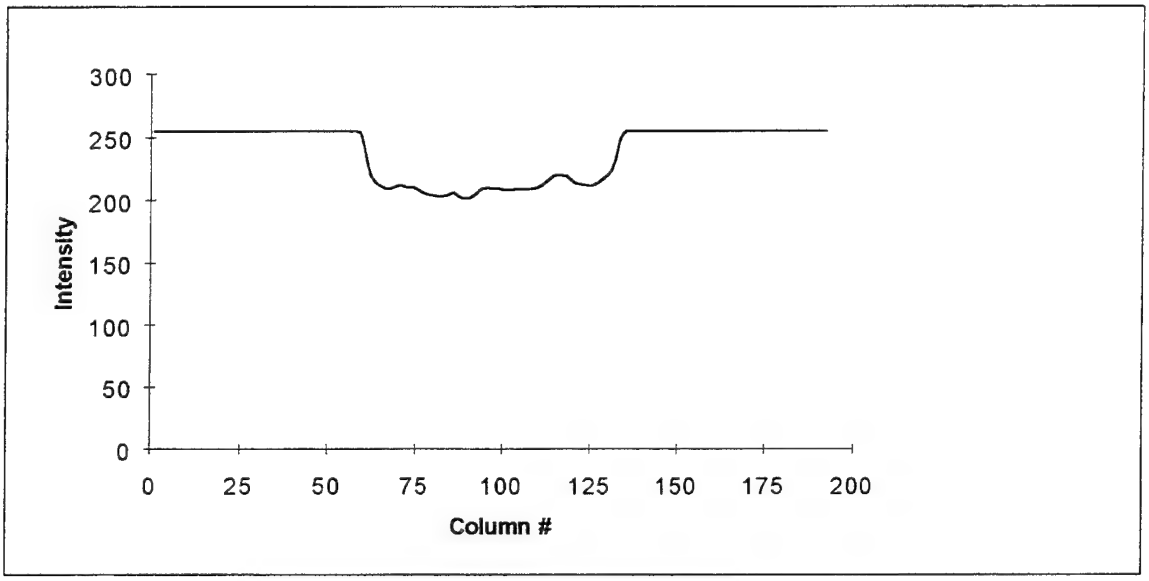

Fig. D-19. T3 squashed to preserve horizontal sequencies

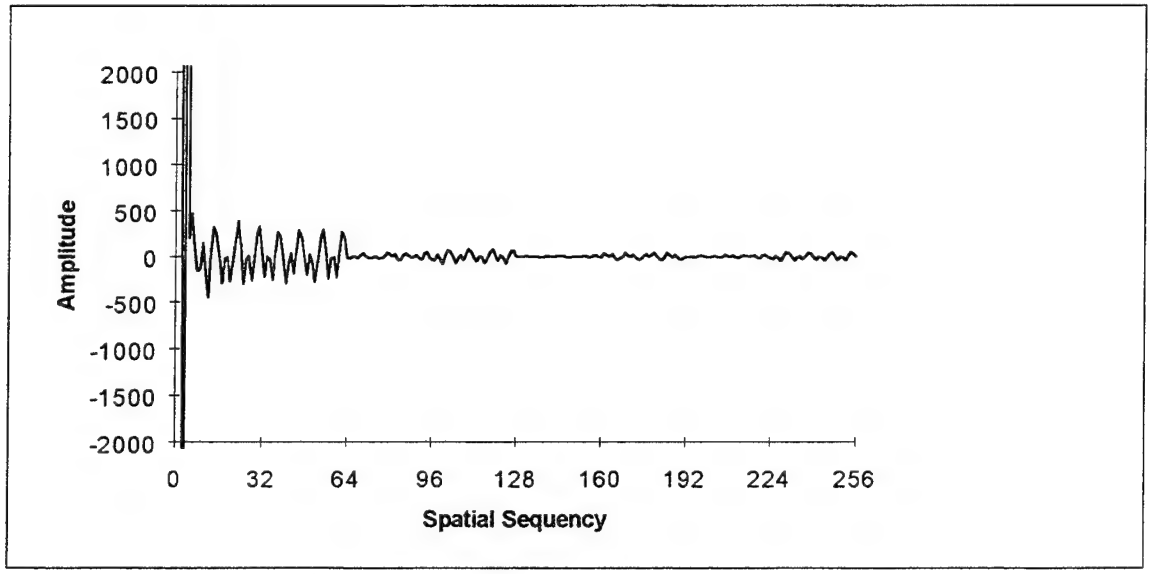

Fig. D-20. Walsh transform of Fig. D-19

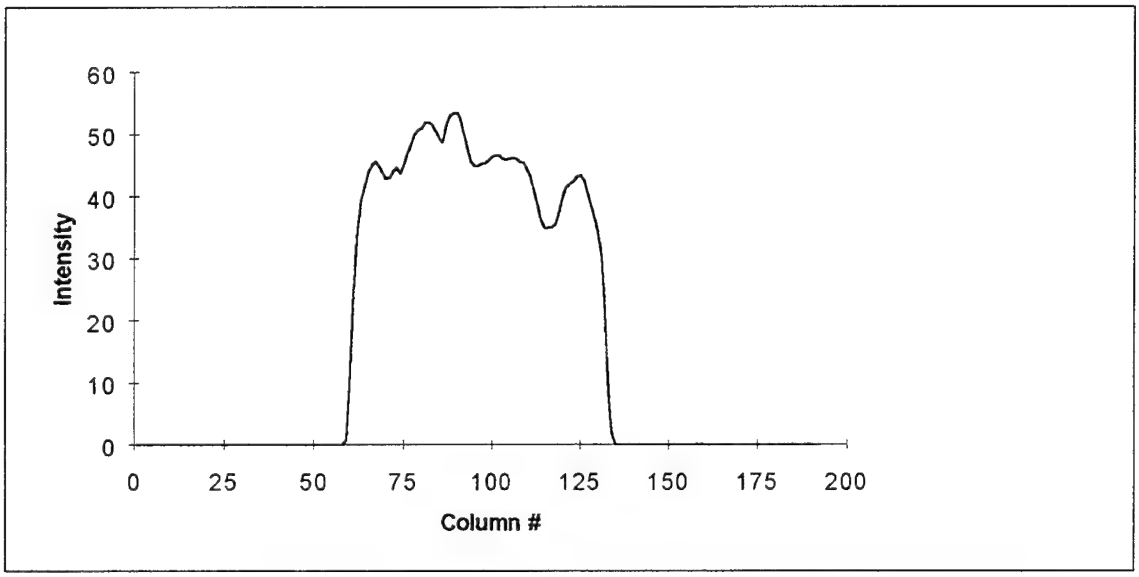

Fig. D-21. Complement of T3 squashed to preserve horizontal sequencies

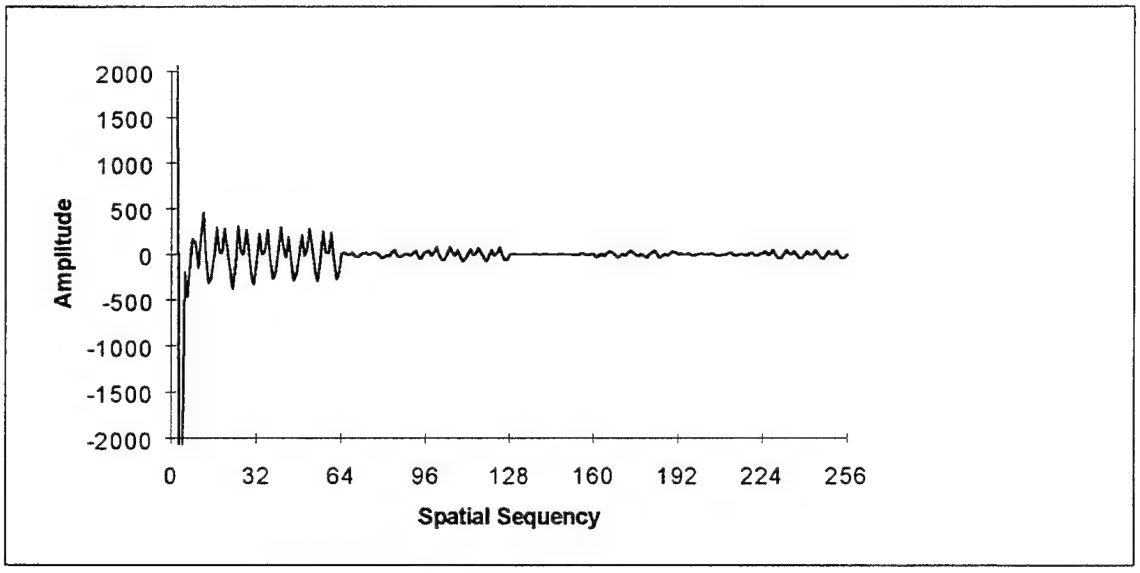

Fig. D-22. Walsh transform of Fig. D-21

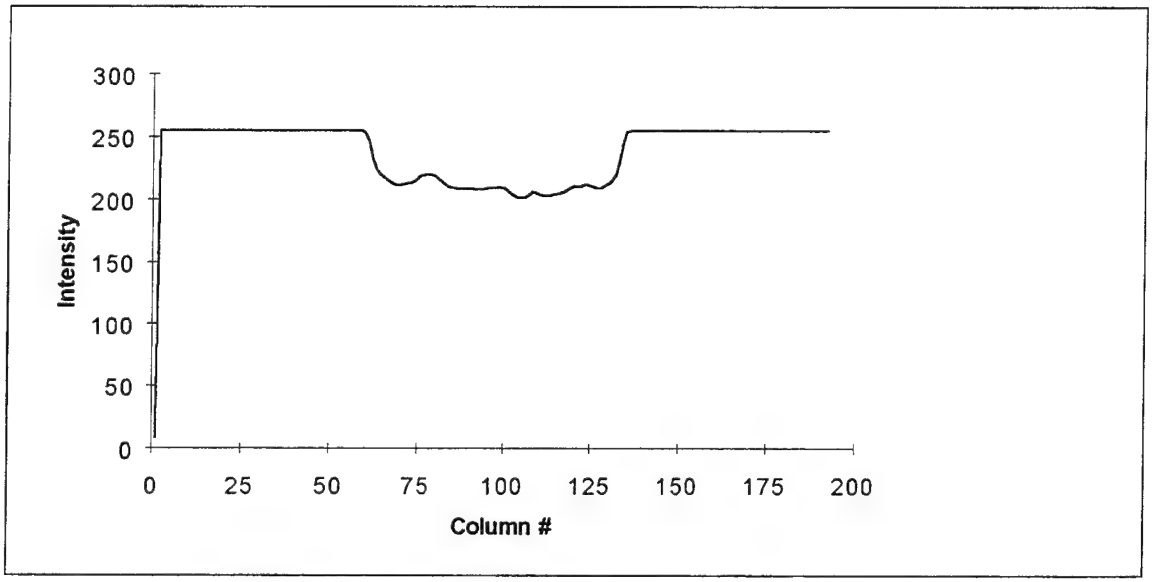

Fig. D-23. Reflection of T3 squashed to preserve horizontal sequencies

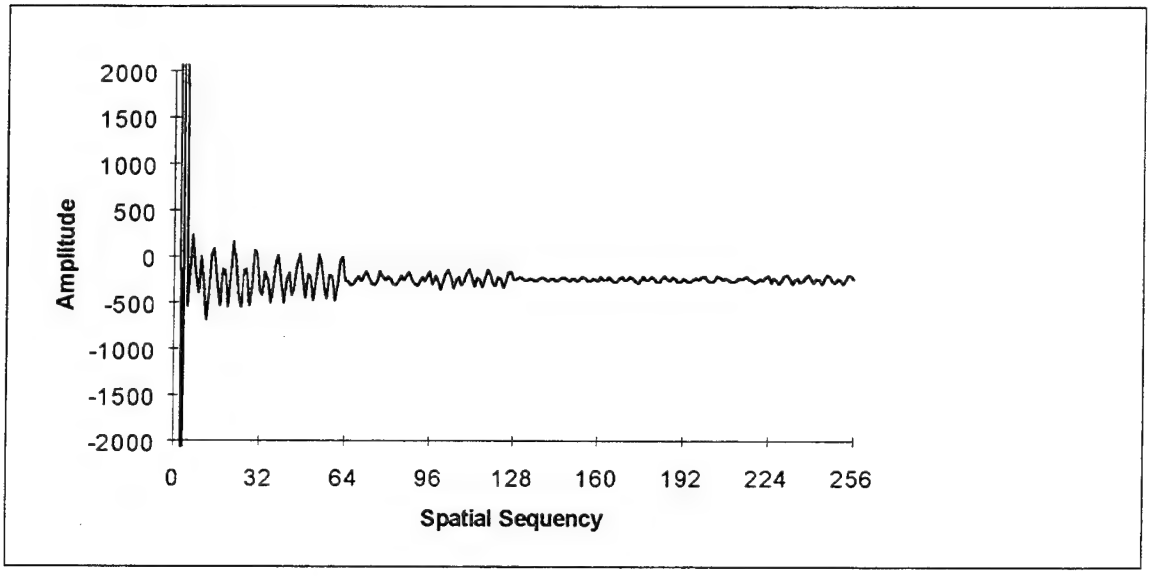

Fig. D-24. Walsh transform of Fig. D-23

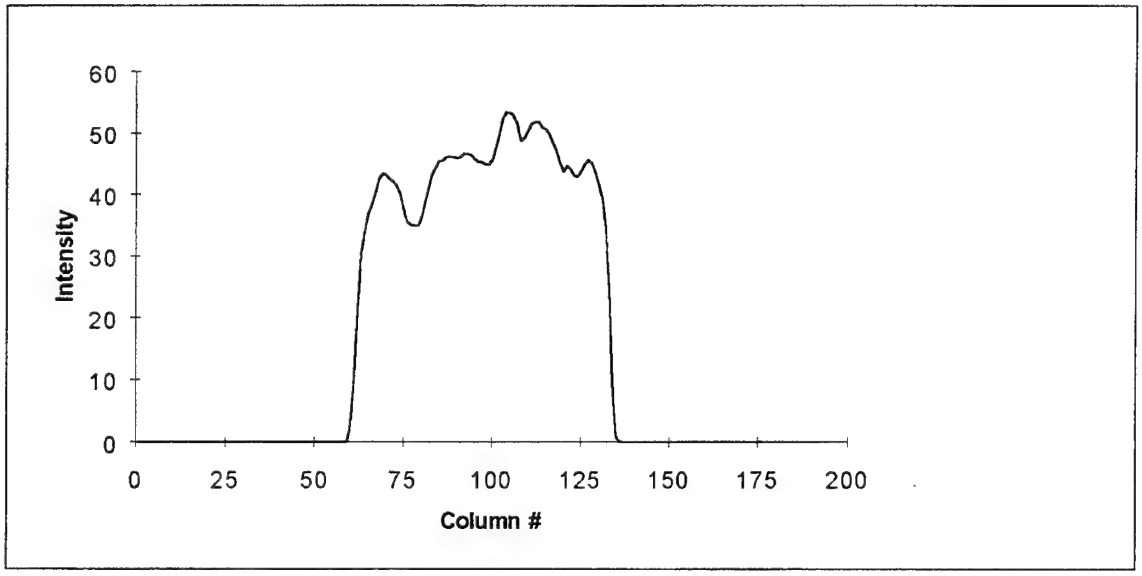

Fig. D-25. Complemented reflection of T3 squashed to preserve horizontal sequencies

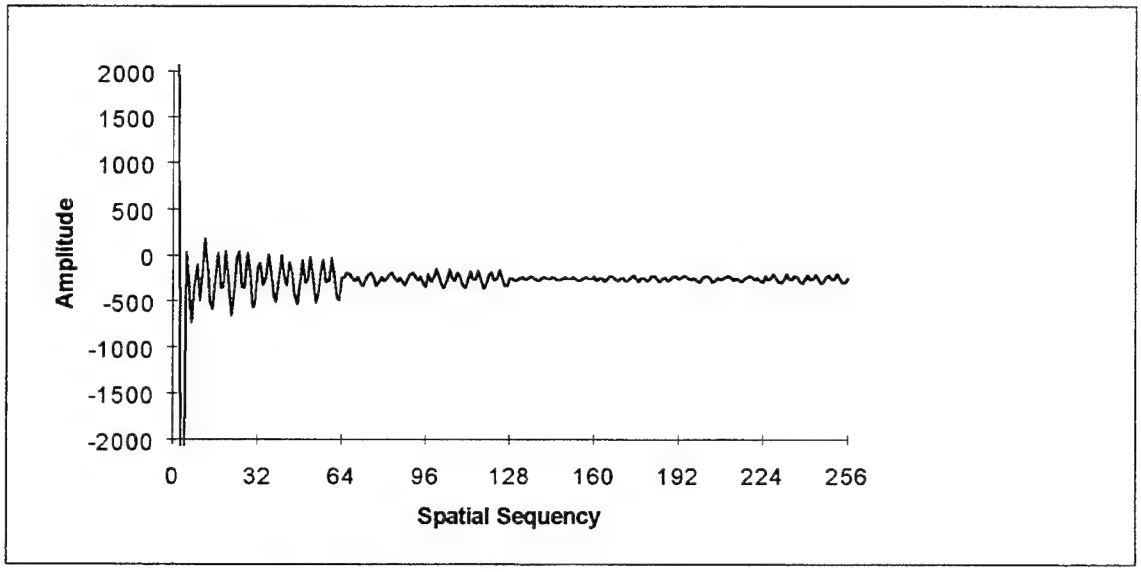

Fig. D-26. Walsh transform of Fig. D-25

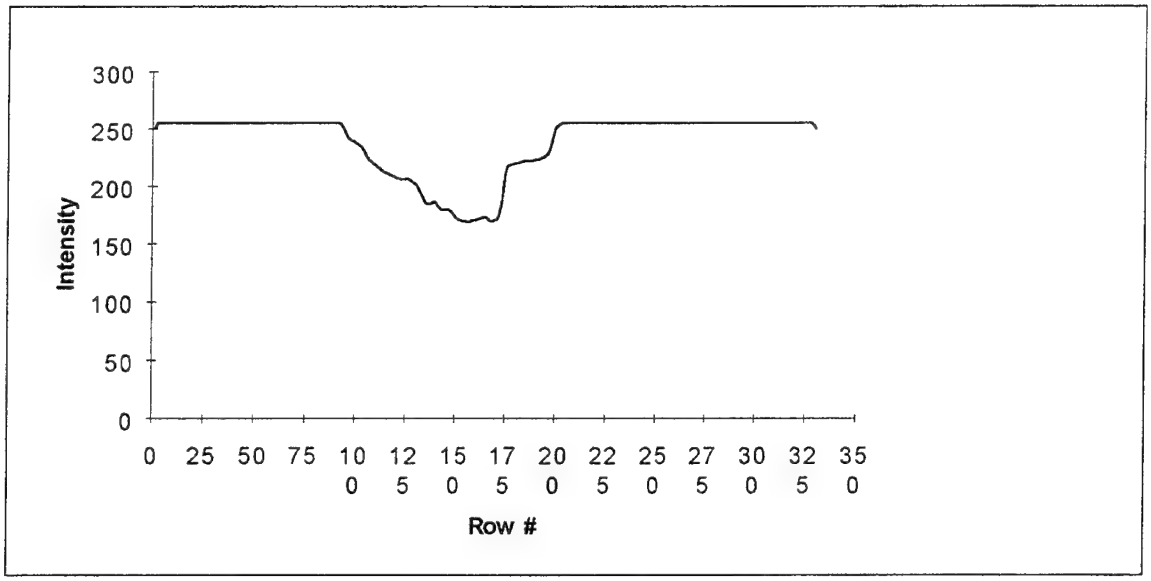

Fig. D-27. T3 squashed to preserve vertical sequencies

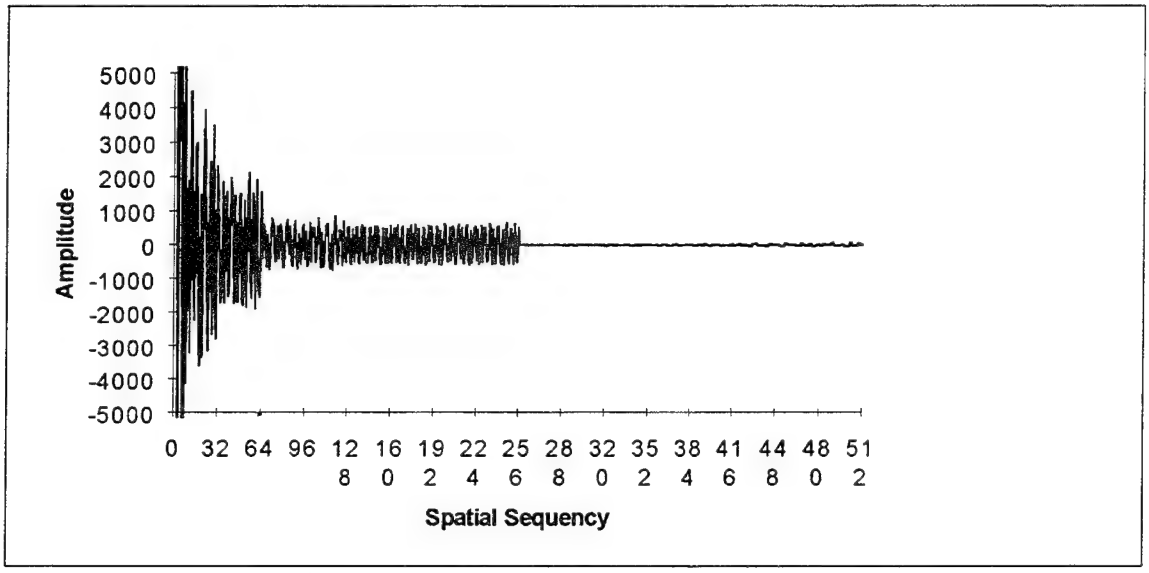

Fig. D-28. Walsh transform of Fig. D-27

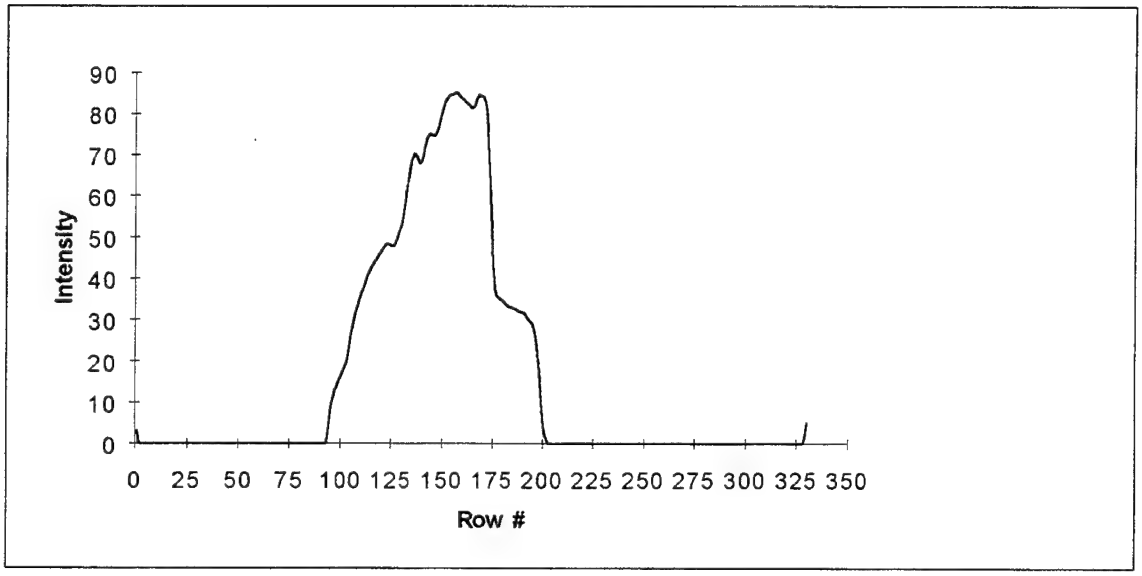

Fig. D-29. Complement of T3 squashed to preserve vertical sequencies

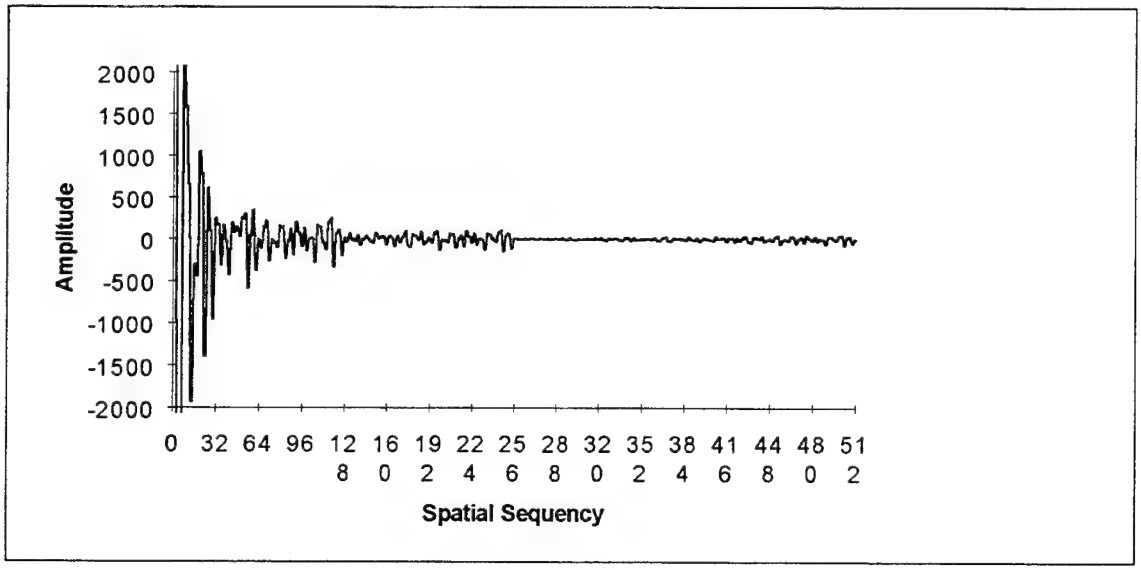

Fig. D-30. Walsh transform of Fig. D-29

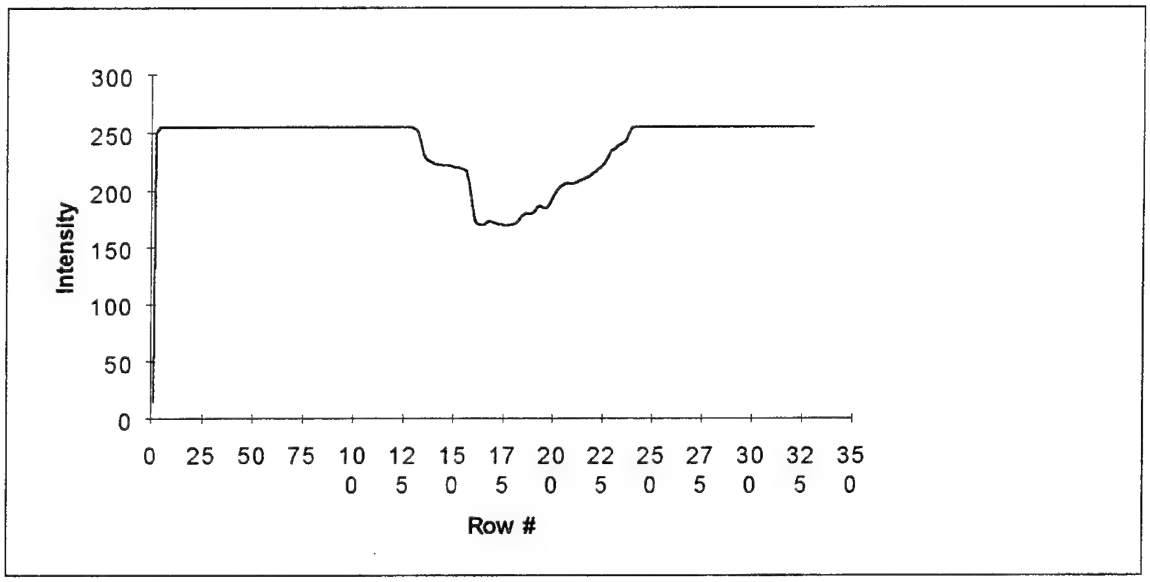

Fig. D-31. Reflection of T3 squashed to preserve vertical sequencies

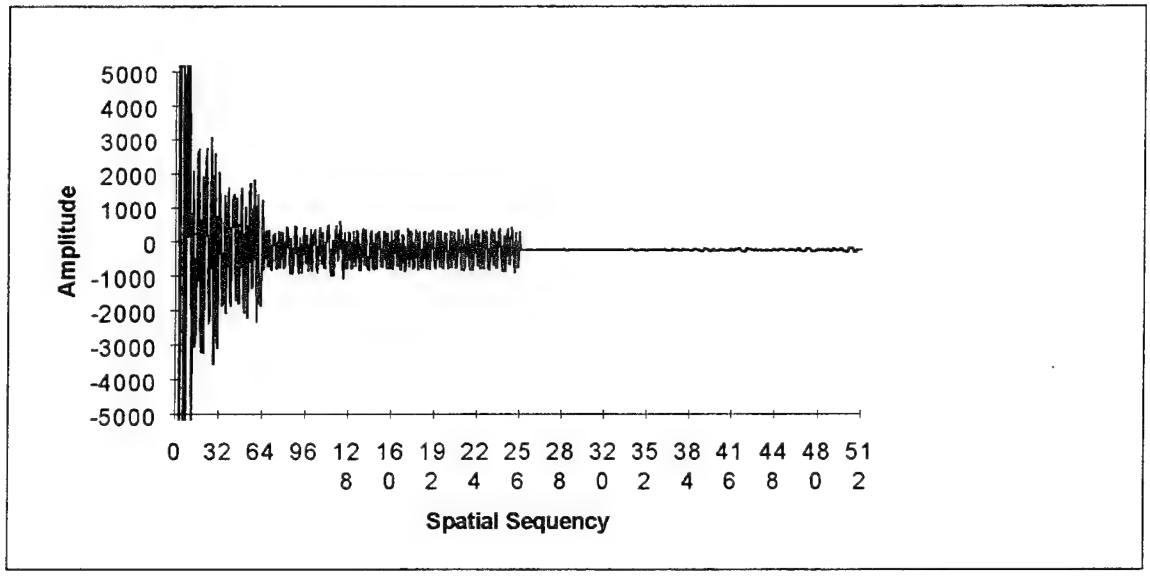

Fig. D-32. Walsh transform of Fig. D-31

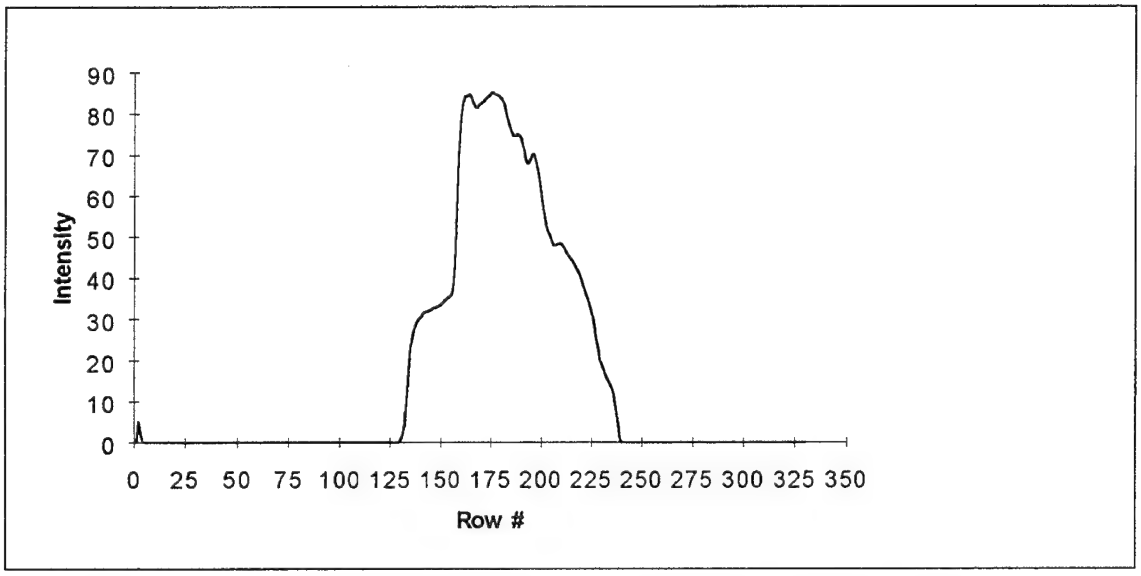

Fig. D-33. Complemented reflection of T3 squashed to preserve vertical sequencies

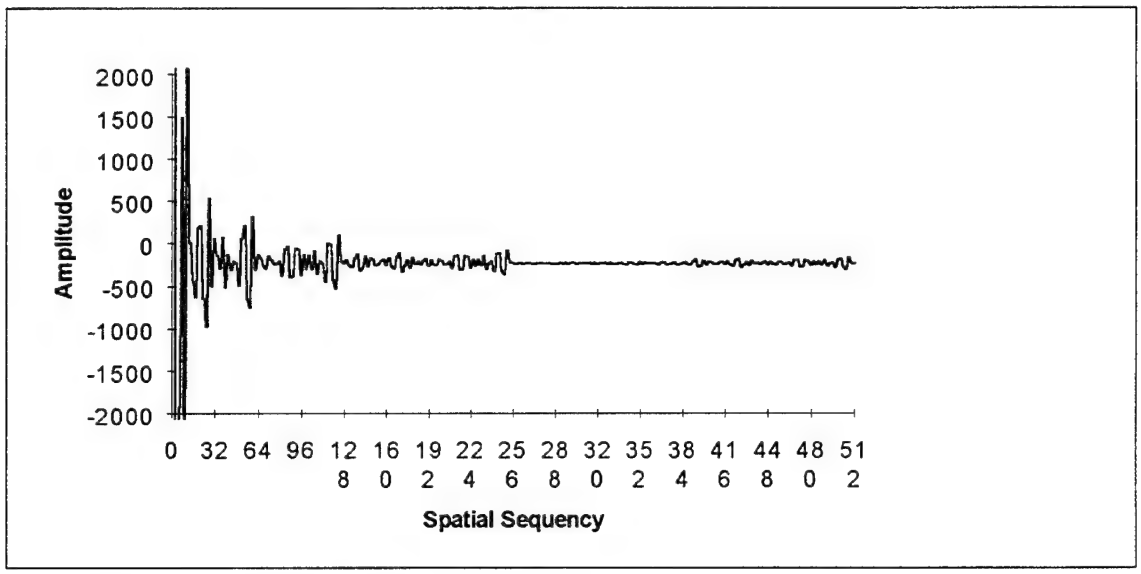

Fig. D-34. Walsh transform of Fig. D-33

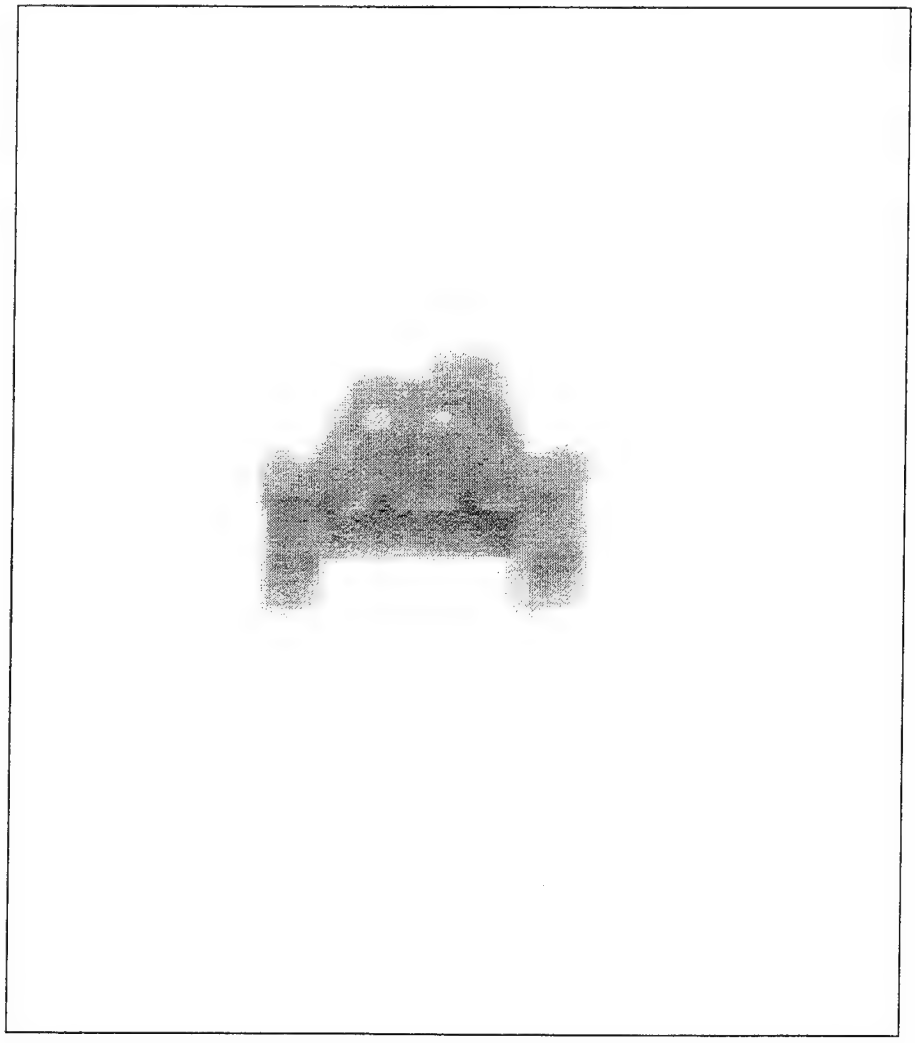

Fig. D-35. T4

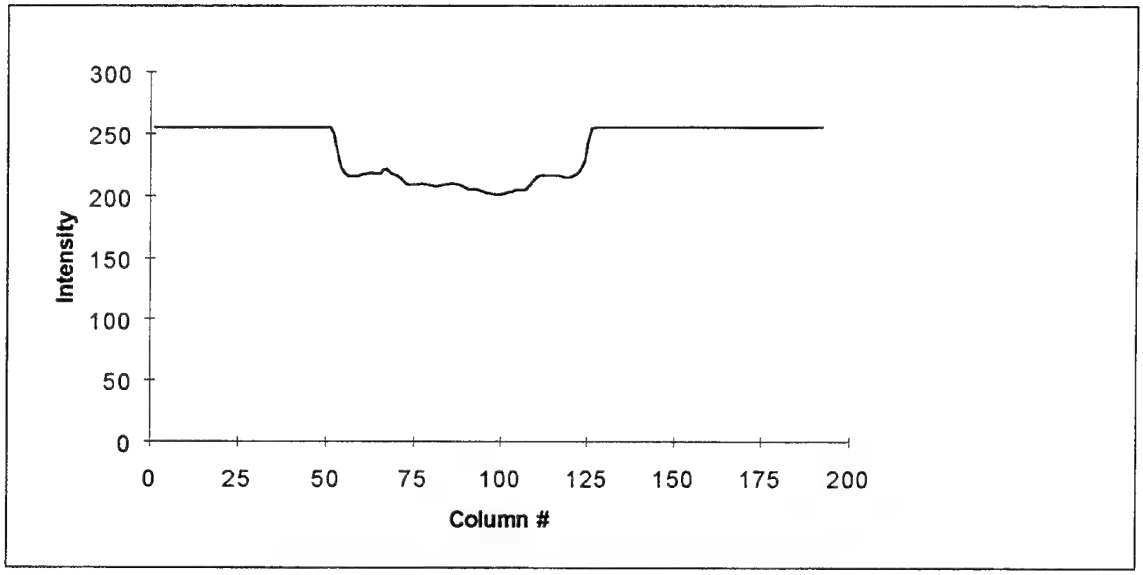

Fig. D-36. T4 squashed to preserve horizontal sequencies

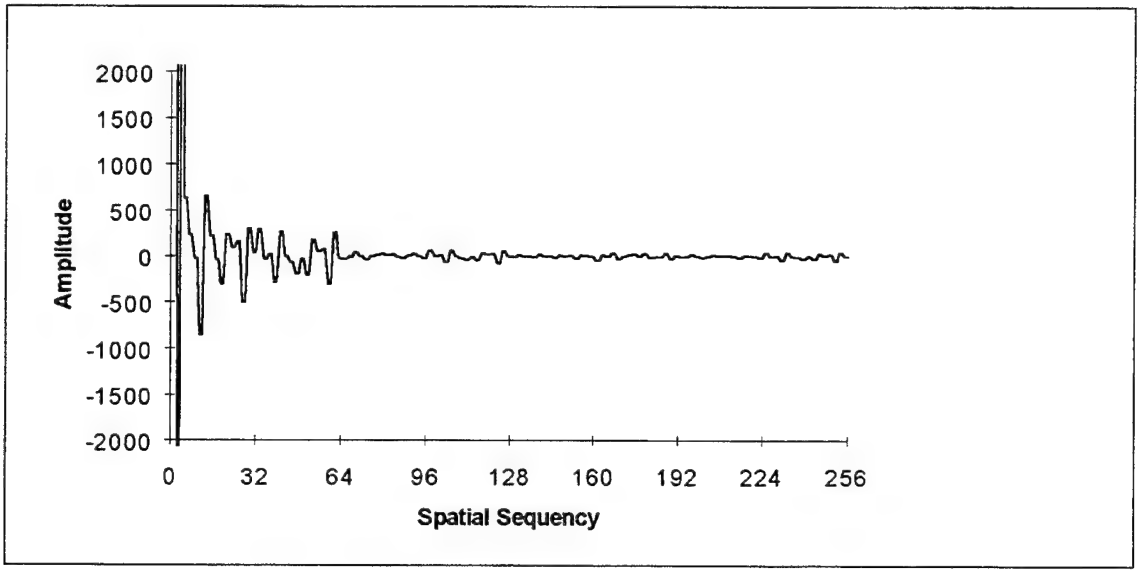

Fig. D-37. Walsh transform of Fig. D-36

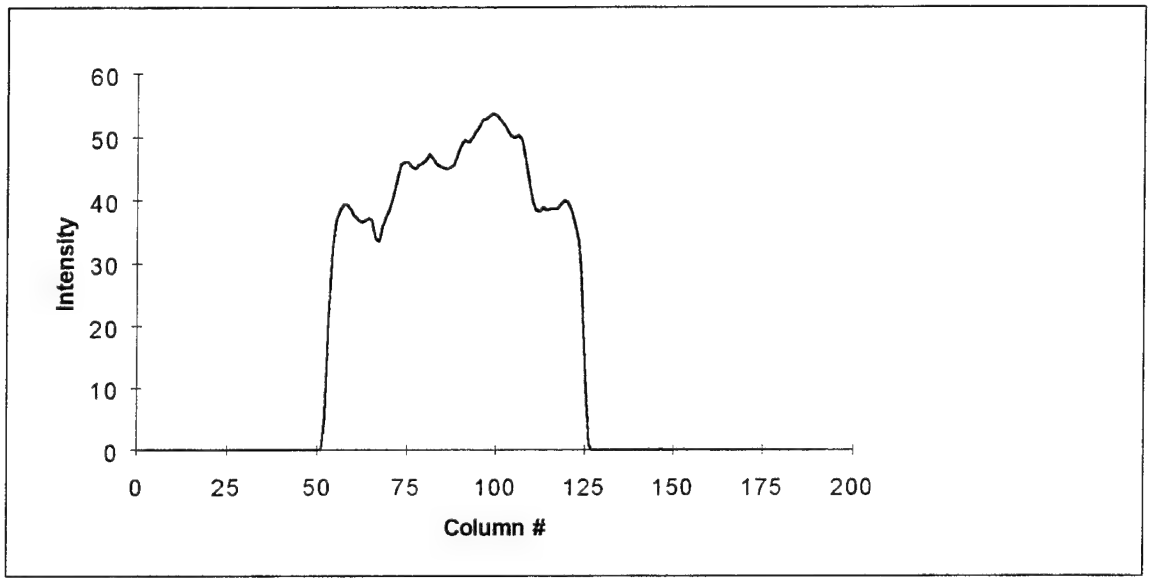

Fig. D-38. Complement of T4 squashed to preserve horizontal sequencies

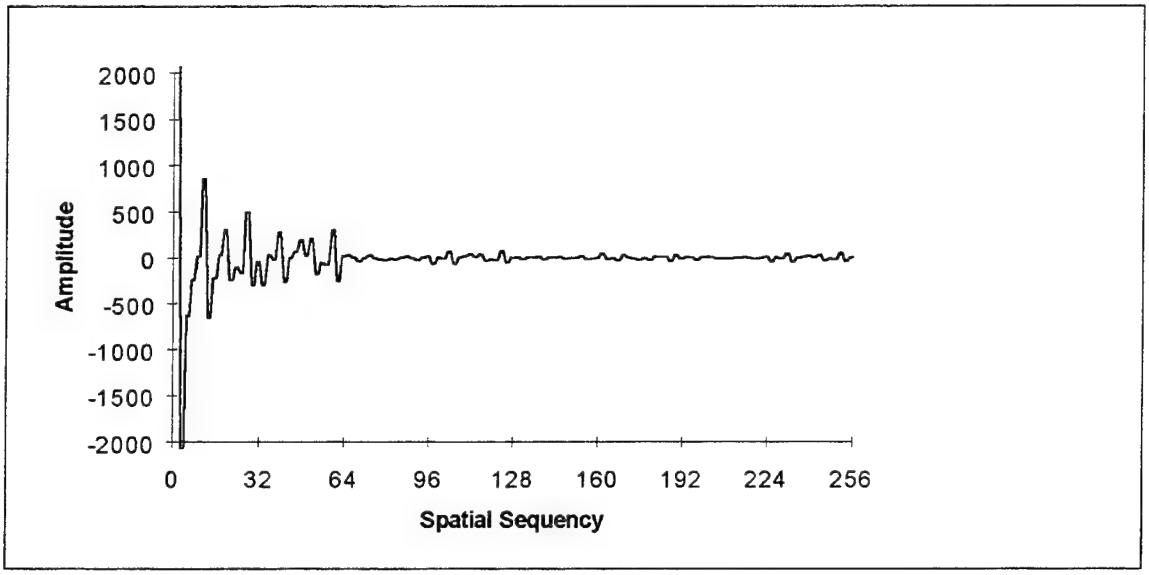

Fig. D-39. Walsh transform of Fig. D-38

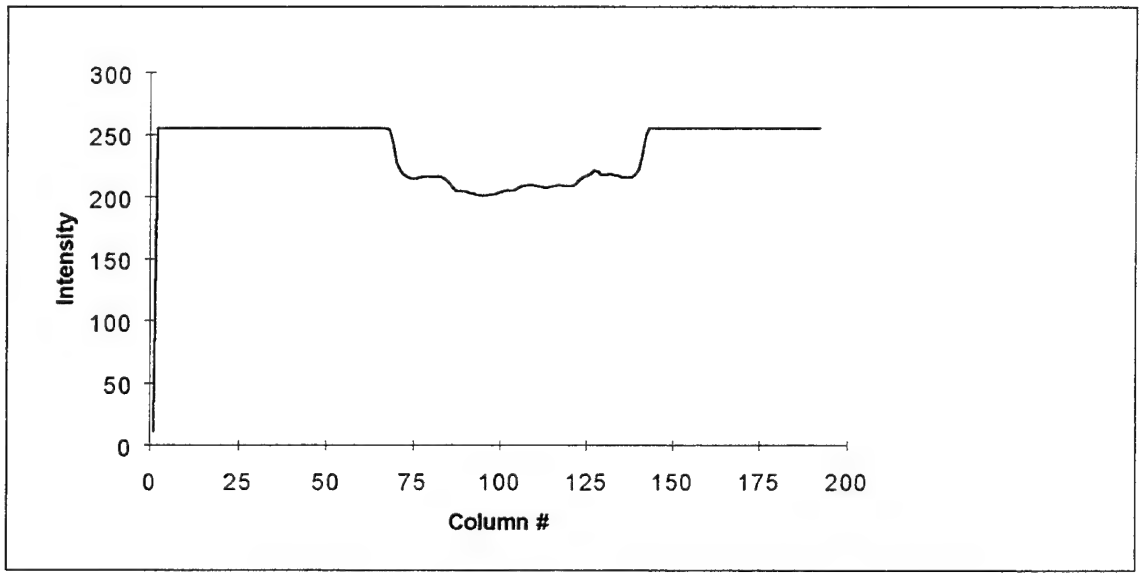

Fig. D-40. Reflection of T4 squashed to preserve horizontal sequencies

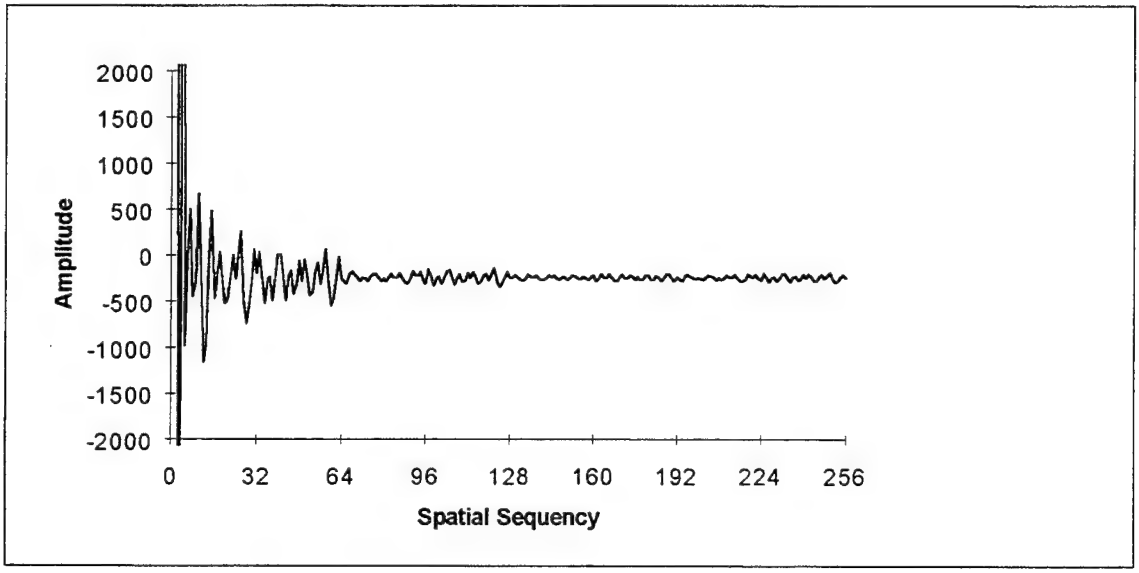

Fig. D-41. Walsh transform of Fig. D-40

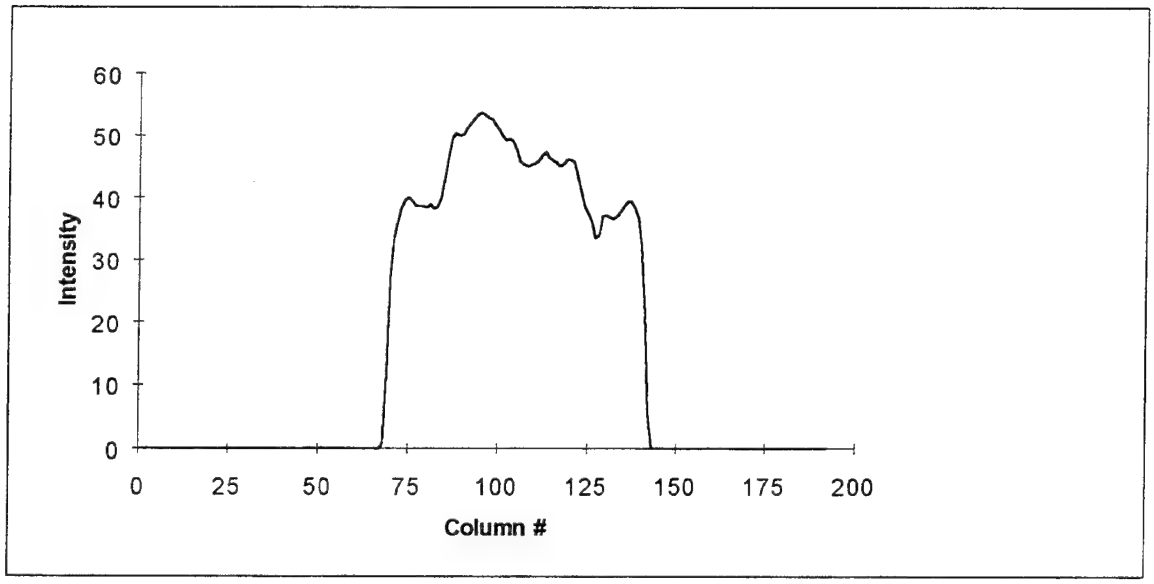

Fig. D-42. Complemented reflection of T4 squashed to preserve horizontal sequencies

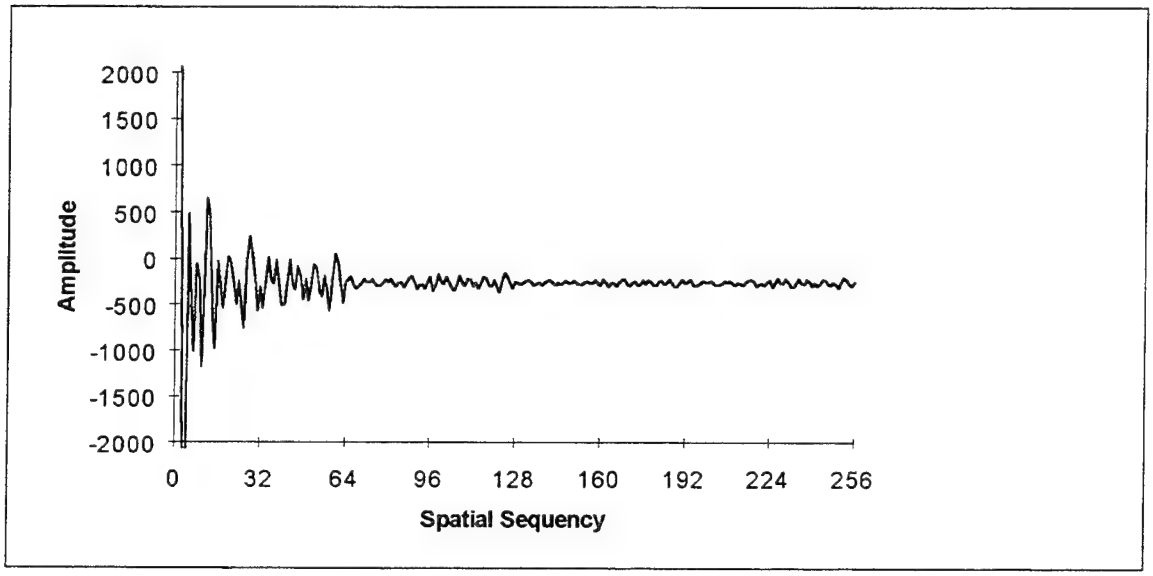

Fig. D-43. Walsh transform of Fig. D-42

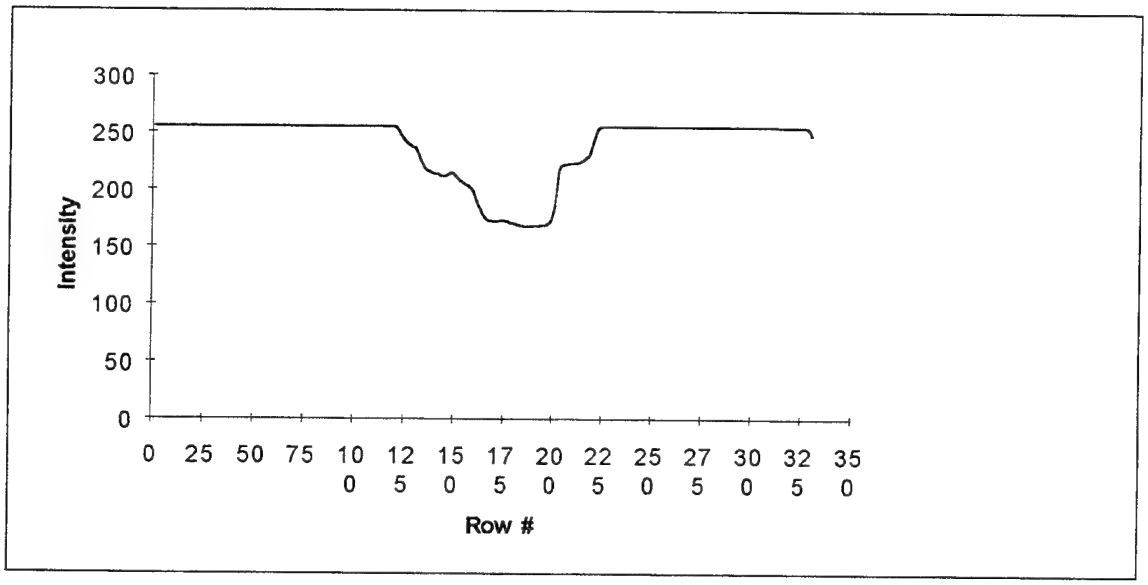

Fig. D-44. T4 squashed to preserve vertical sequencies

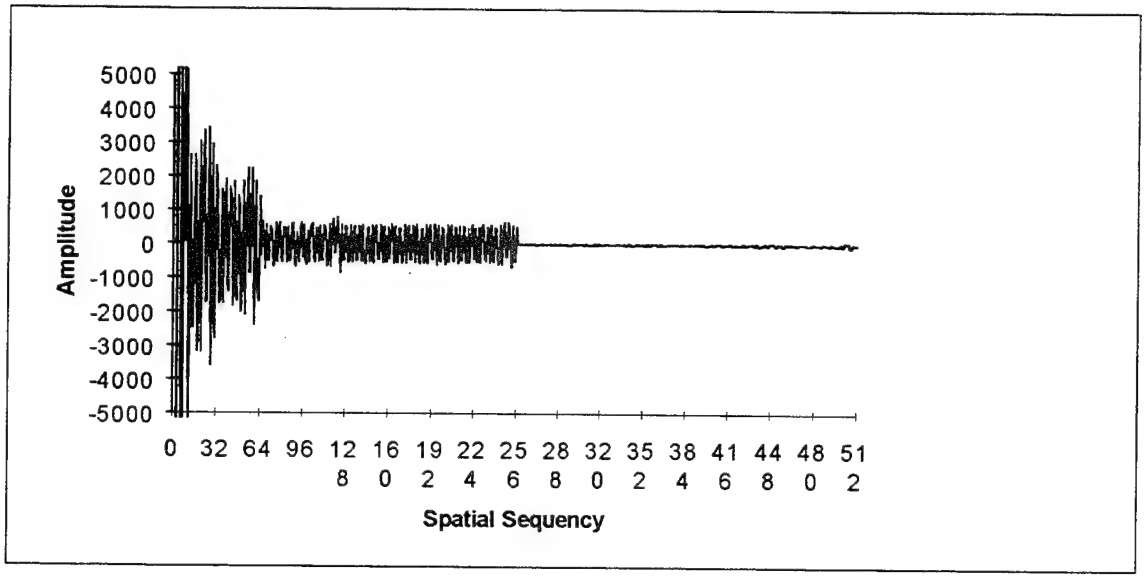

Fig. D-45. Walsh transform of Fig. D-44

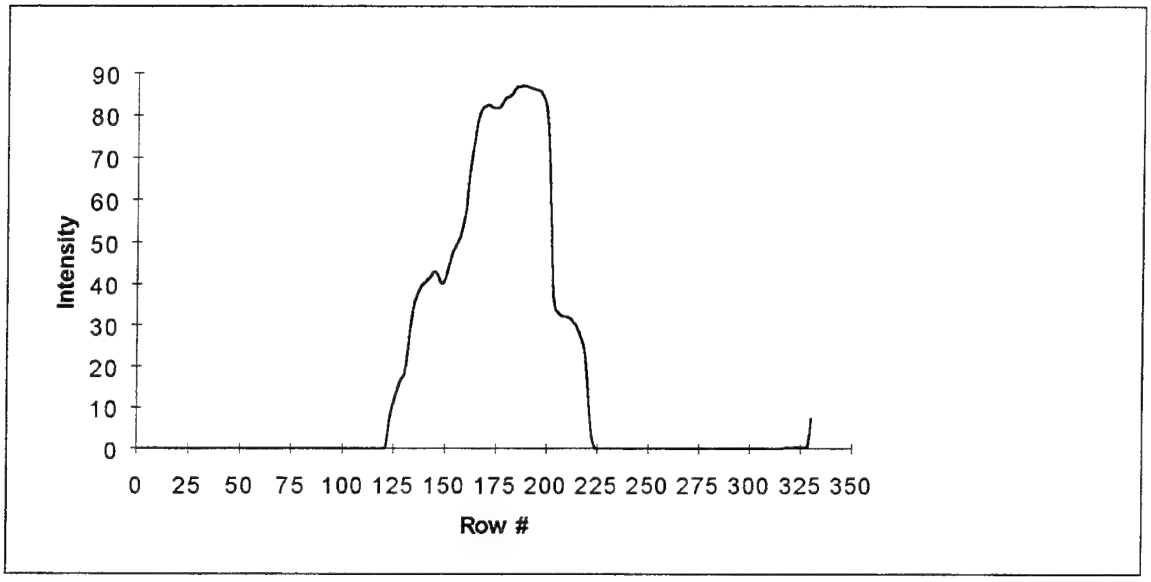

Fig. D-46. Complement of T4 squashed to preserve vertical sequencies

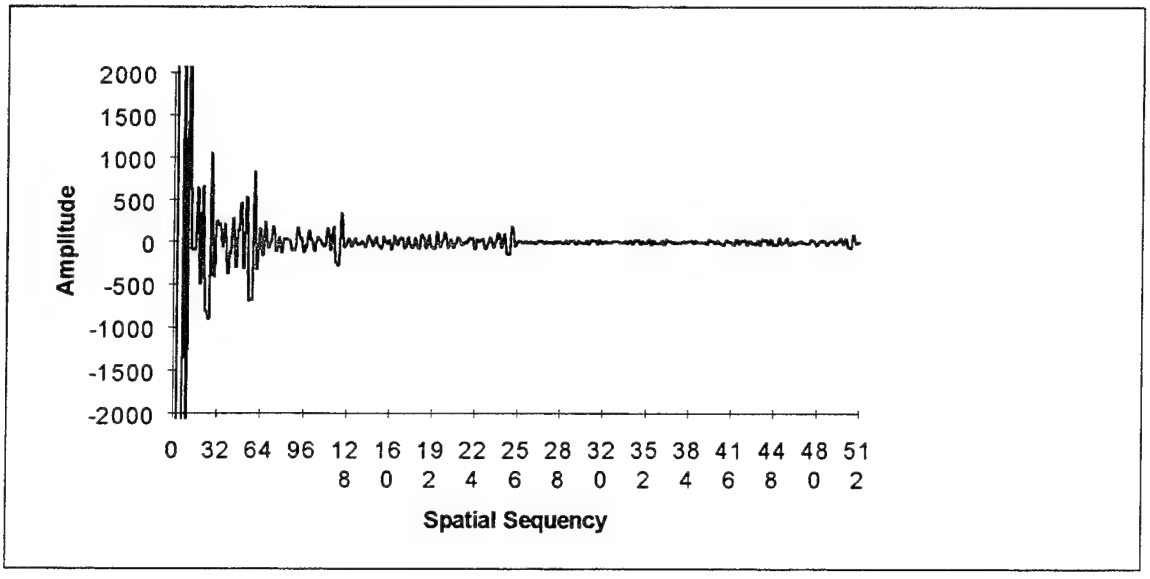

Fig. D-47. Walsh transform of Fig. D-46

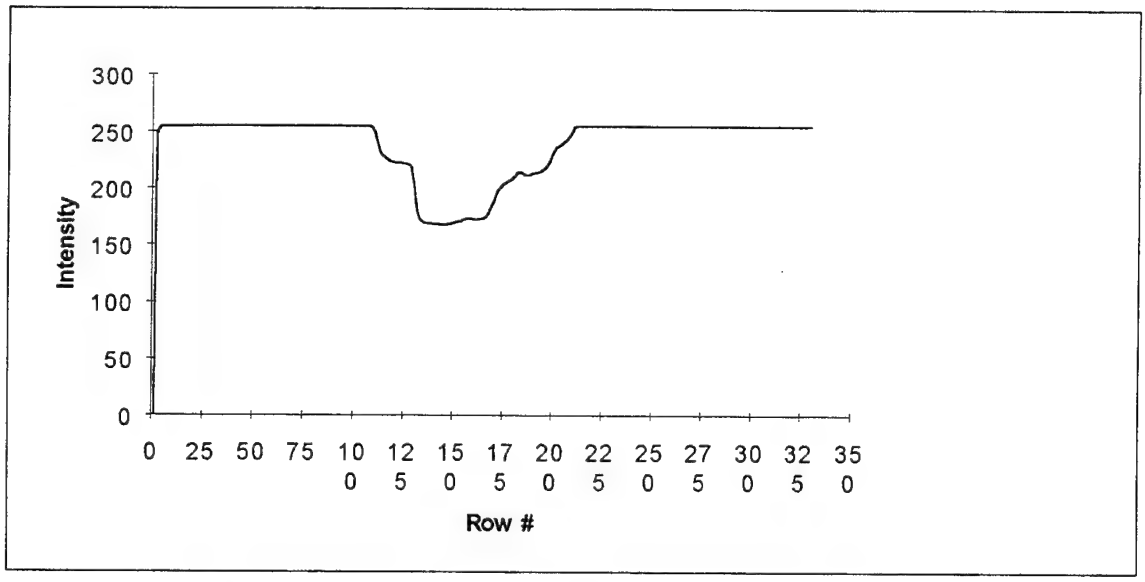

Fig. D-48. Reflection of T4 squashed to preserve vertical sequencies

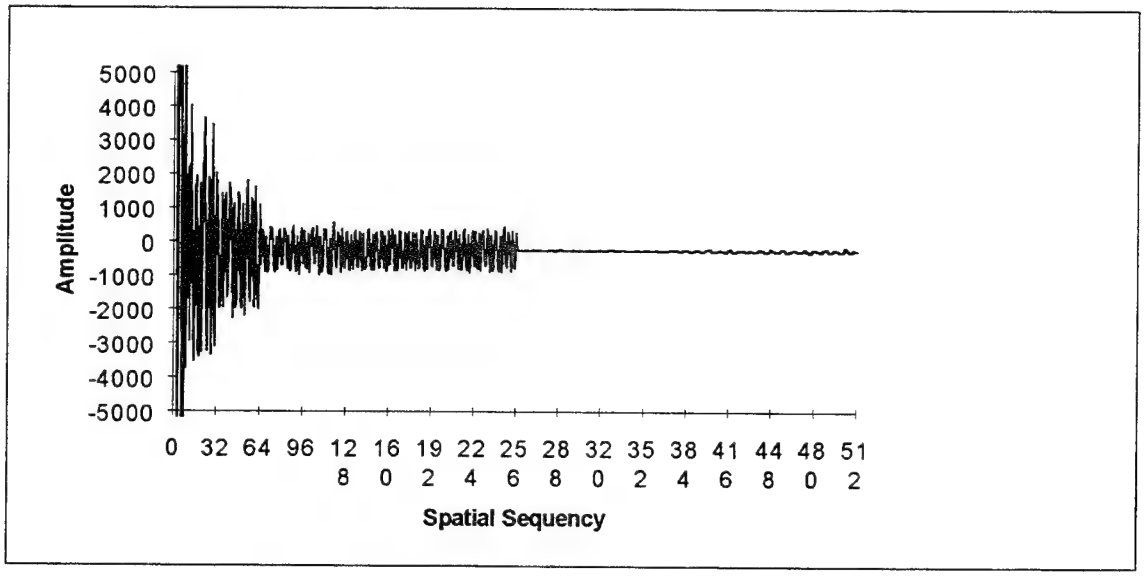

Fig. D-49. Walsh transform of Fig. D-48

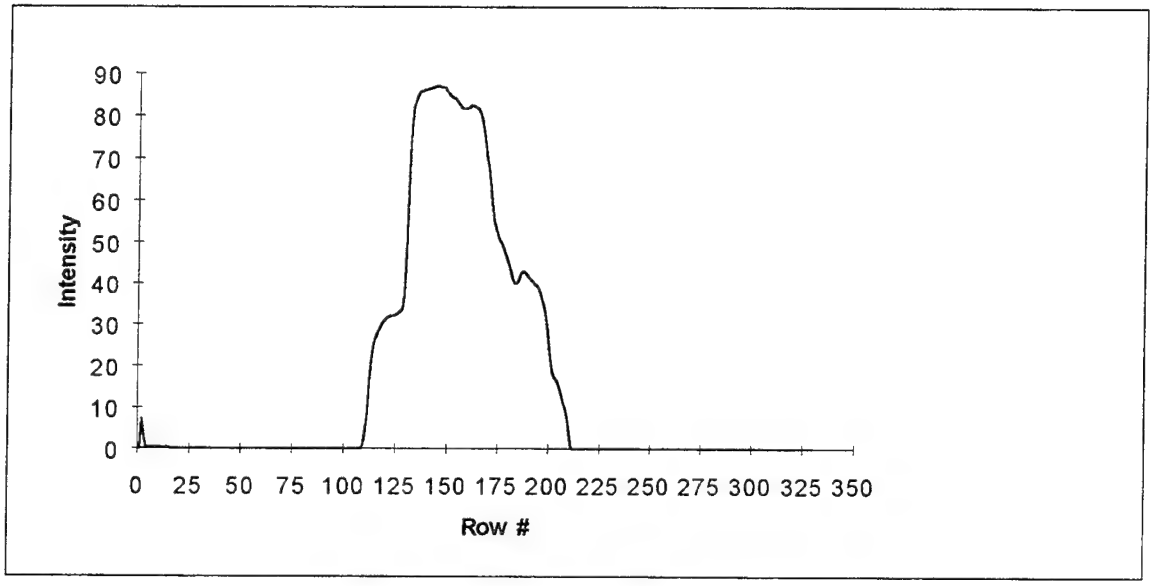

Fig. D-50. Complemented reflection of T4 squashed to preserve vertical sequencies

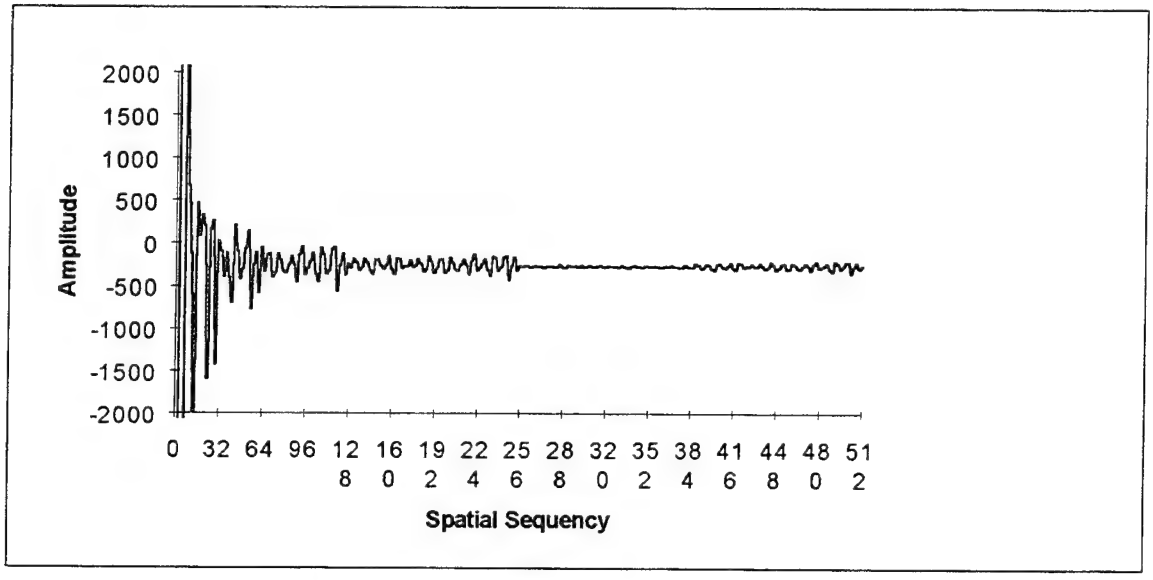

Fig. D-51. Walsh transform of Fig. D-50

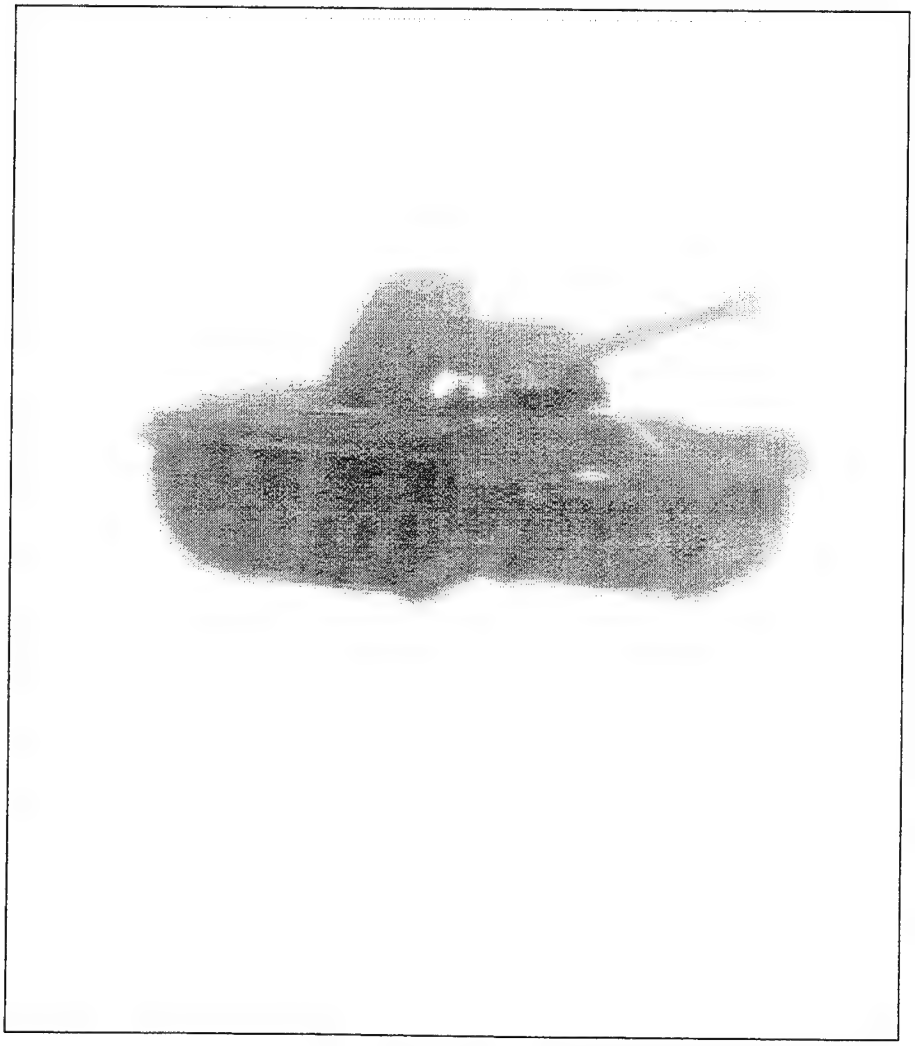

Fig. D-52. T5

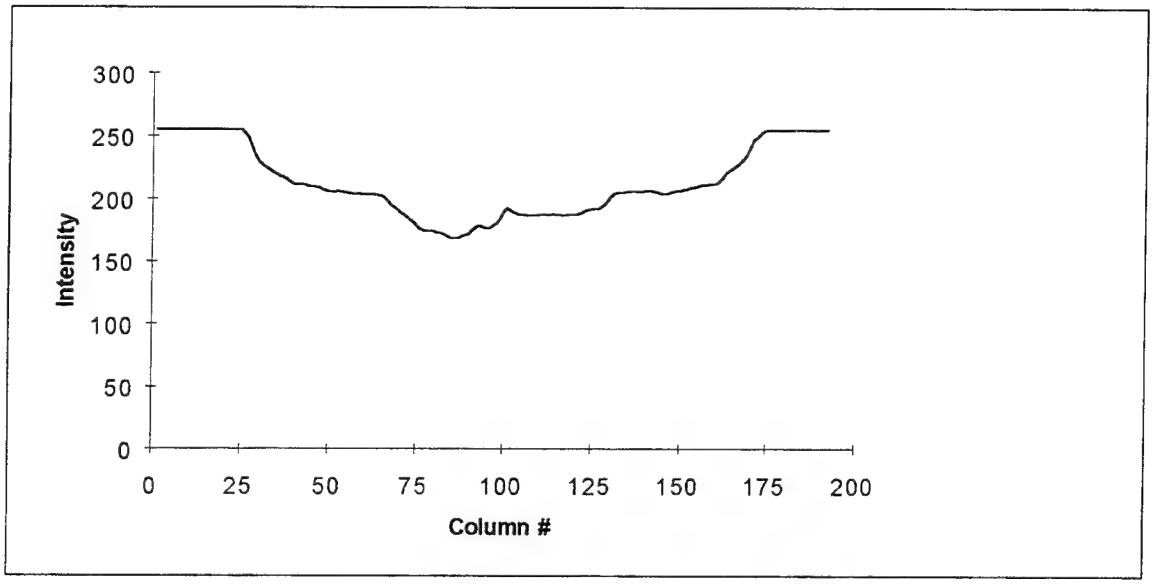

Fig. D-53. T5 squashed to preserve horizontal sequencies

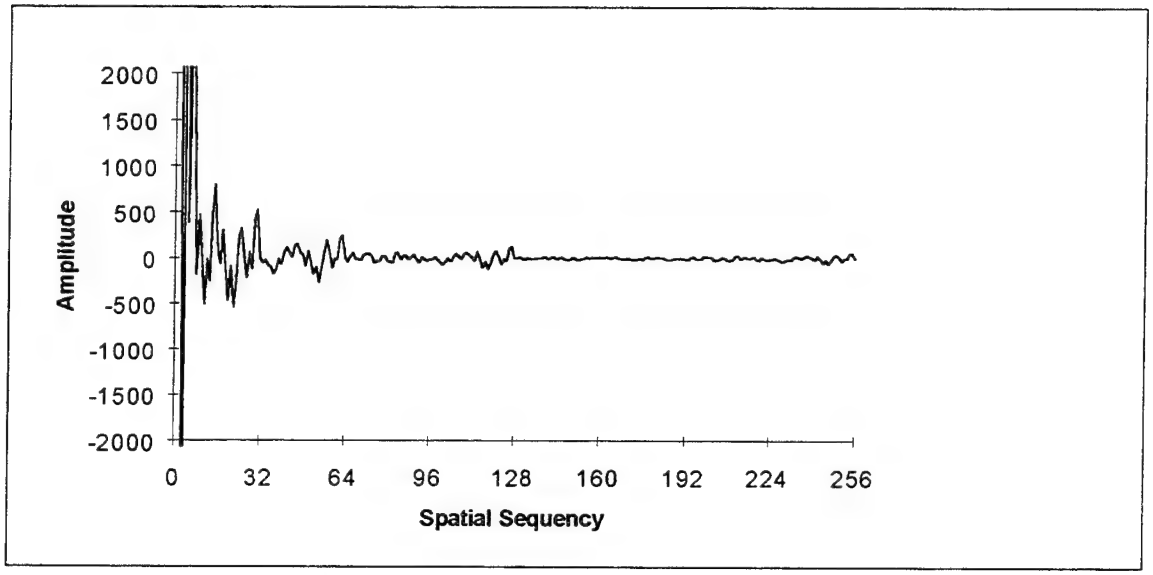

Fig. D-54. Walsh transform of Fig. D-53

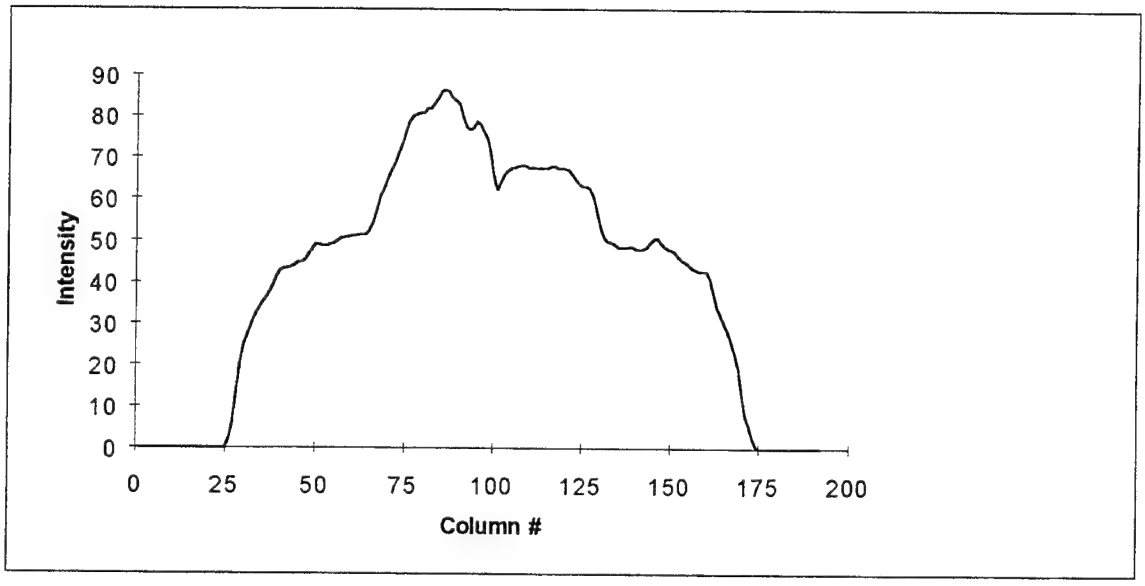

Fig. D-55. Complement of T5 squashed to preserve horizontal sequencies

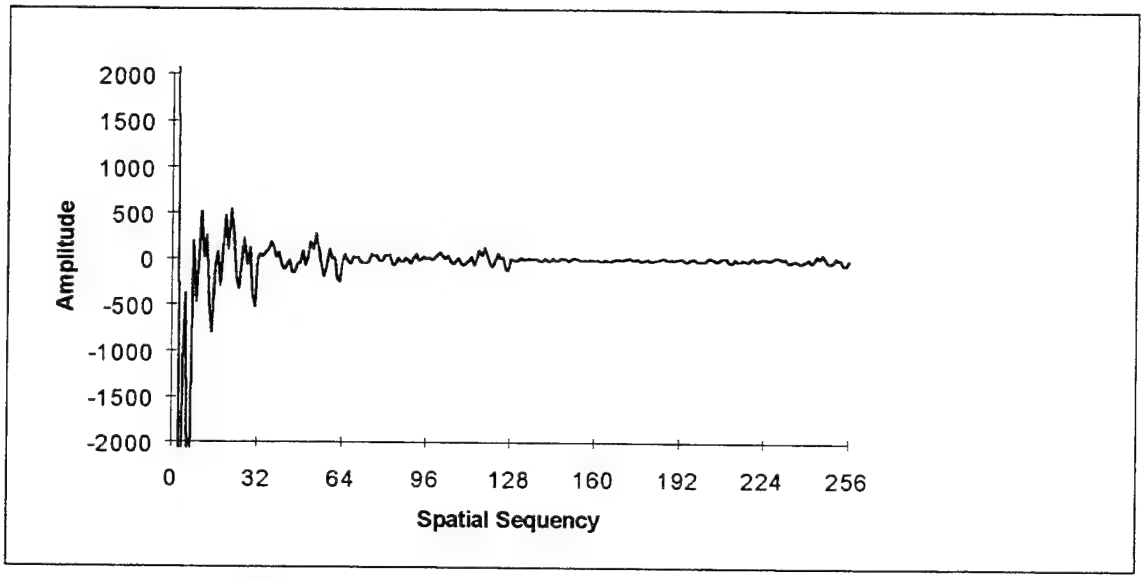

Fig. D-56. Walsh transform of Fig. D-55

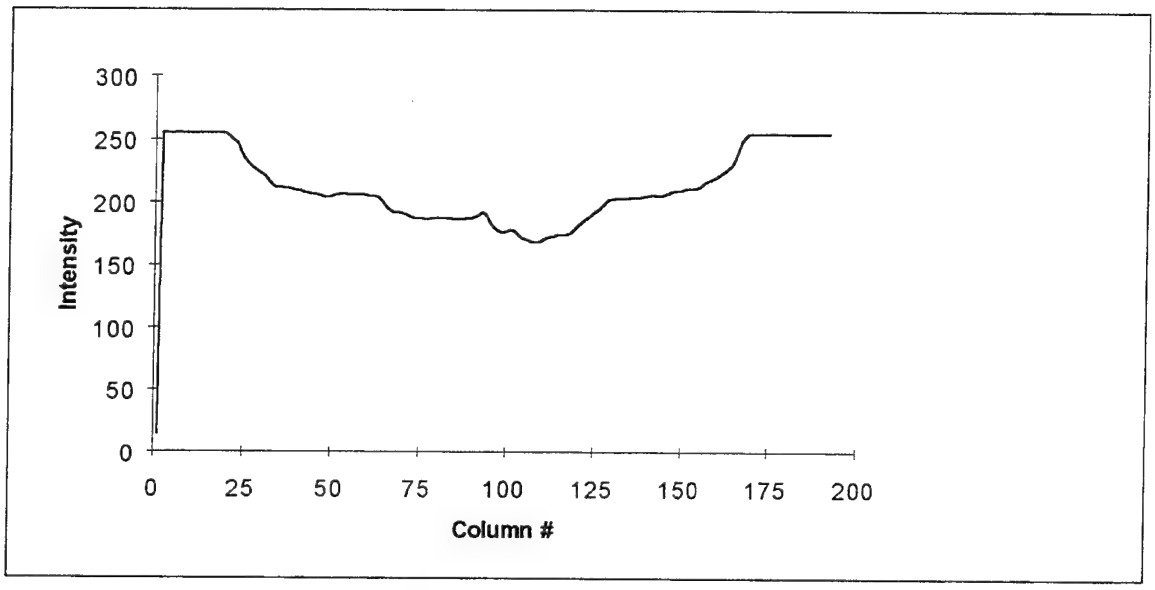

Fig. D-57. Reflection of T5 squashed to preserve horizontal sequencies

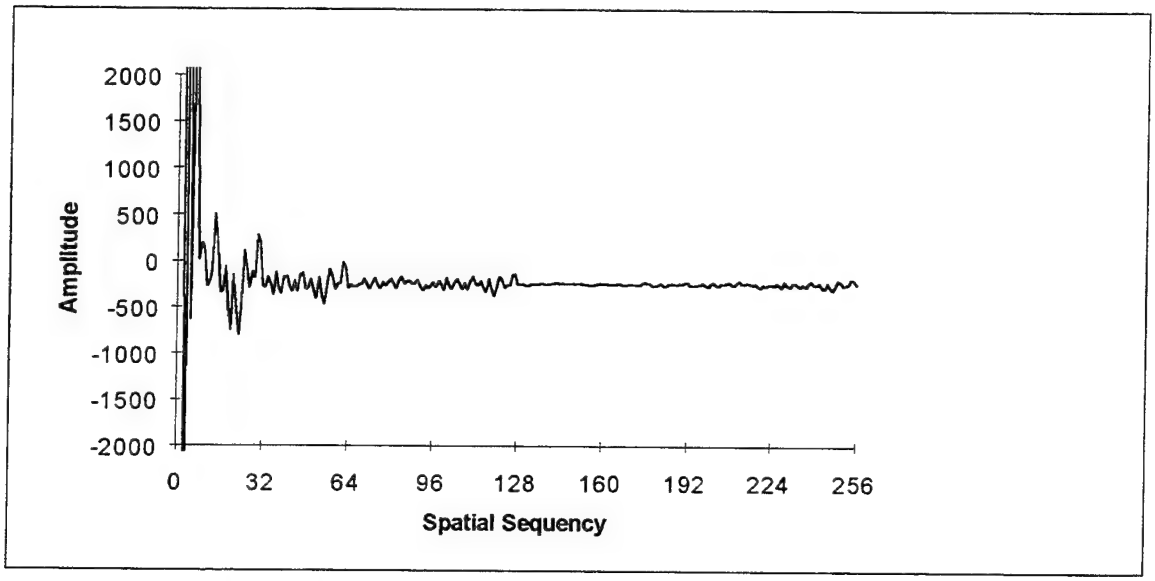

Fig. D-58. Walsh transform of Fig. D-57

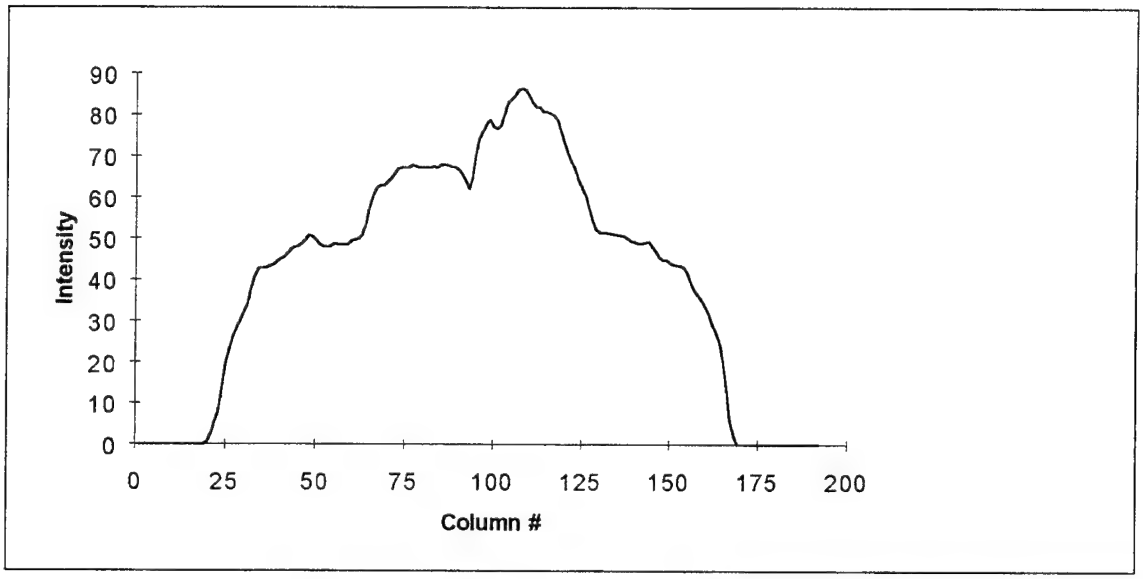

Fig. D-59. Complemented reflection of T5 squashed to preserve horizontal sequencies

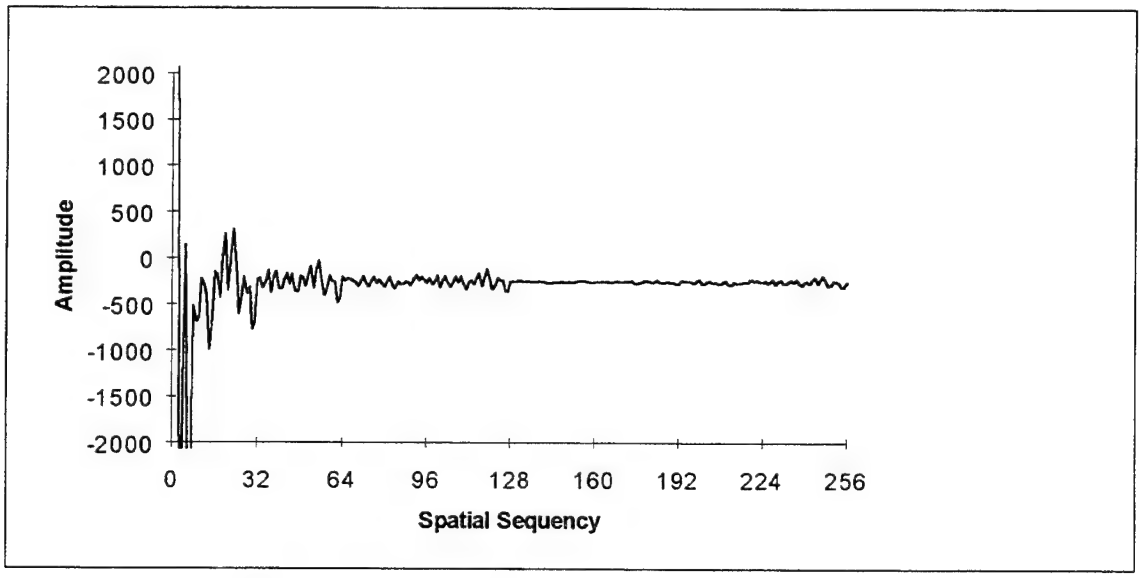

Fig. D-60. Walsh transform of Fig. D-59

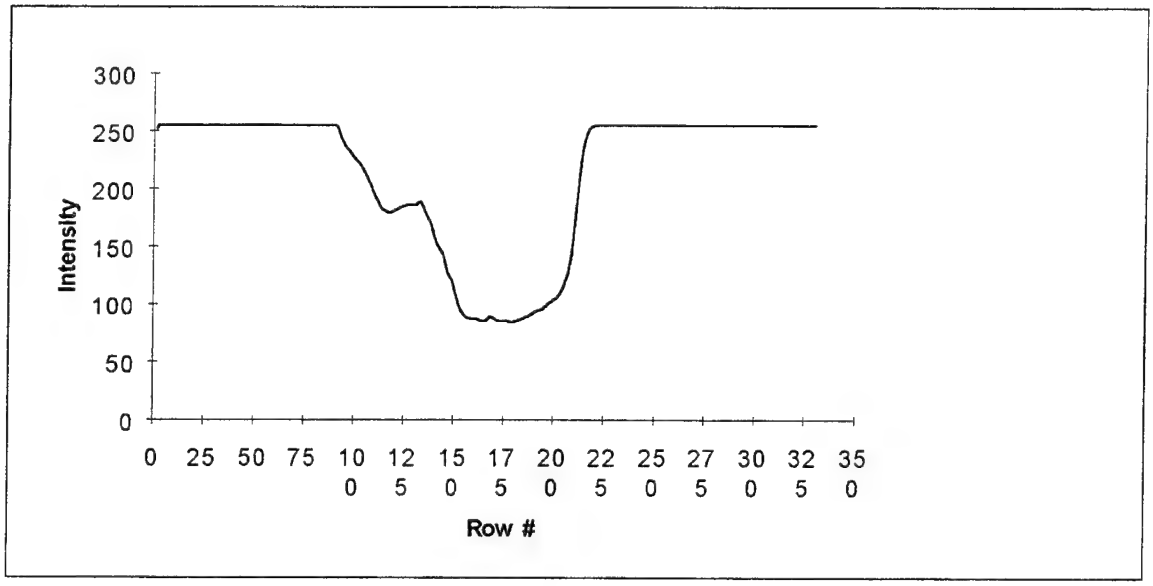

Fig. D-61. T5 squashed to preserve vertical sequencies

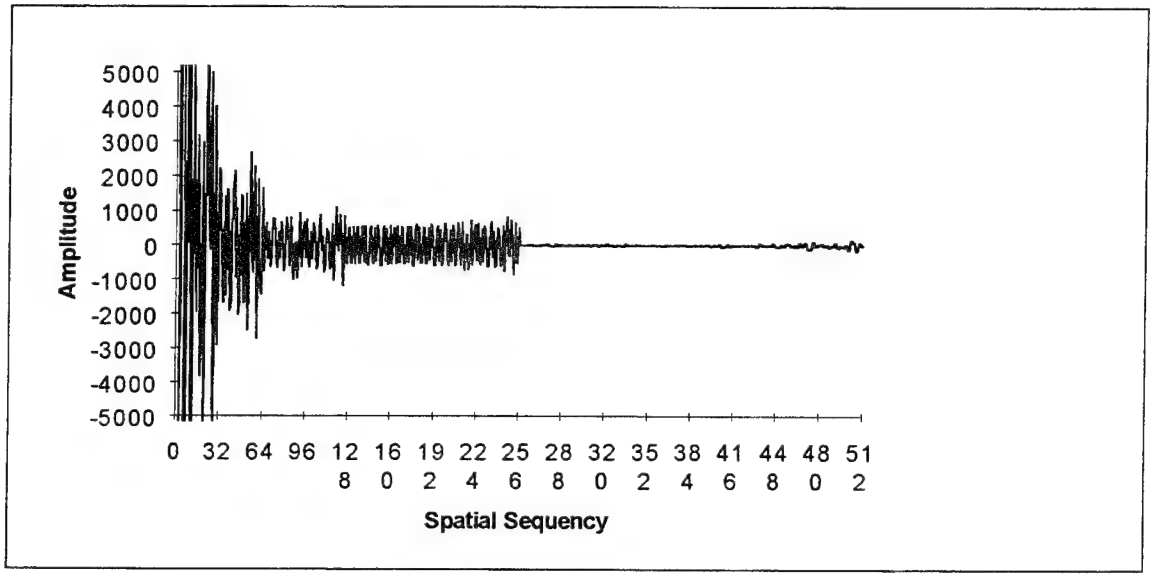

Fig. D-62. Walsh transform of Fig. D-61

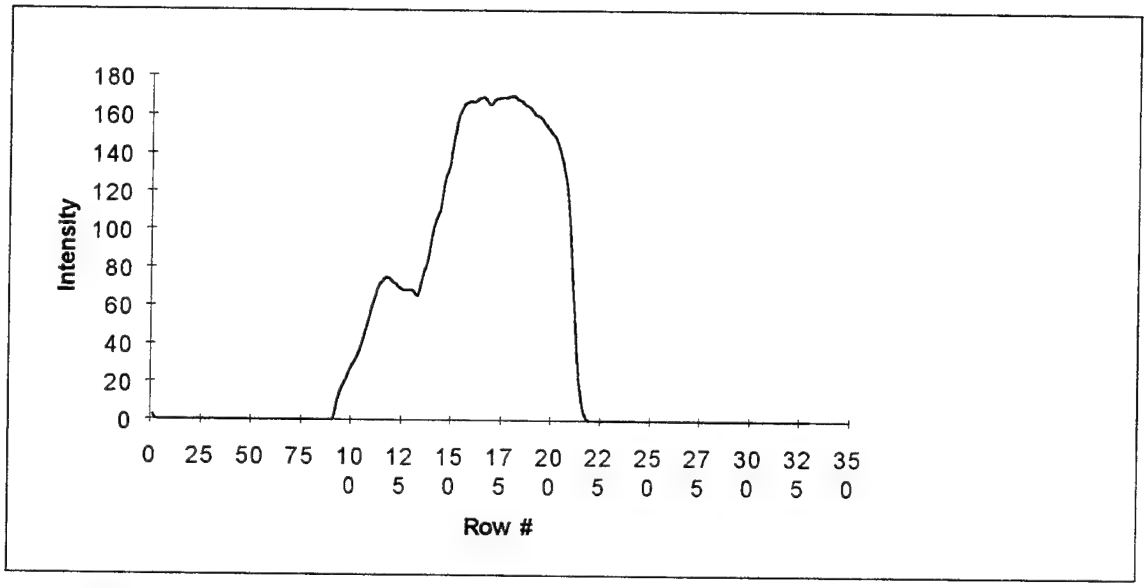

Fig. D-63. Complement of T5 squashed to preserve vertical sequencies

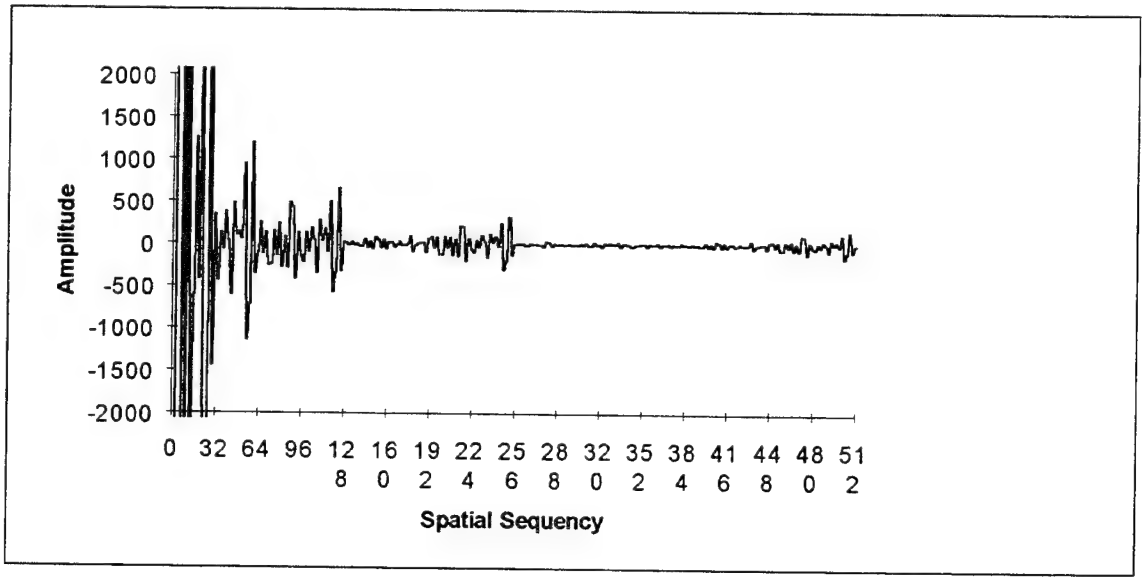

Fig. D-64. Walsh transform of Fig. D-63

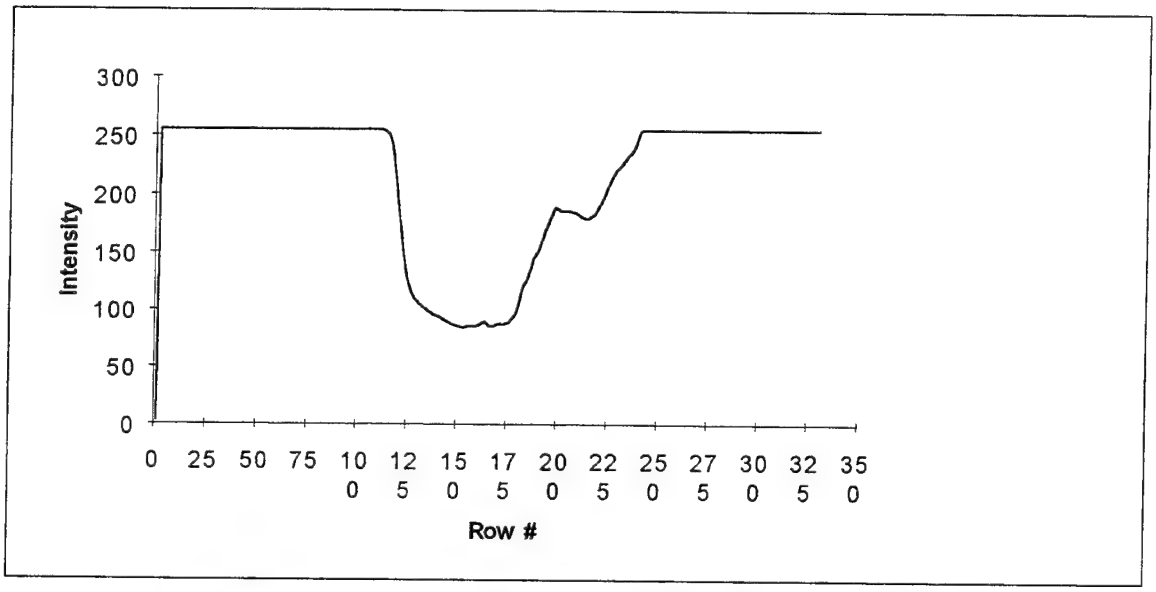

Fig. D-65. Reflection of T5 squashed to preserve vertical sequencies

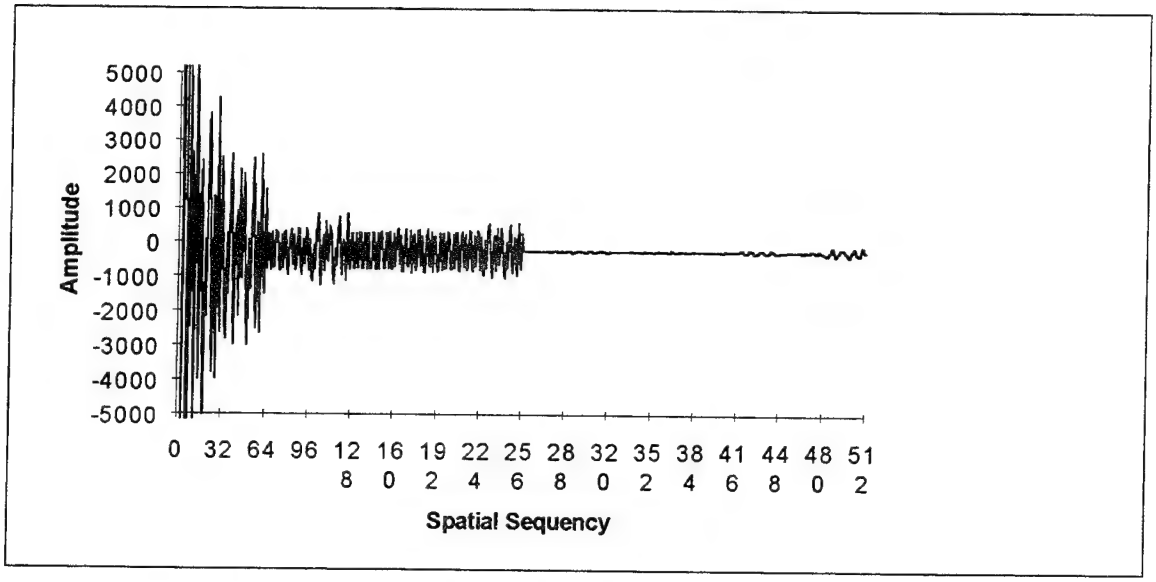

Fig. D-66. Walsh transform of Fig. D-65

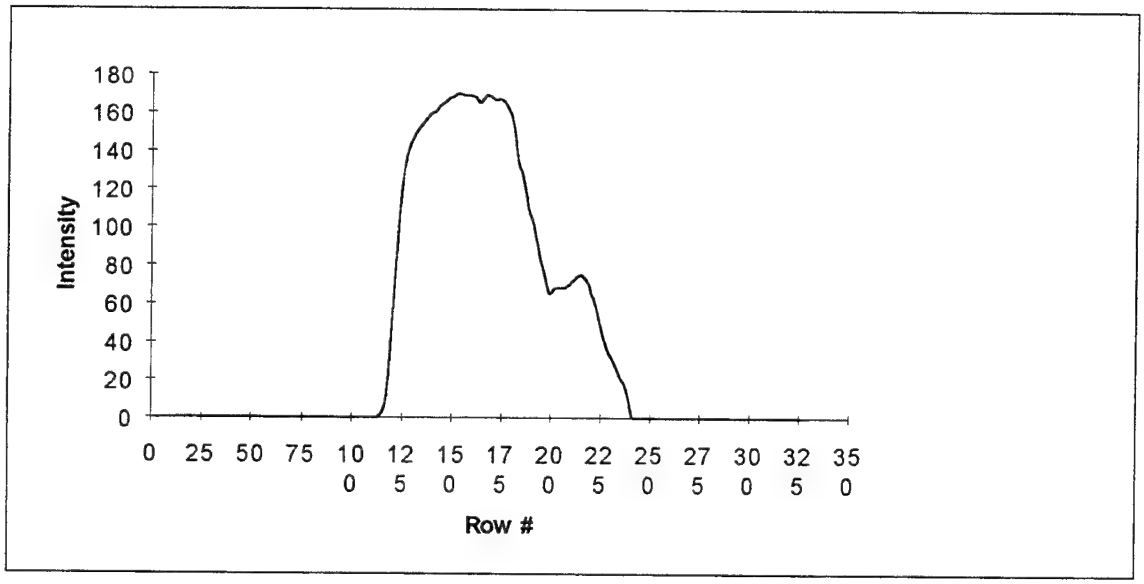

Fig. D-67. Complemented reflection of T5 squashed to preserve vertical sequencies

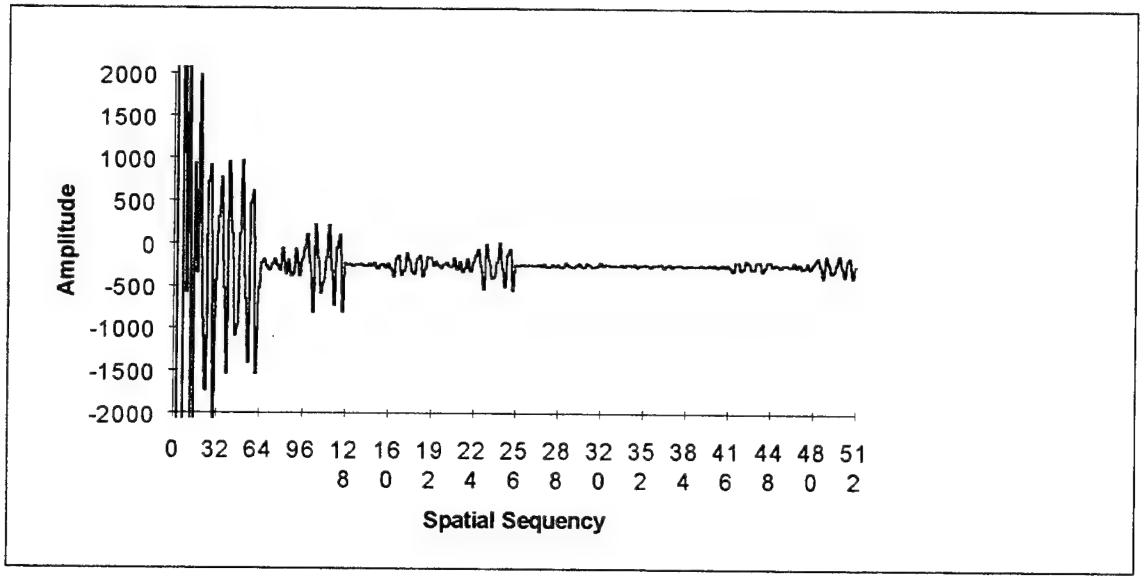

Fig. D-68. Walsh transform of Fig. D-67

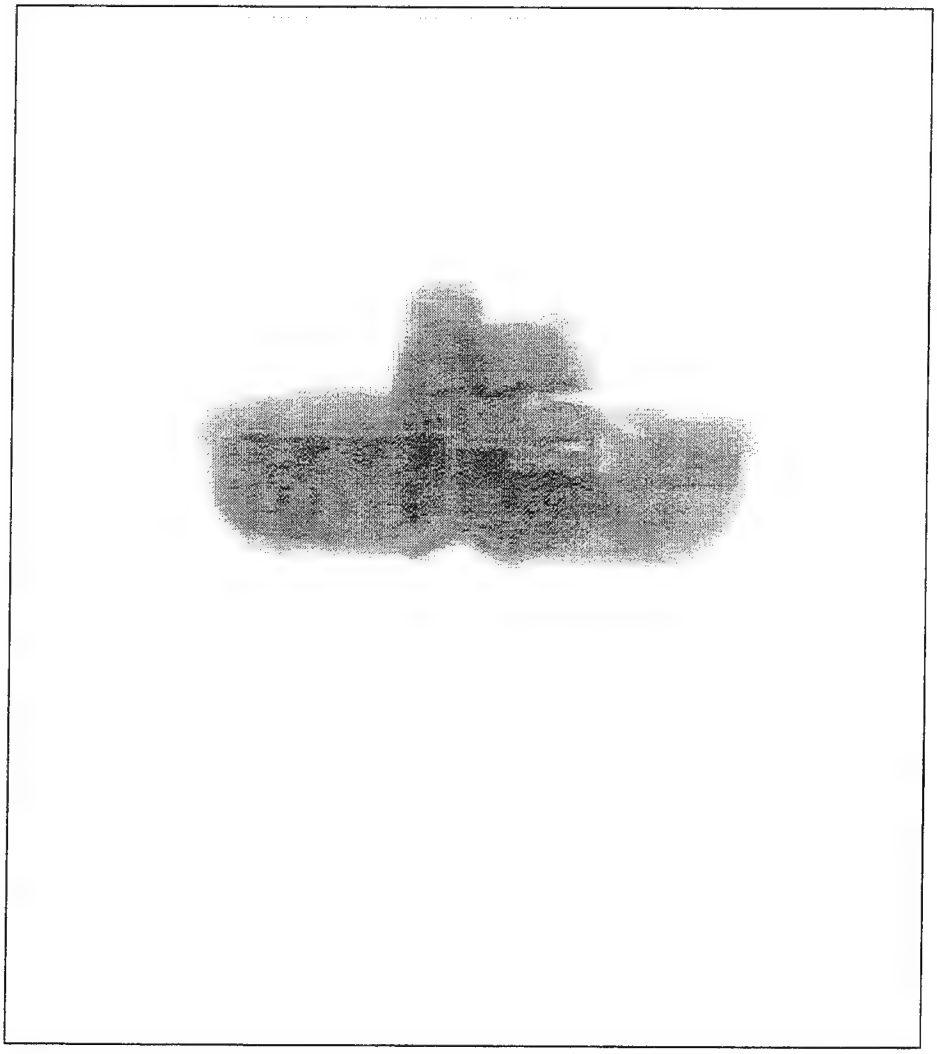

Fig. D-69. T6

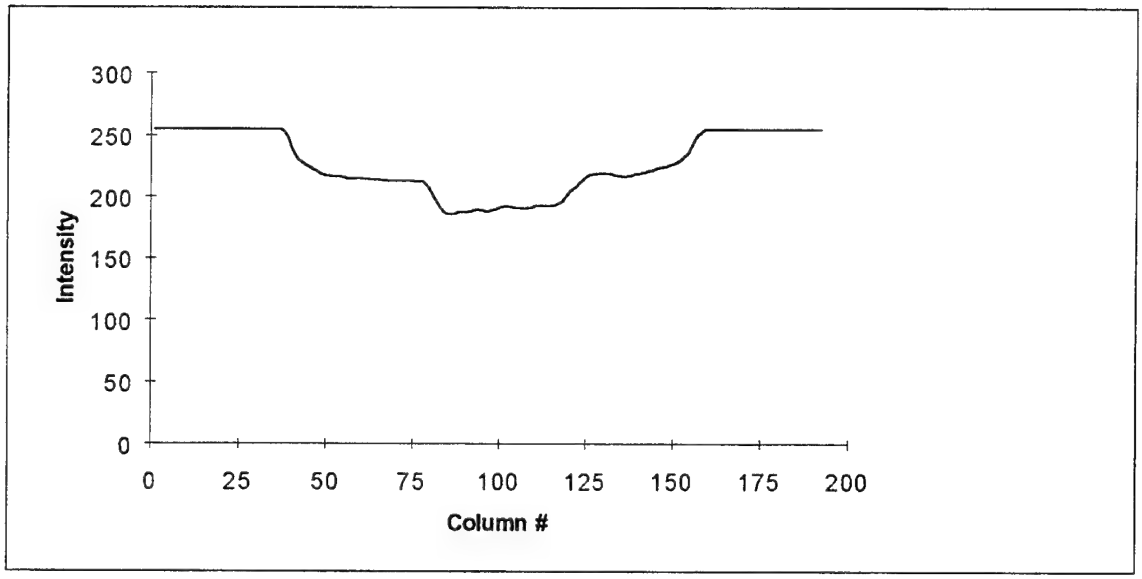

Fig. D-70. T6 squashed to preserve horizontal sequencies

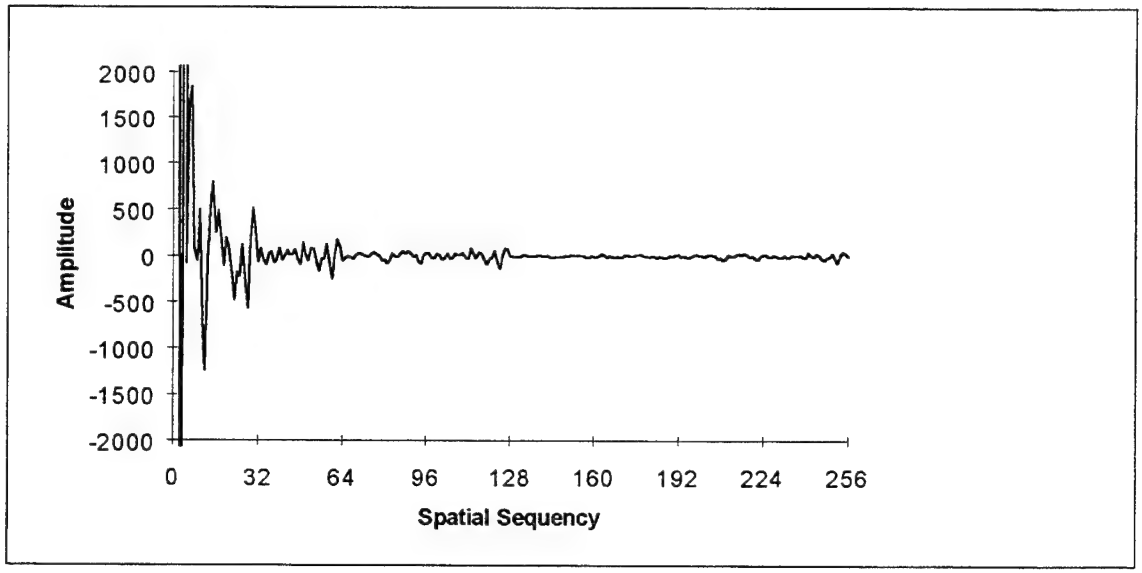

Fig. D-71. Walsh transform of Fig. D-70

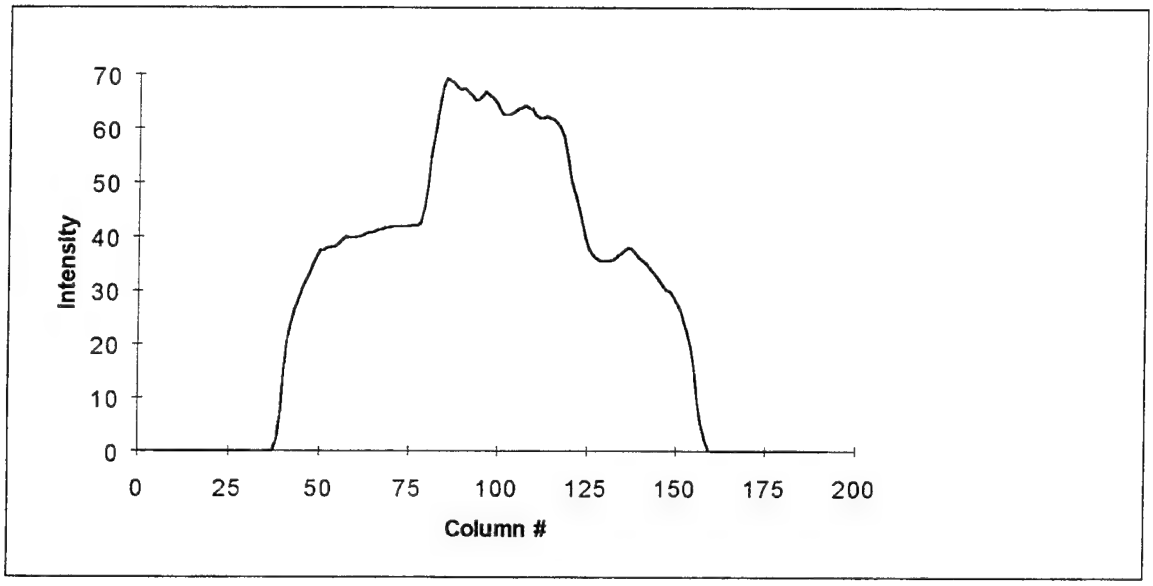

Fig. D-72. Complement of T6 squashed to preserve horizontal sequencies

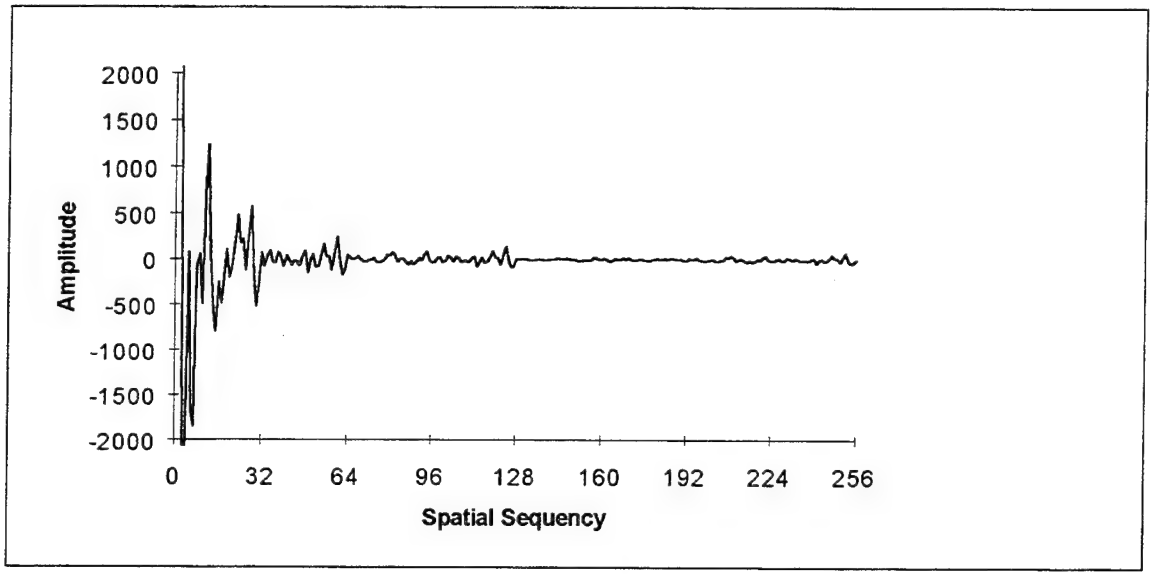

Fig. D-73. Walsh transform of Fig. D-72

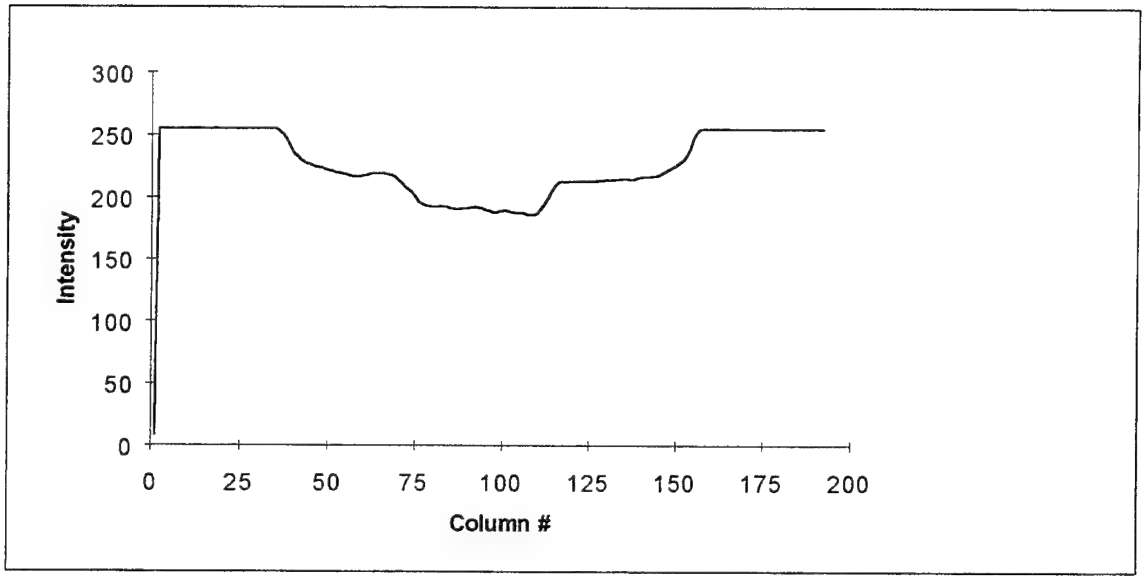

Fig. D-74. Reflection of T6 squashed to preserve horizontal sequencies

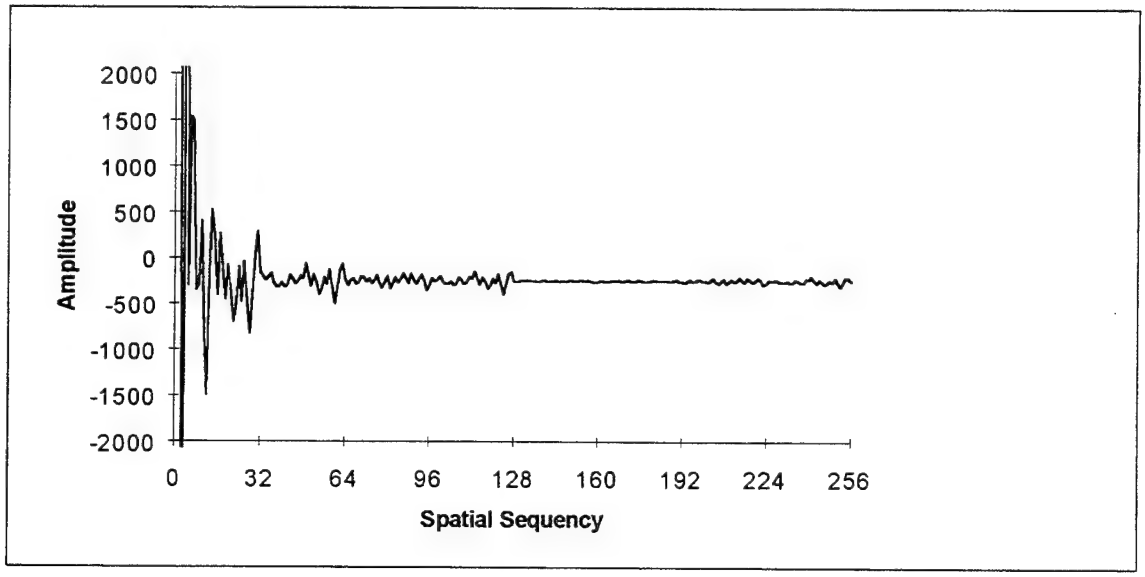

Fig. D-75. Walsh transform of Fig. D-74

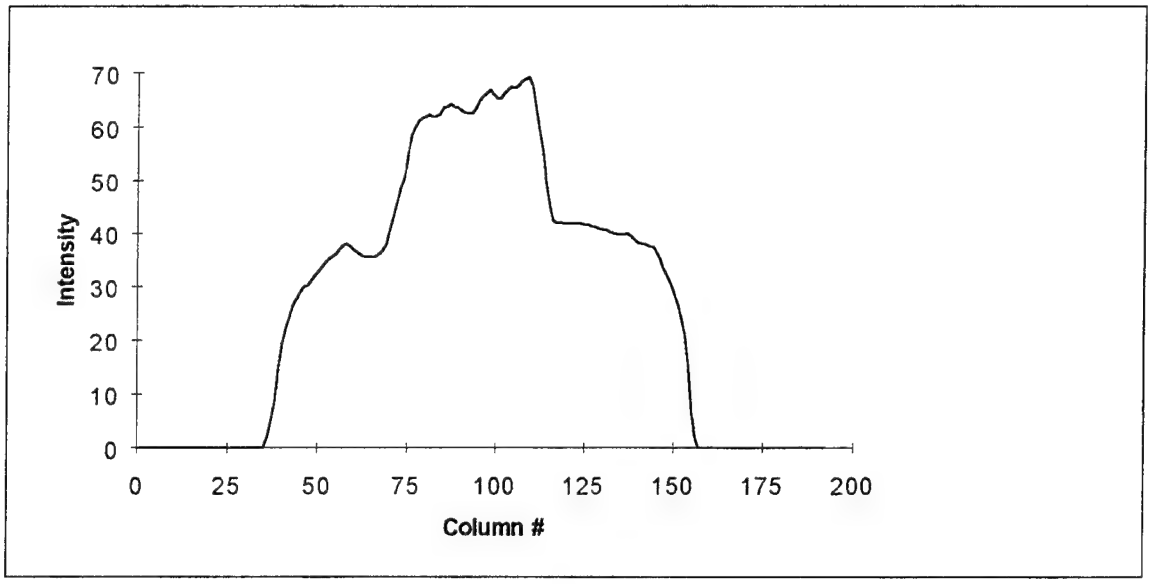

Fig. D-76. Complemented reflection of T6 squashed to preserve horizontal sequencies

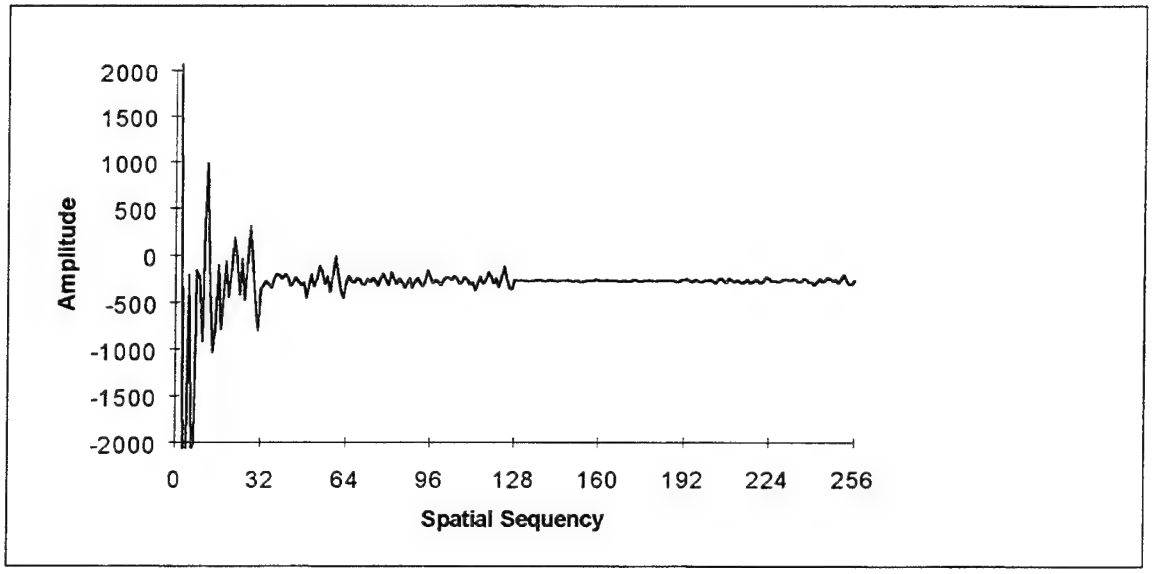

Fig. D-77. Walsh transform of Fig. D-76

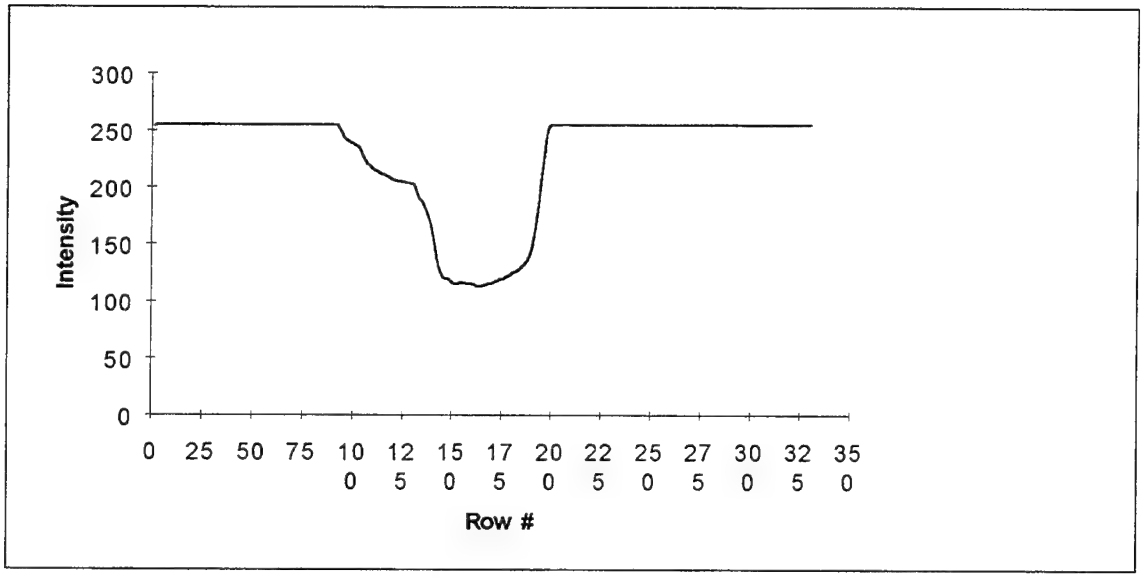

Fig. D-78. T6 squashed to preserve vertical sequencies

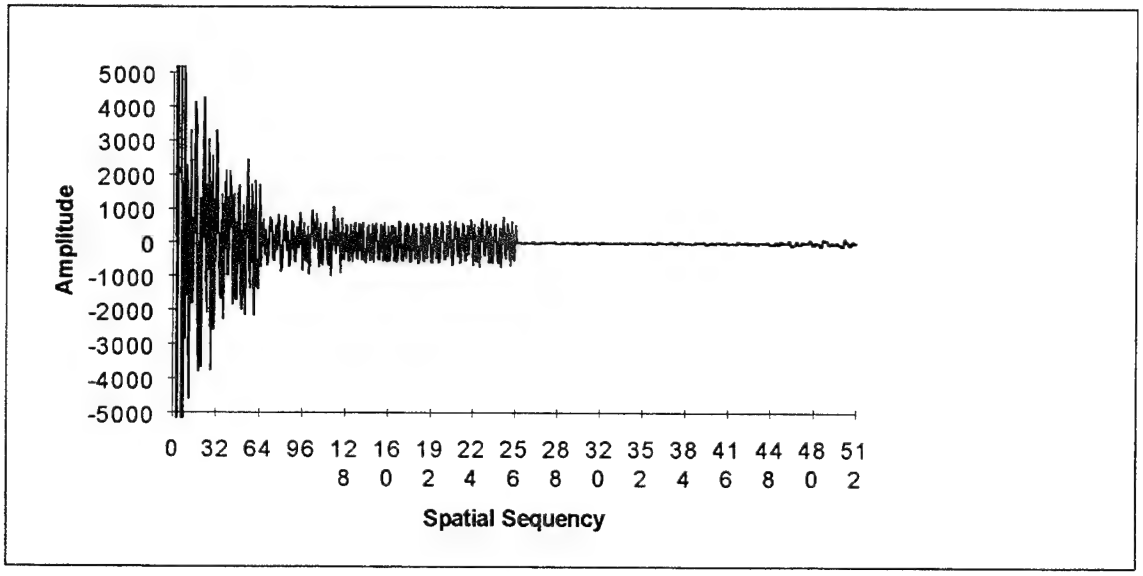

Fig. D-79. Walsh transform of Fig. D-78

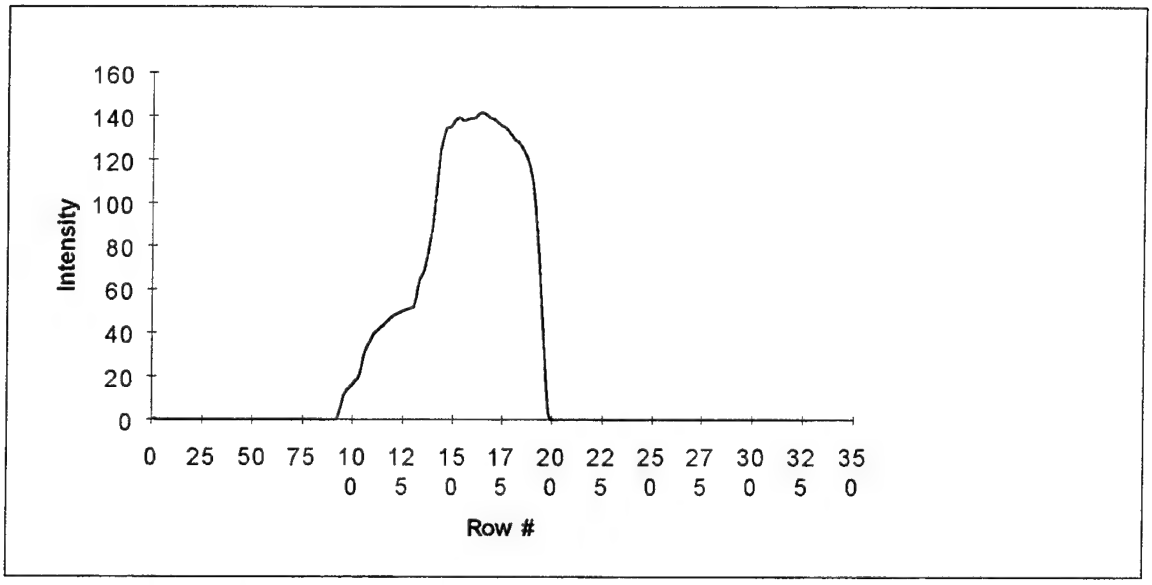

Fig. D-80. Complement of T6 squashed to preserve vertical sequencies

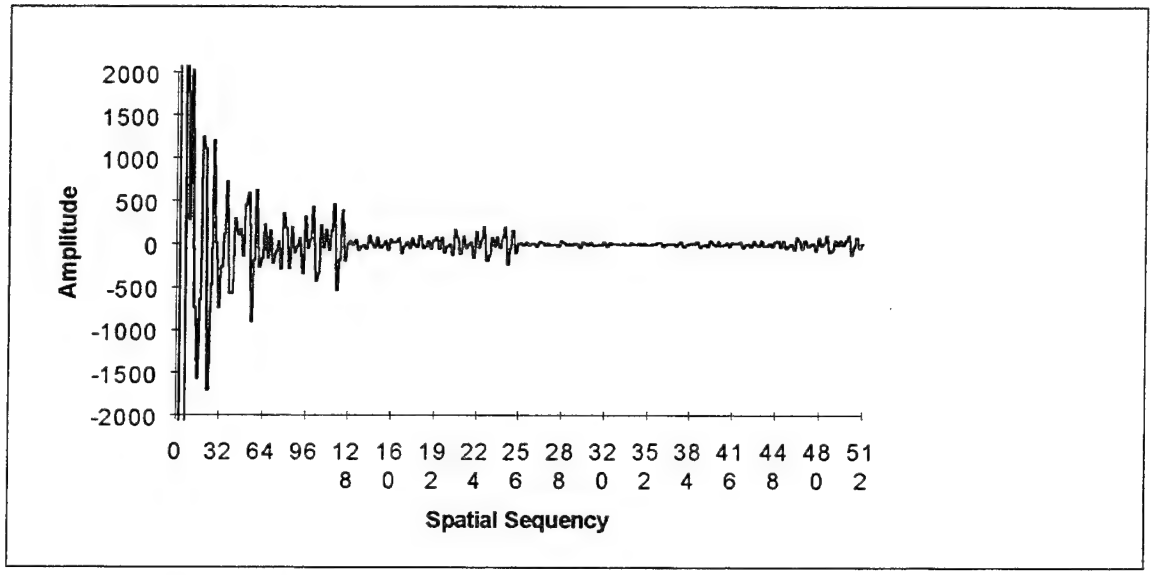

Fig. 81. Walsh transform of Fig. D-80

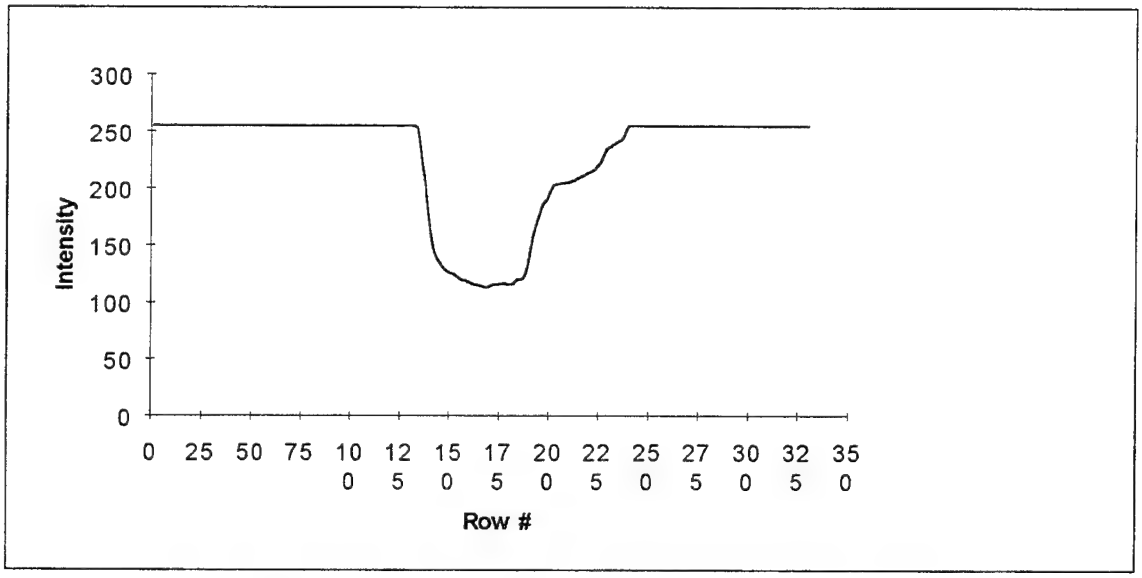

Fig. D-82. Reflection of T6 squashed to preserve vertical sequencies

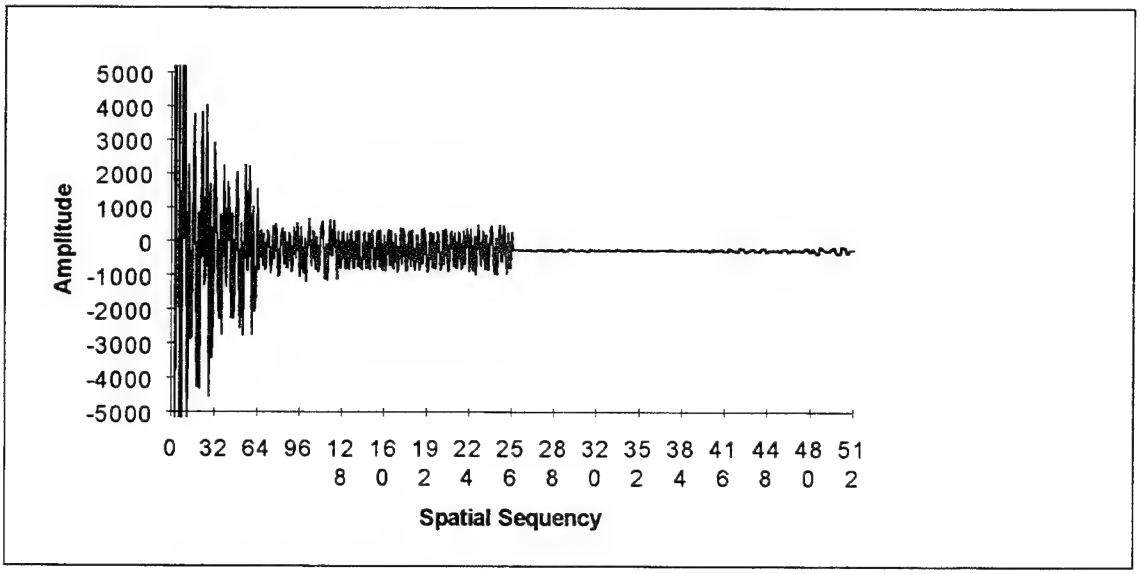

Fig. D-83. Walsh transform of Fig. D-82

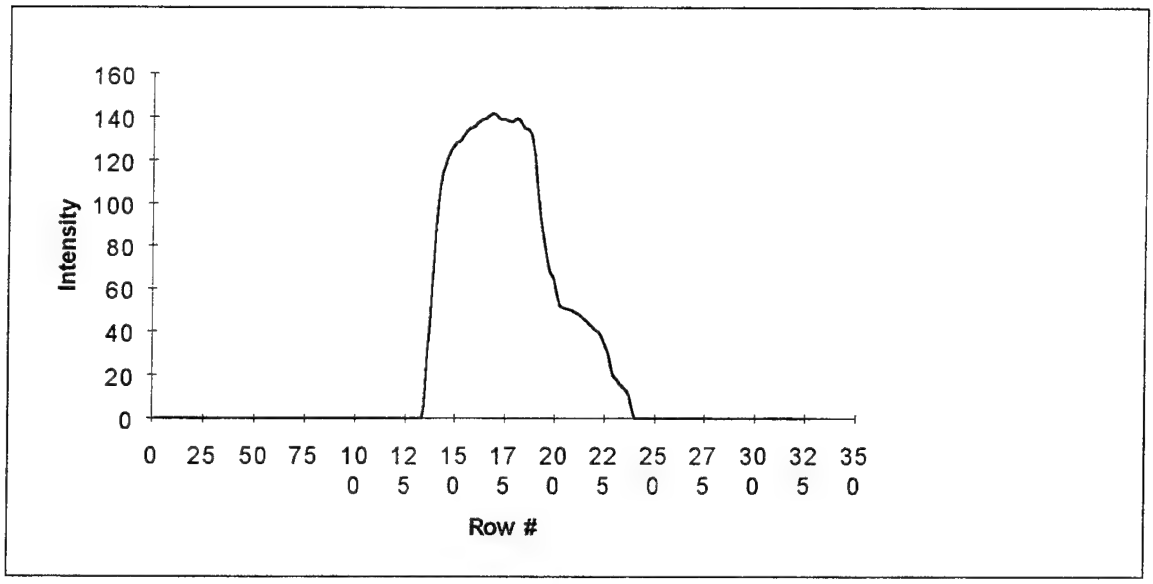

Fig. D-84. Complemented reflection of T6 squashed to preserve vertical sequencies

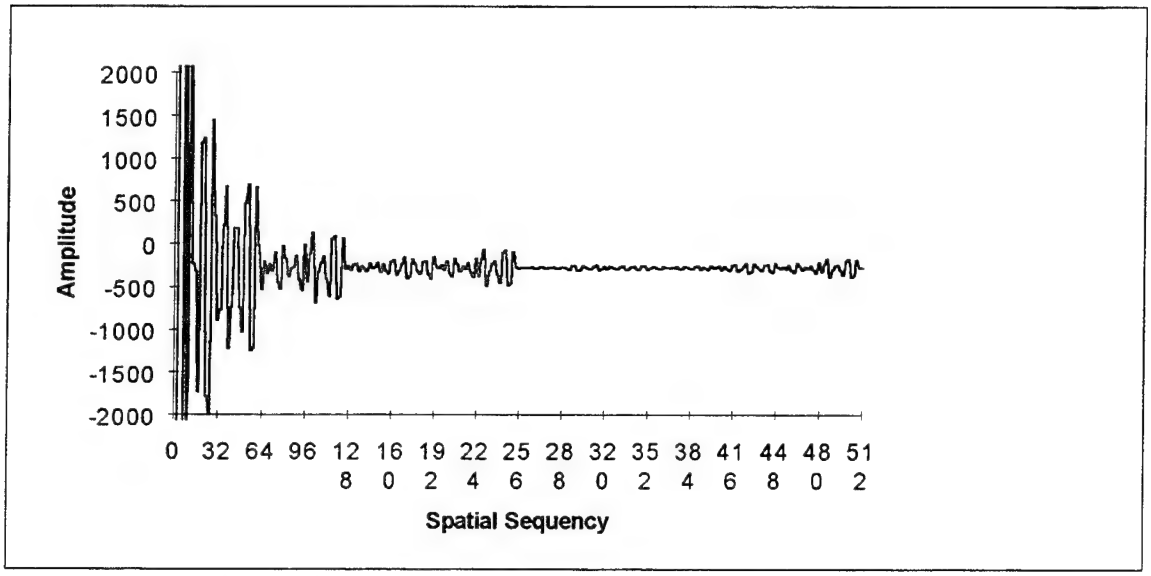

Fig. D-85. Walsh transform of Fig. D-84

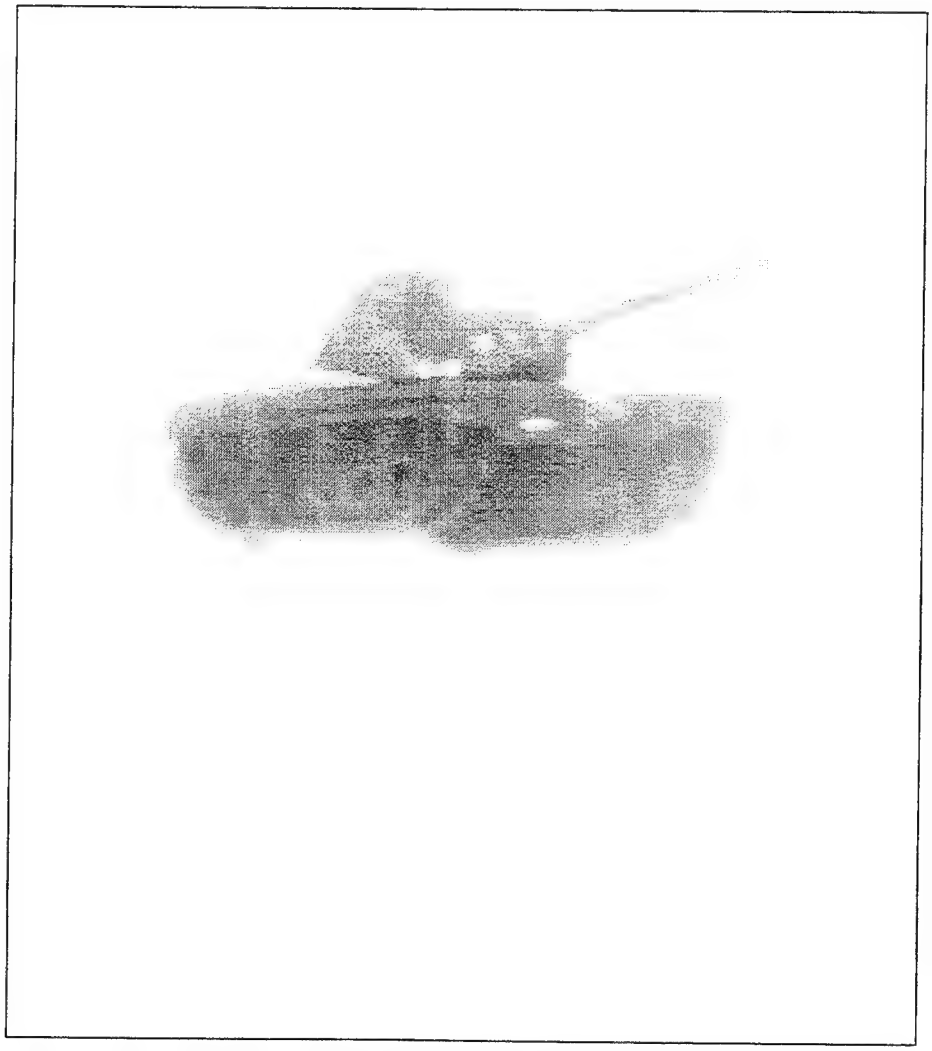

Fig. D-86. T7

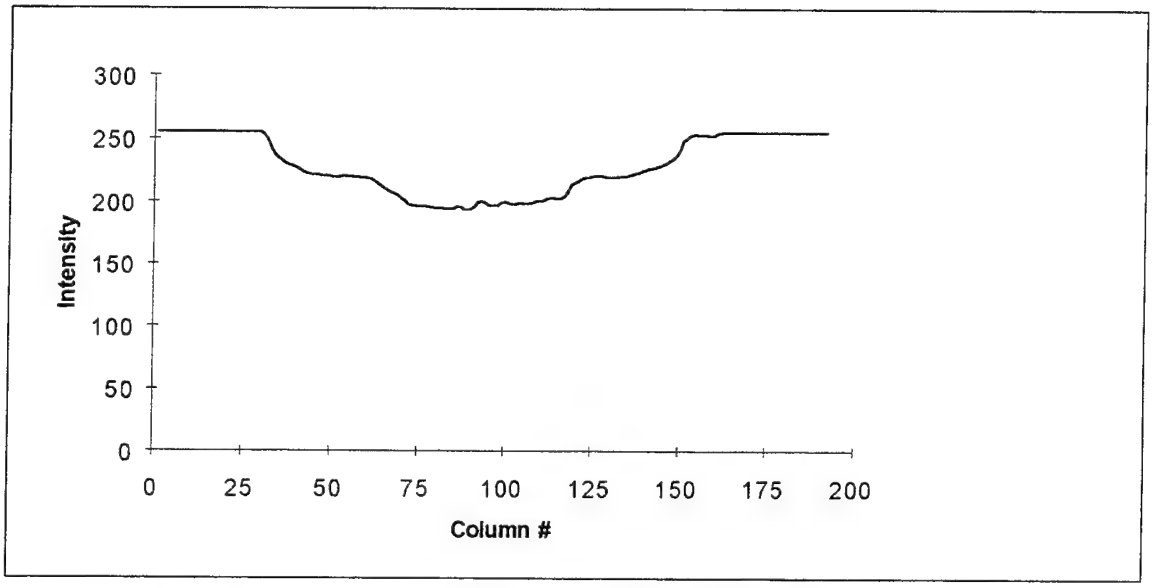

Fig. D-87. T7 squashed to preserve horizontal sequencies

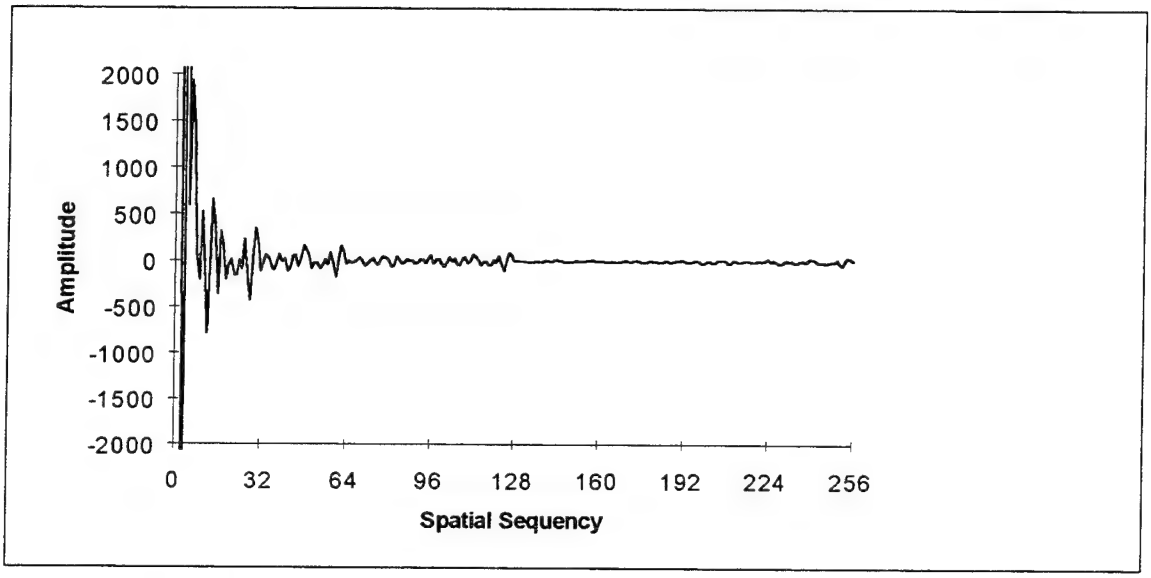

Fig. D-88. Walsh transform of Fig. D-87

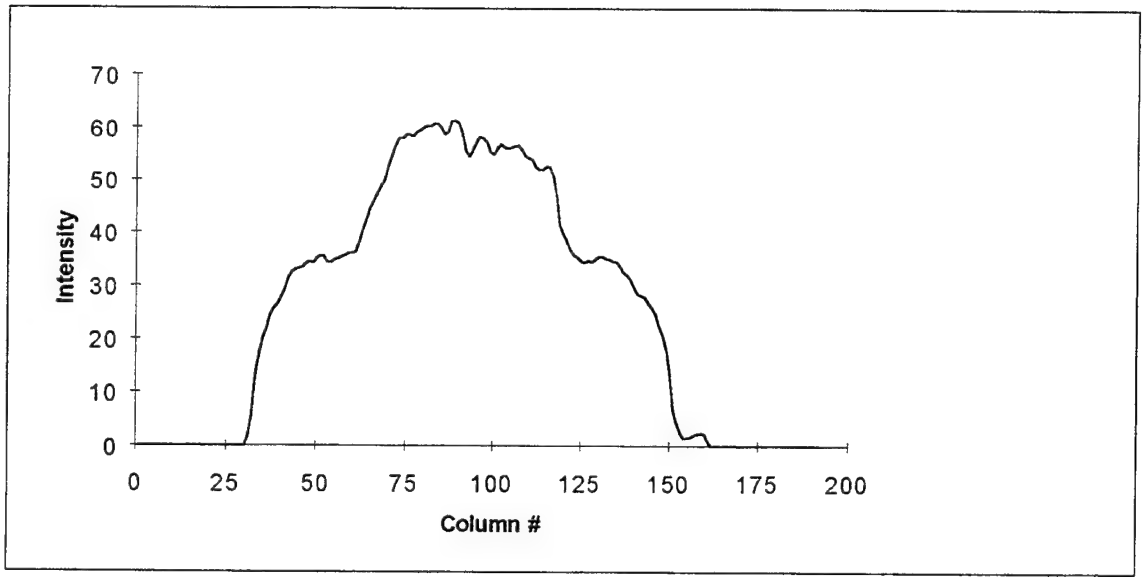

Fig. D-89. Complement of T7 squashed to preserve horizontal sequencies

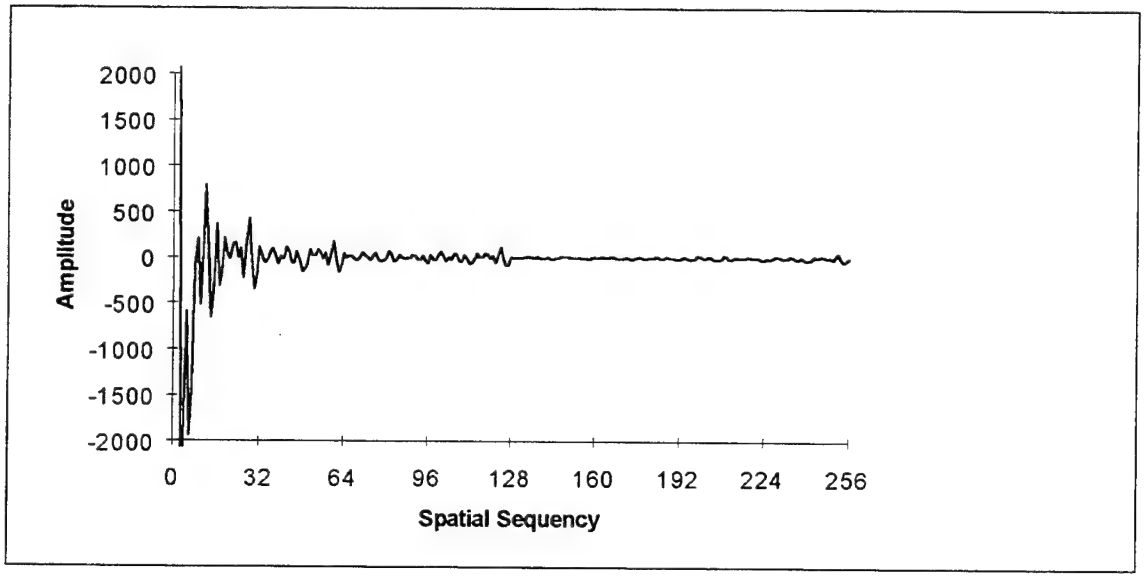

Fig. D-90. Walsh transform of Fig. D-89

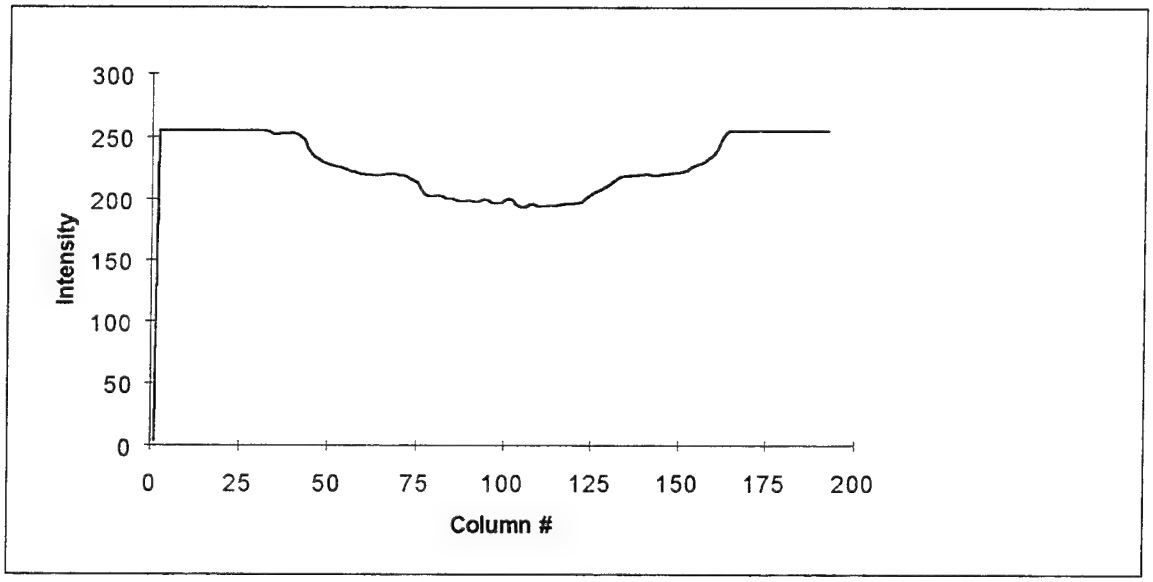

Fig. D-91. Reflection of T7 squashed to preserve horizontal sequencies

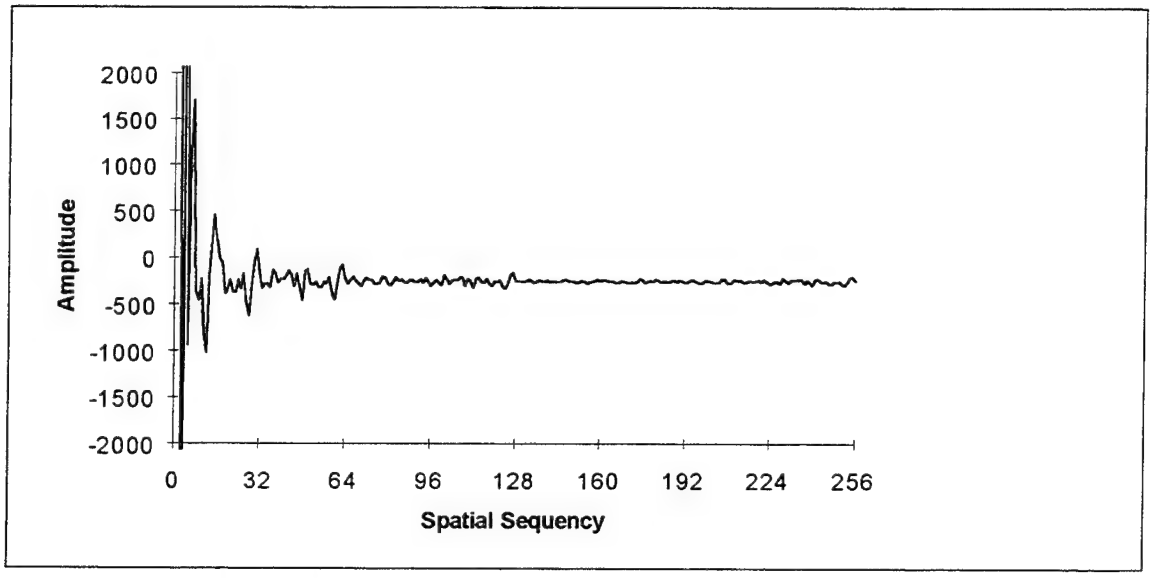

Fig. D-92. Walsh transform of Fig. D-91

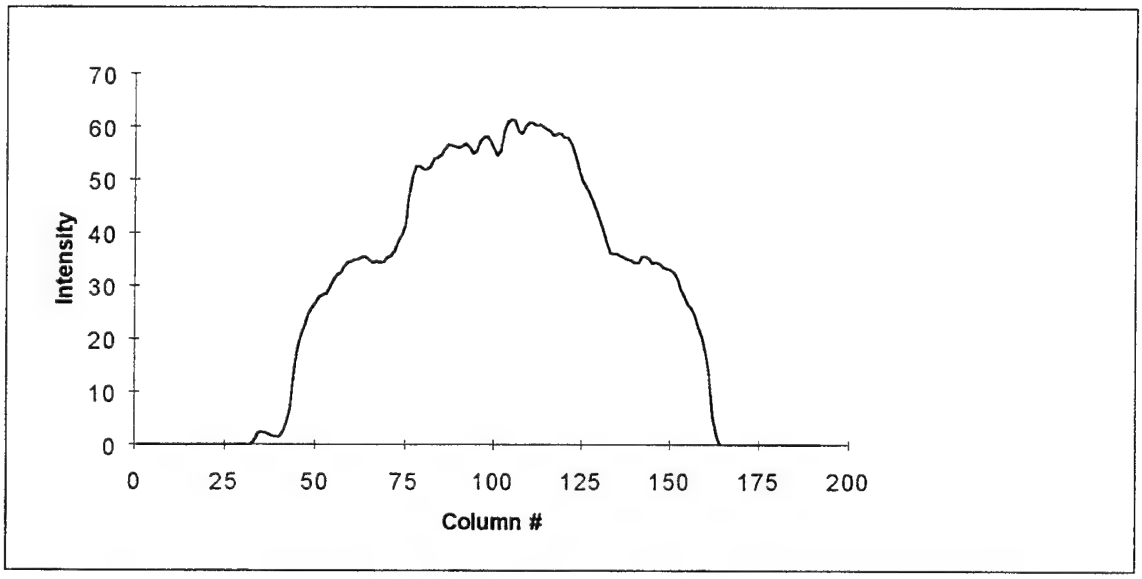

Fig. D-93. Complemented reflection of T7 squashed to preserve horizontal sequencies

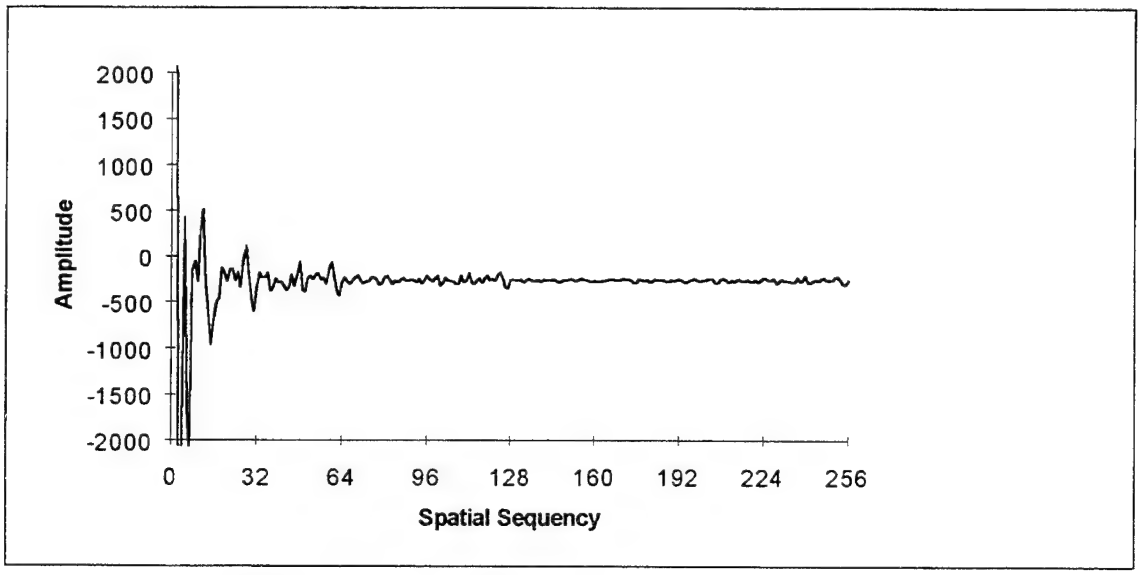

Fig. D-94. Walsh transform of Fig. D-93

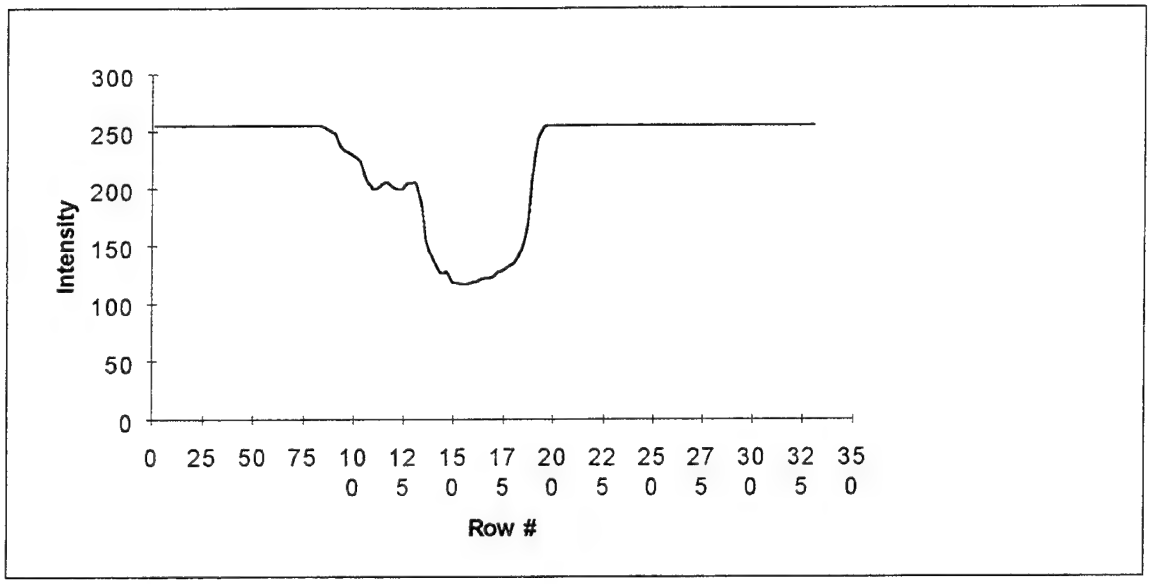

Fig. D-95. T7 squashed to preserve vertical sequencies

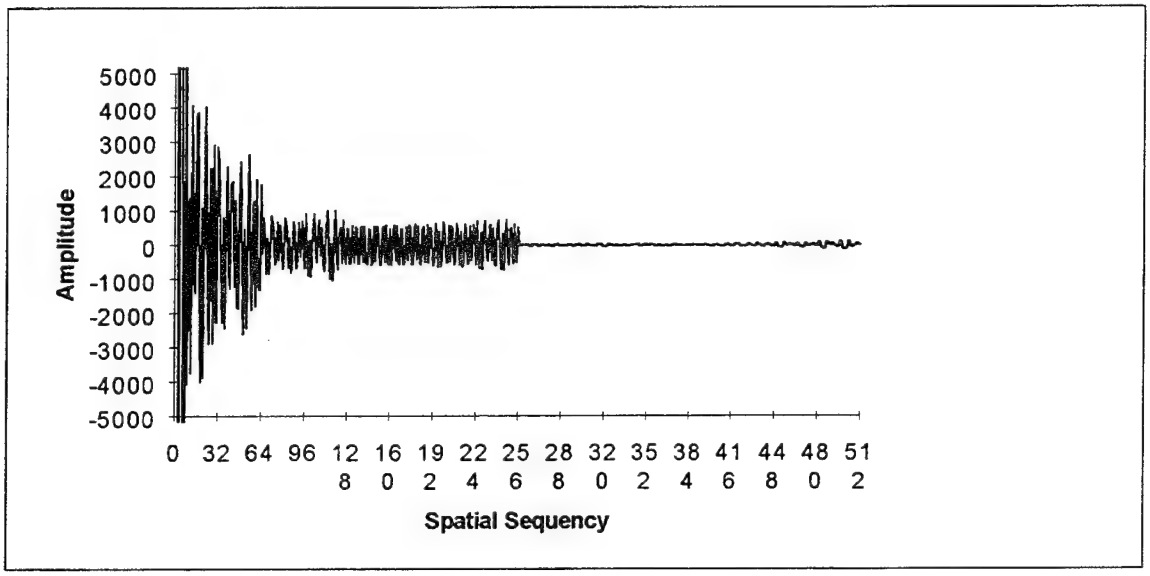

Fig. D-96. Walsh transform of Fig. D-95

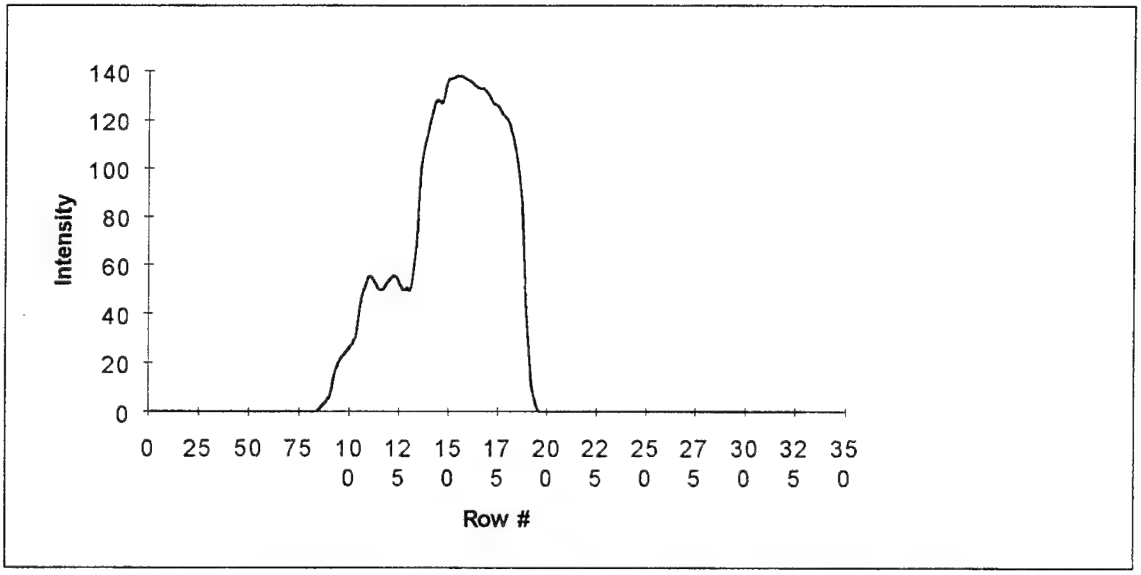

Fig. D-97. Complement of T7 squashed to preserve vertical sequencies

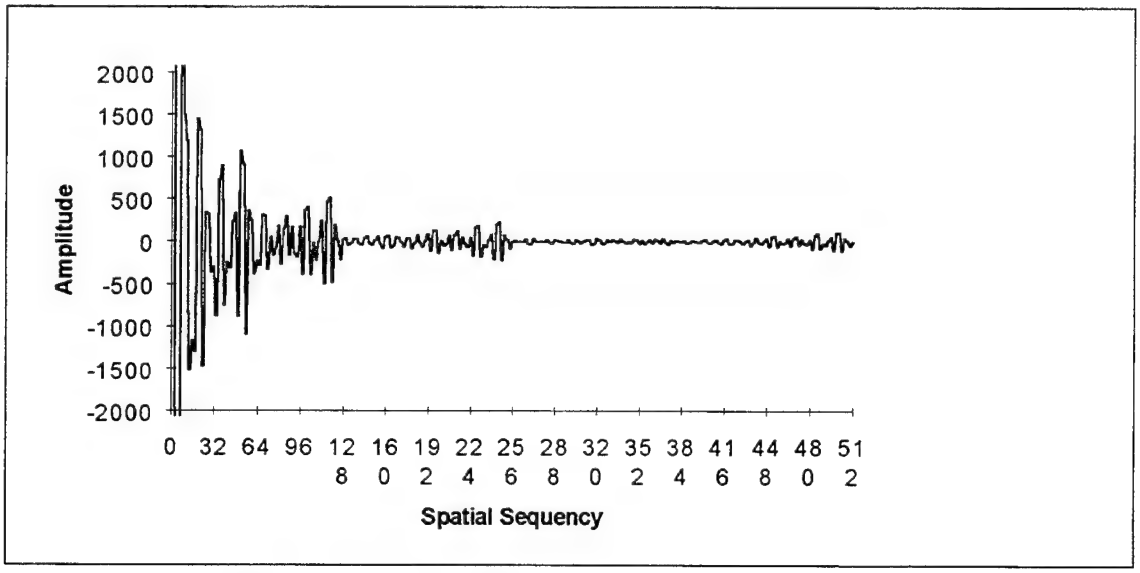

Fig. D-98. Walsh transform of Fig. D-97

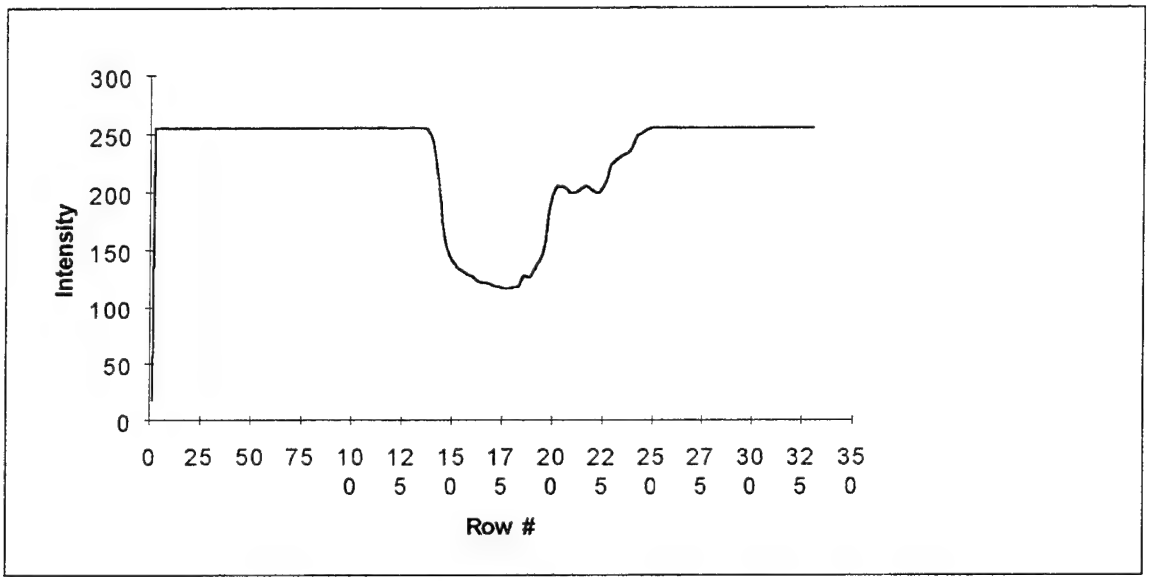

Fig. D-99. Reflection of T7 squashed to preserve vertical sequencies

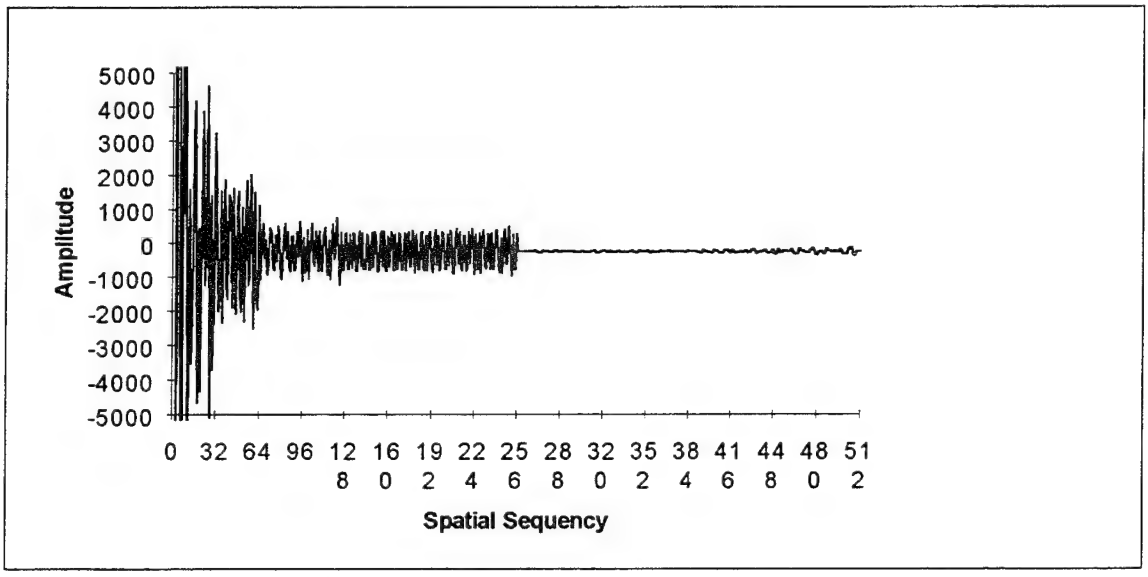

Fig. D-100. Walsh transform of Fig. D-99

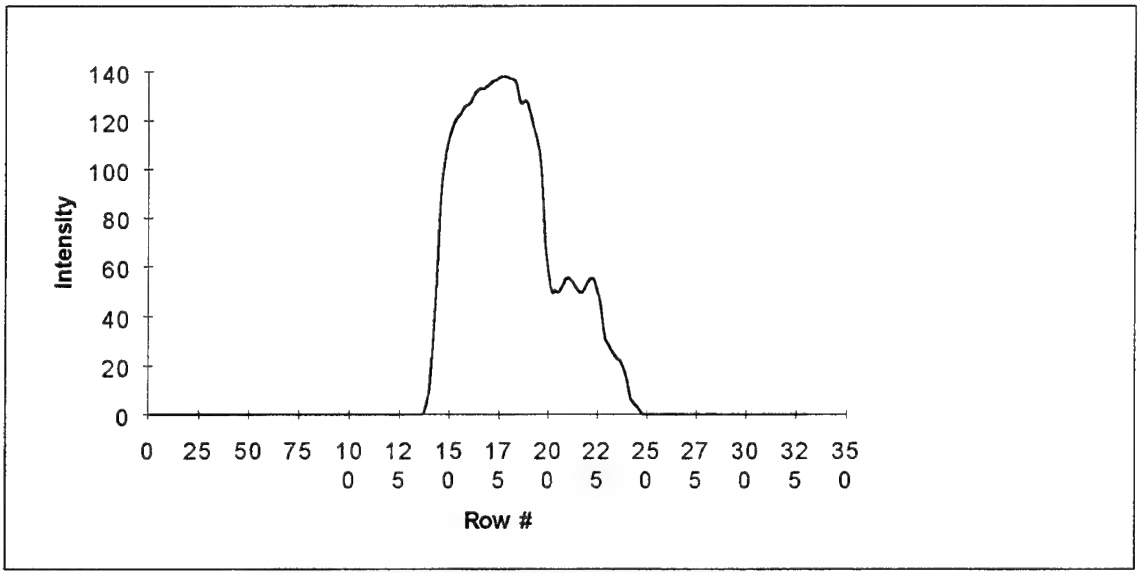

Fig. D-101. Complemented reflection of T7 squashed to preserve vertical sequencies

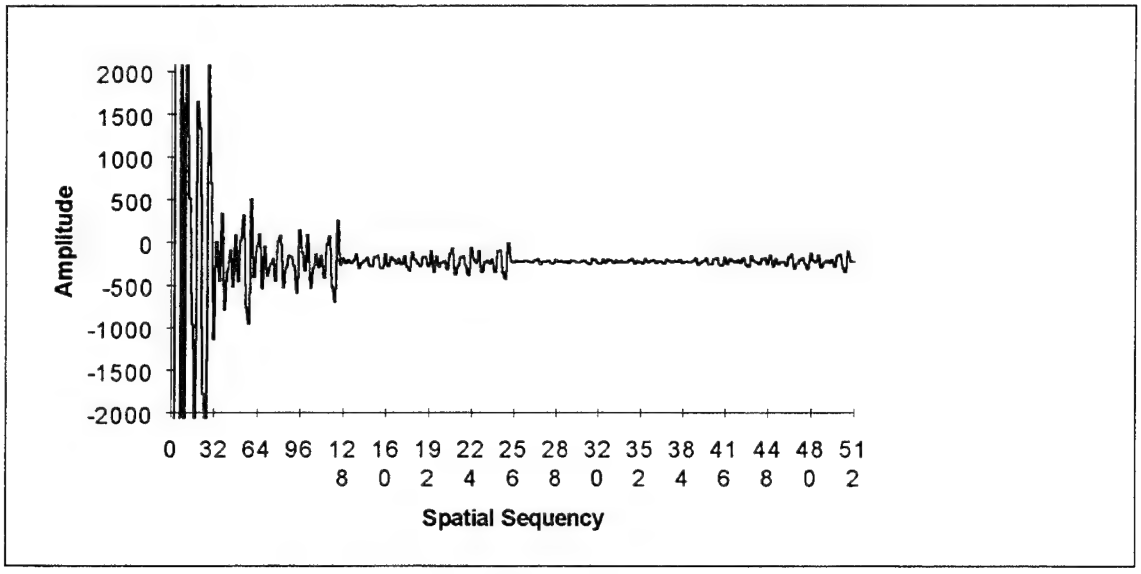

Fig. D-102. Walsh transform of Fig. D-101

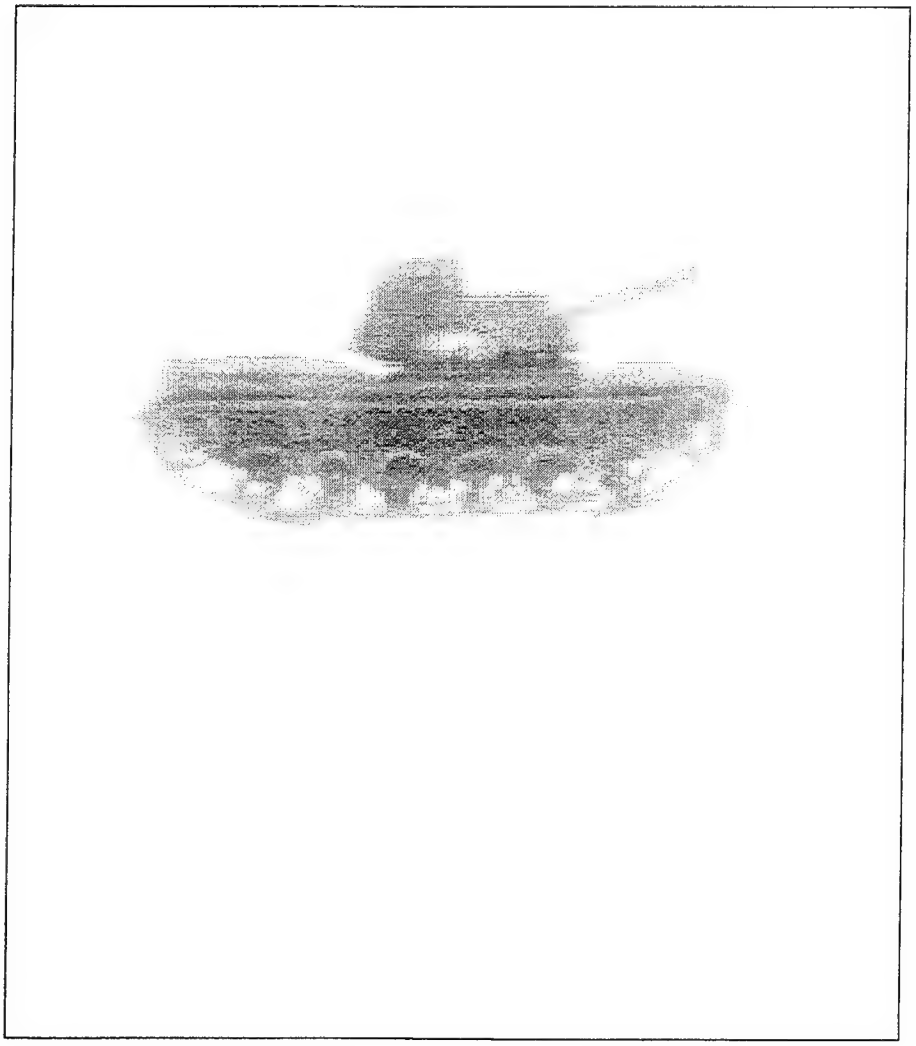

Fig. D-103. T8

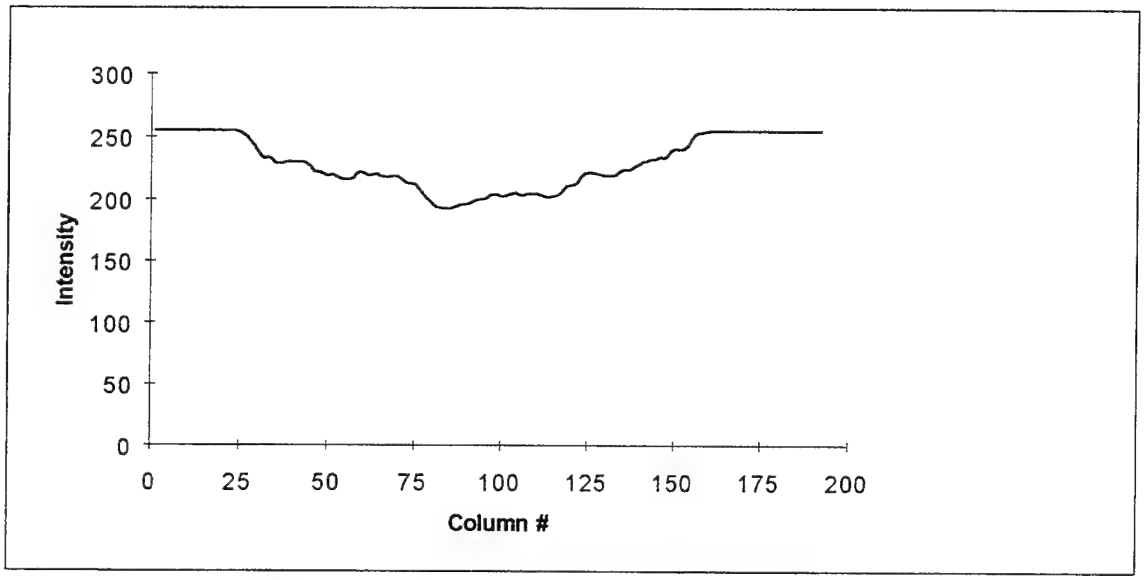

Fig. D-104. T8 squashed to preserve horizontal sequencies

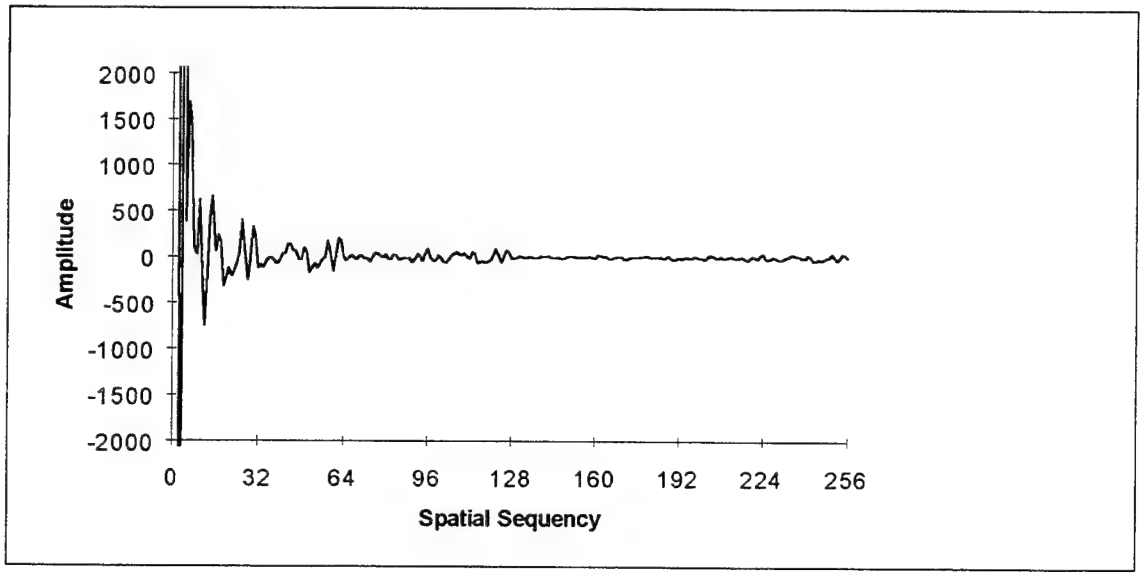

Fig. D-105. Walsh transform of Fig. D-104

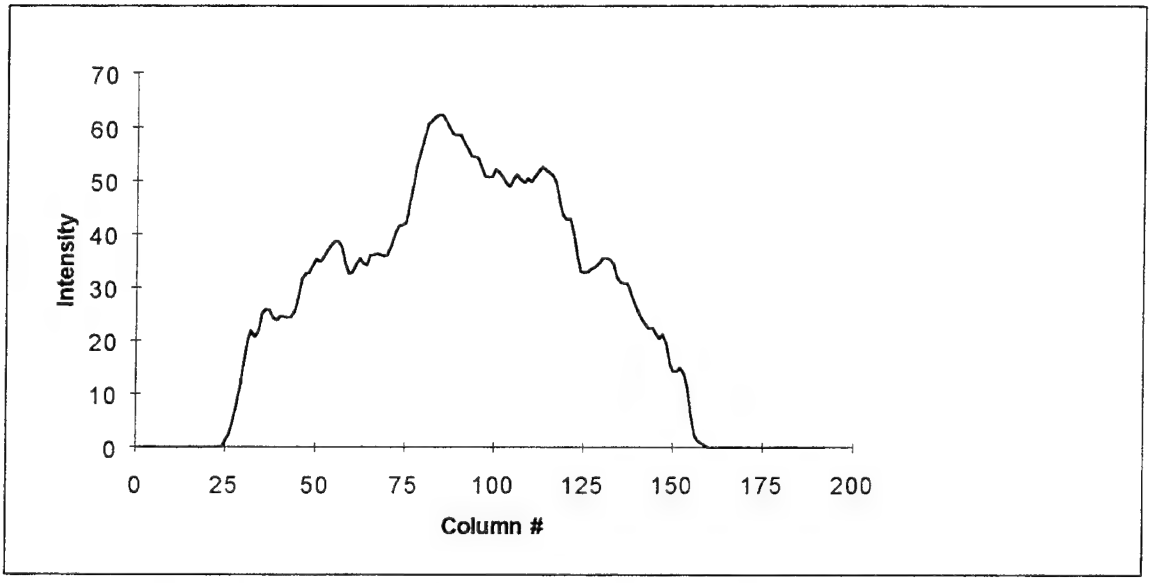

Fig. D-106. Complement of T8 squashed to preserve horizontal sequencies

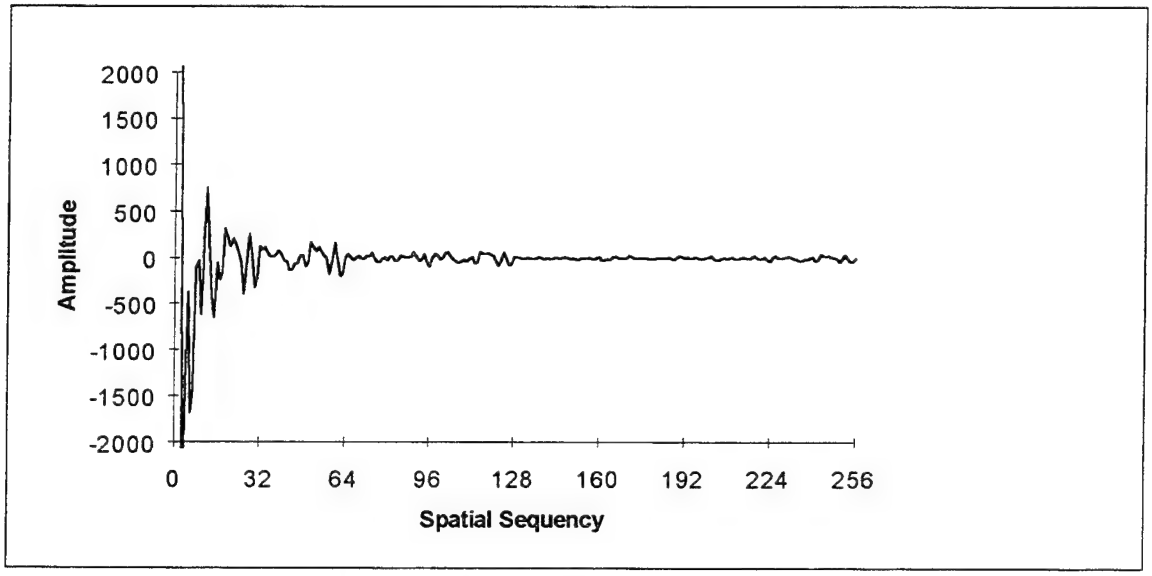

Fig. D-107. Walsh transform of Fig. D-106

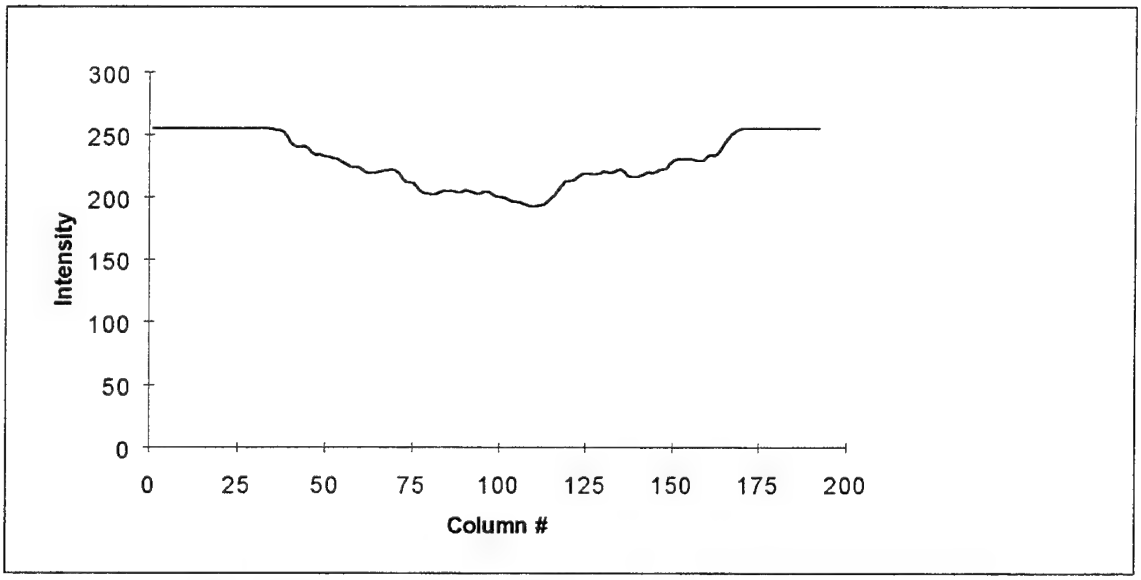

Fig. D-108. Reflection of T8 squashed to preserve horizontal sequencies

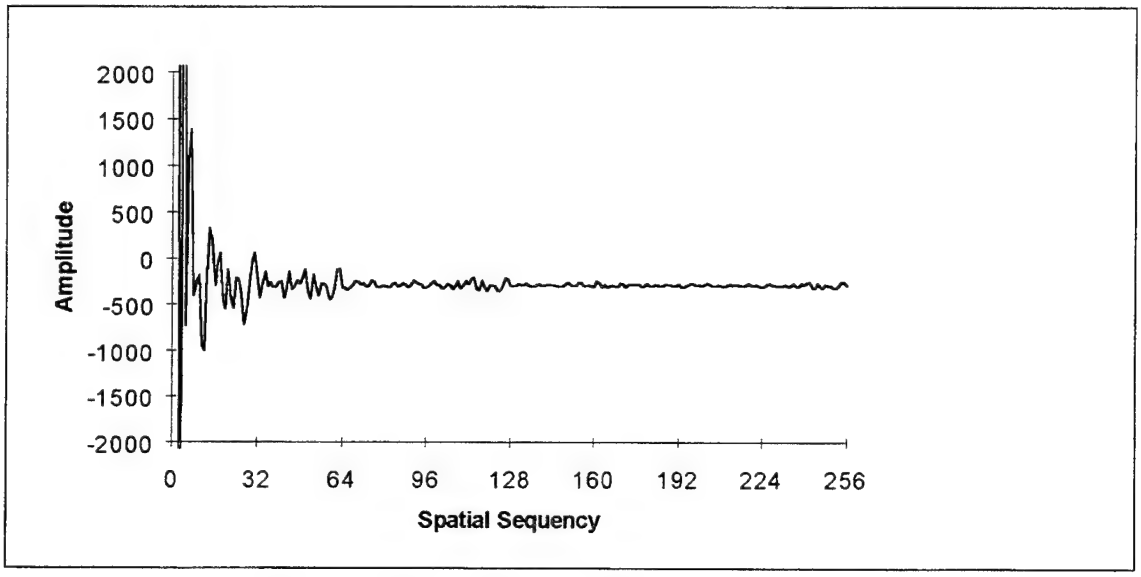

Fig. D-109. Walsh transform of Fig. D-108

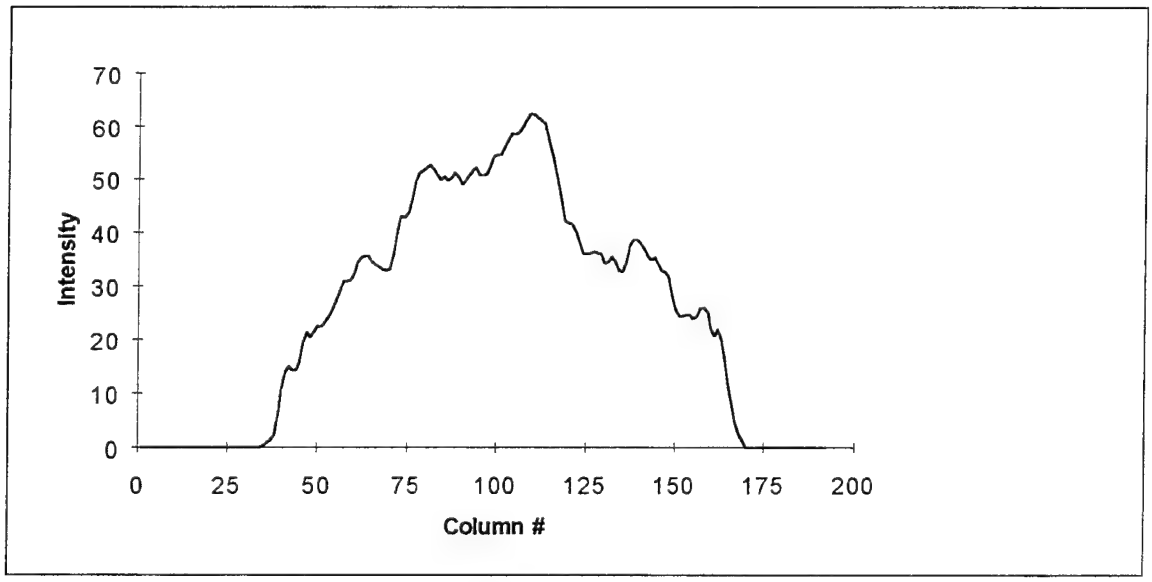

Fig. D-110. Complemented reflection of T8 squashed to preserve horizontal sequencies

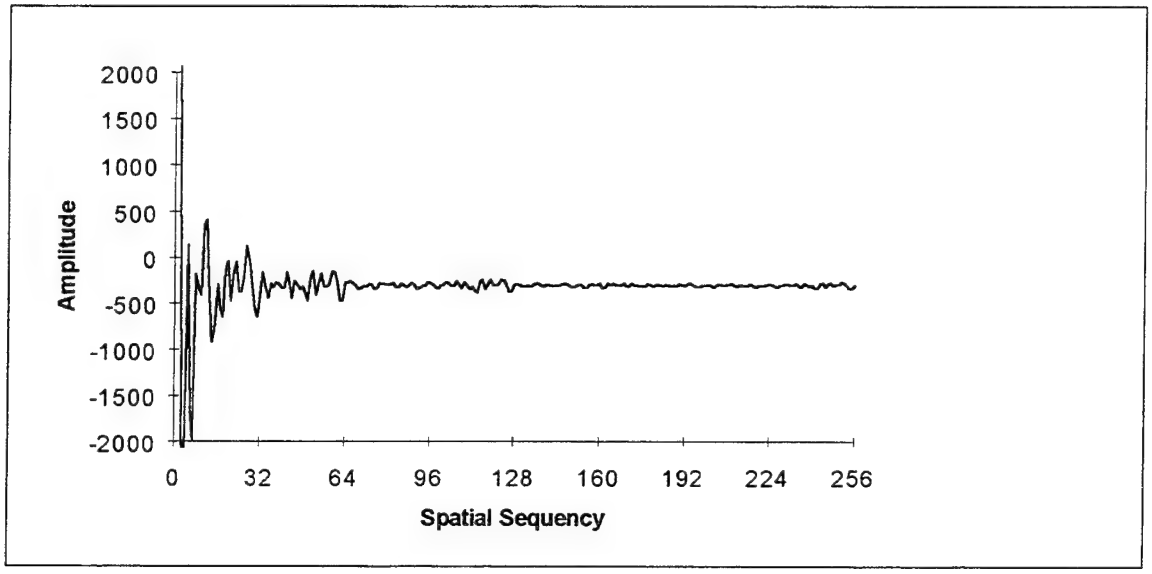

Fig. D-111. Walsh transform of Fig. D-110

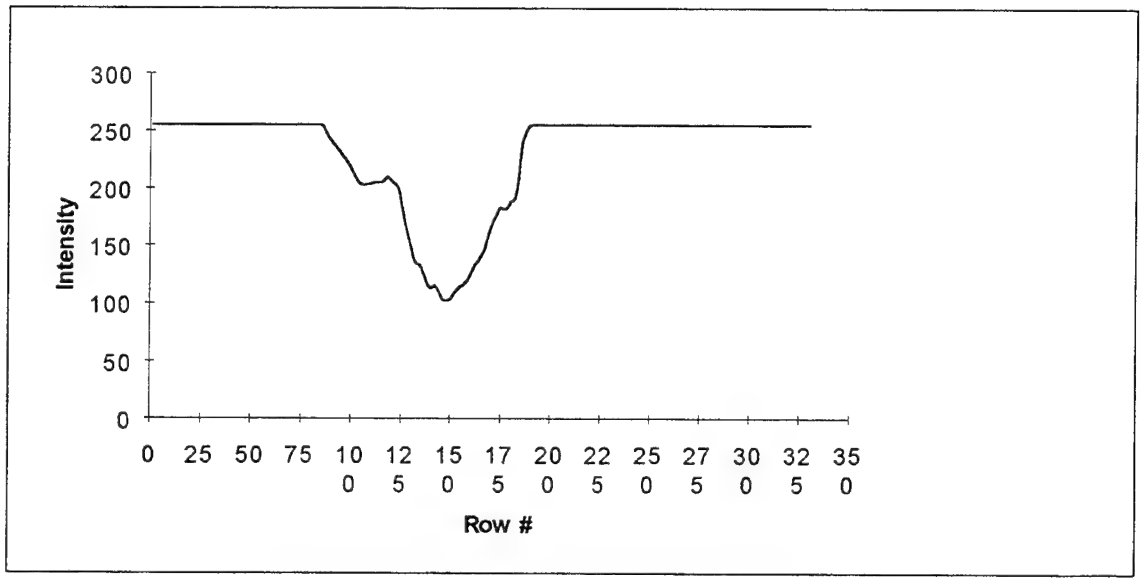

Fig. D-112. T8 squashed to preserve vertical sequencies

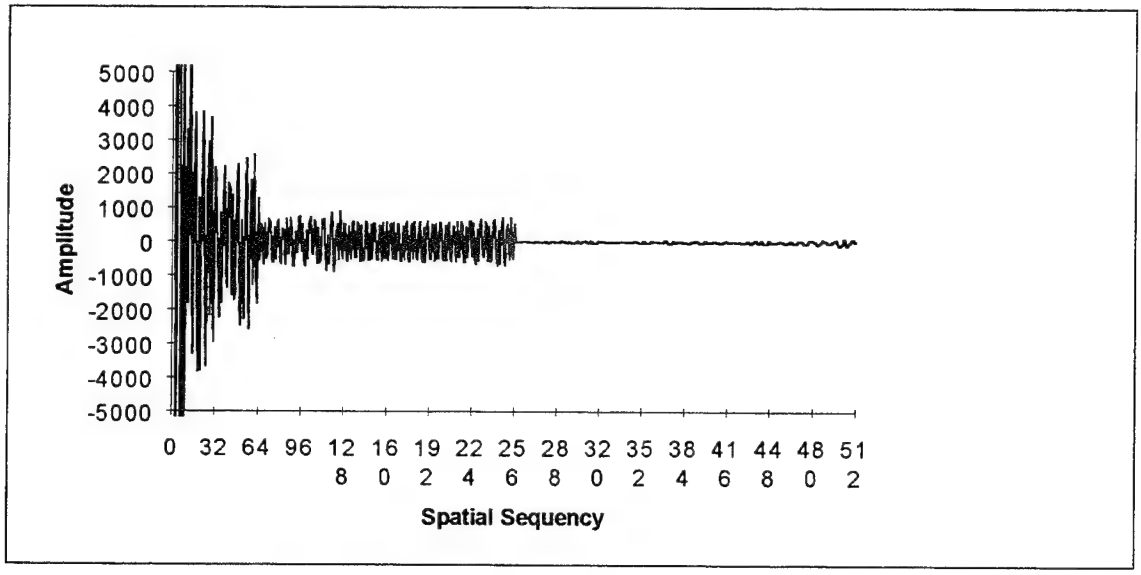

Fig. D-113. Walsh transform of Fig. D-112

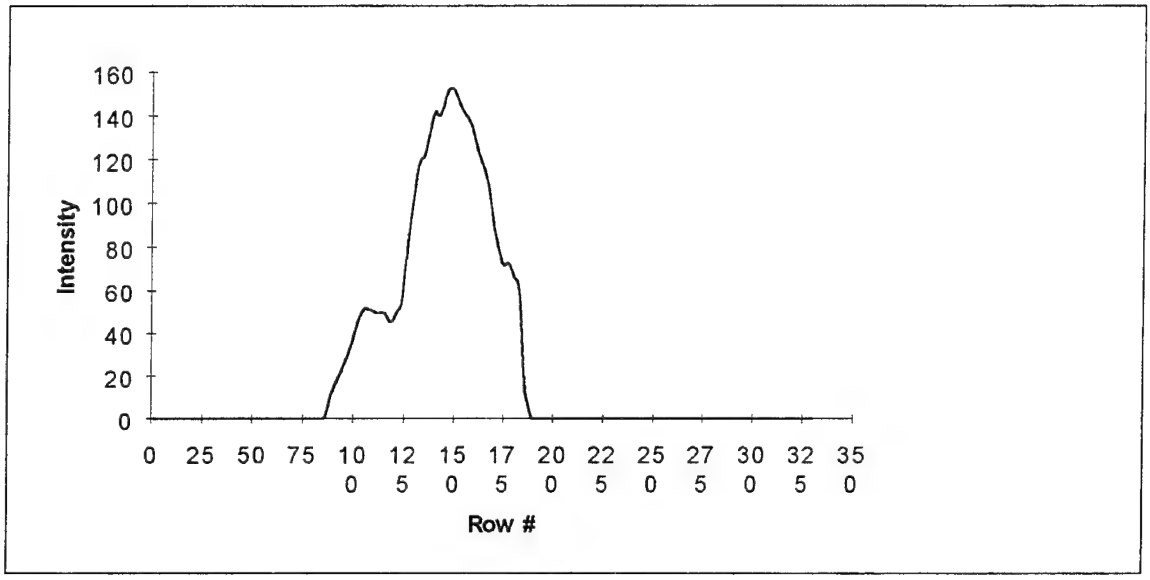

Fig. D-114. Complement of T8 squashed to preserve vertical sequencies

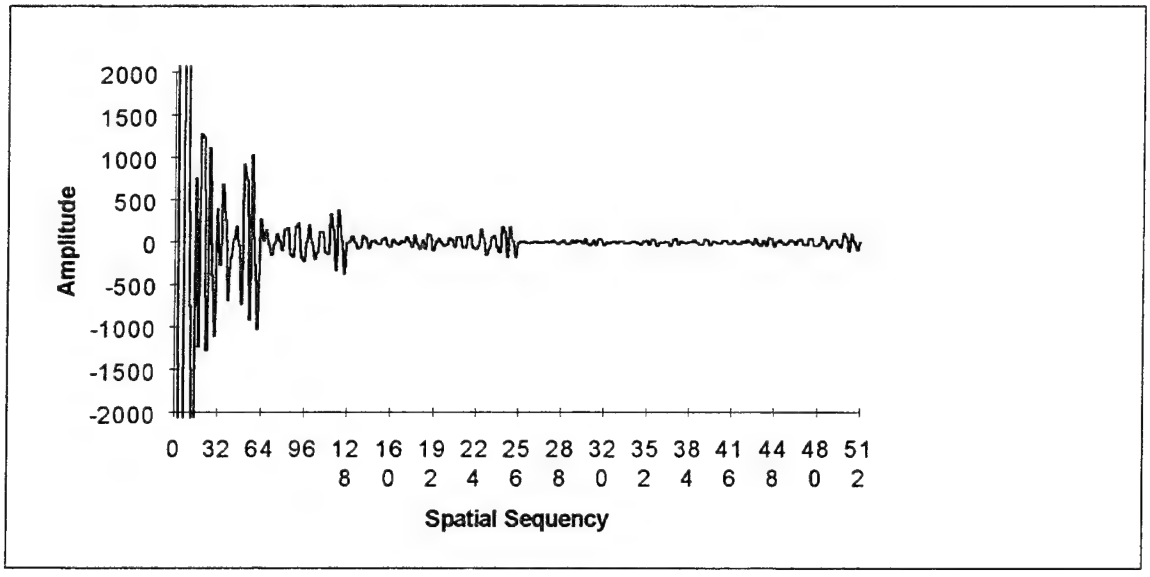

Fig. D-115. Walsh transform of Fig. D-114

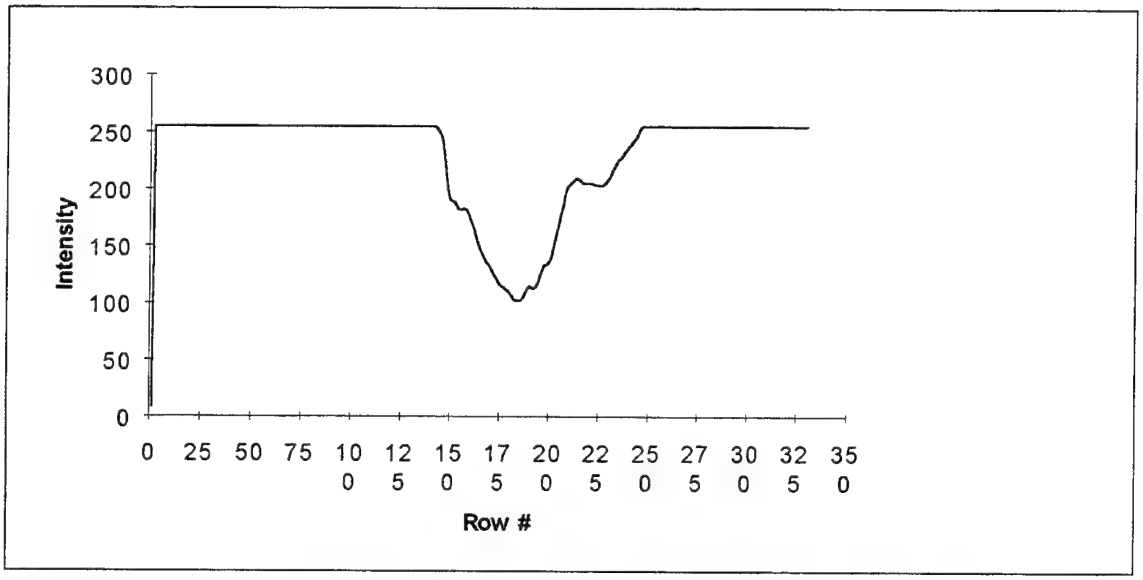

Fig. D-116. Reflection of T8 squashed to preserve vertical sequencies

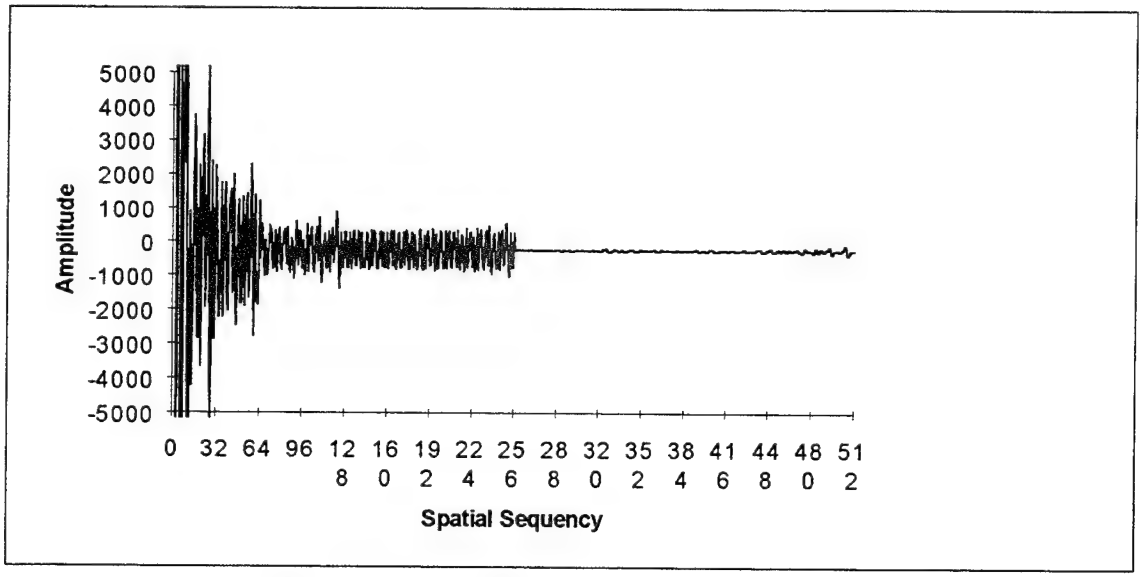

Fig. D-117. Walsh transform of Fig. D-116

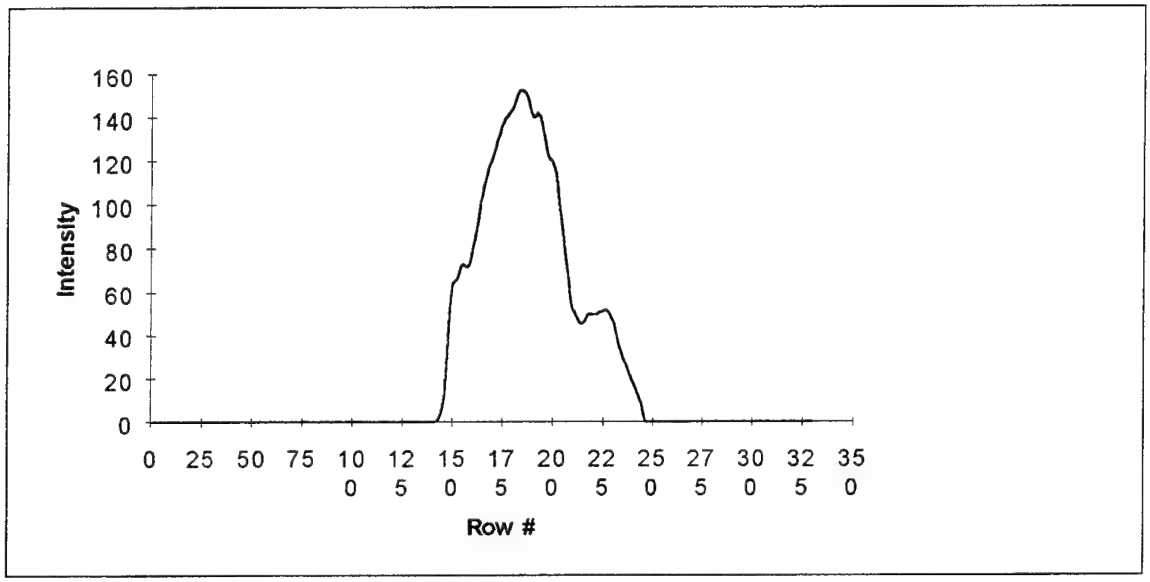

Fig. D-118. Complemented reflection of T8 squashed to preserve vertical sequencies

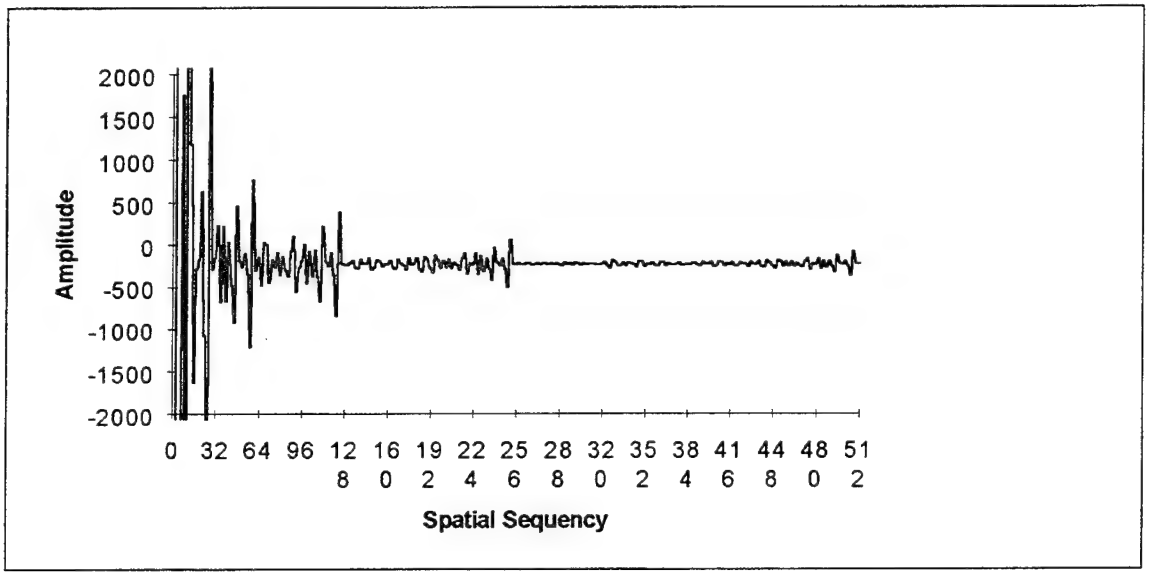

Fig. D-119. Walsh transform of Fig. D-118

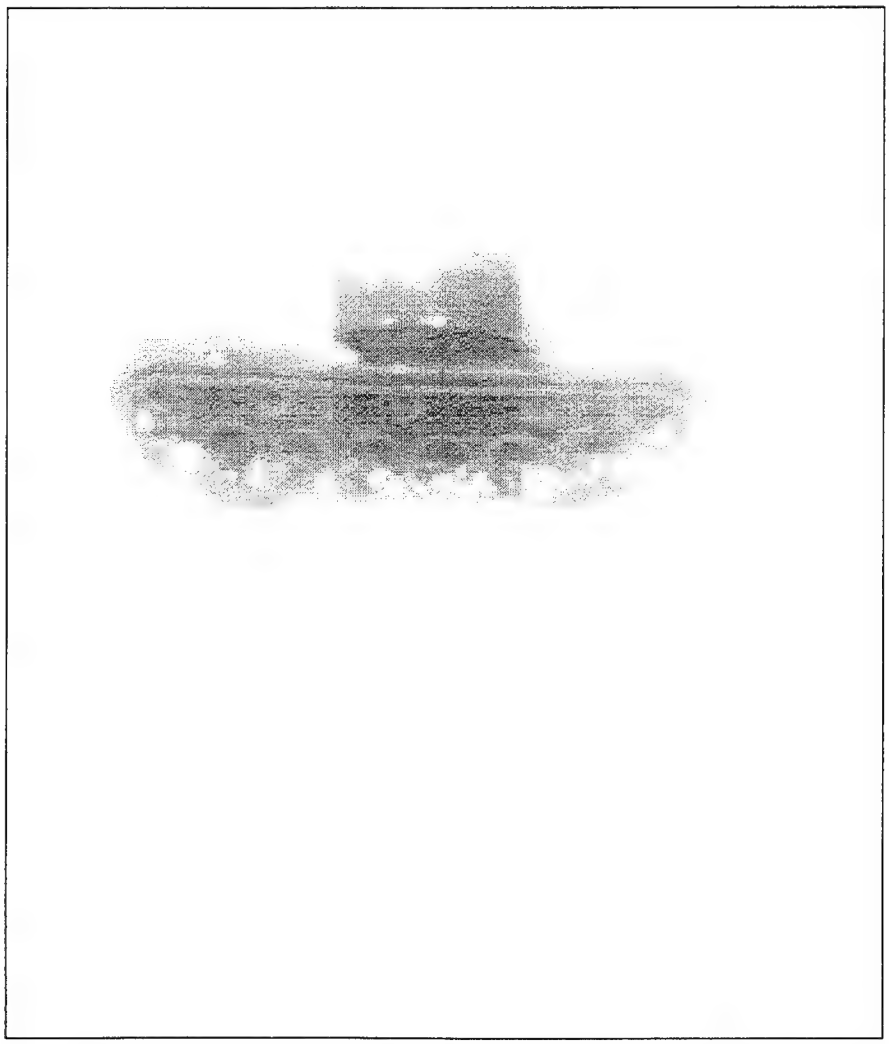

Fig. D-120. T9

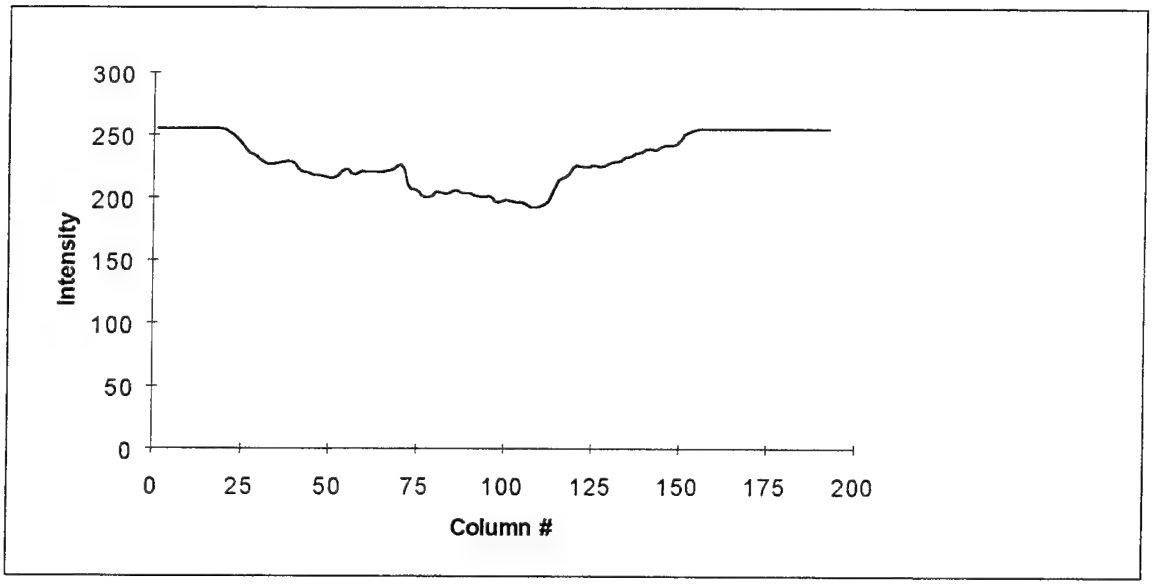

Fig. D-121. T9 squashed to preserve horizontal sequencies

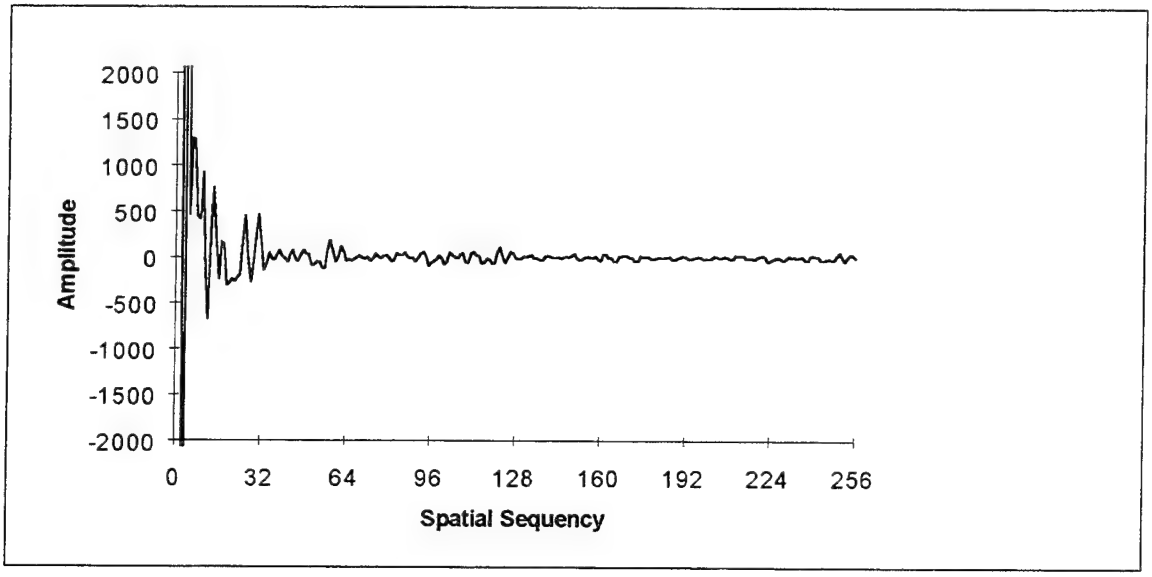

Fig. D-122. Walsh transform of Fig. D-121

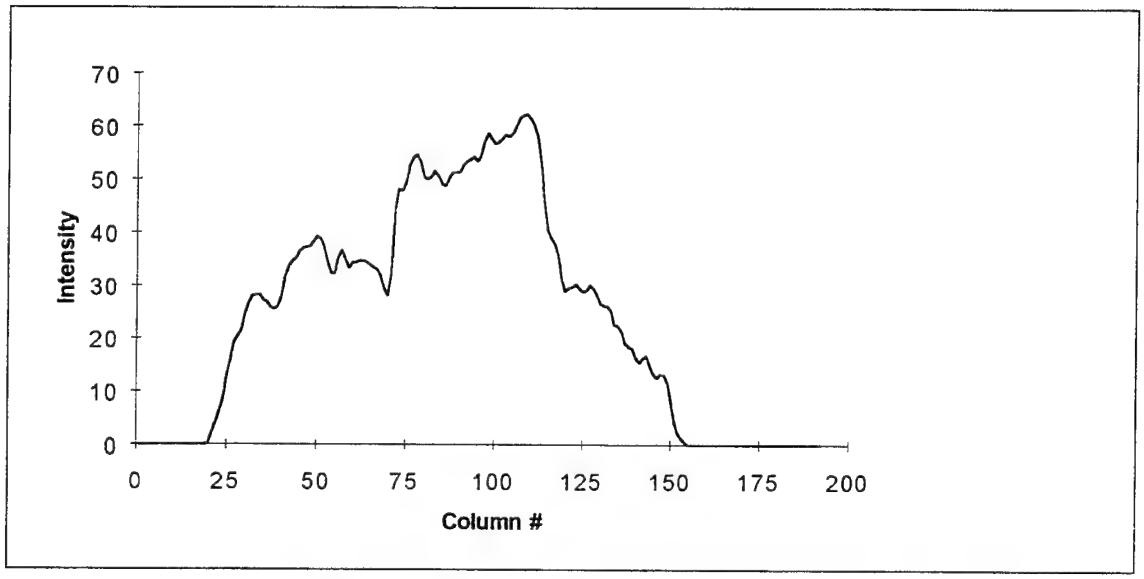

Fig. D-123. Complement of T9 squashed to preserve horizontal sequencies

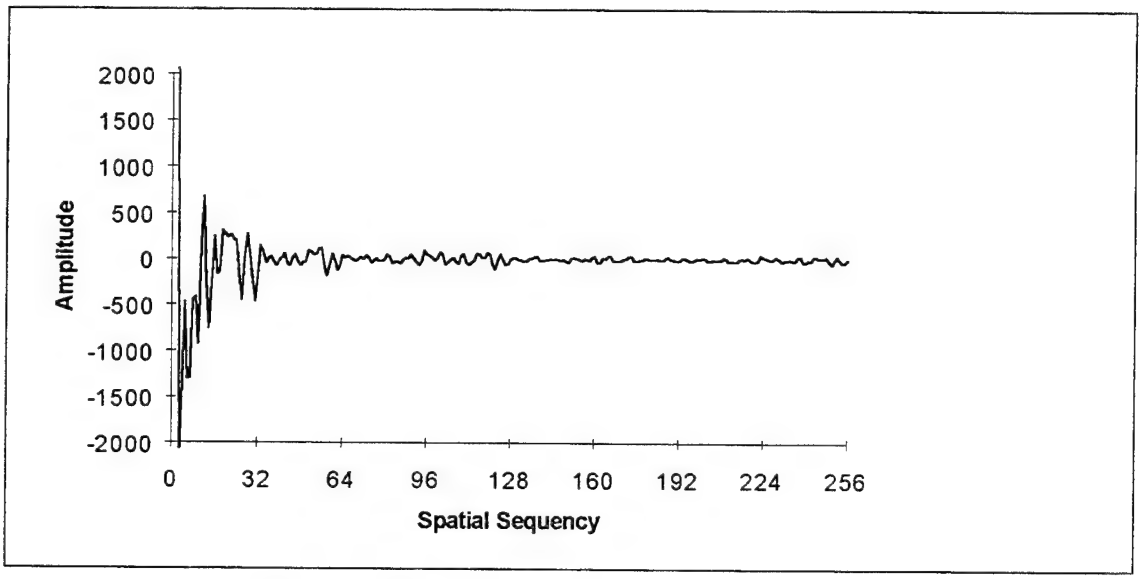

Fig. D-124. Walsh transform of Fig. D-123

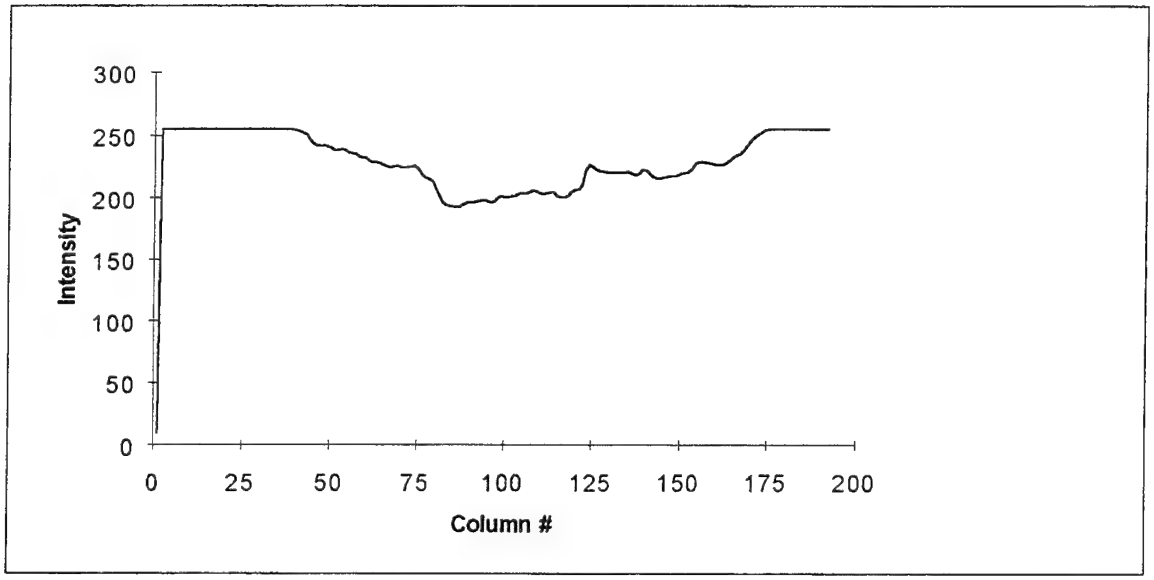

Fig. D-125. Reflection of T9 squashed to preserve horizontal sequency

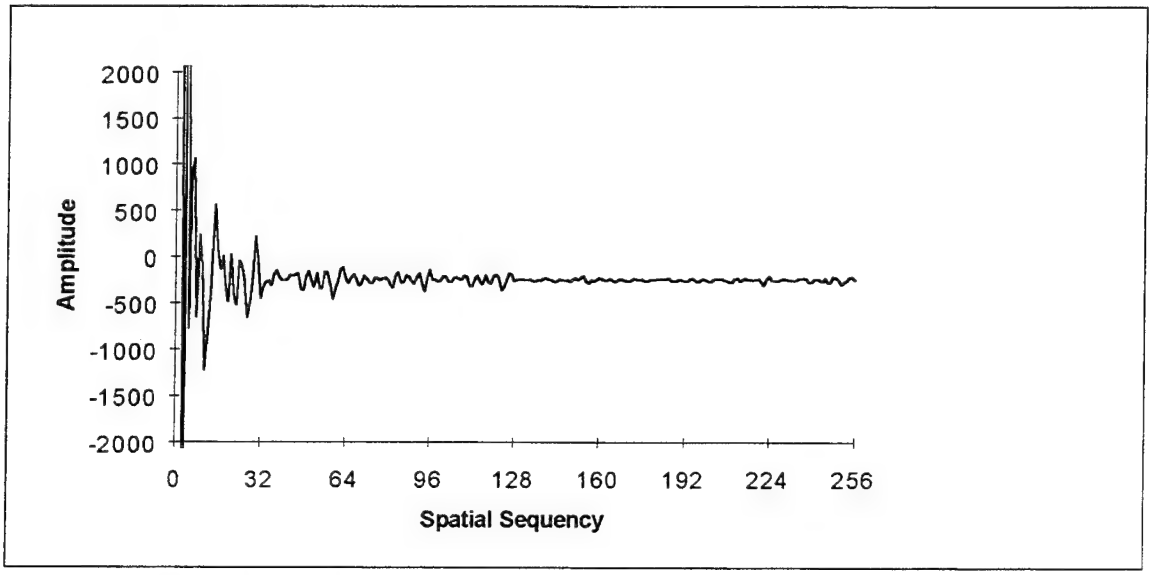

Fig. D-126. Walsh transform of Fig. D-125

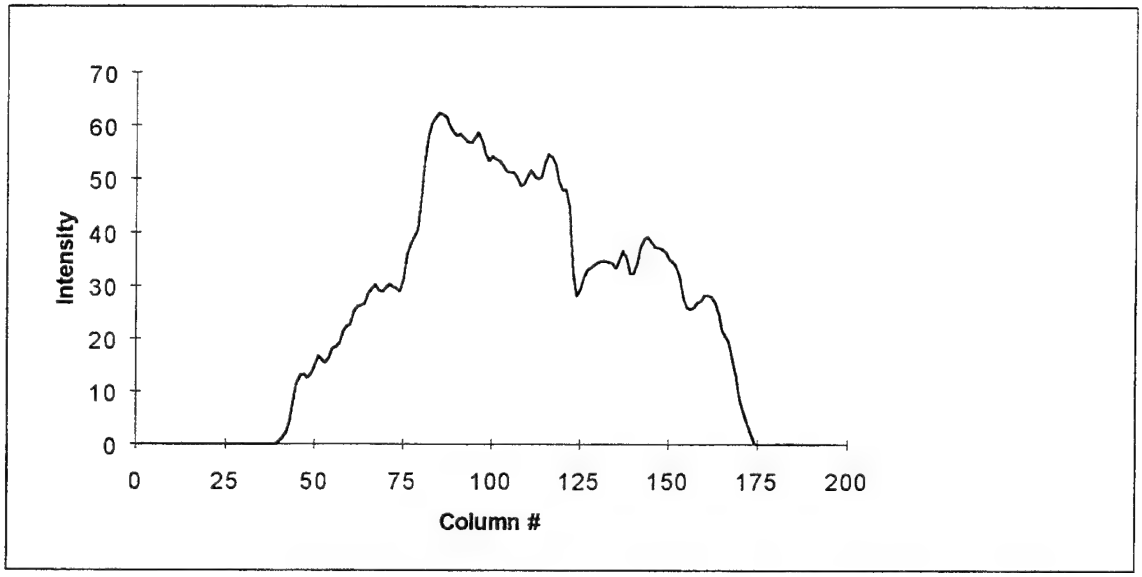

Fig. D-127. Complemented reflection of T9 squashed to preserve horizontal sequencies

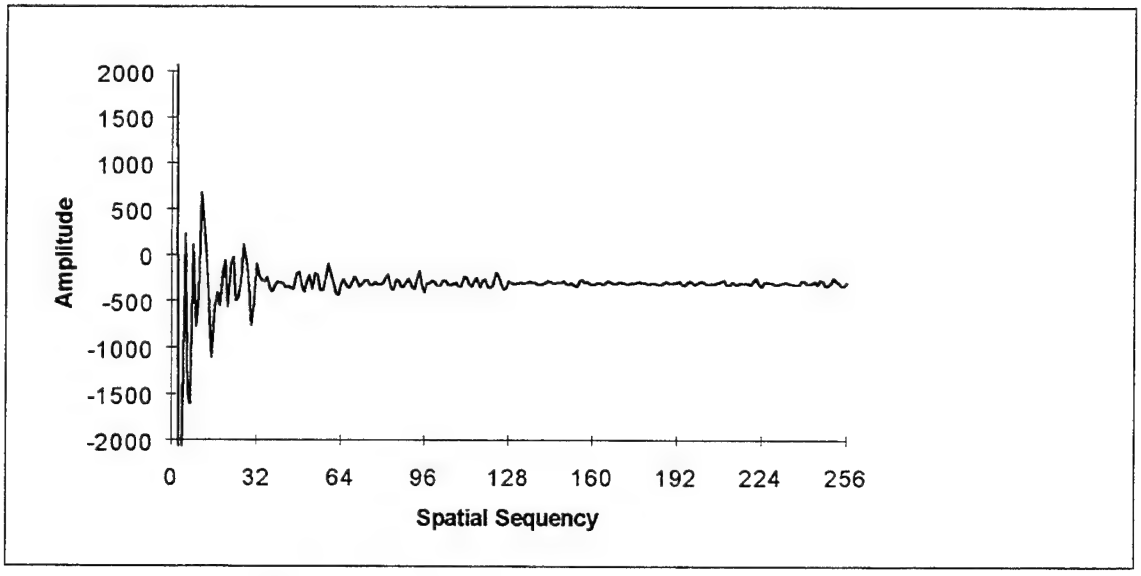

Fig. D-128. Walsh transform of Fig. D-127

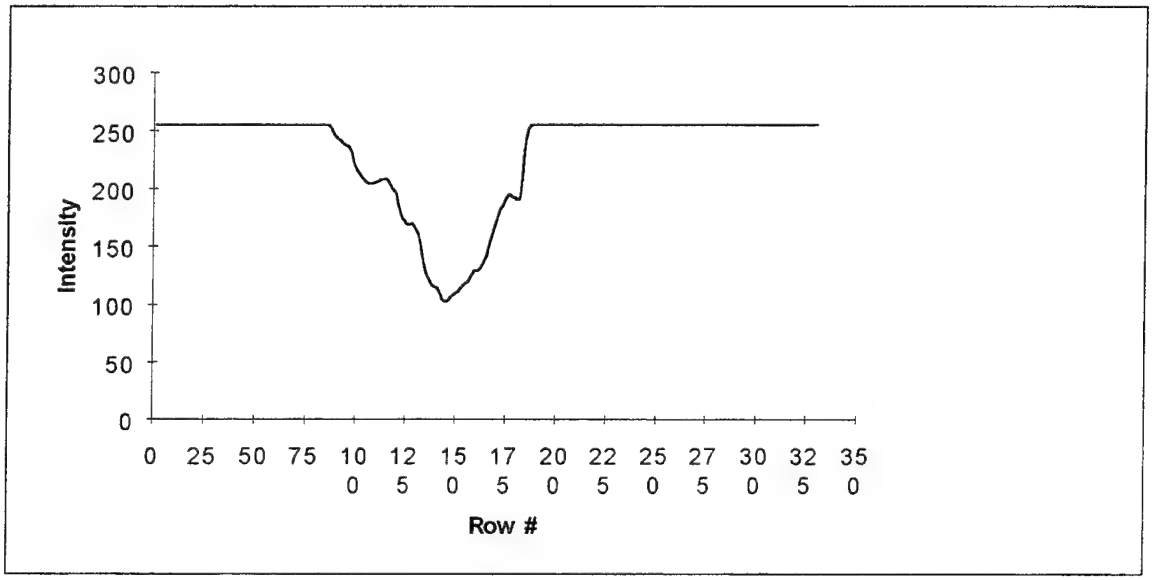

Fig. D-129. T9 squashed to preserve vertical sequencies

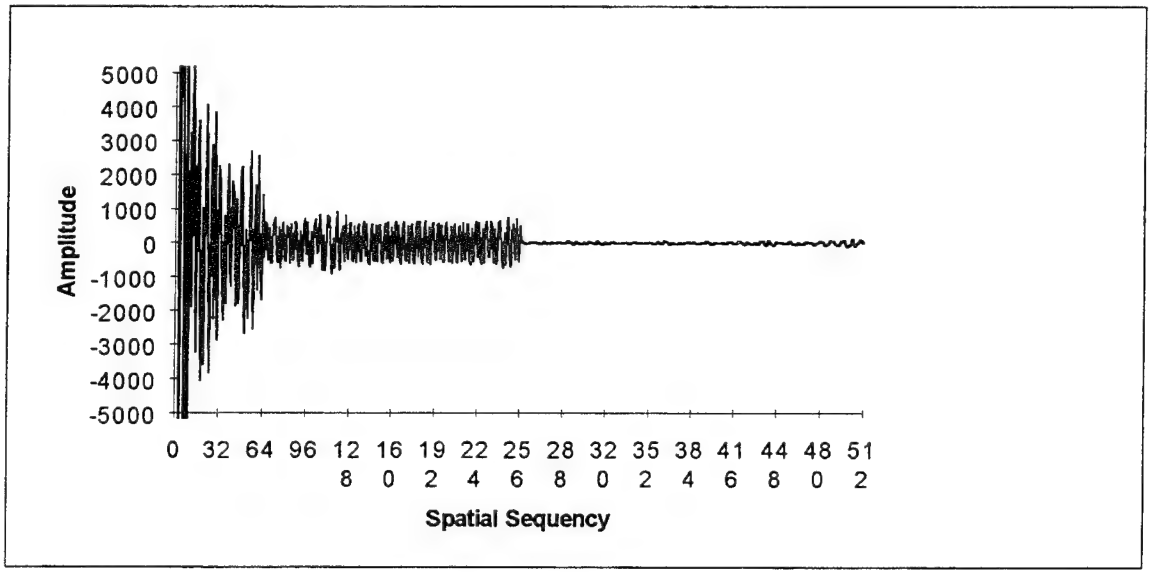

Fig. D-130. Walsh transform of Fig. D-129

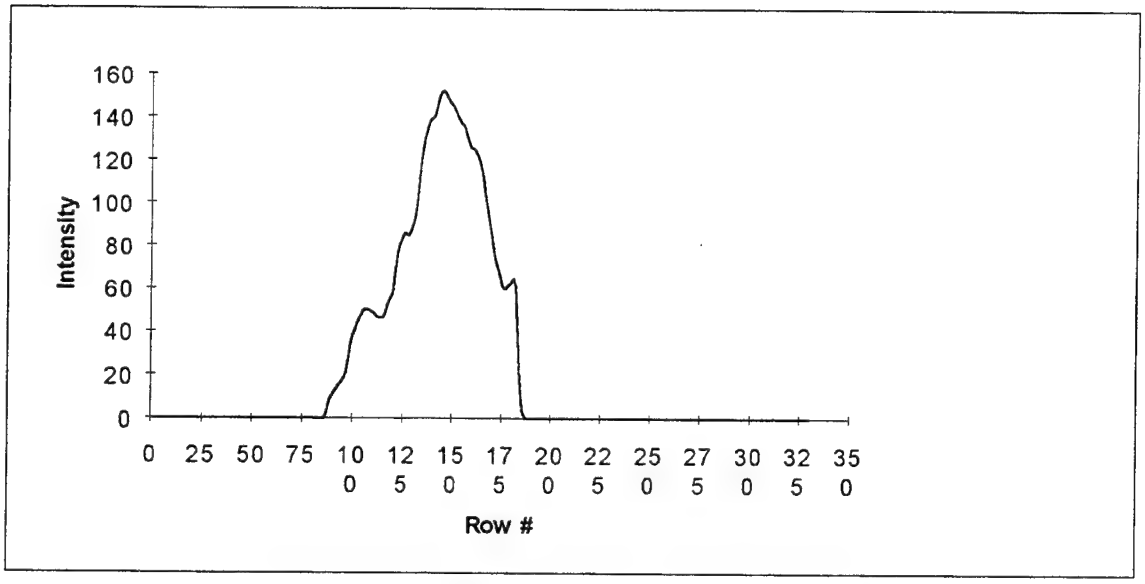

Fig. D-131. Complement of T9 squashed to preserve vertical sequencies

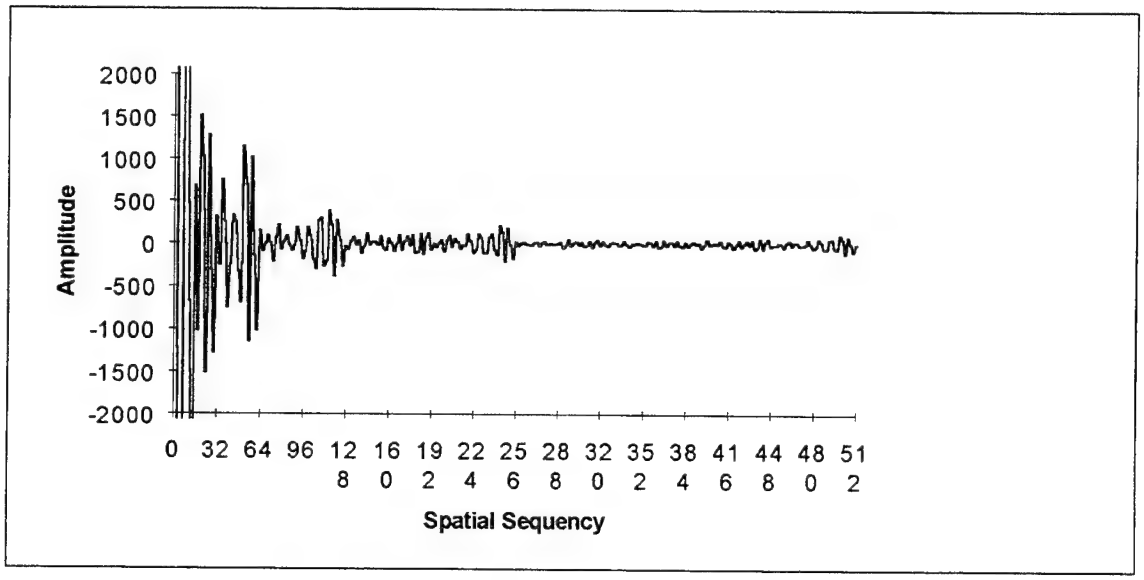

Fig. D-132. Walsh transform of Fig. D-131

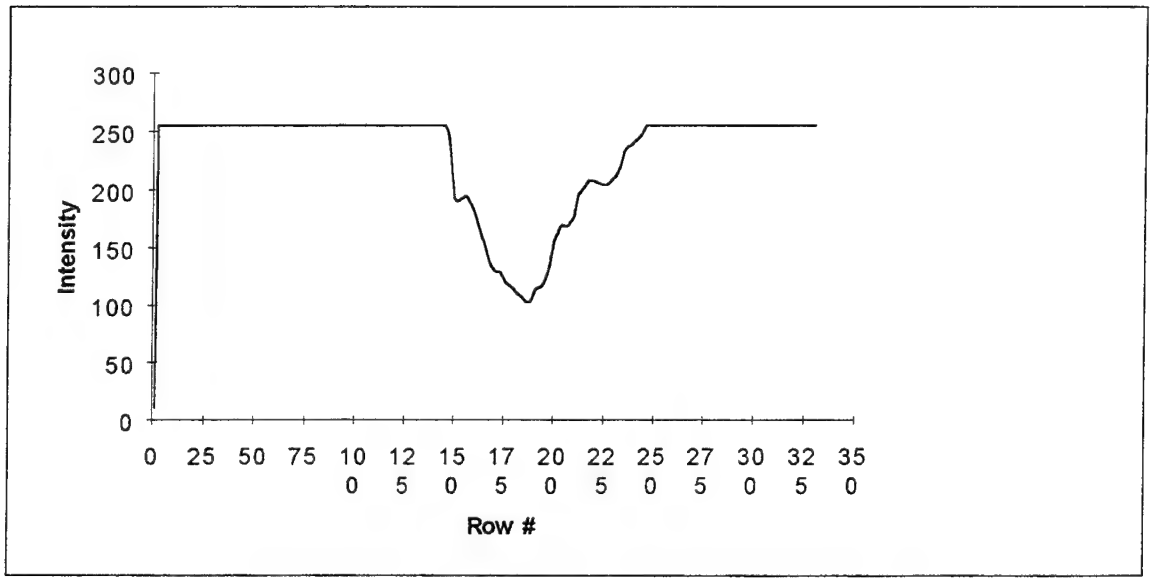

Fig. D-133. Reflection of T9 squashed to preserve vertical sequencies

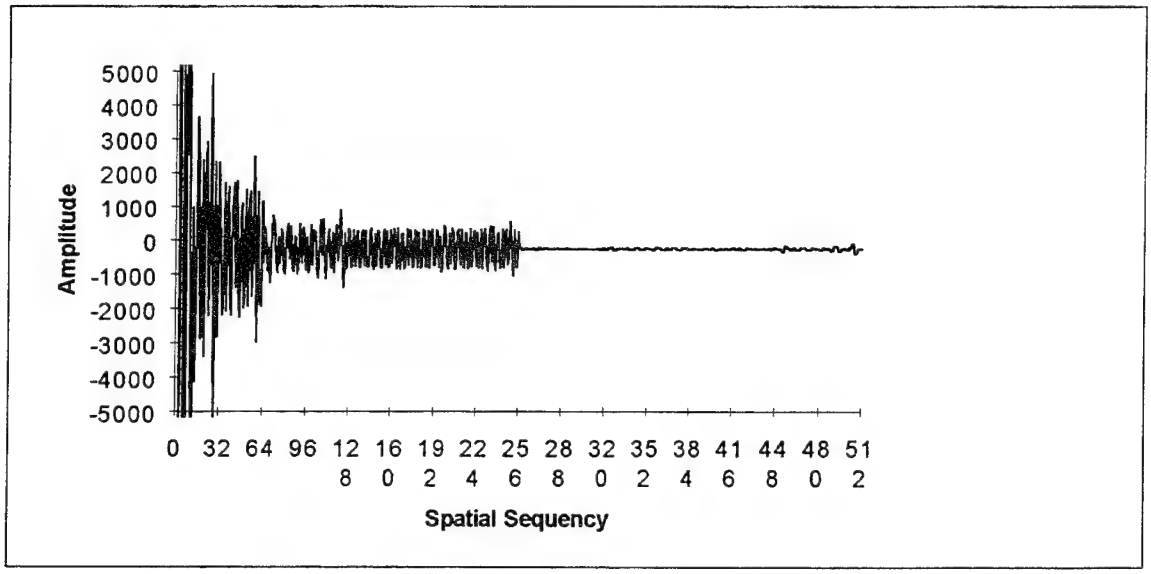

Fig. D-134. Walsh transform of Fig. D-133

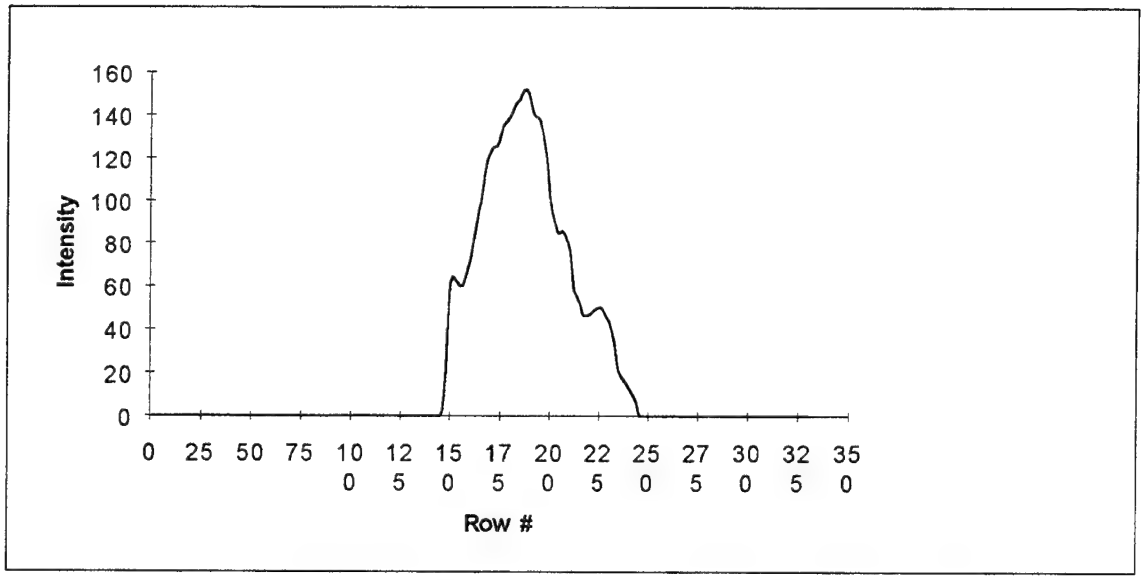

Fig. D-135. Complemented reflection of T9 squashed to preserve vertical sequencies

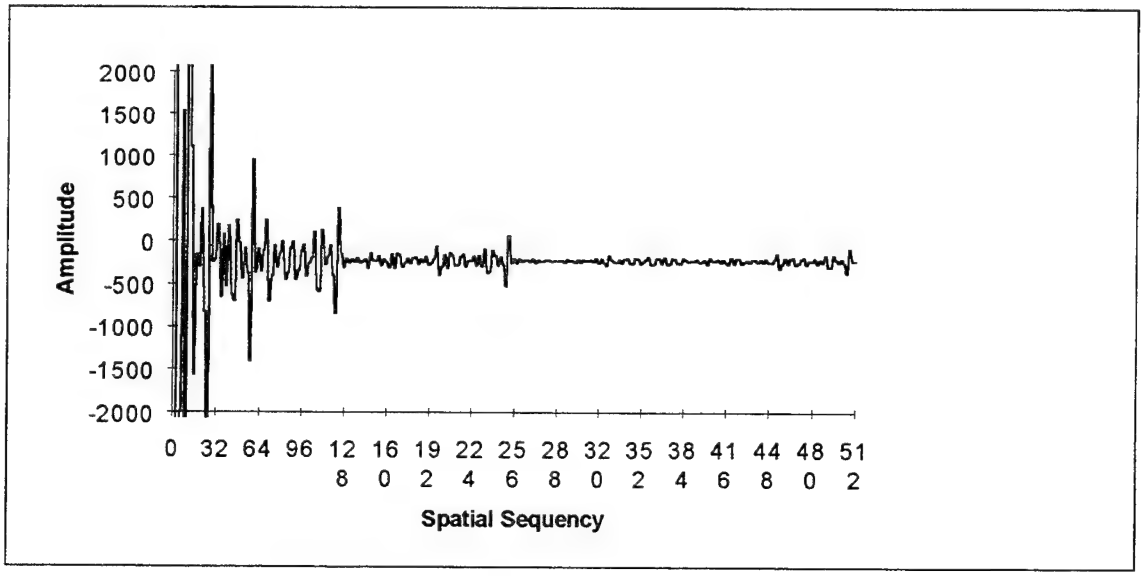

Fig. D-136. Walsh transform of Fig. D-135

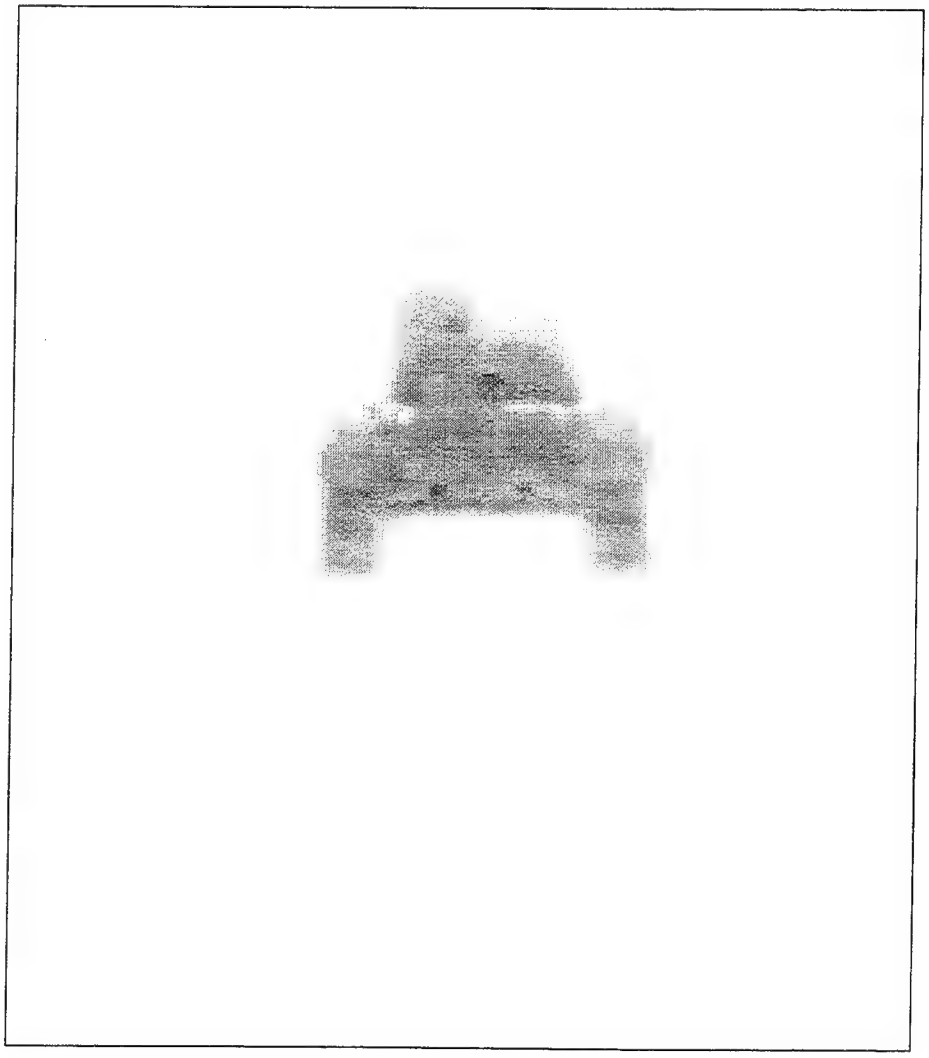

Fig. D-137. T10

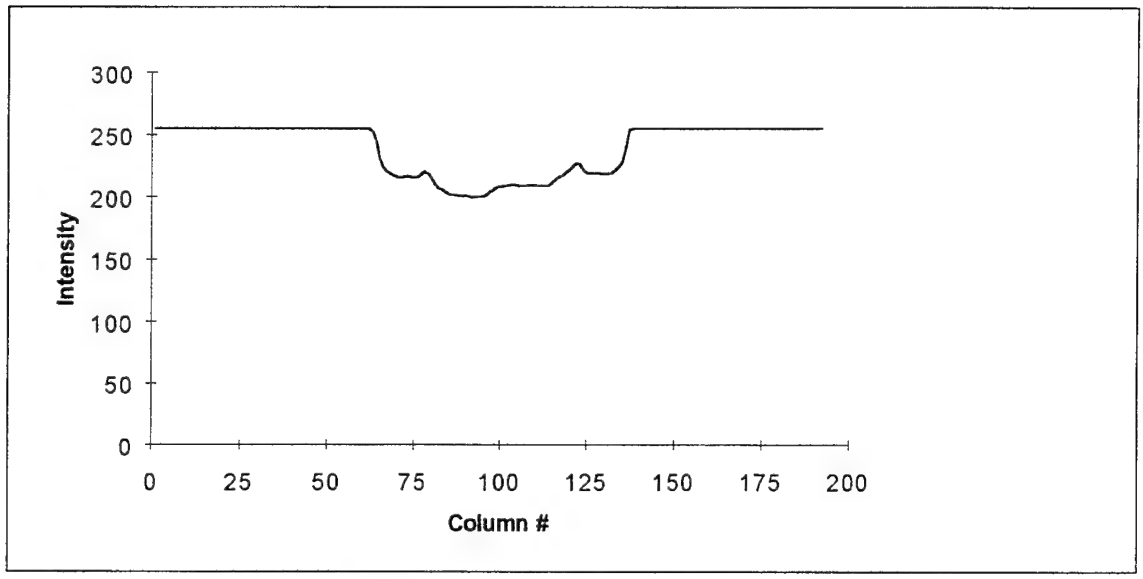

Fig. D-138. T10 squashed to preserve horizontal sequencies

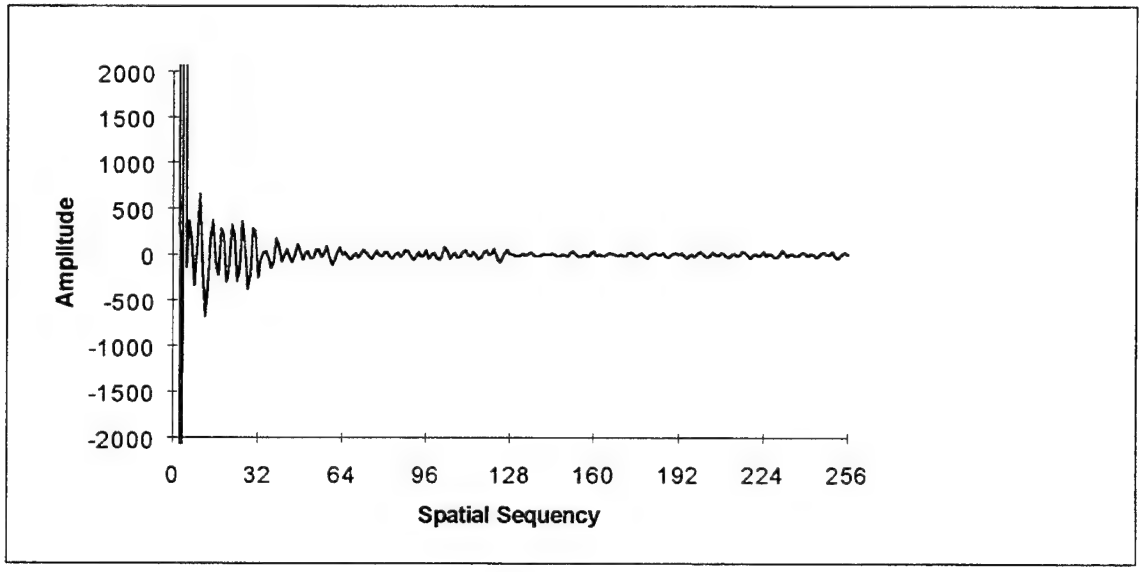

Fig. D-139. Walsh transform of Fig. D-138

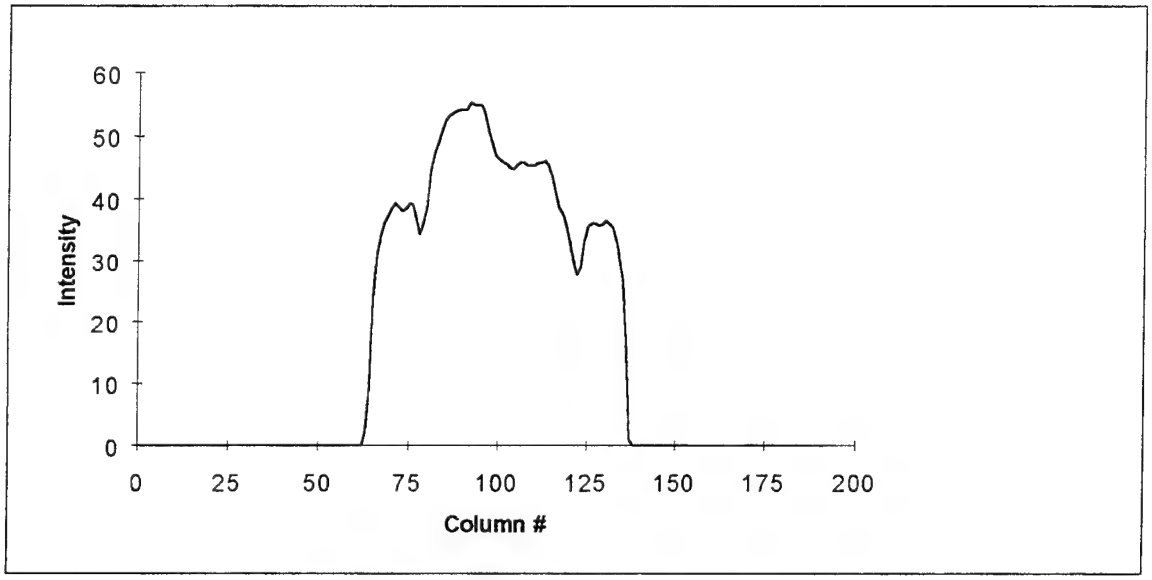

Fig. D-140. Complement of T10 squashed to preserve horizontal sequencies

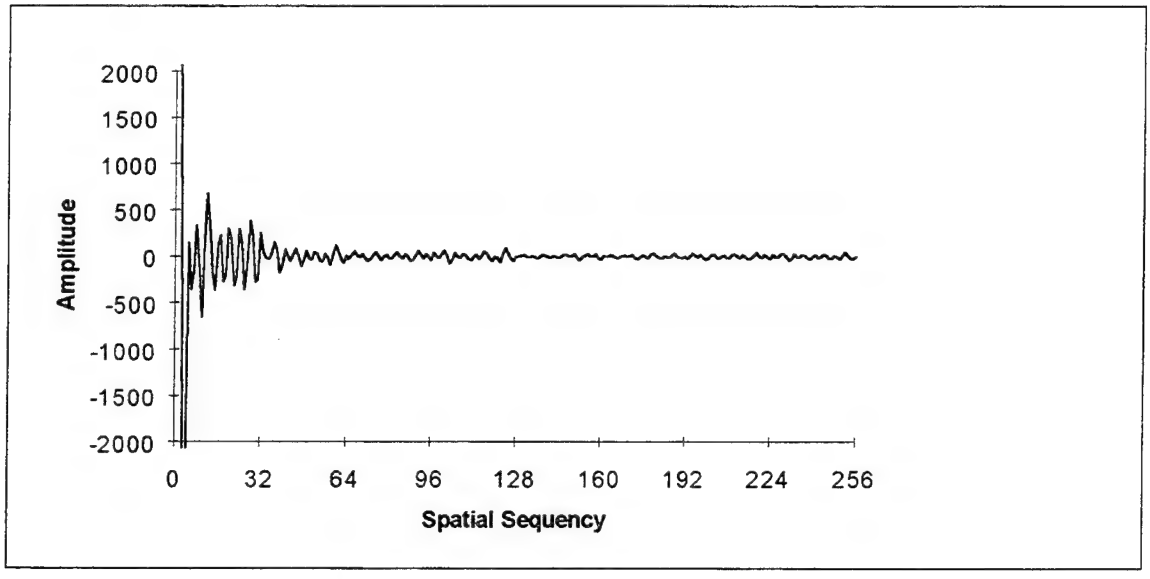

Fig. D-141. Walsh transform of Fig. D-140

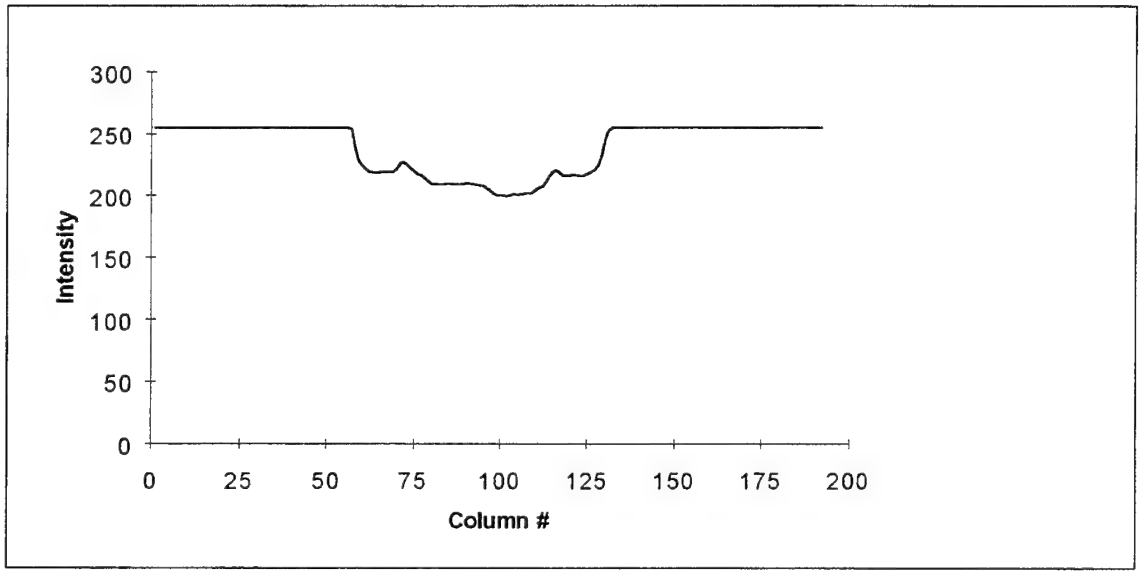

Fig. D-142. Reflection of T10 squashed to preserve horizontal sequencies

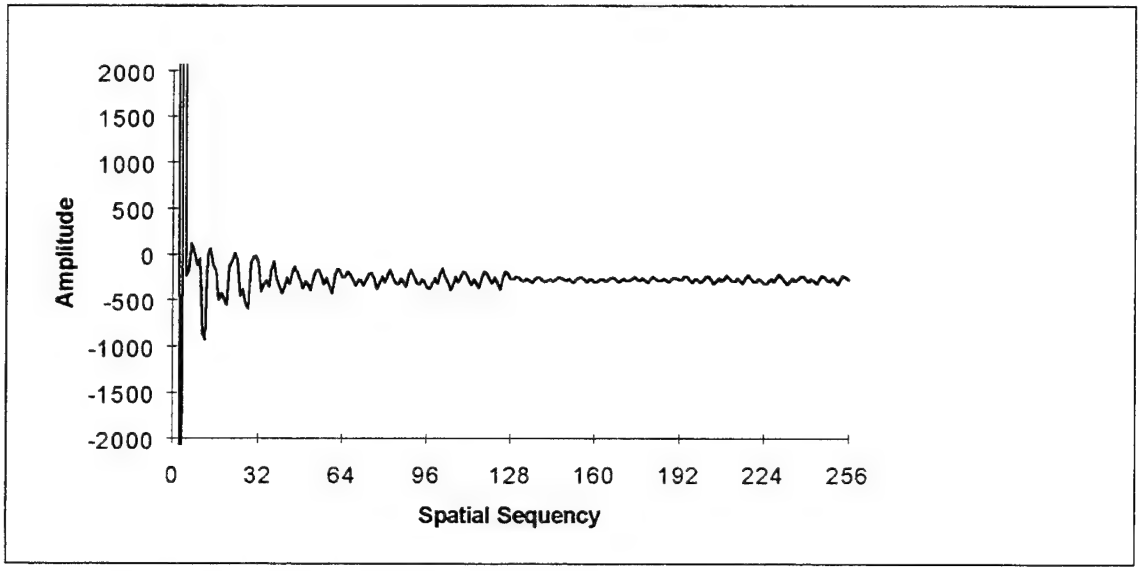

Fig. D-143. Walsh transform of Fig. D-142

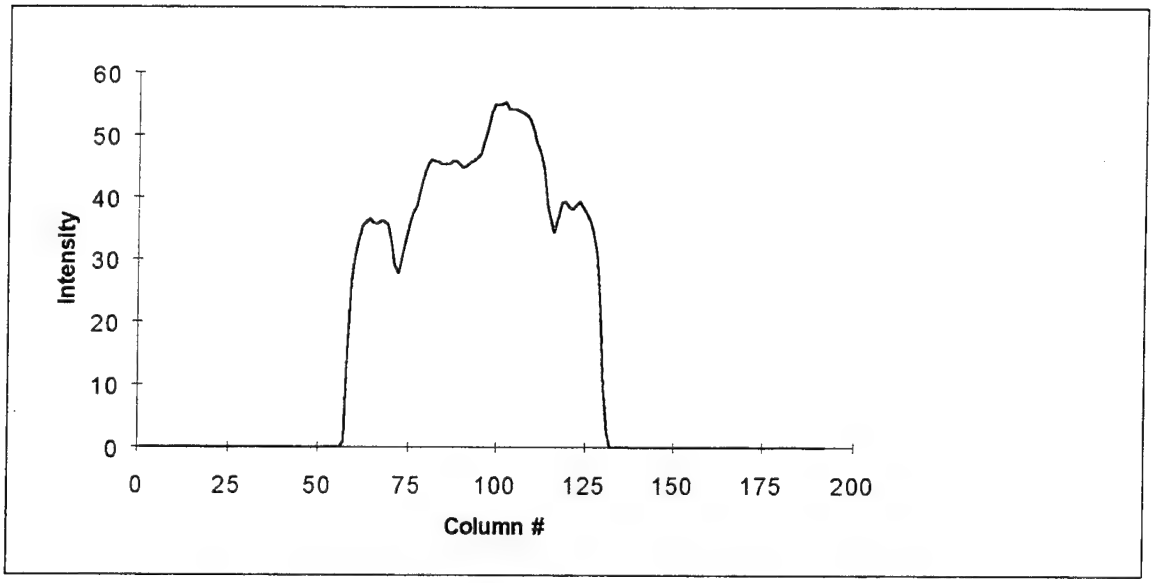

Fig. D-144. Complemented reflection of T10 squashed to preserve horizontal sequencies

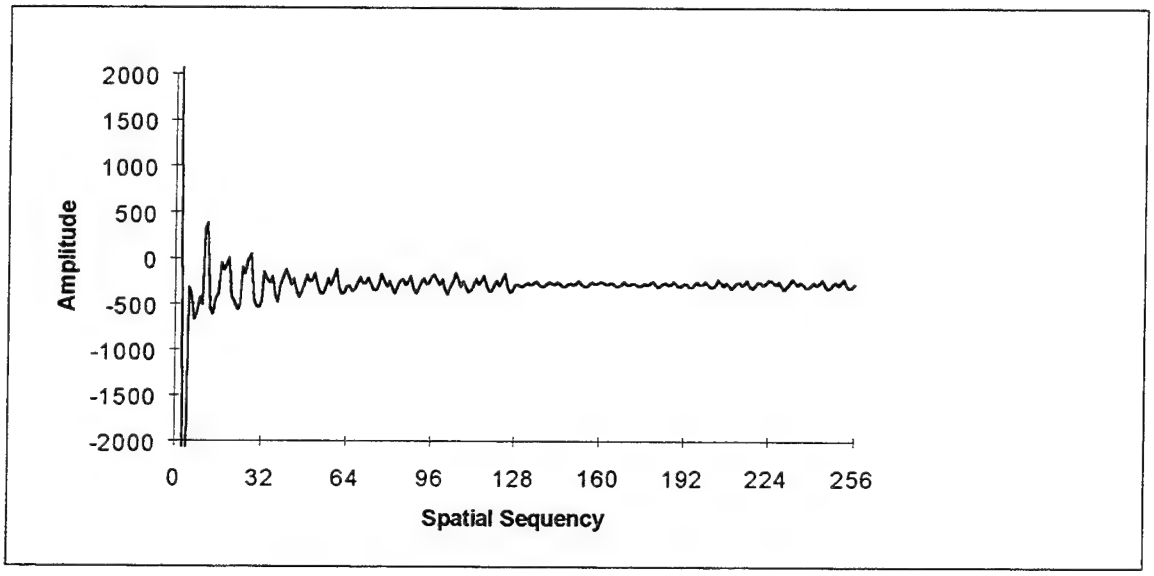

Fig. D-145. Walsh transform of Fig. D-144

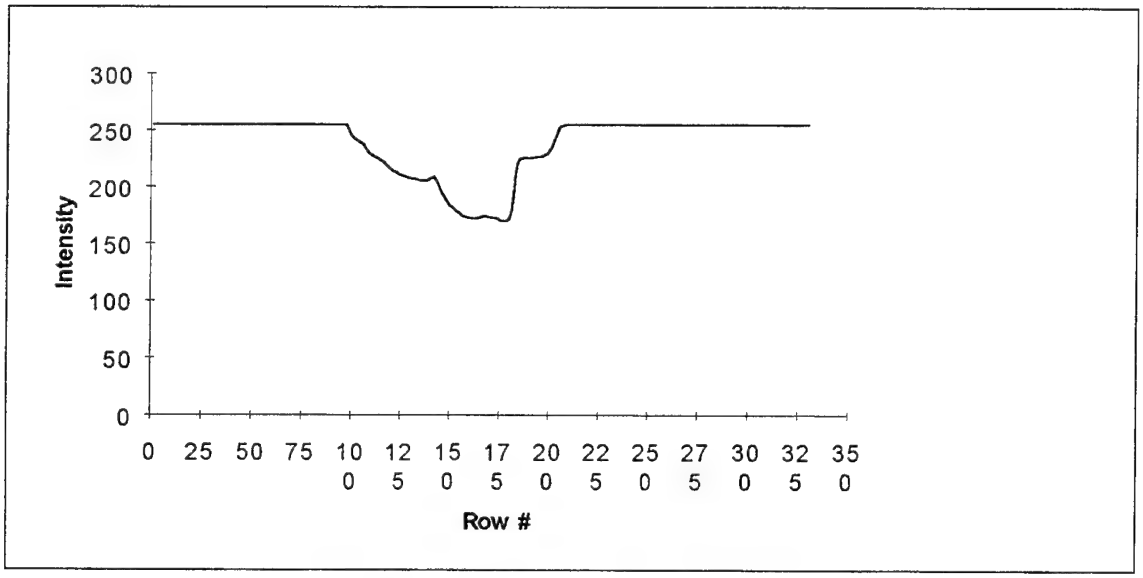

Fig. D-146. T10 squashed to preserve vertical sequencies

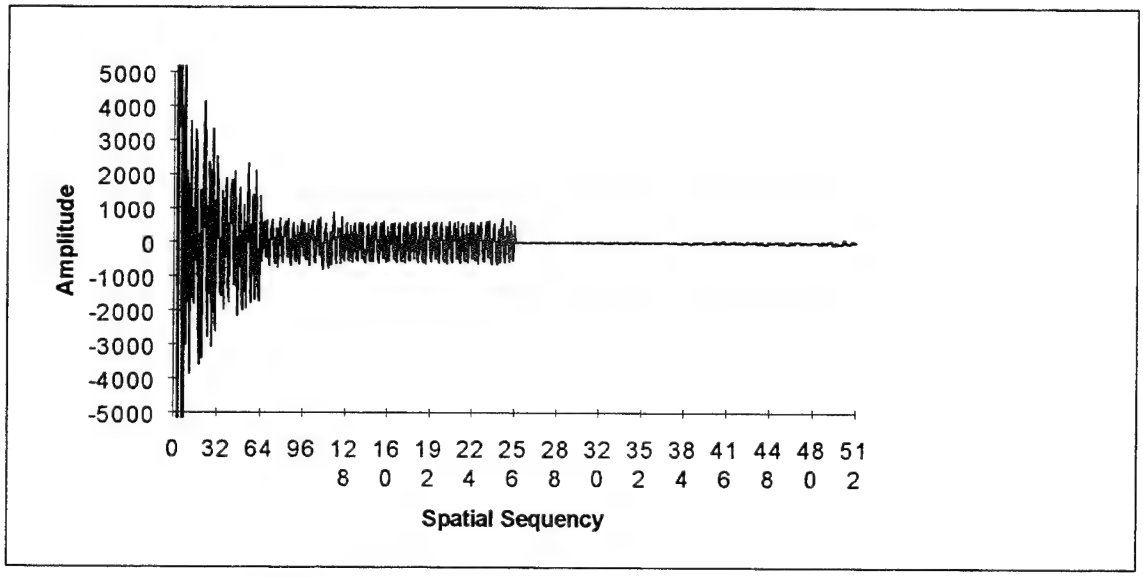

Fig. D-147. Walsh transform of Fig. D-146

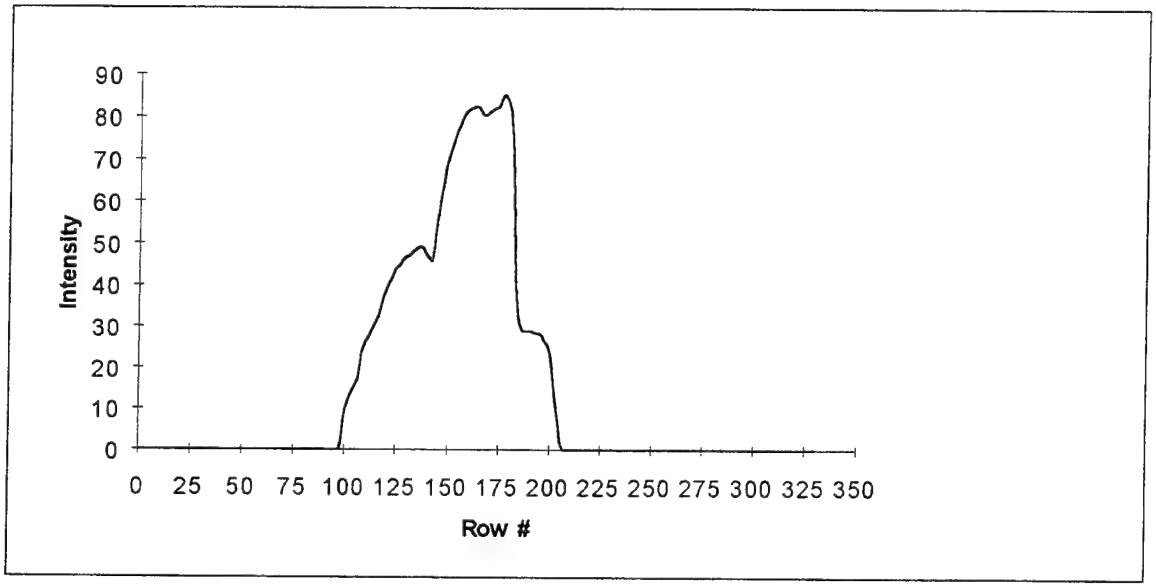

Fig. D-148. Complement of T10 squashed to preserve vertical sequencies

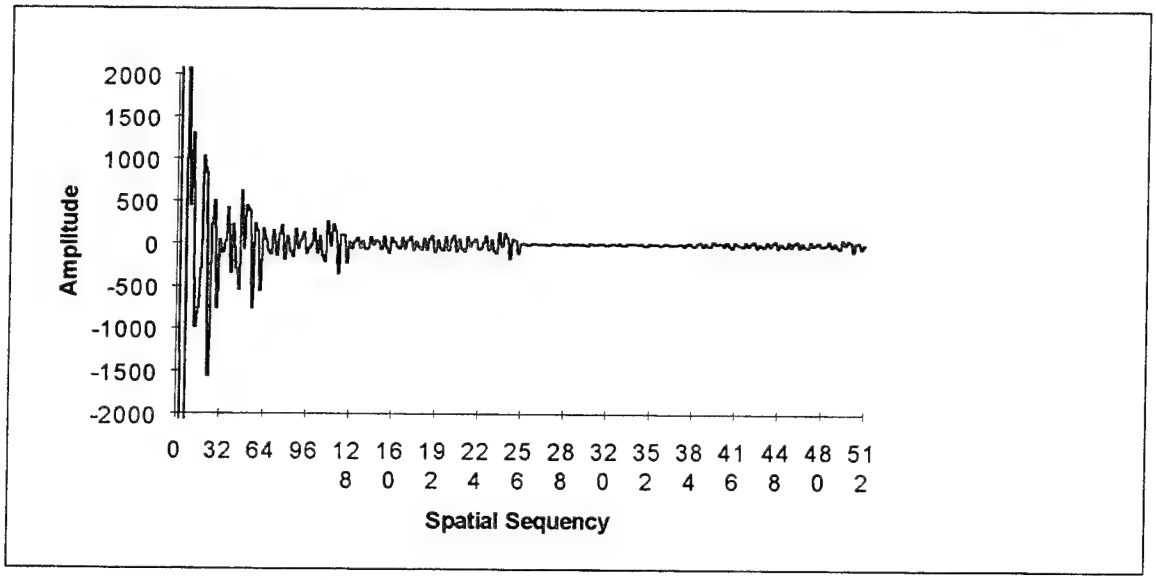

Fig. D-149. Walsh transform of Fig. D-148

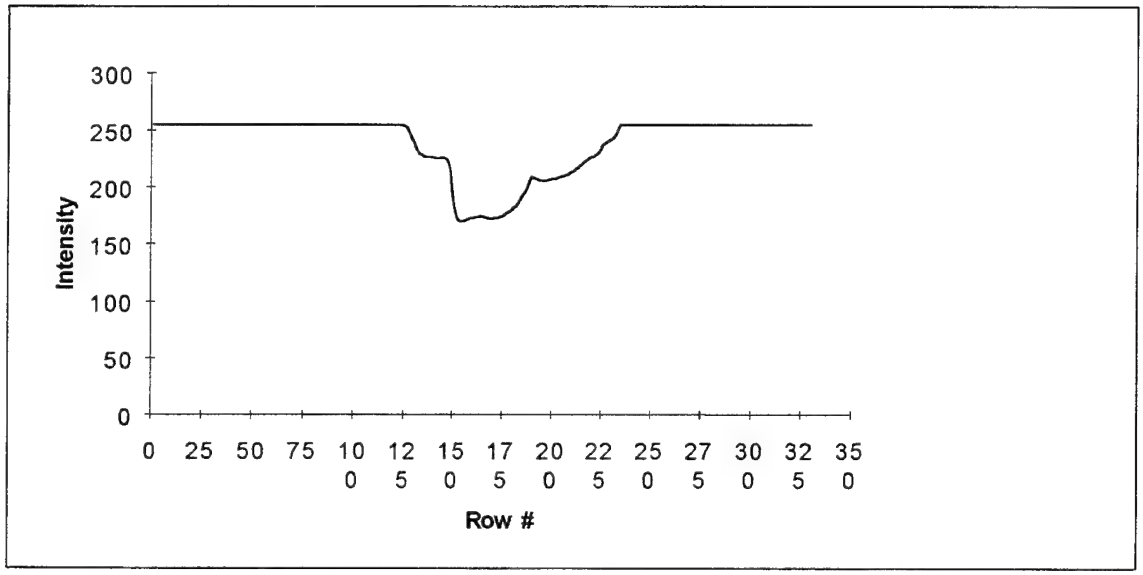

Fig. D-150. Reflection of T10 squashed to preserve vertical sequency

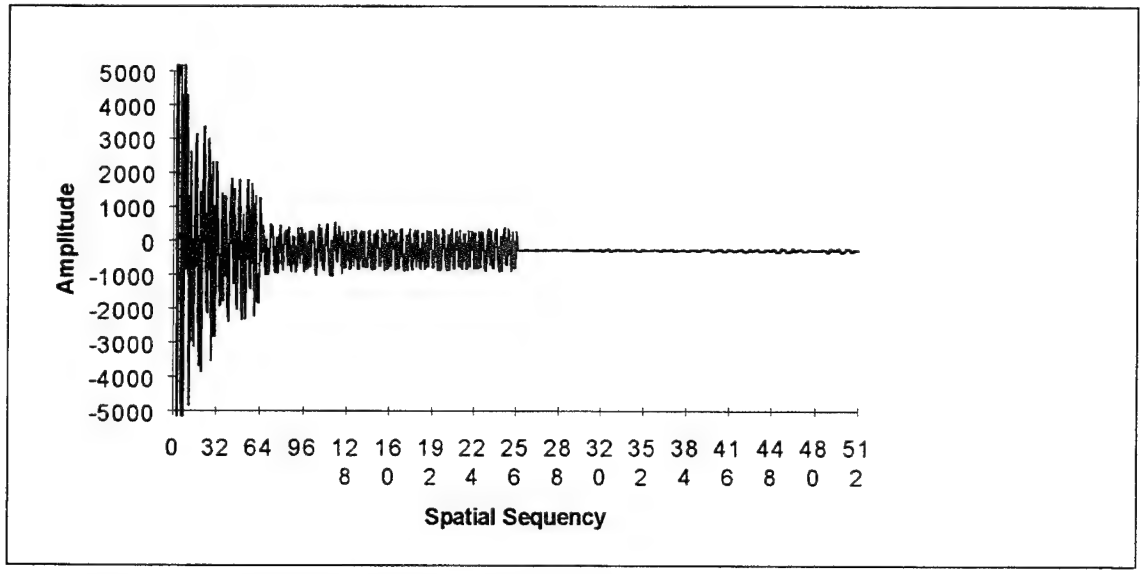

Fig. D-151. Walsh transform of Fig. D-150

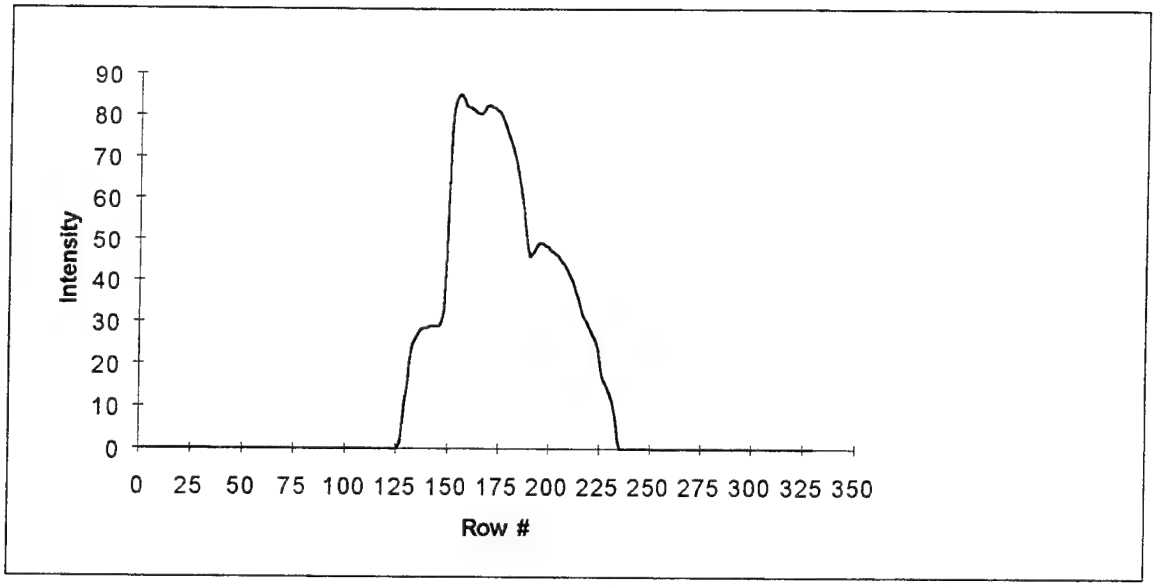

Fig. D-152. Complemented reflection of T10 squashed to preserve vertical sequencies

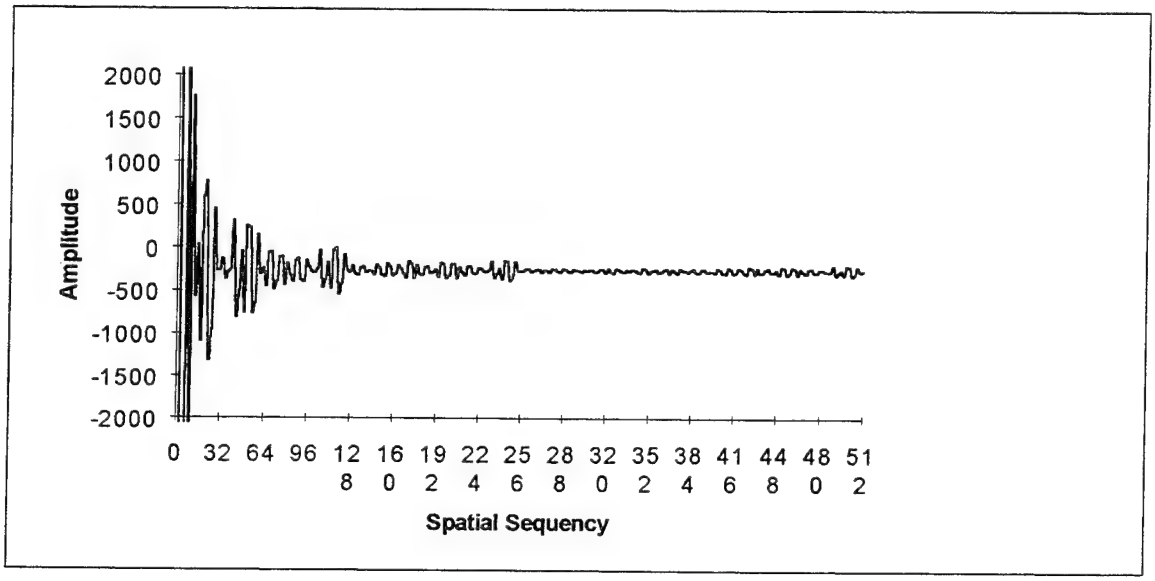

Fig. D-153. Walsh transform of Fig. D-152

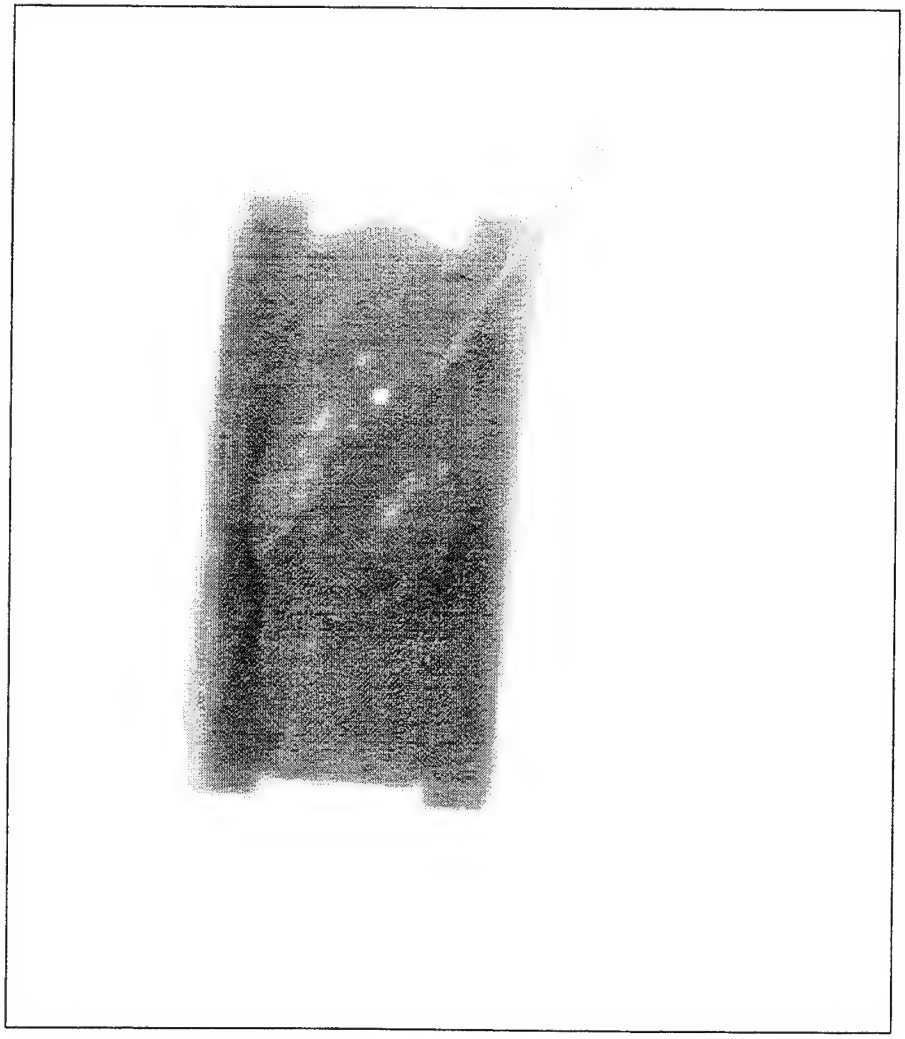

Fig. D-154. T11

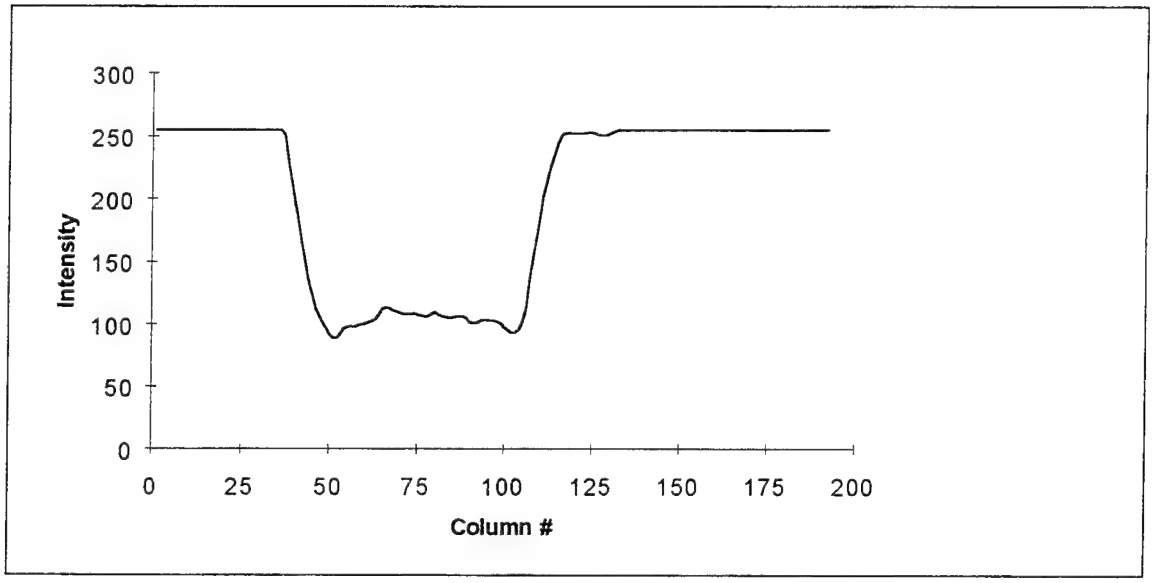

Fig. D-155. T11 squashed to preserve horizontal sequencies

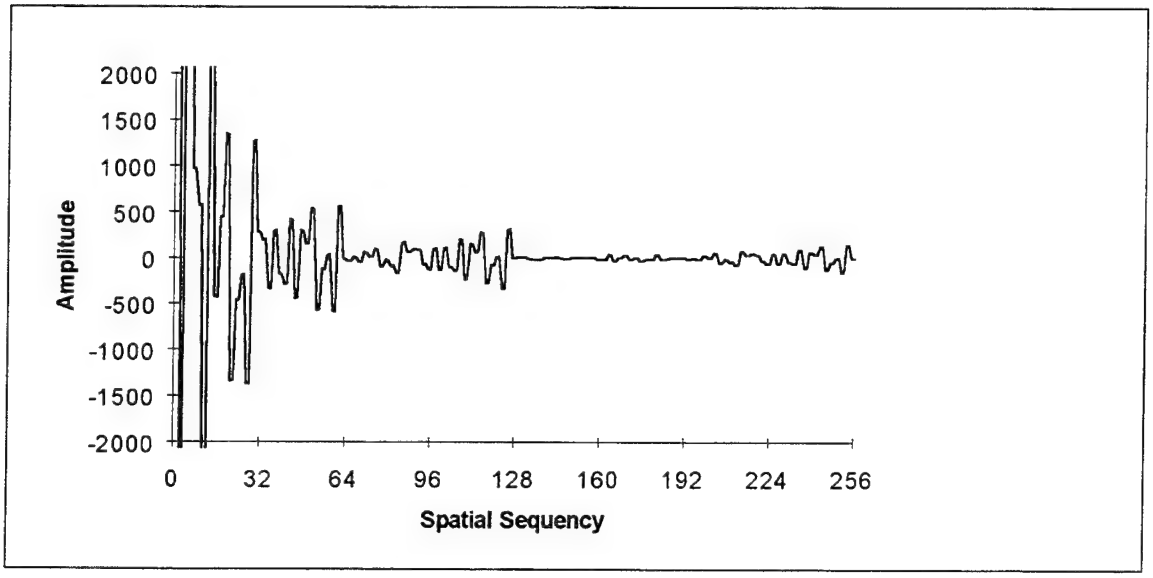

Fig. D-156. Walsh transform of Fig. D-155

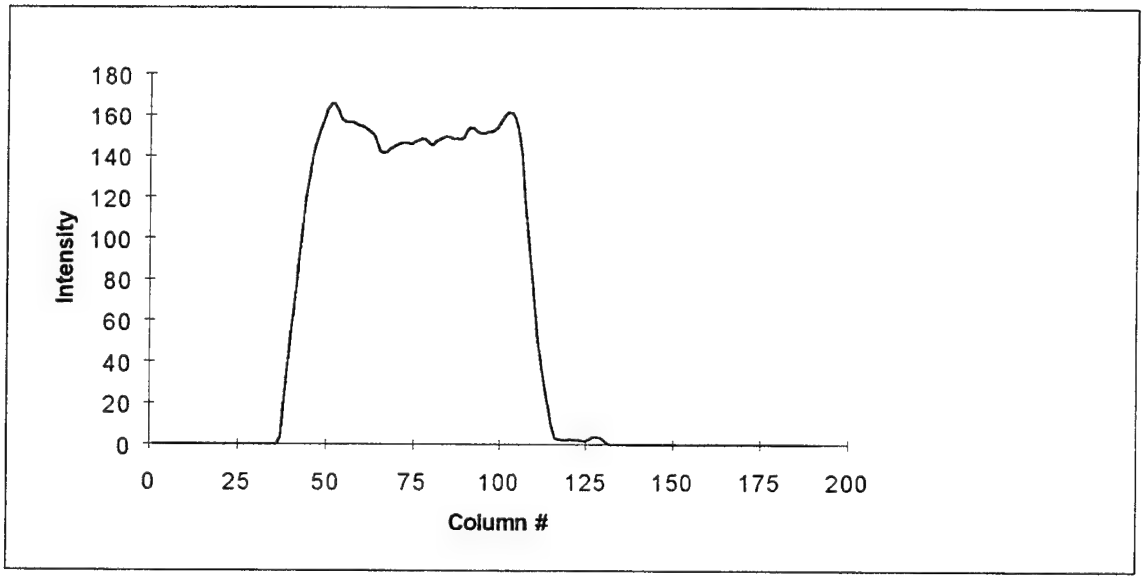

Fig. D-157. Complement of T11 squashed to preserve horizontal sequencies

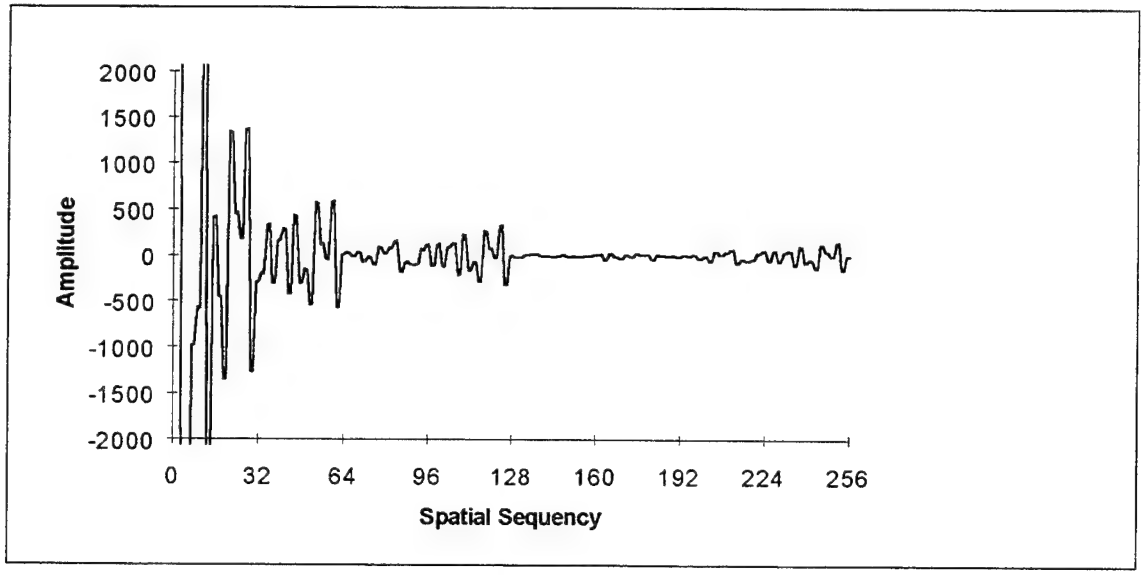

Fig. D-158. Walsh transform of Fig. D-157

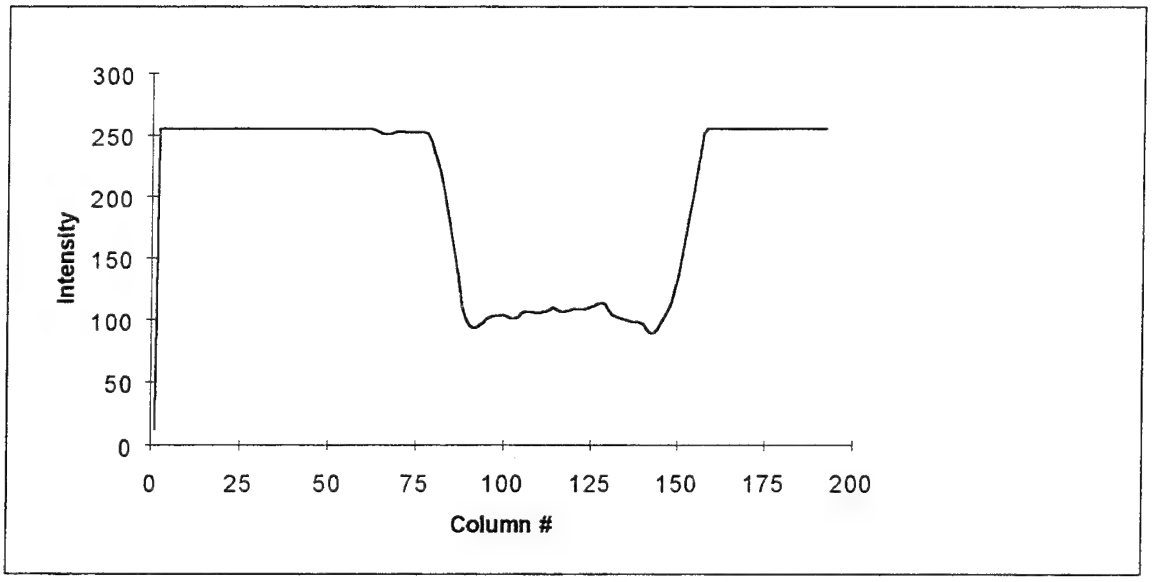

Fig. D-159. Reflection of T11 squashed to preserve horizontal sequencies

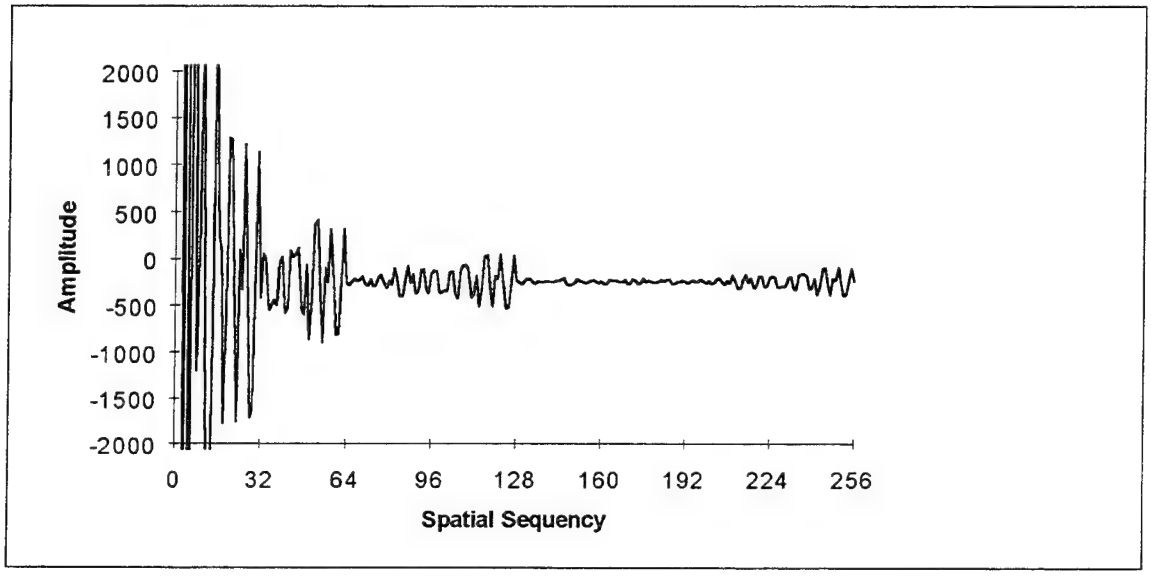

Fig. D-160. Walsh transform of Fig. D-159

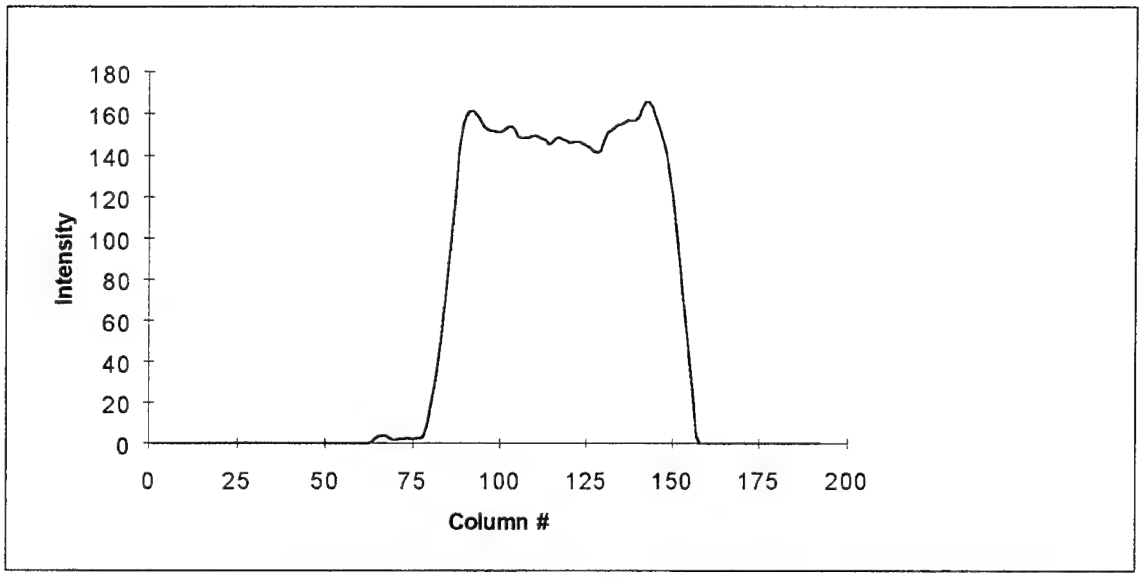

Fig. D-161. Complemented reflection of T11 squashed to preserve horizontal sequencies

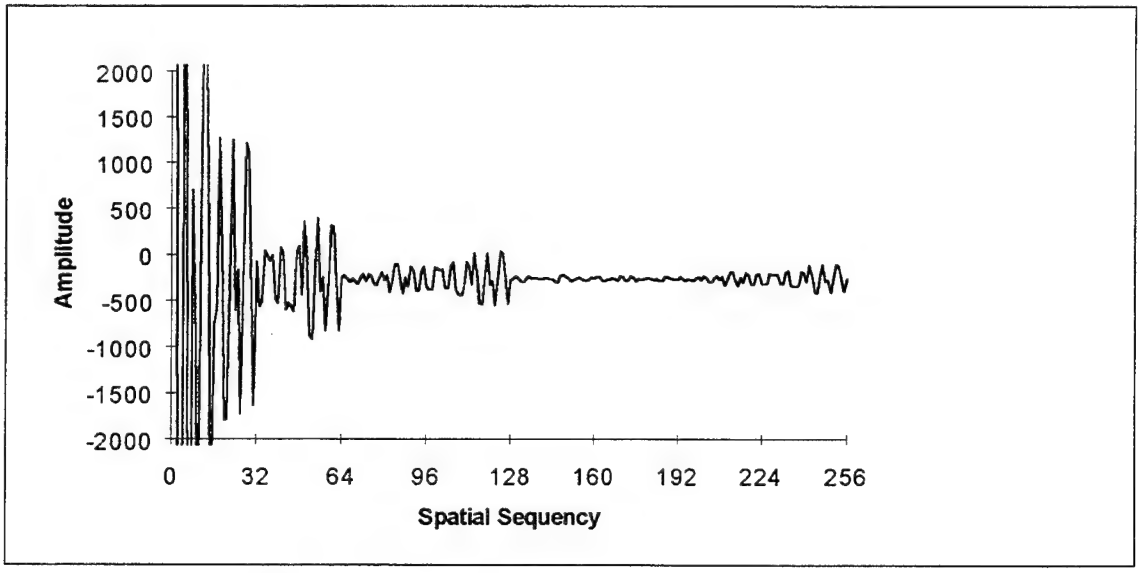

Fig. D-162. Walsh transform of Fig. D-161

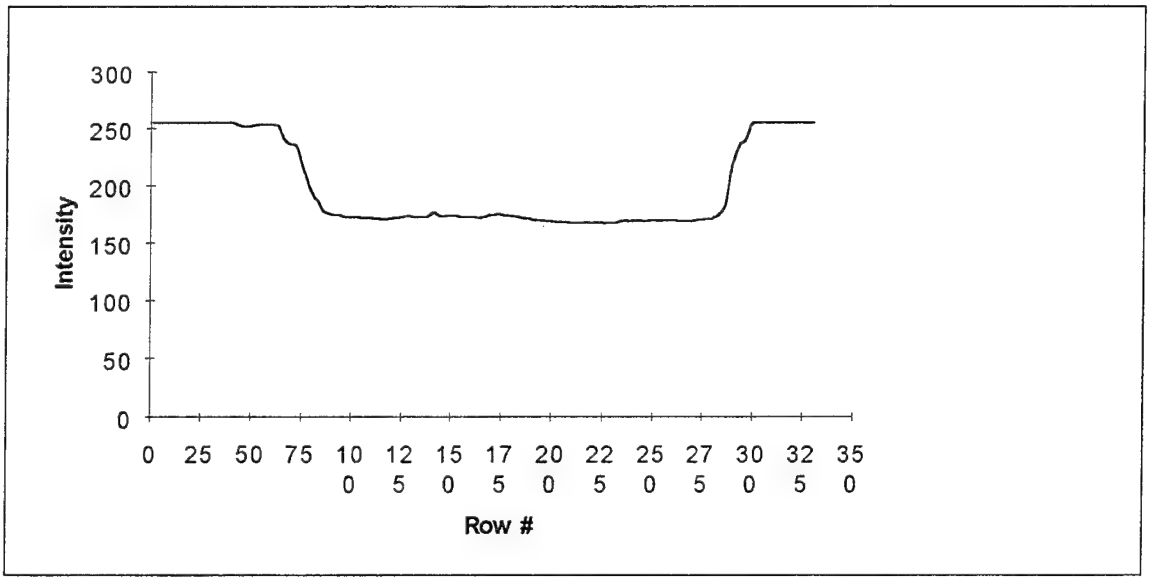

Fig. D-163. T11 squashed to preserve vertical sequencies

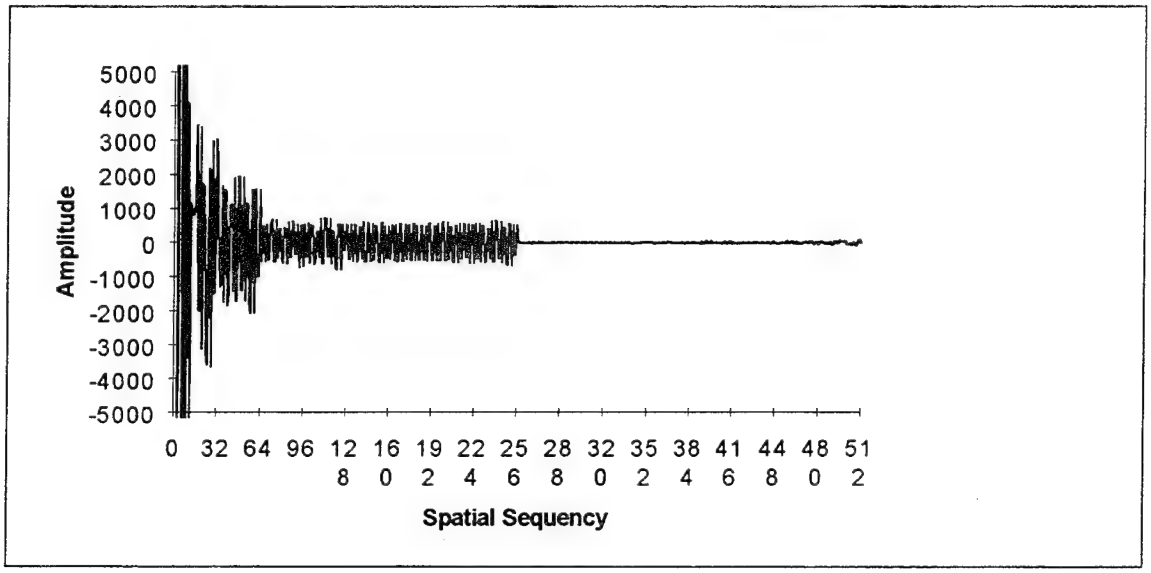

Fig. D-164. Walsh transform of Fig. D-163

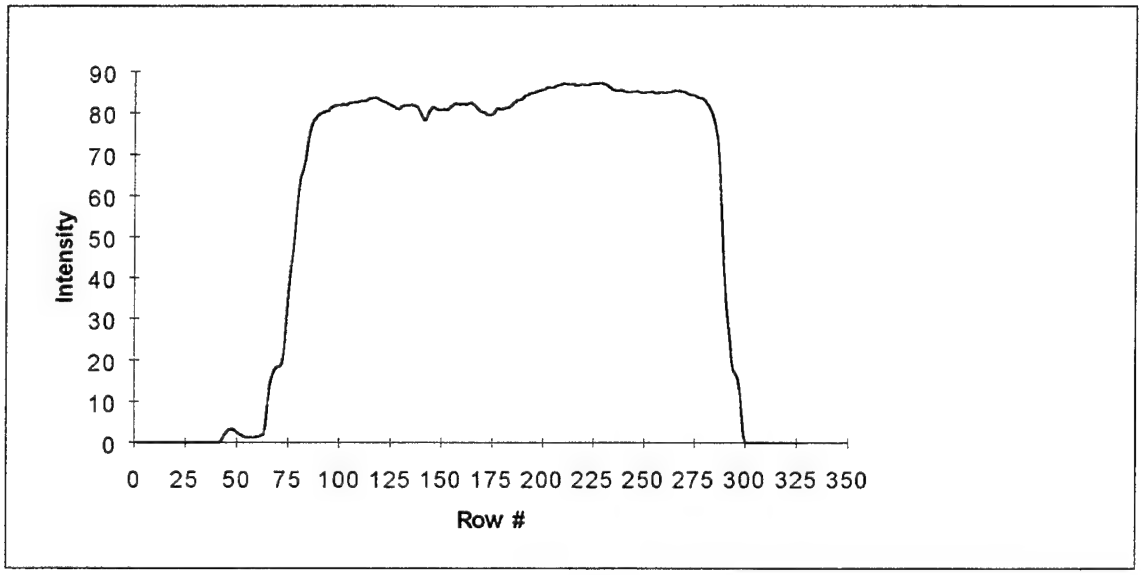

Fig. D-165. Complement of T11 squashed to preserve vertical sequencies

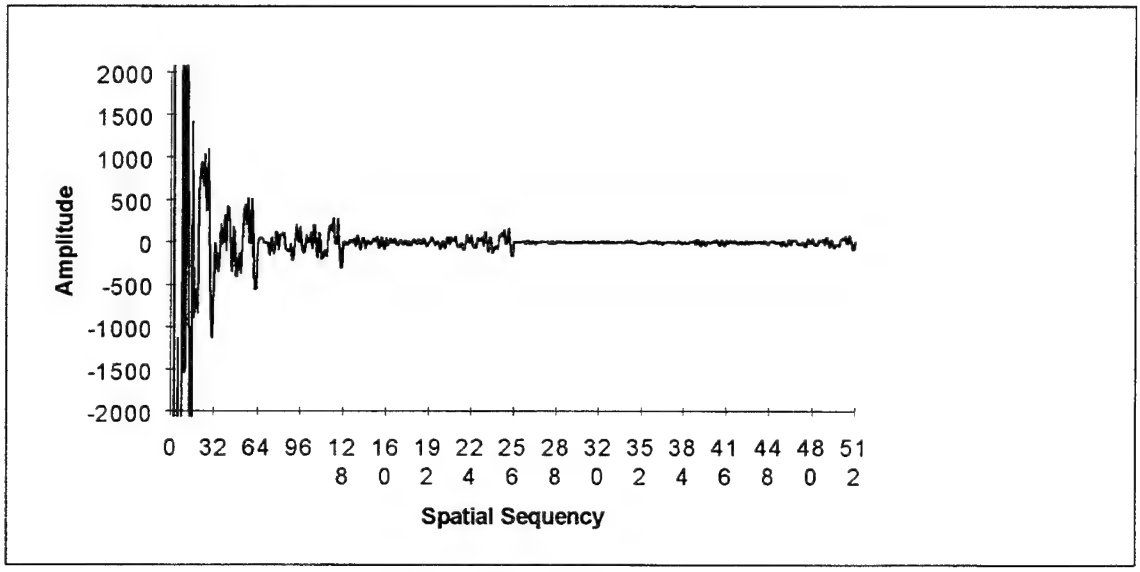

Fig. D-166. Walsh transform of Fig. D-165

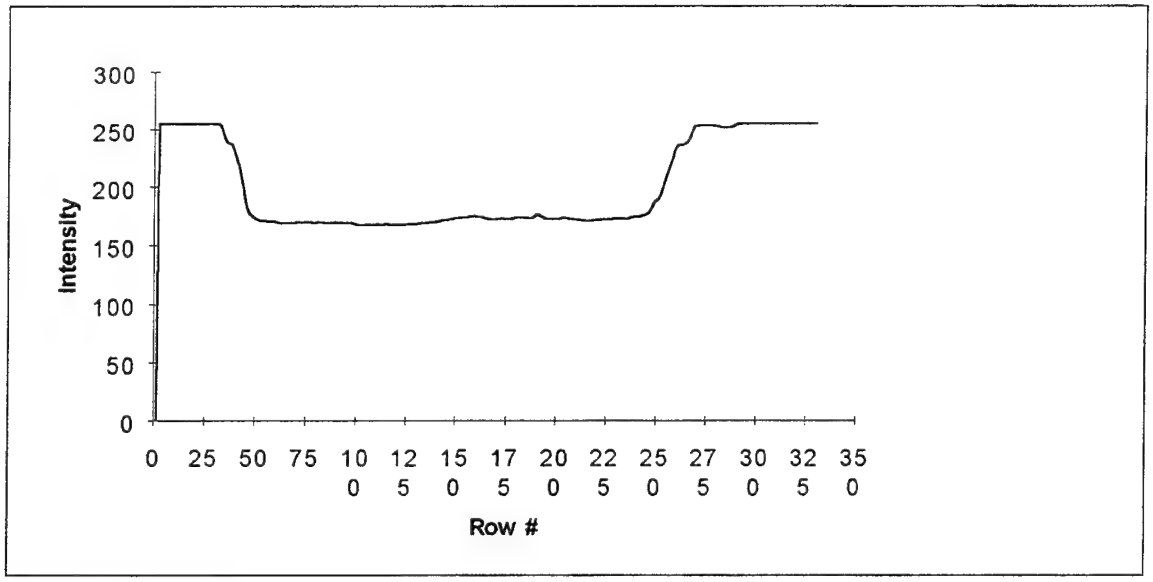

Fig. D-167. Reflection of T11 squashed to preserve vertical sequencies

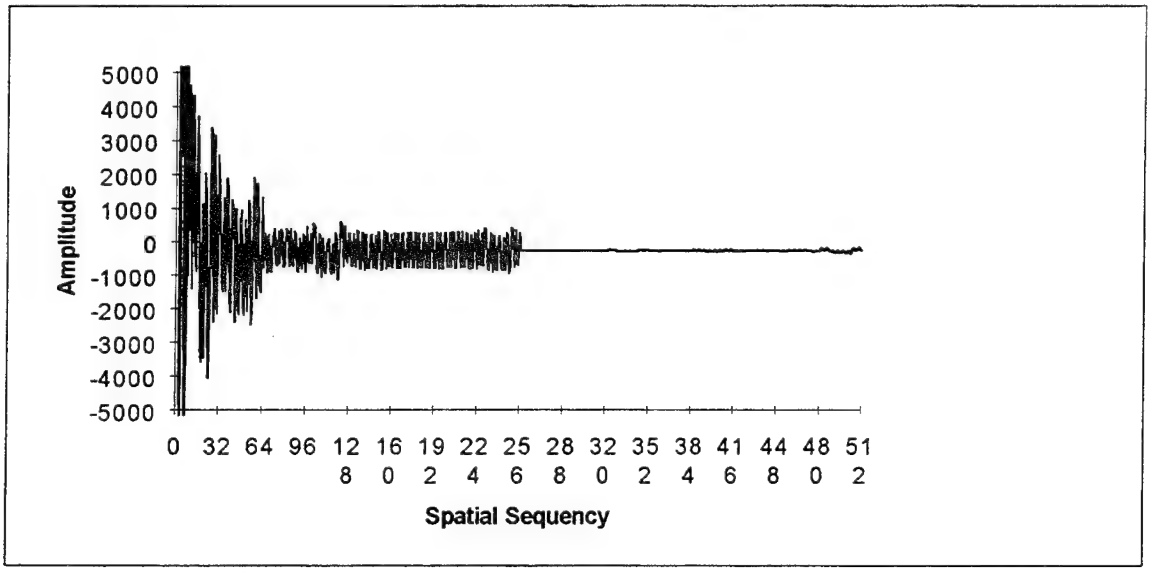

Fig. D-168. Walsh transform of Fig. D-167

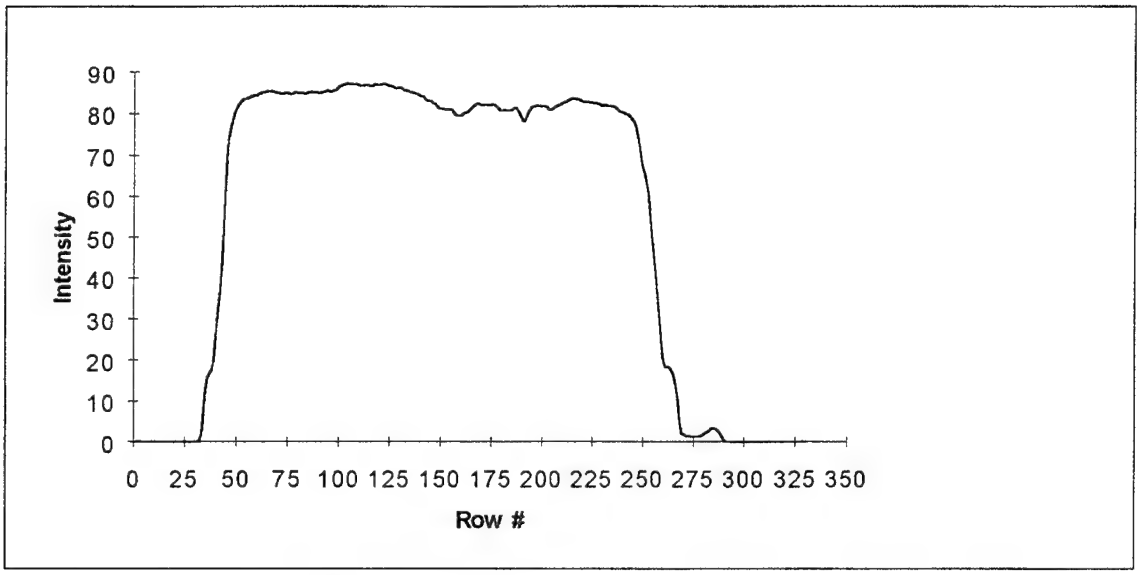

Fig. D-169. Complemented reflection of T11 squashed to preserve vertical sequencies

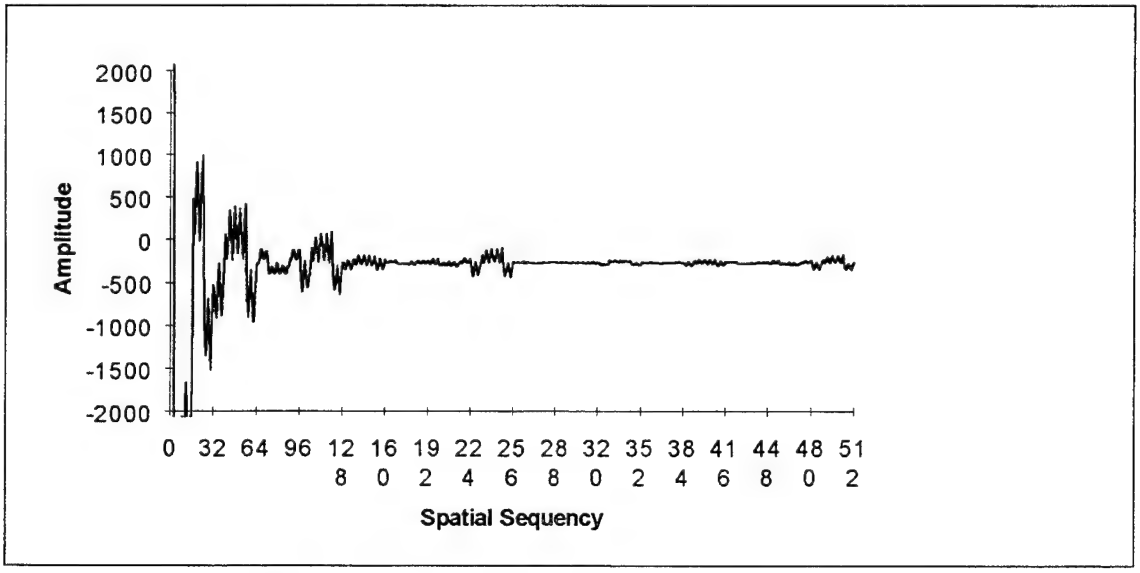

Fig. D-170. Walsh transform of Fig. D-169

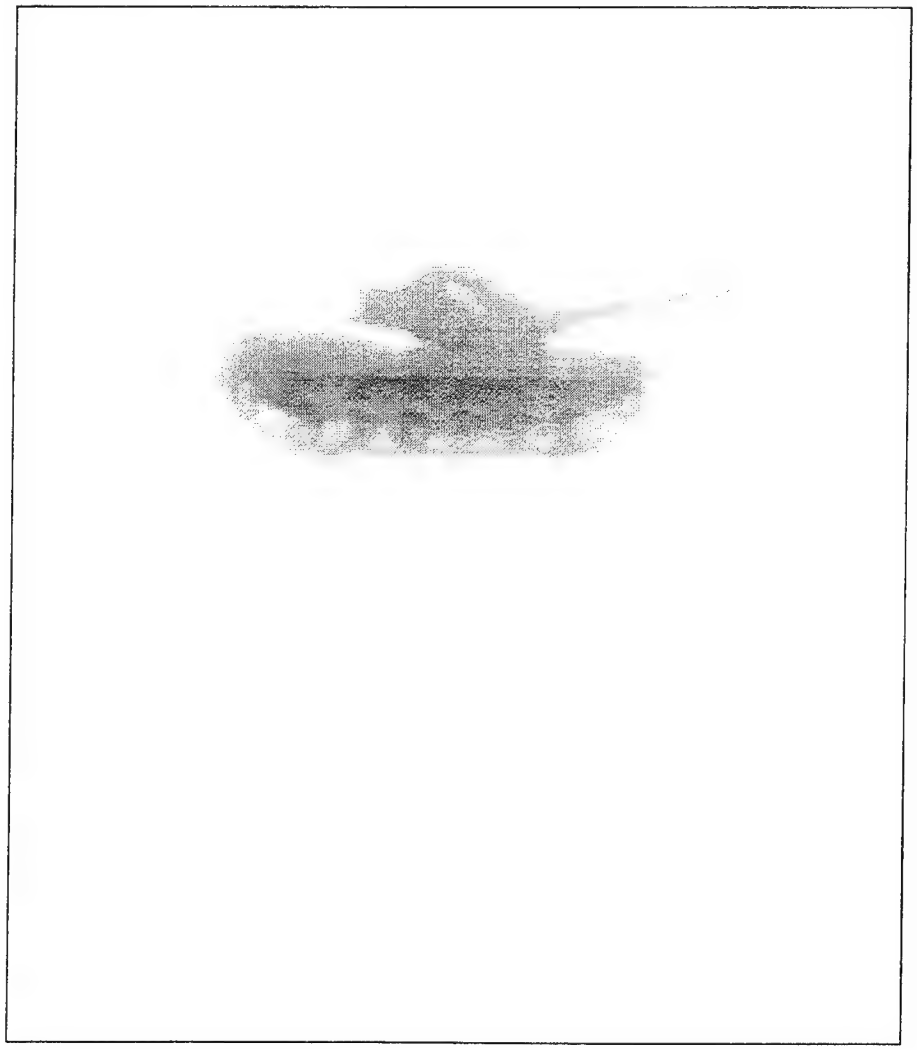

Fig. D-171. T13

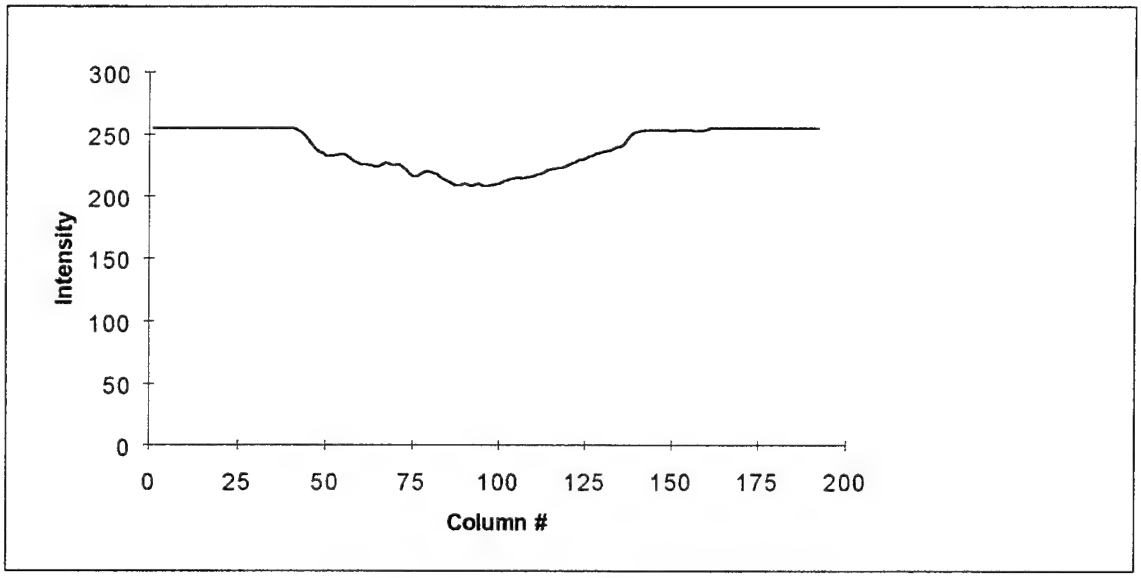

Fig. D-172. T13 squashed to preserve horizontal sequencies

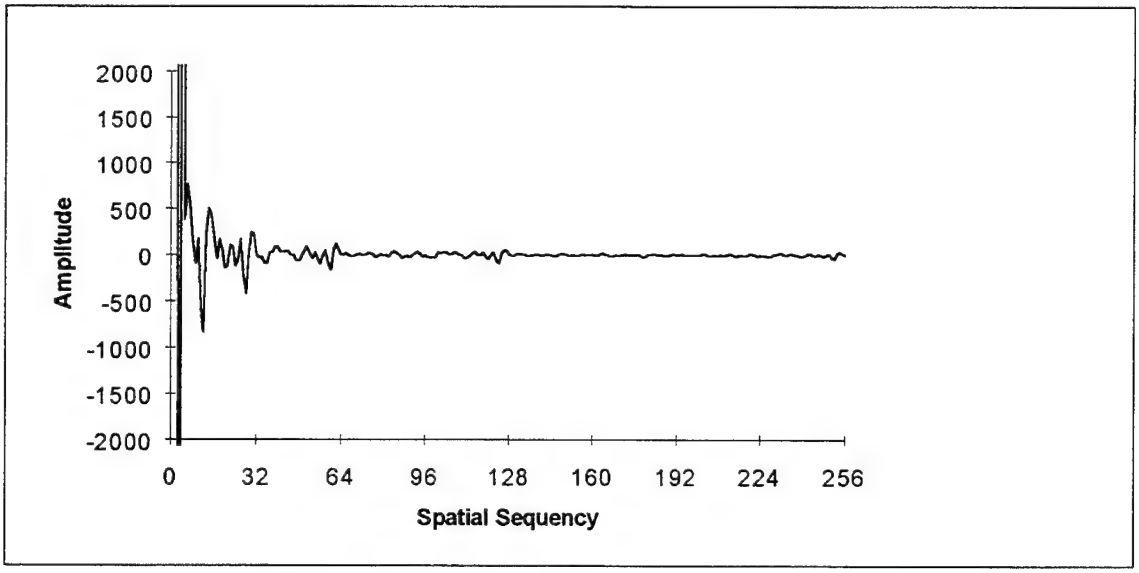

Fig. D-173. Walsh transform of Fig. D-172

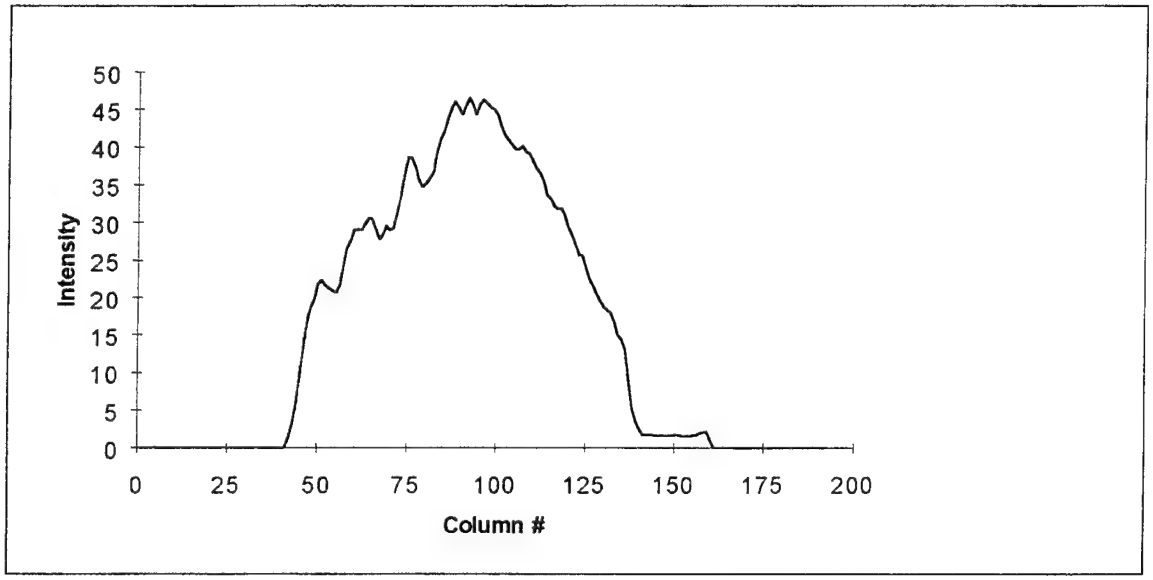

Fig. D-174. Complement of T13 squashed to preserve horizontal sequencies

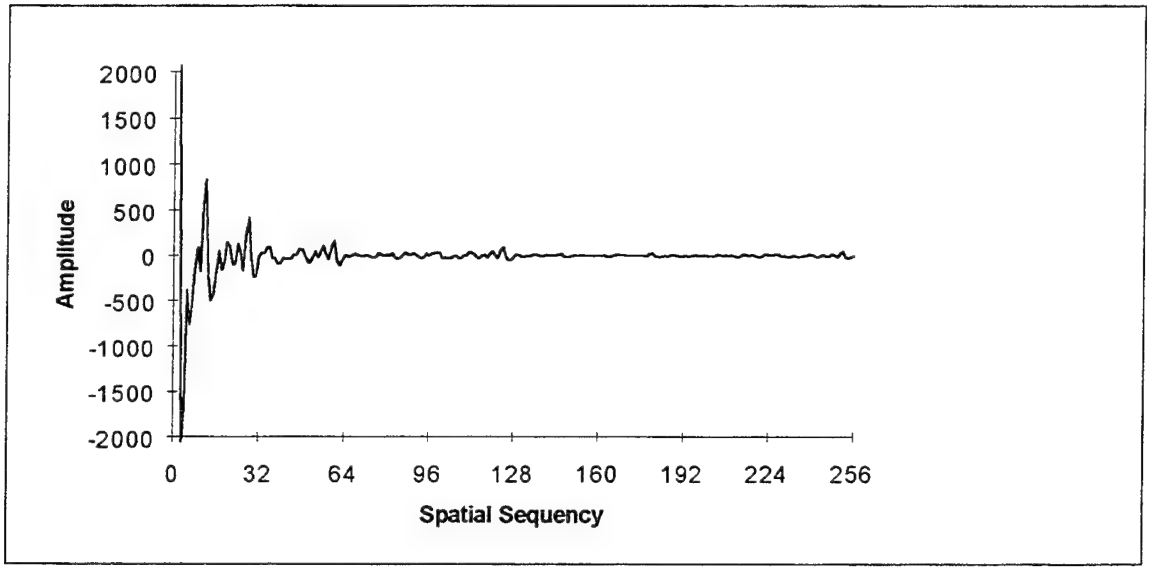

Fig. D-175. Walsh transform of Fig. D-174

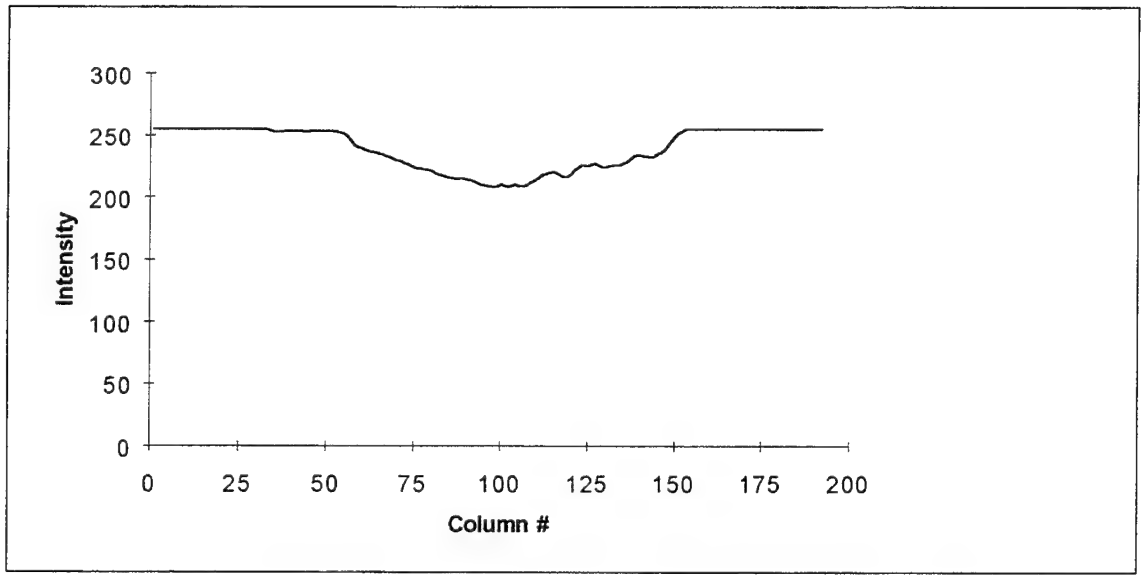

Fig. D-176. Reflection of T13 squashed to preserve horizontal sequencies

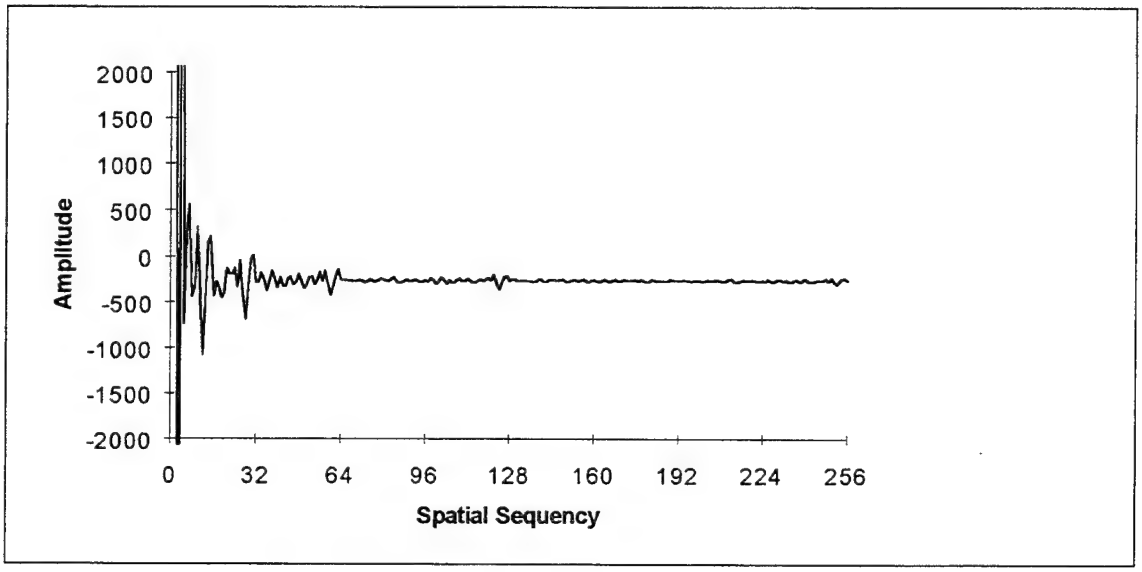

Fig. D-177. Walsh transform of Fig. D-176

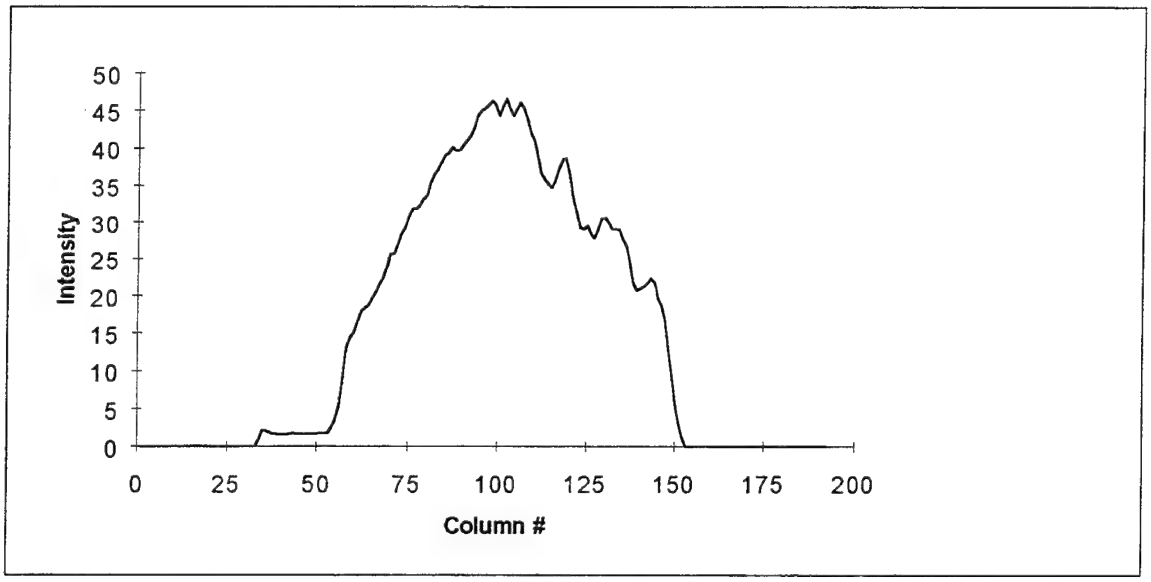

Fig. D-178. Complemented reflection of T13 squashed to preserve horizontal sequencies

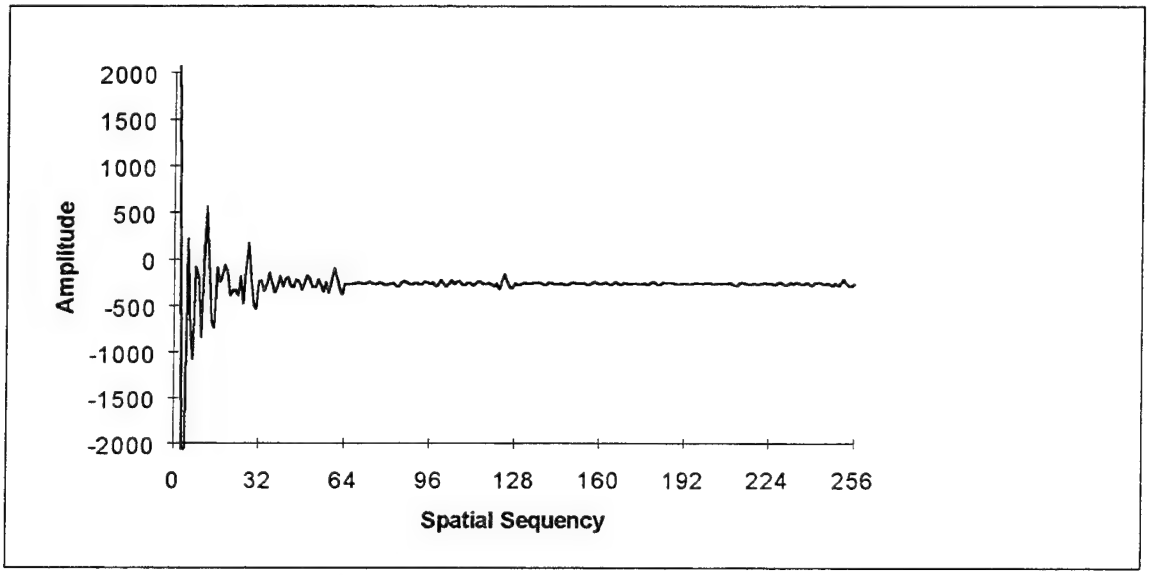

Fig. D-179. Walsh transform of Fig. D-178

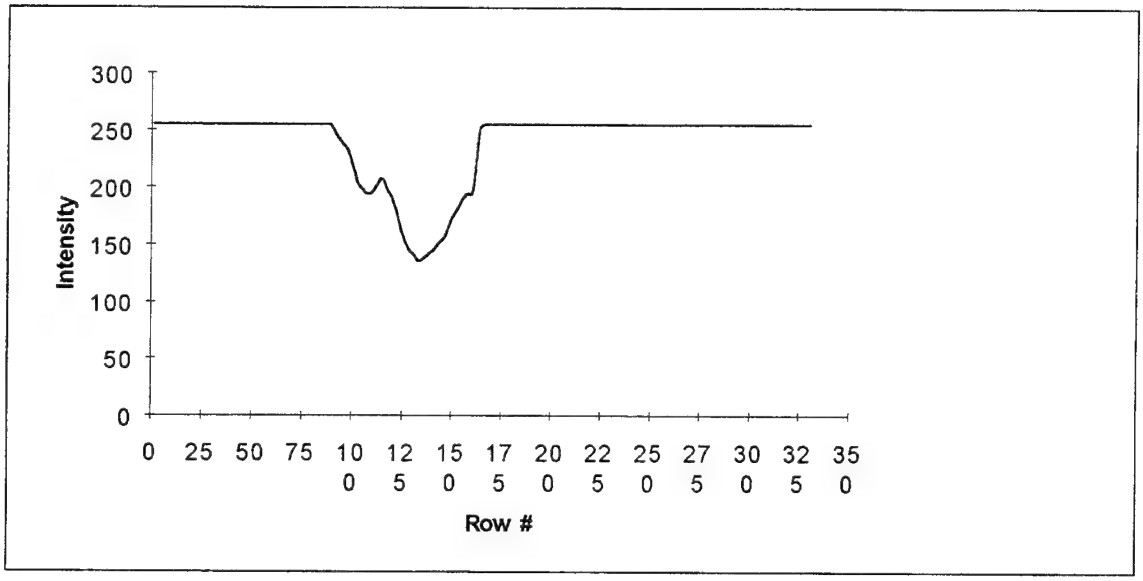

Fig. D-180. T13 squashed to preserve vertical sequencies

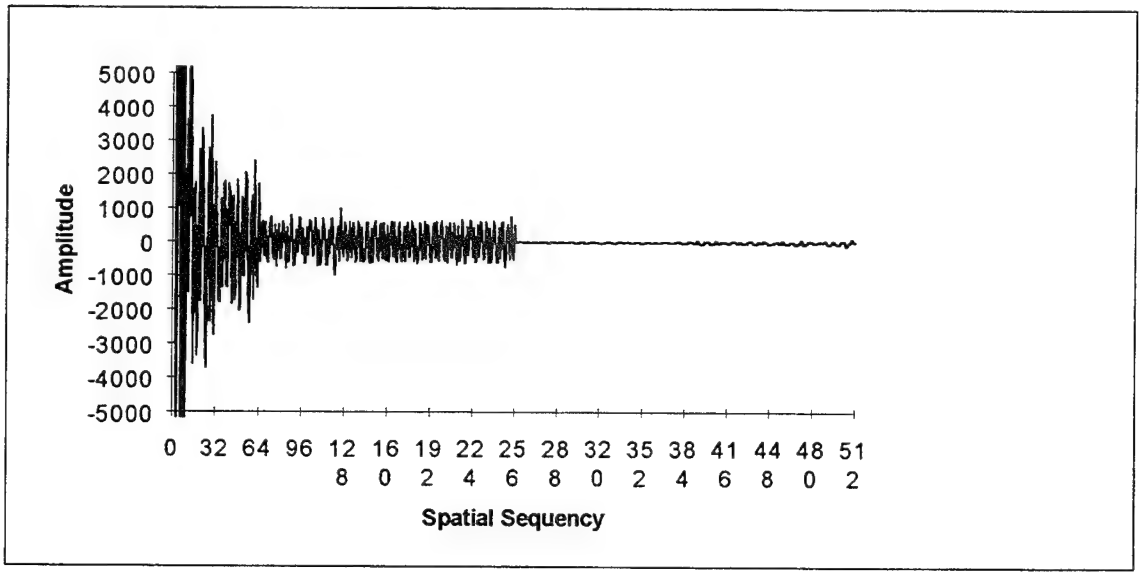

Fig. D-181. Walsh transform of Fig. D-180

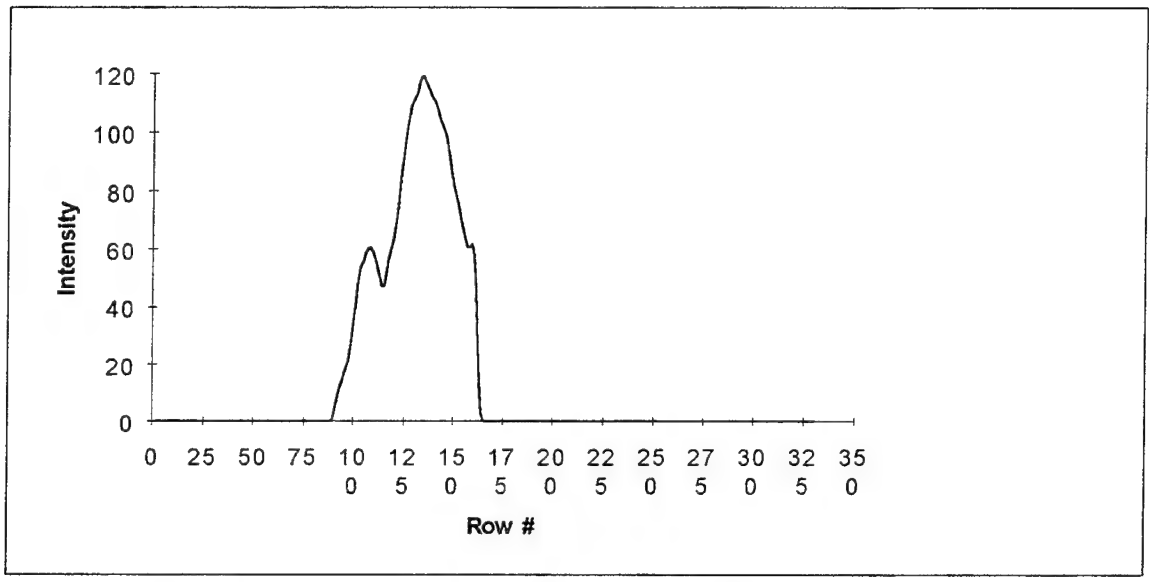

Fig. D-182. Complement of T13 squashed to preserve vertical sequencies

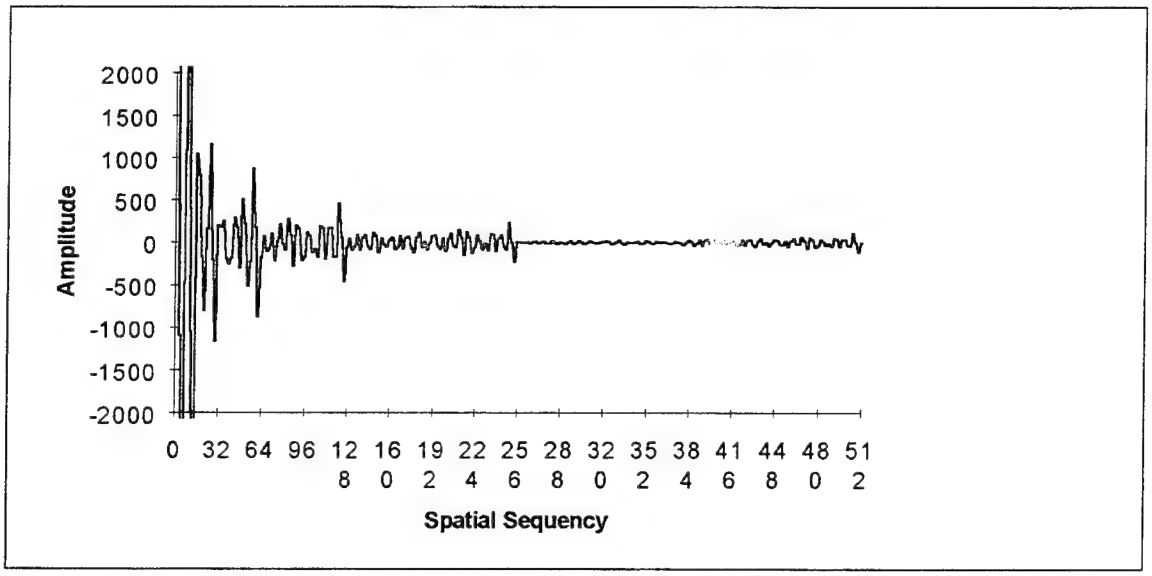

Fig. D-183. Walsh transform of Fig. D-182

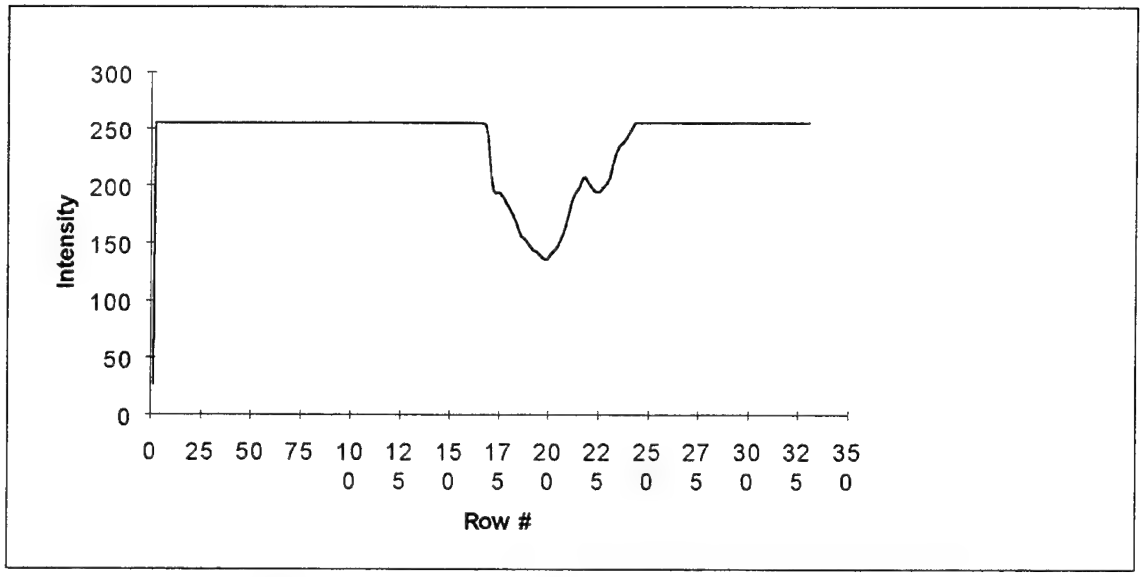

Fig. D-184. Reflection of T13 squashed to preserve vertical sequencies

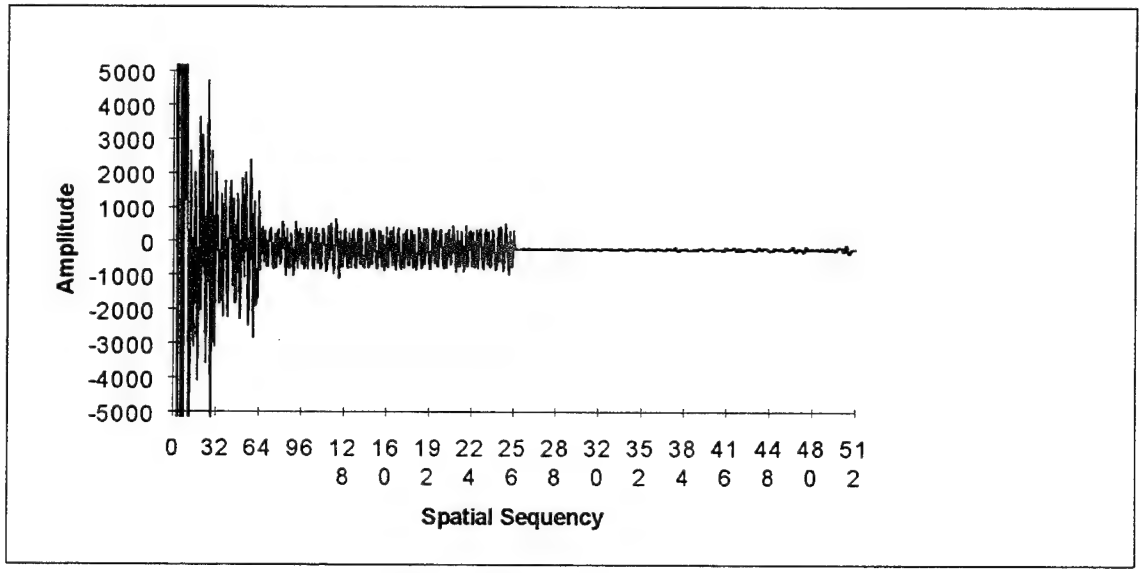

Fig. D-185. Walsh transform of Fig. D-184

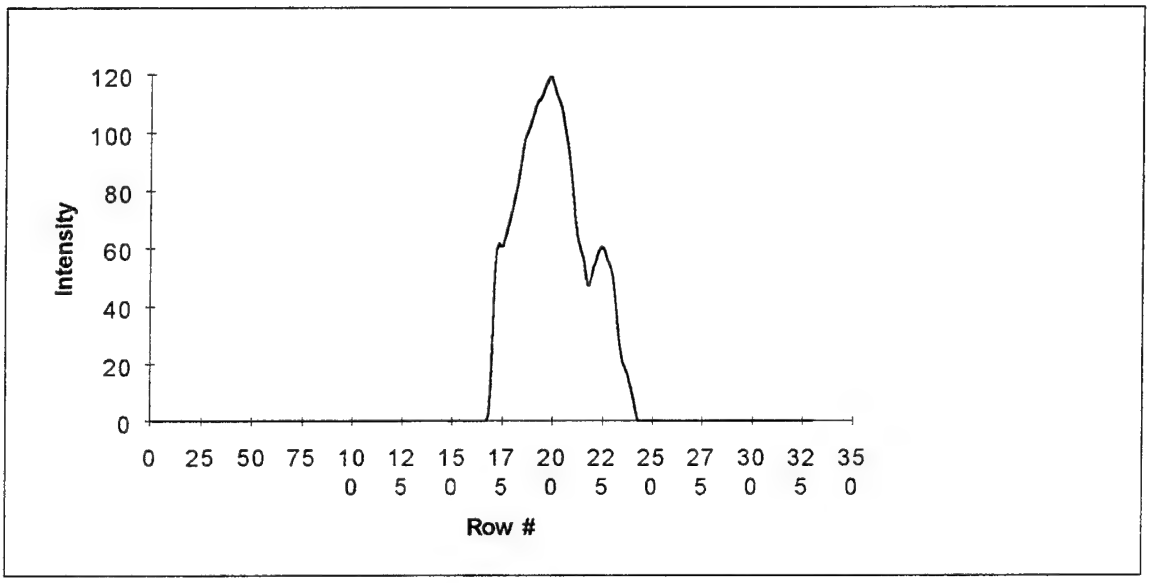

Fig. D-186. Complemented reflection of T13 squashed to preserve vertical sequencies

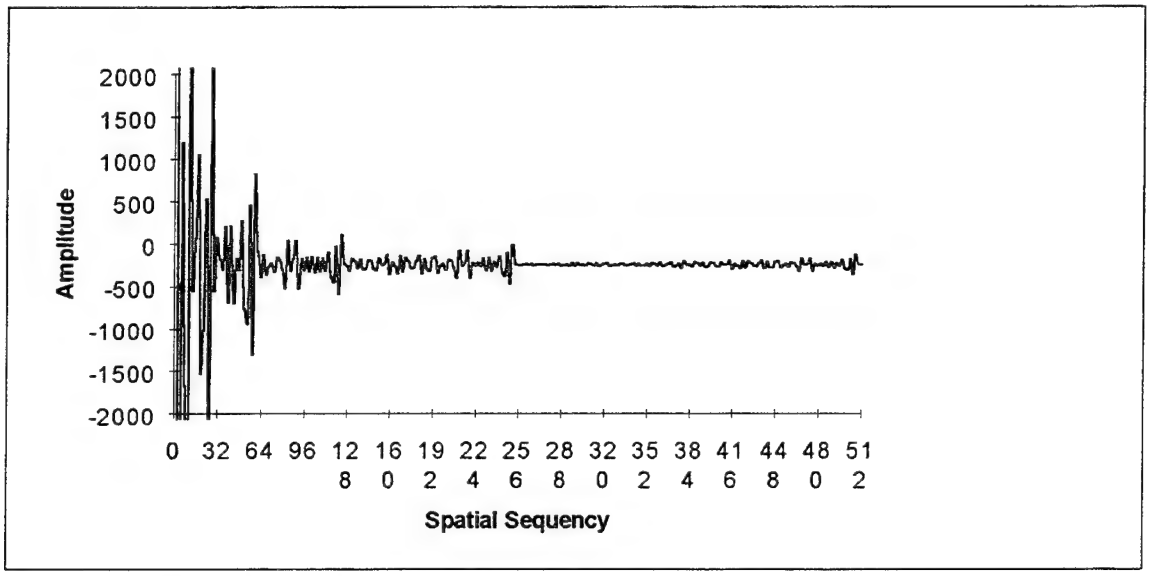

Fig. D-187. Walsh transform of Fig. D-186

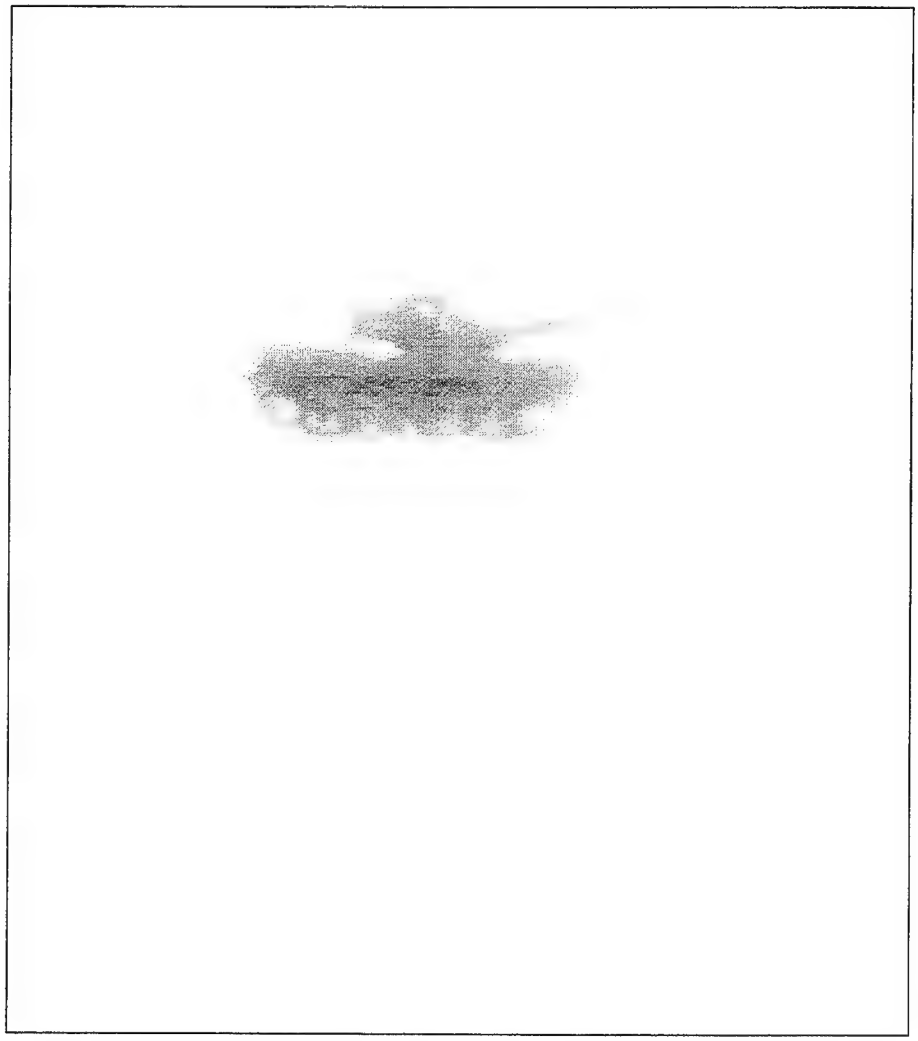

Fig. D-188. T14

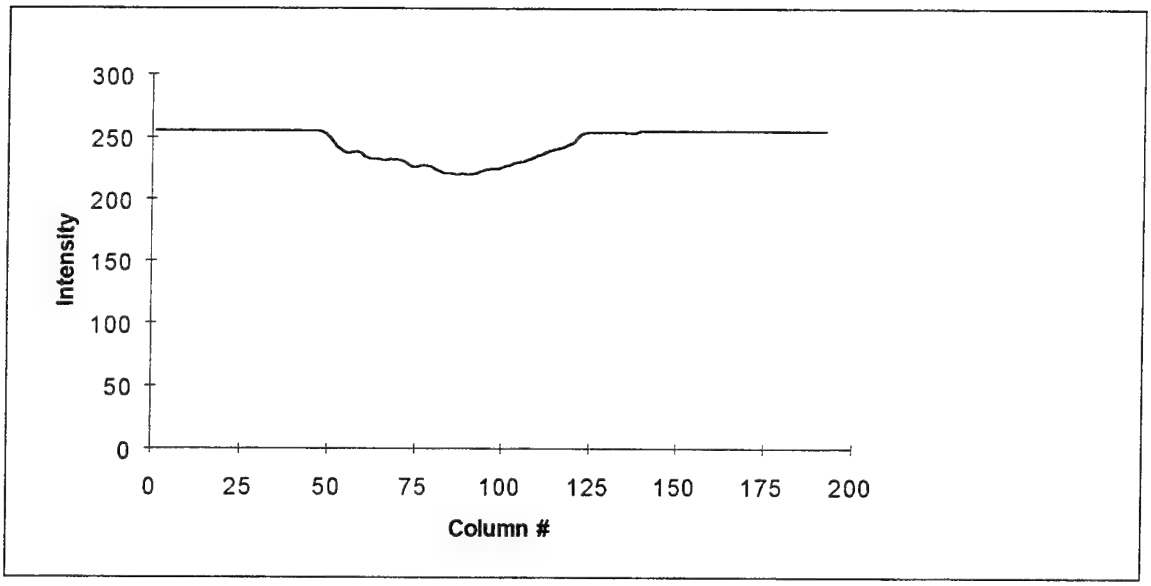

Fig. D-189. T14 squashed to preserve horizontal sequencies

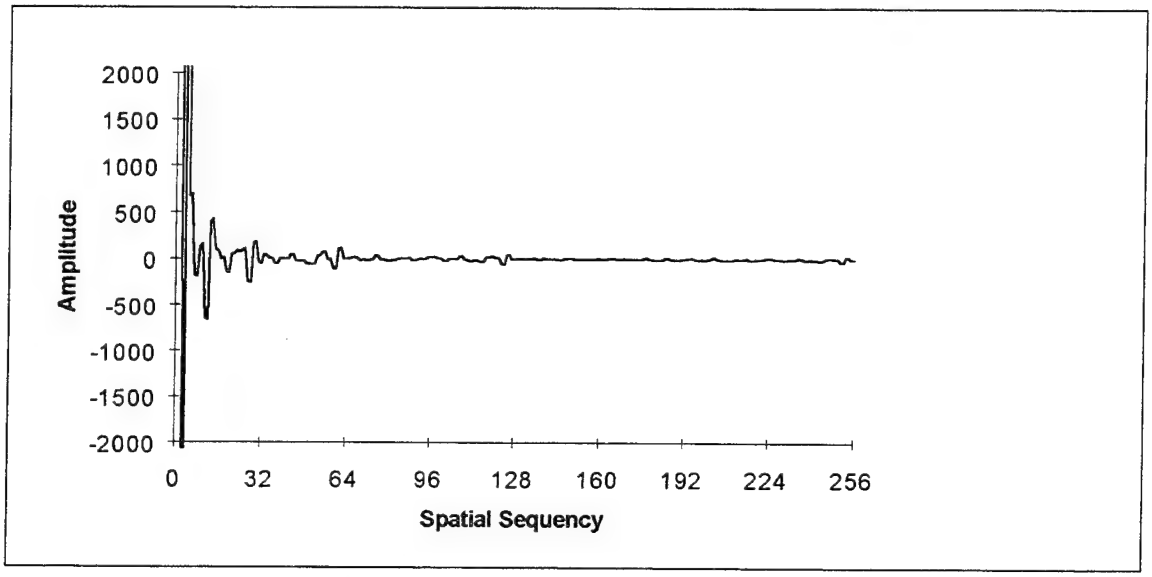

Fig. D-190. Walsh transform of Fig. D-189

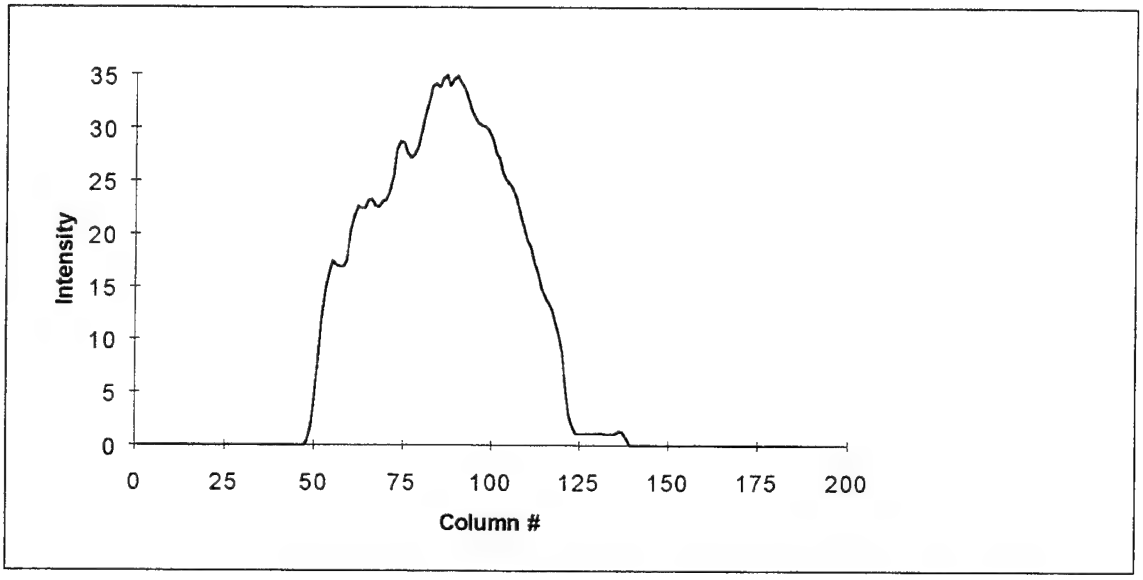

Fig. D-191. Complement of T14 squashed to preserve horizontal sequencies

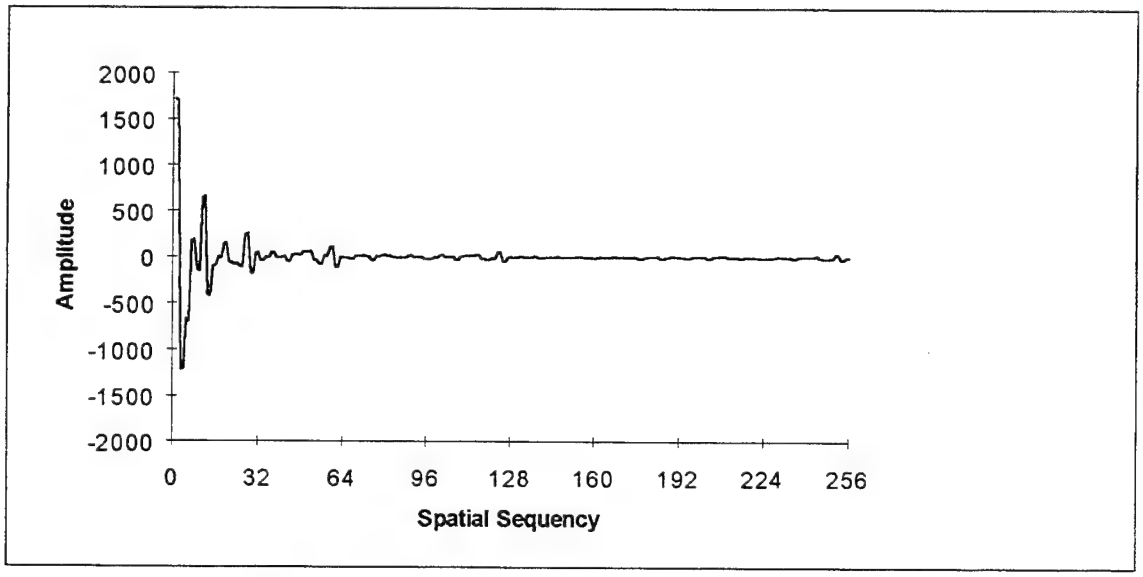

Fig. D-192. Walsh transform of Fig. D-191

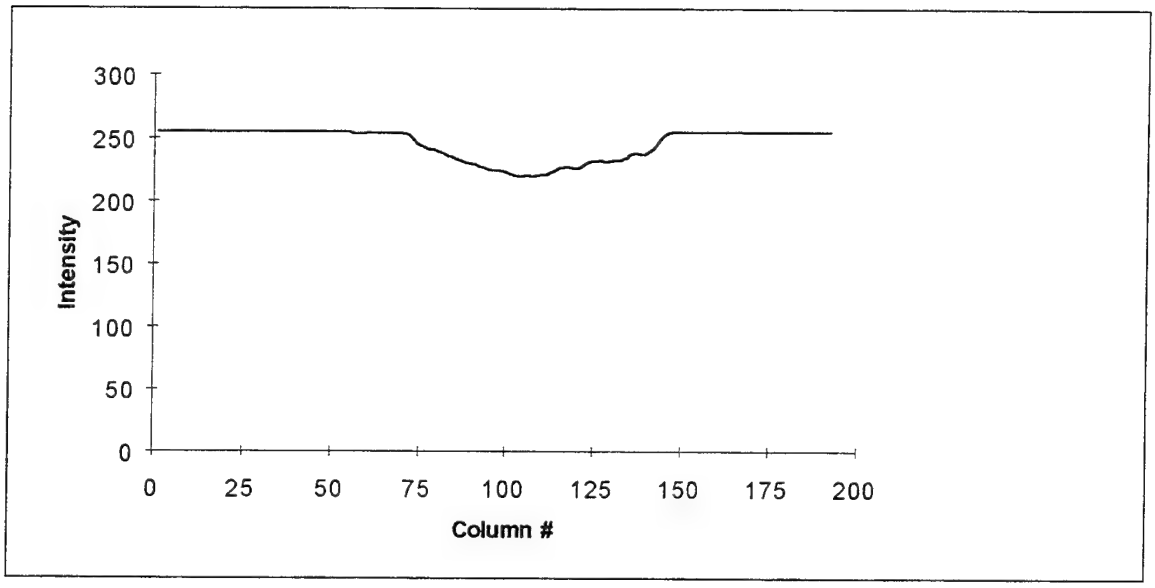

Fig. D-193. Reflection of T14 squashed to preserve horizontal sequencies

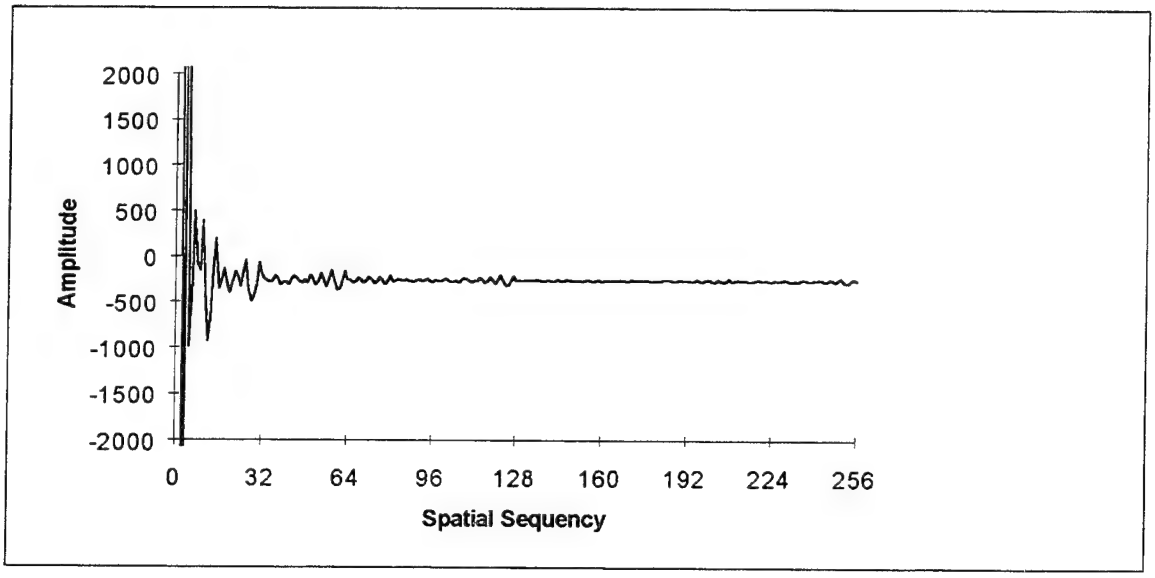

Fig. D-194. Walsh transform of Fig. D-193

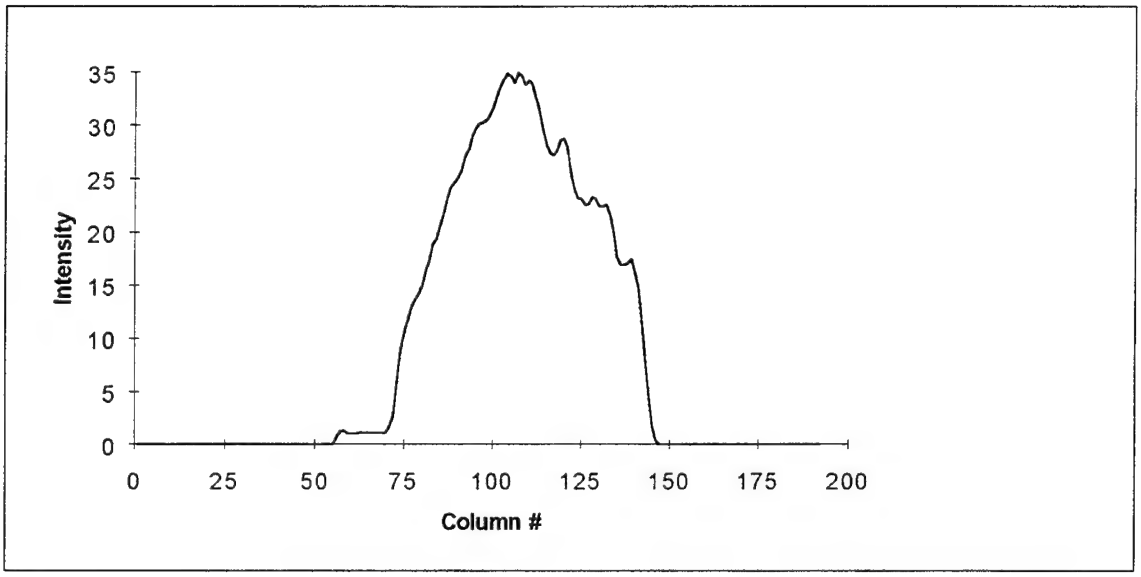

Fig. D-195. Complemented reflection of T14 squashed to preserve horizontal sequencies

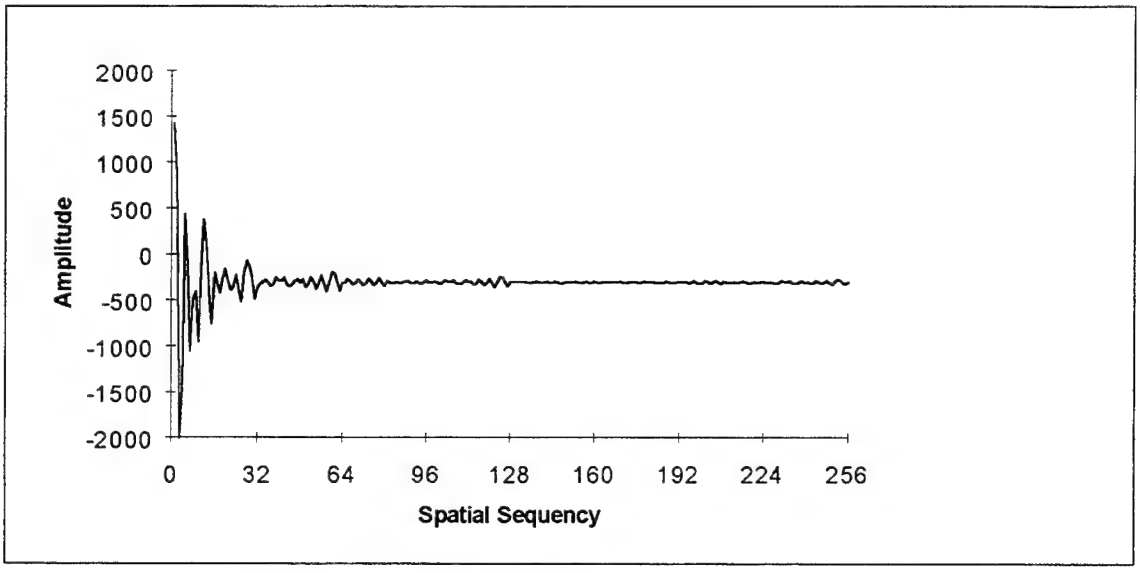

Fig. D-196. Walsh transform of Fig. D-195

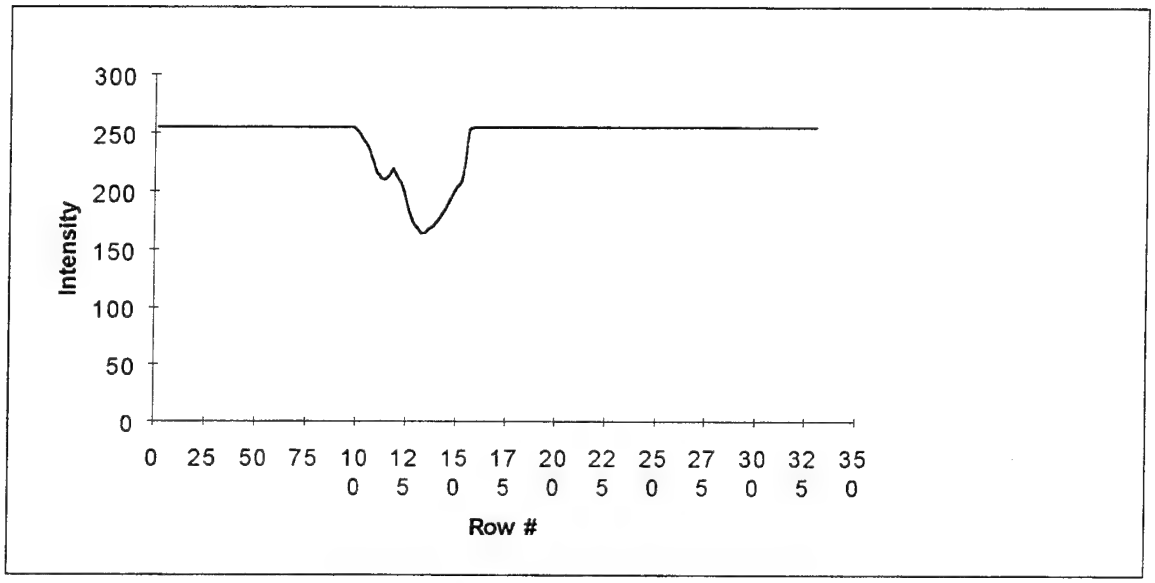

Fig. D-197. T14 squashed to preserve vertical sequencies

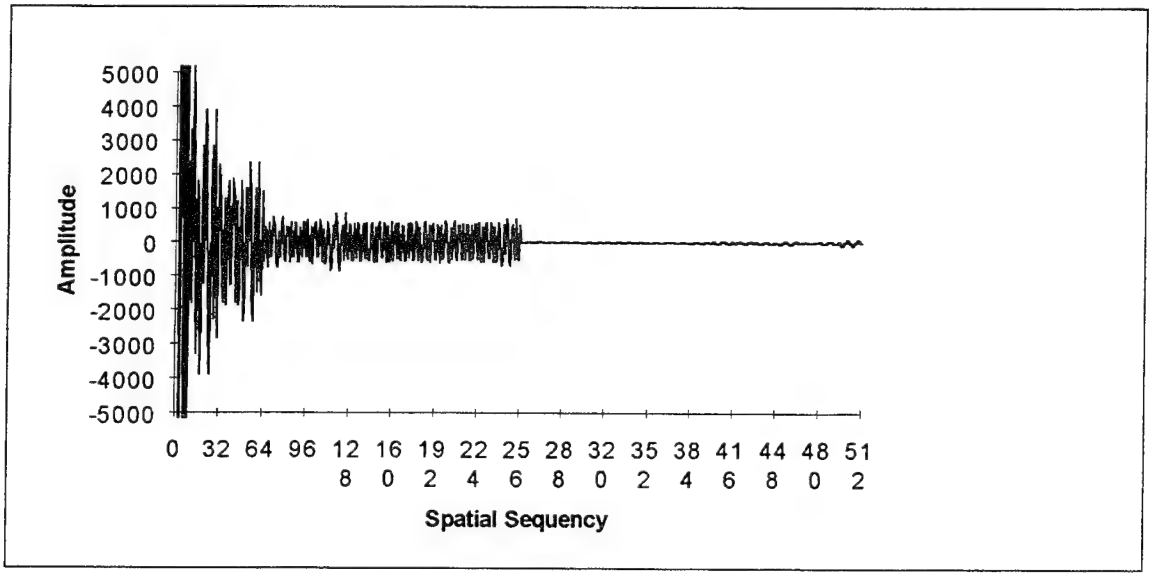

Fig. D-198. Walsh transform of Fig. D-197

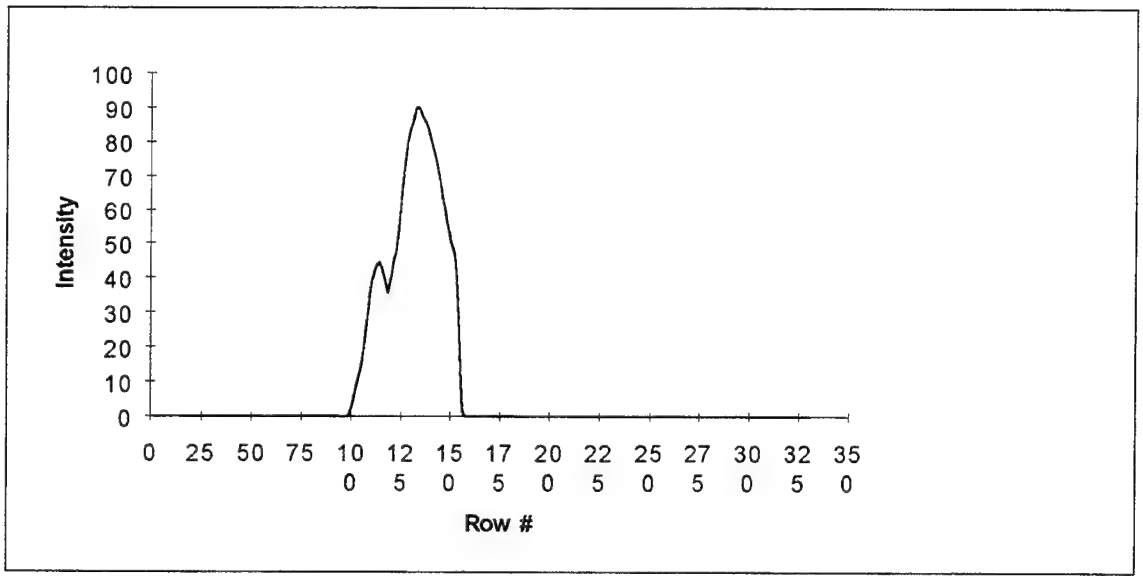

Fig. D-199. Complement of T14 squashed to preserve vertical sequencies

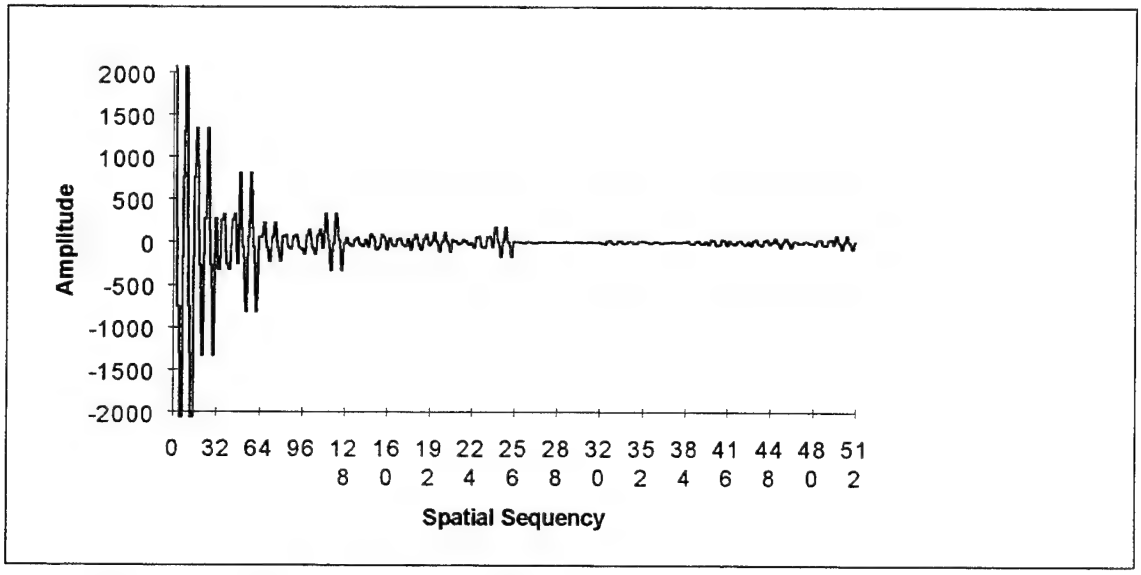

Fig. D-200. Walsh transform of Fig. D-199

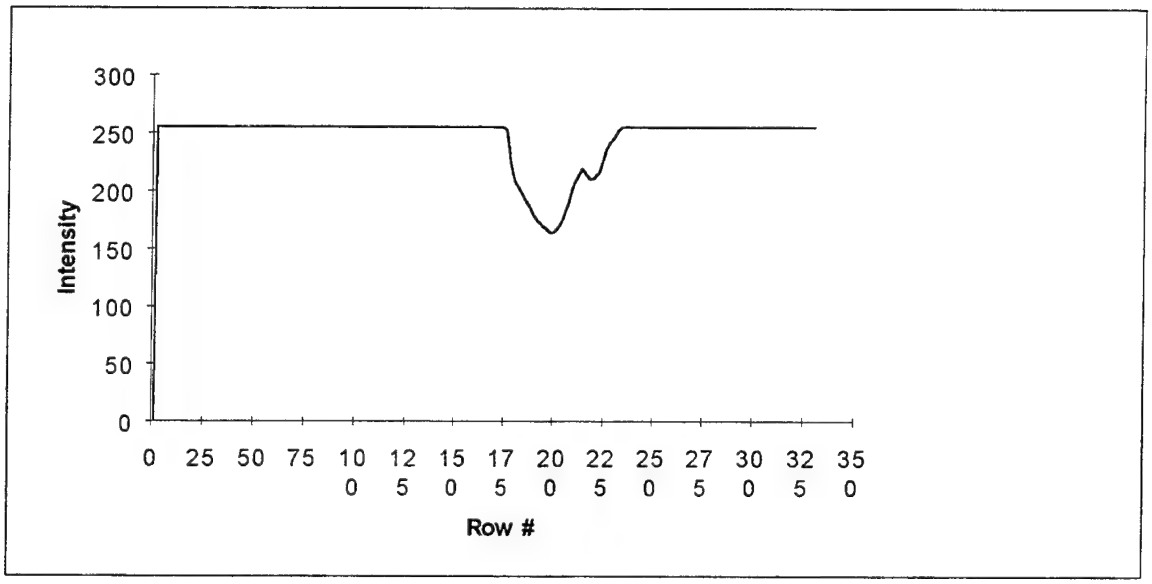

Fig. D-201. Reflection of T14 squashed to preserve vertical sequencies

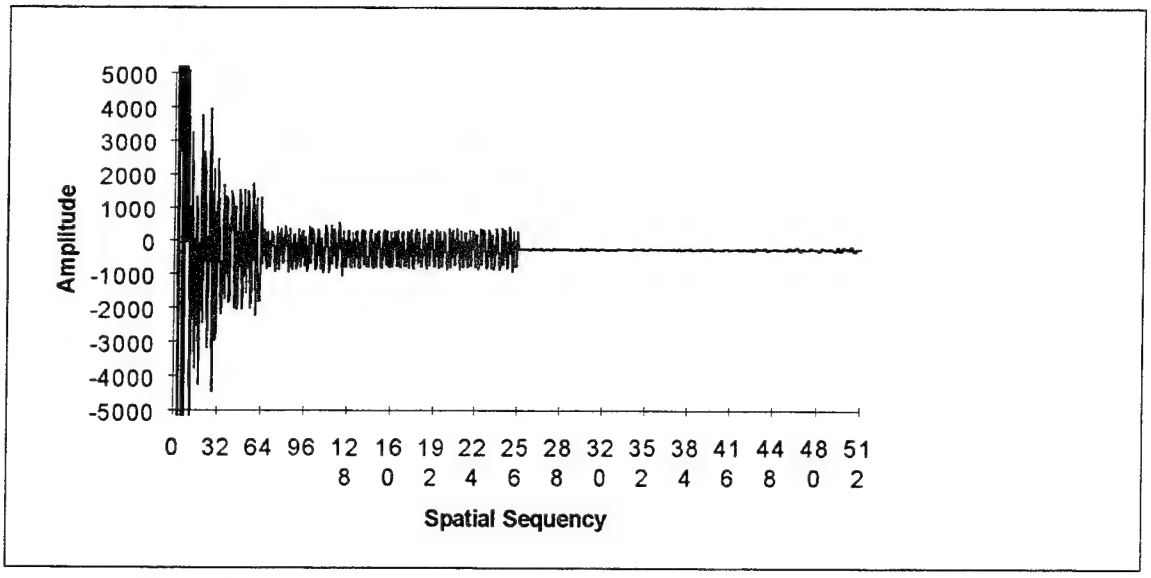

Fig. D-202. Walsh transform of Fig. D-201

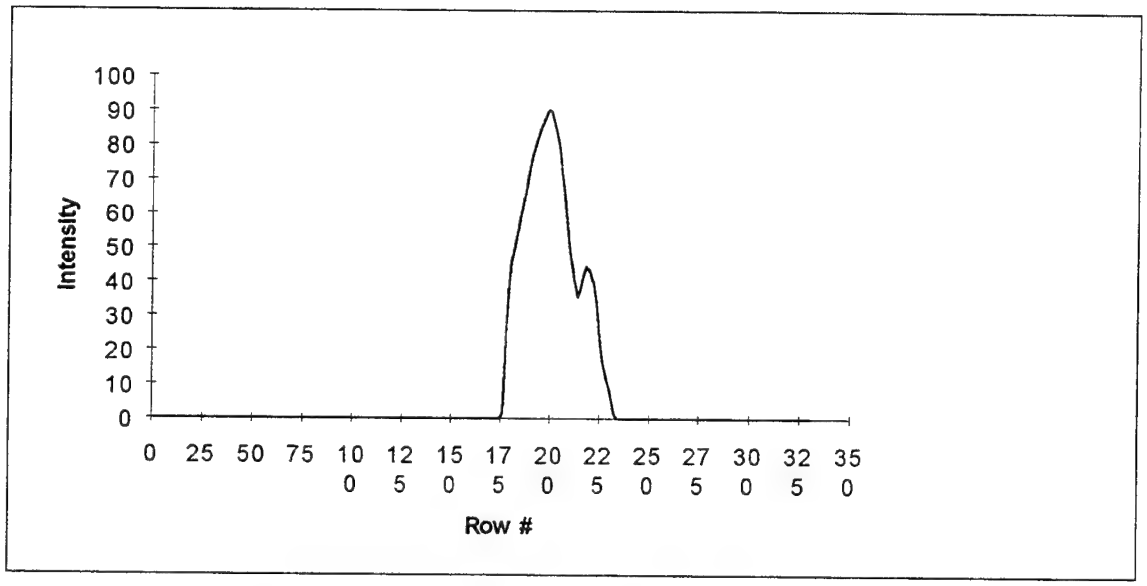

Fig. D-203. Complemented reflection of T14 squashed to preserve vertical sequencies

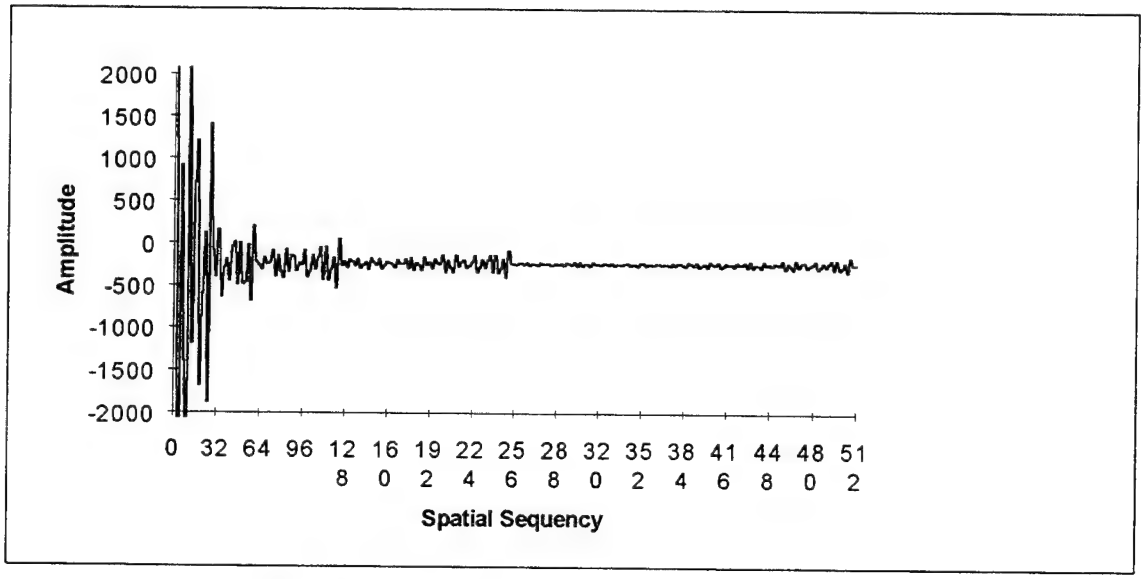

Fig. D-204. Walsh transform of Fig. D-203

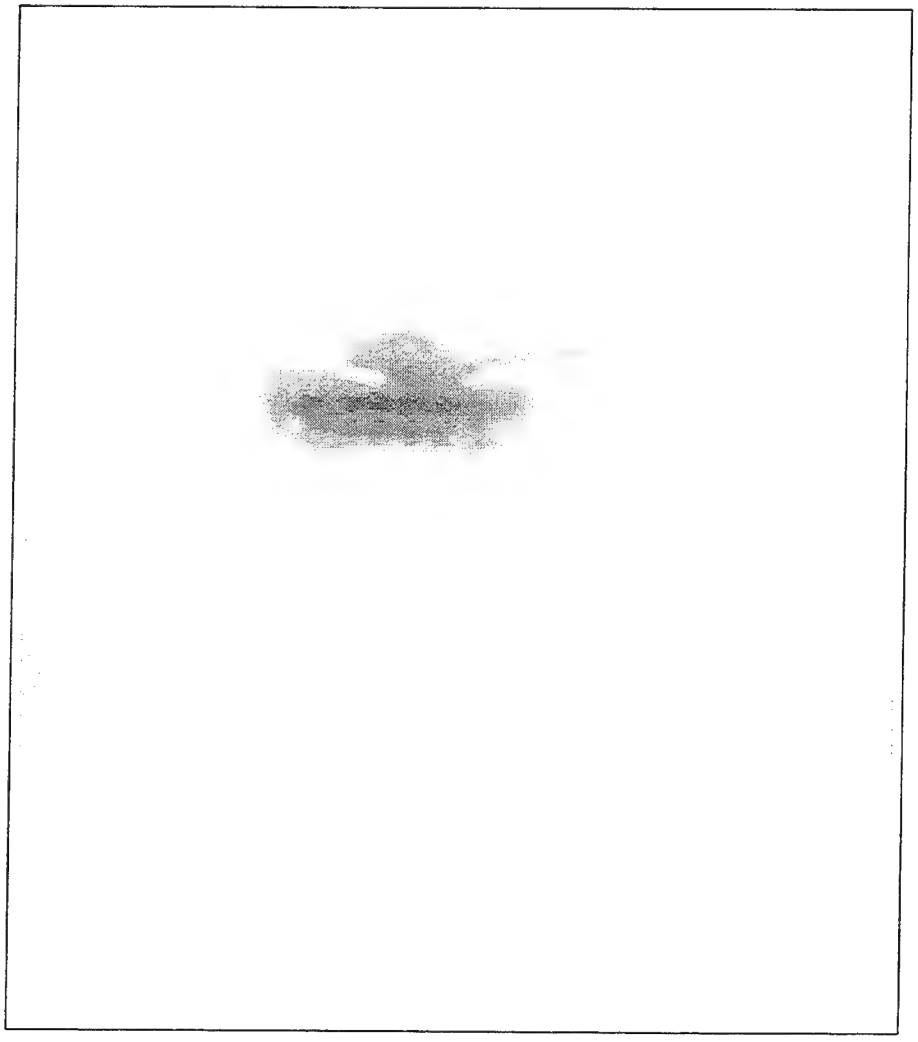

Fig. D-205. T15

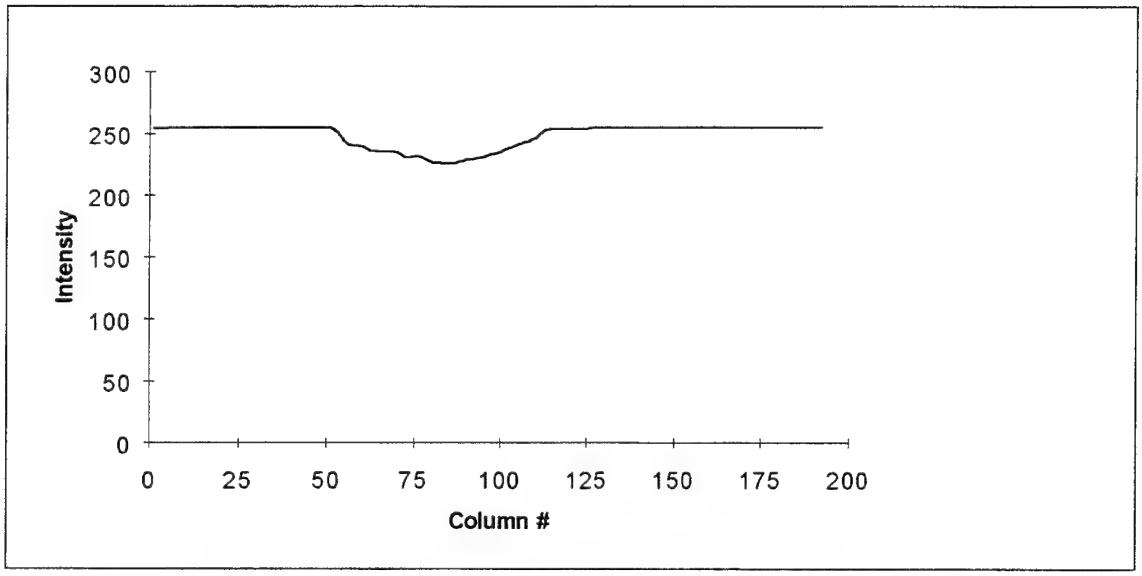

Fig. D-206. T15 squashed to preserve horizontal sequencies

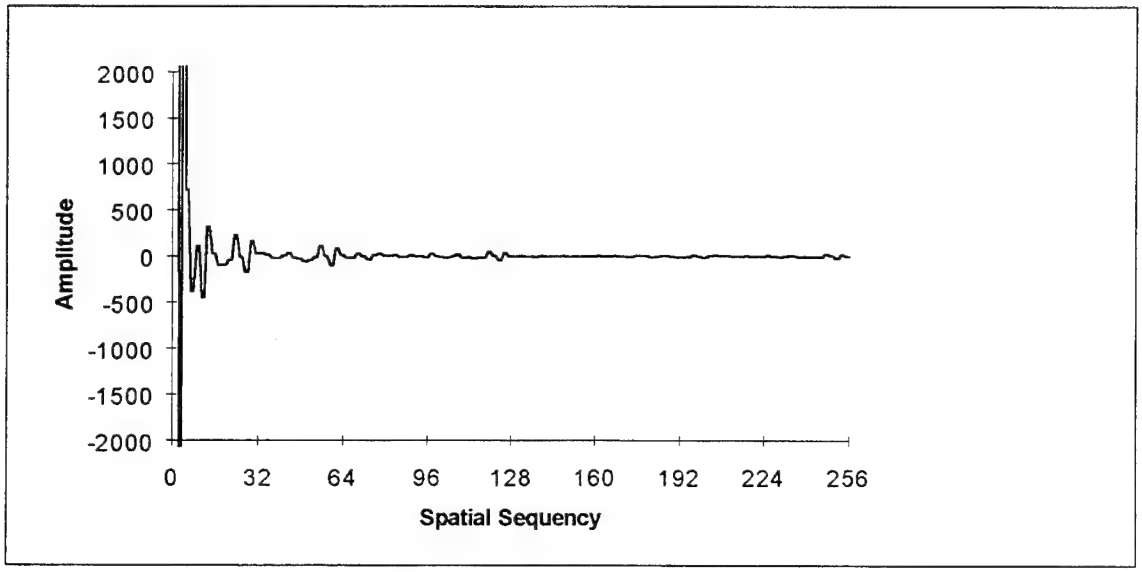

Fig. D-207. Walsh transform of Fig. D-206

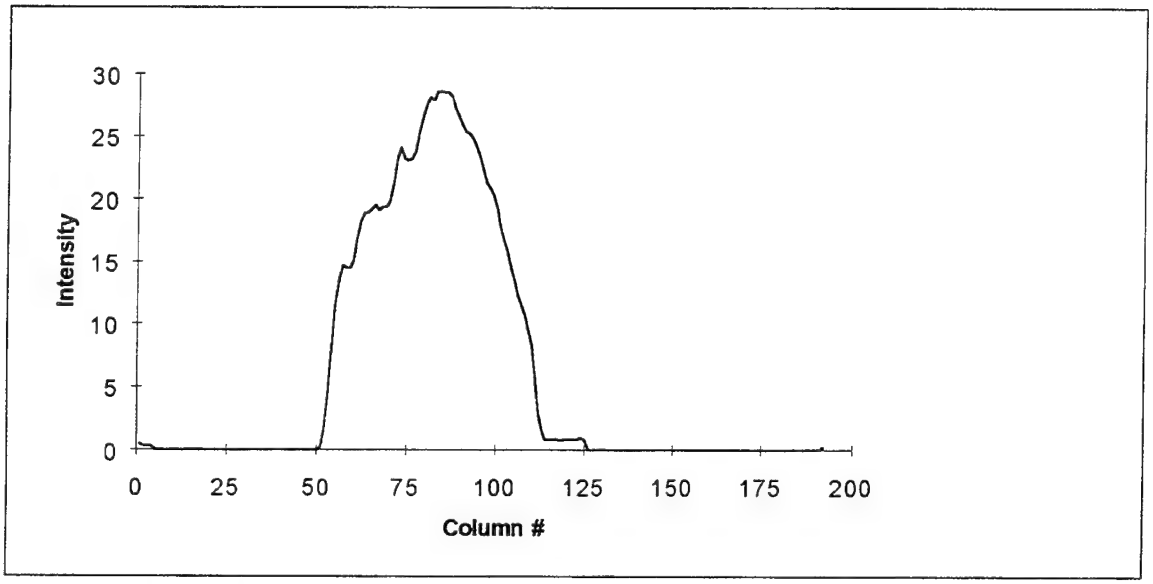

Fig. D-208. Complement of T15 squashed to preserve horizontal sequencies

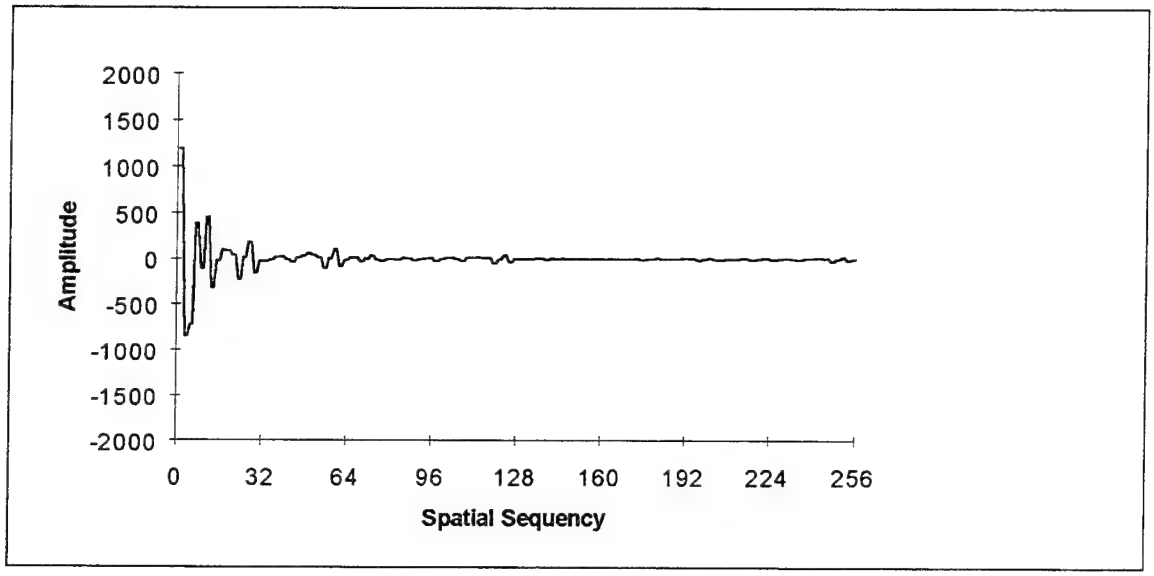

Fig. D-209. Walsh transform of Fig. D-208

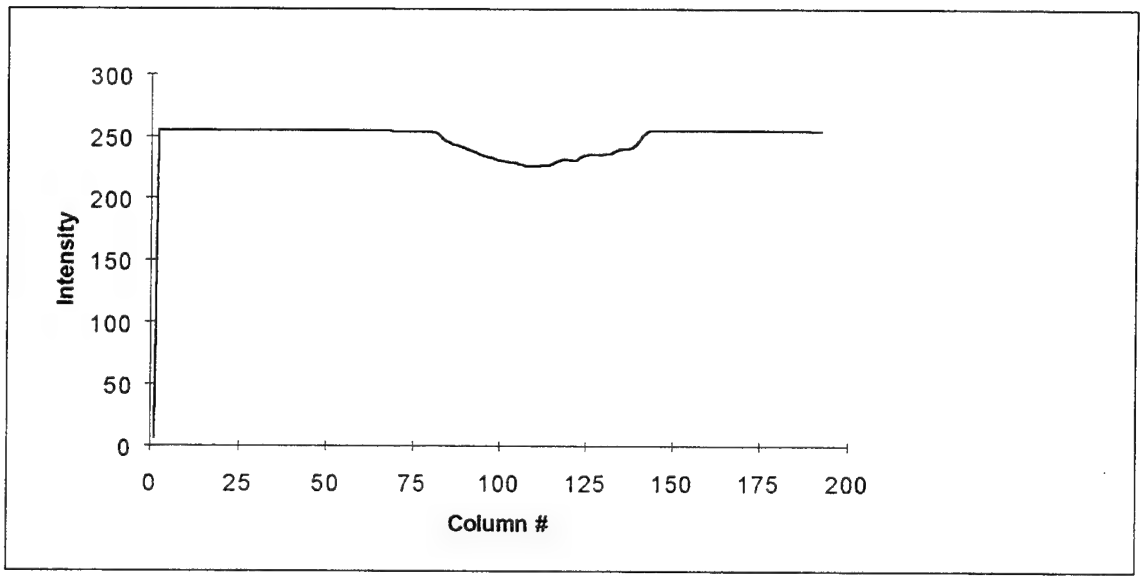

Fig. D-210. Reflection of T15 squashed to preserve horizontal sequencies

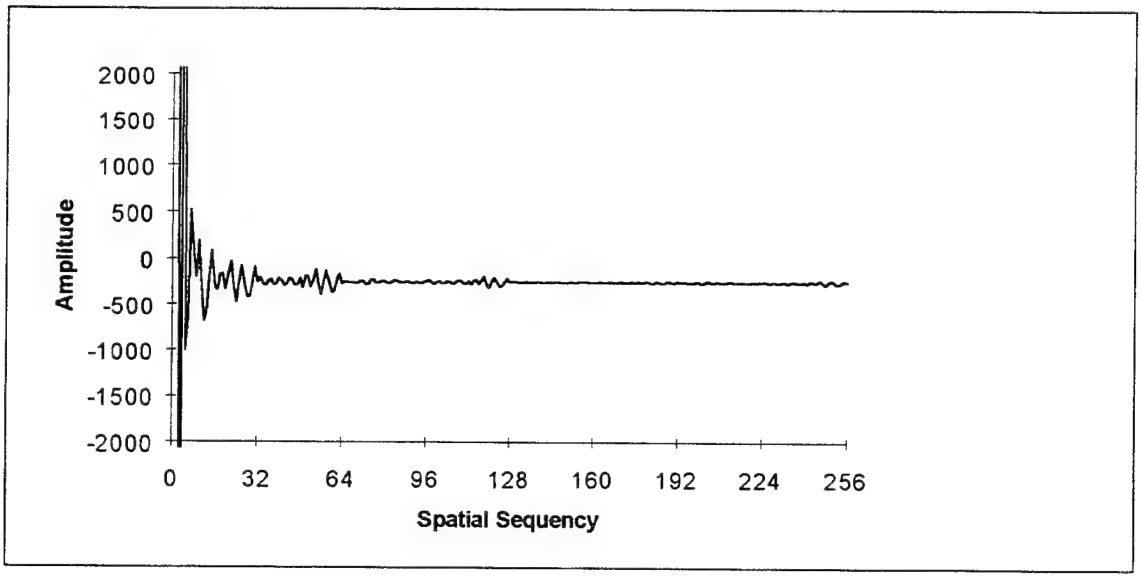

Fig. D-211. Walsh transform of Fig. D-210

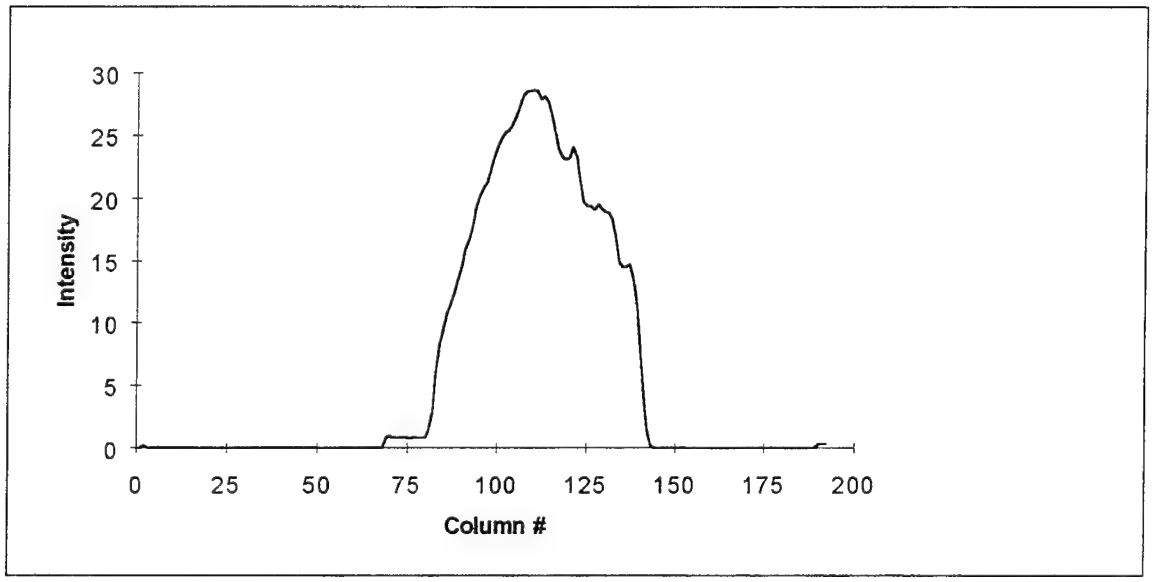

Fig. D-212. Complemented reflection of T15 squashed to preserve horizontal sequencies

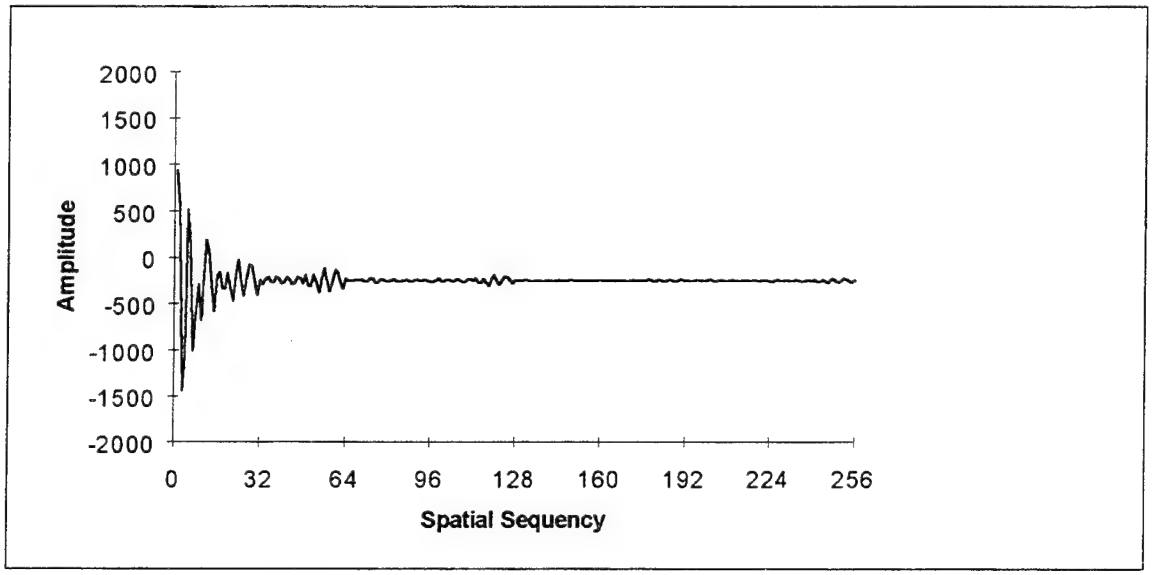

Fig. D-213. Walsh transform of Fig. D-212

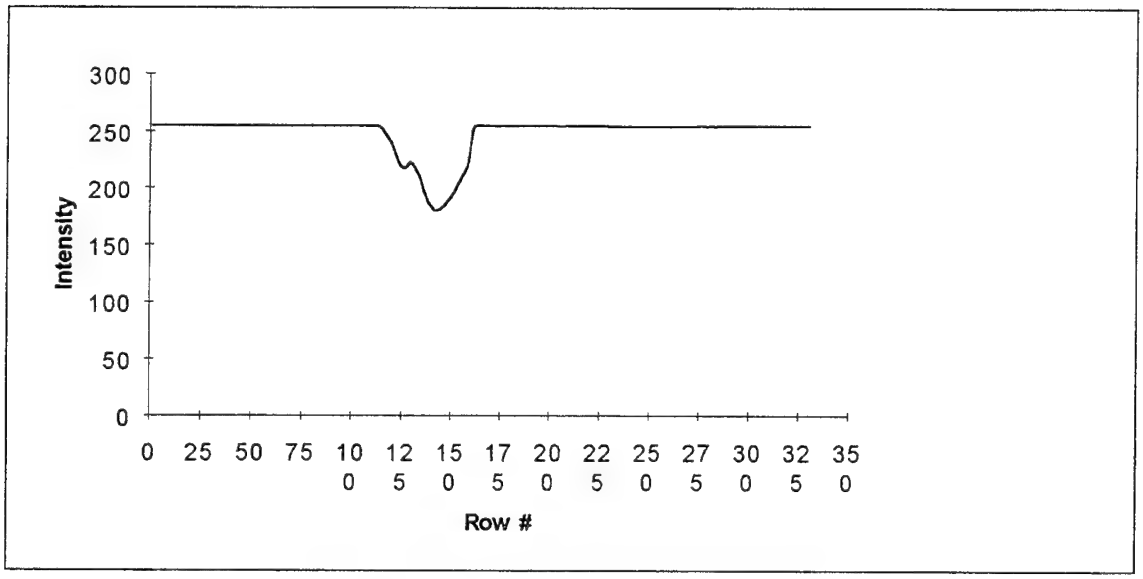

Fig. D-214. T15 squashed to preserve vertical sequencies

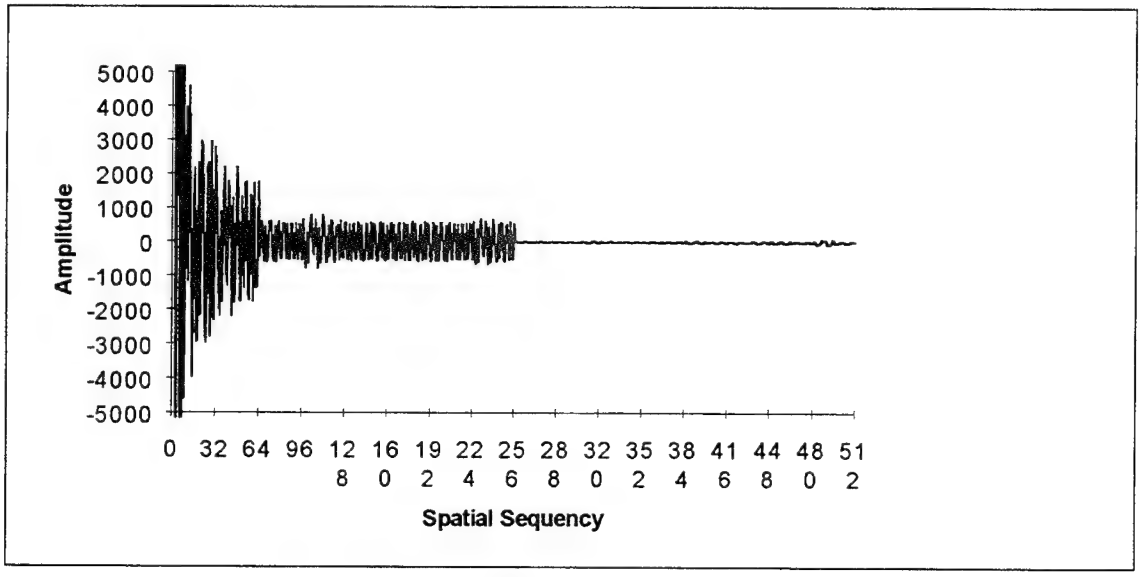

Fig. D-215. Walsh transform of Fig. D-214

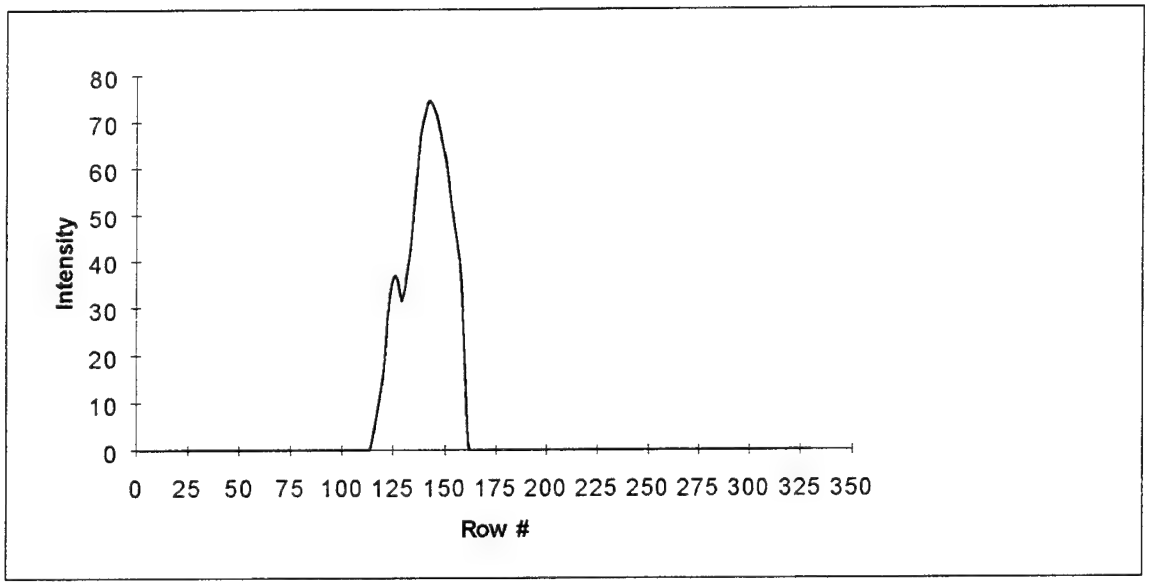

Fig. D-216. Complement of T15 squashed to preserve vertical sequencies

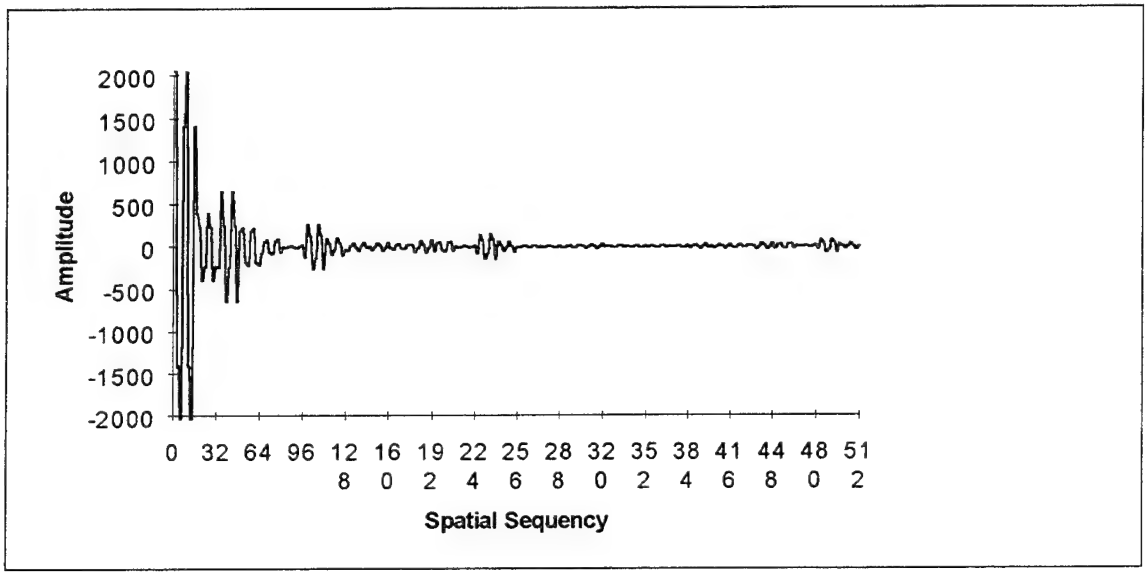

Fig. D-217. Walsh transform of Fig. D-216

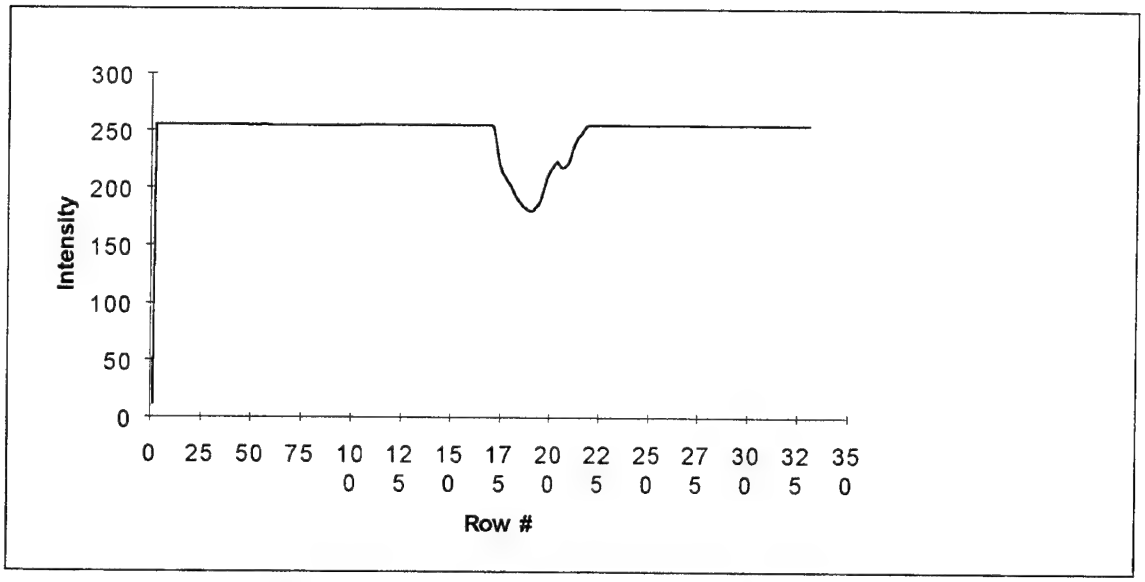

Fig. D-218. Reflection of T15 squashed to preserve vertical sequencies

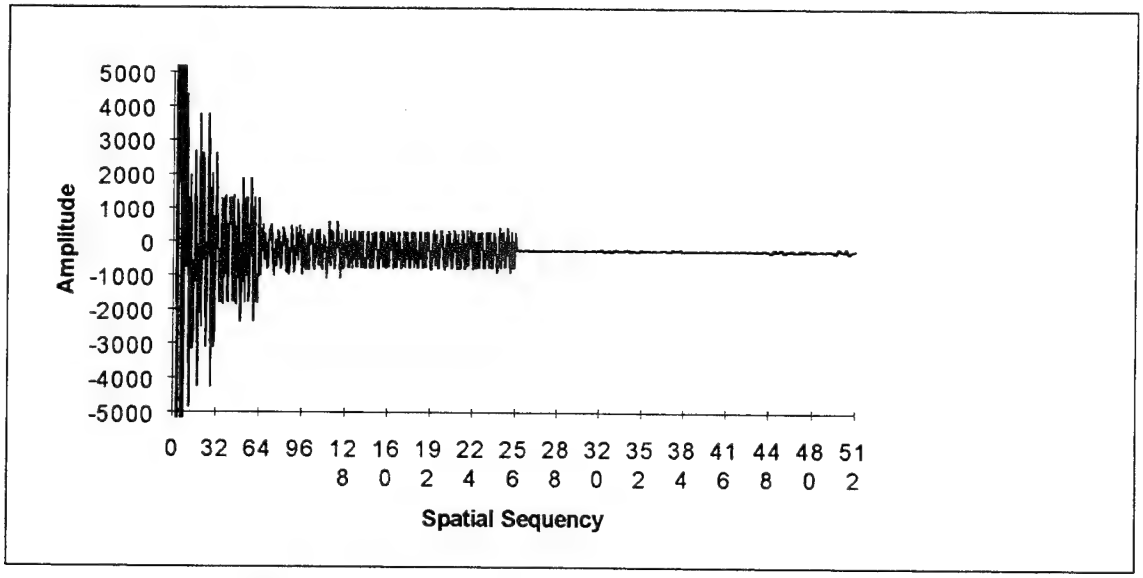

Fig. D-219. Walsh transform of Fig. D-218

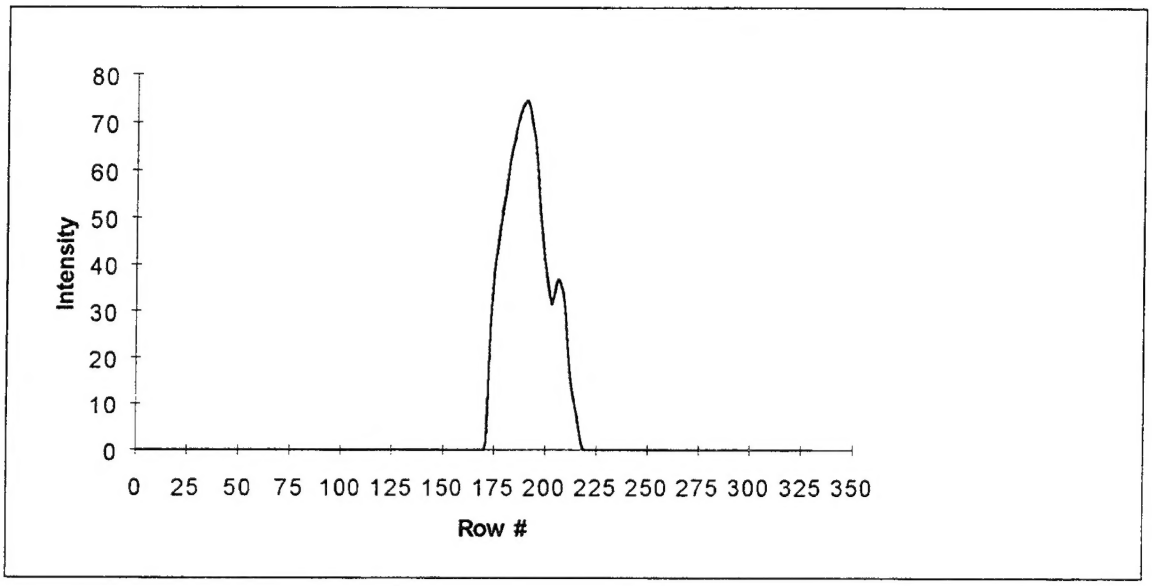

Fig. D-220. Complemented reflection of T15 squashed to preserve vertical sequencies

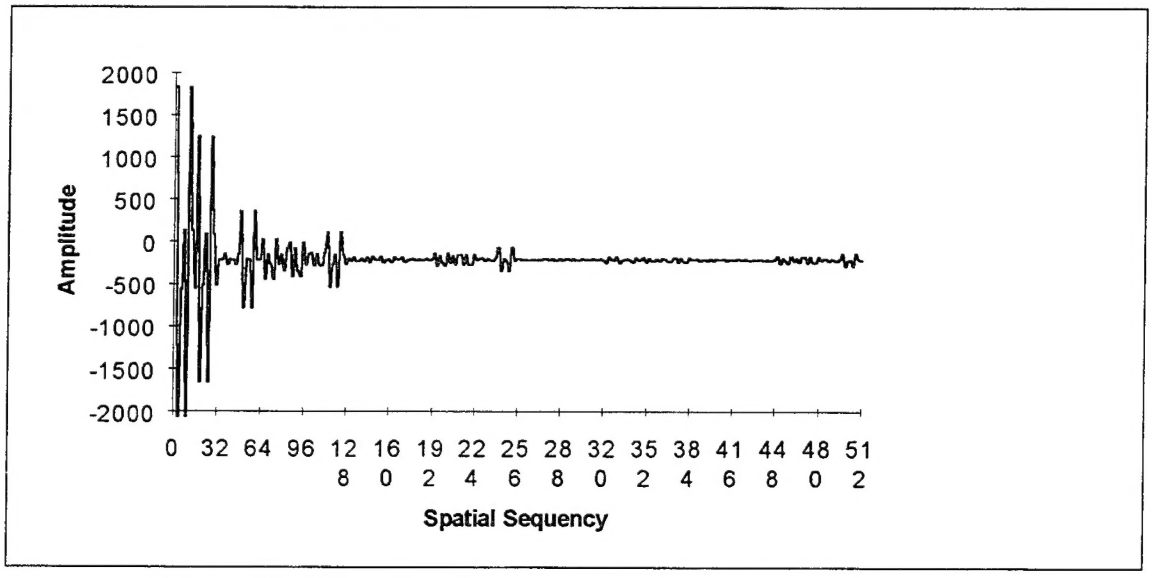

Fig. D-221. Walsh transform of Fig. D-220

REFERENCES

Beauchamp, K. G., Applications of Walsh and Related Functions, With an Introduction to Sequency Theory, Academic Press, 1984.

Bracewell, Ron, The Fourier Transform and Its Applications, McGraw-Hill, 1965.

Davis, D. S. , *Multiplexed Imaging By Means of Optically Generated Kronecker Products: 1. The Basic Concept*, A paper to appear in Applied Optics in 1994.

Dereniak, Eustace L. and Devon G. Crowe, Optical Radiation Detectors, John Wiley and Sons, 1984.

Harmuth, H. F., *Sequency Theory: Foundations and Applications*, Advances in Electronics and Electron Physics, Marton, L. (ed.),pp. 1-65,Academic Press, 1977.

Hecht, E. Optics, 2nd ed., Addison-Wesley, 1987.

Huguenin, Blake D. *Design, Development and Testing of a Prototype Optical System for a Next Generation Multiplexed Imager*, Master's Thesis, Naval Postgraduate School, Monterey, California, June 1992.

Kadin, A. M., M. Leung, A. D. Smith, and J. M. Murduck, *Photofluxonic Detection: A New Mechanism for Infrared Detection in Superconducting Thin Films*, Applied Physics, Vol 57, pp. 2847-2849, 1990.

Lindley, C. A., Practical Image Processing in C, John Wiley and Sons, 1991.

McKenzie, R. H. *A Demonstration of the Use of Walsh Functions for Multiplexed Imaging*, Master's Thesis, Naval Postgraduate School, Monterey, California, December 1990.

Metzger, Ferdinand Joseph, Jr. *Investigation of a Background Suppression Transimpedance Amplifier for Photovoltaic Detectors*, Master's Thesis, Naval Postgraduate School, Monterey, California, December 1992.

Middleton, Mark, *Design, Development, and Testing of a Preceision Angular Positioning System for a Next Generation Multiplexed Imager*, Master's Thesis, Naval Postgraduate School, Monterey, California, December 1994.

Musselman, Brian Jay, *A Study of the Diffraction Behavior and Resolution Criteria for Pattern Recognition for a Proposed Multiplexed Imaging Technique*, Master's Thesis, Naval Postgraduate School, Monterey, California, September 1991.

Pratt, W. K., Digital Image Processing, 2nd Edition, John Wiley and Sons, 1991.

Sargent, Joseph P., *A Design, Fabrication and Test of a Precision Positioning Servo Drive for a Multiplexed Imaging System*, Master's Thesis, Naval Postgraduate School, Monterey, California, September 1991.

INITIAL DISTRIBUTION LIST

1. Defense Technical Information Center 2
   Cameron Station
   Alexandria, VA 22304-6145

2. Library, Code 52 2
   Naval Postgraduate School
   Monterey, CA 93943-5000

3. Professor William B. Colson, Code PH/Cw 1
   Chairman, Department of Physics
   Naval Postgraduate School
   Monterey, CA 93943-5000

4. Professor D. S. Davis, Code PH/Dv 2
   Department of Physics
   Naval Postgraduate School
   Monterey, CA 93943-5000

5. Professor Michael E. Melich, Code PH/Mm 2
   Department of Physics
   Naval Postgraduate School
   Monterey, CA 93943-5000

6. Department of Physics Library 2
   Naval Postgraduate School
   Monterey, CA 93943-5000

7. MAJ Jeffrey H. Davis 2
   USA ELE DNA FLD CMD
   Kirtland AFB, NM 87115-5000